SPACE SCIENCES LABORATORY

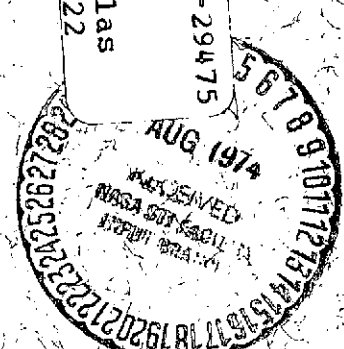

FINAL REPORT

NASA Grant NGR 05-003-134

Analytical Techniques for Identification and Study of Organic Matter in Returned Lunar Samples

6/1/66 - 5/31/68

Principal Investigator:

Prof. A. L. Burlingame

March 15, 1974

UNIVERSITY OF CALIFORNIA, BERKELEY

Space Sciences Laboratory Series 15 Issue 15

Space Sciences Laboratory
University of California
Berkeley, California 94720

FINAL REPORT

NASA Grant NGR 05-003-134

Analytical Techniques for Identification and Study of Organic Matter in Returned Lunar Samples

Period of Performance

6/1/66 - 5/31/68

Principal Investigator

Prof. A. L. Burlingame

March 15, 1974

Series 15 Issue 15

TABLE OF CONTENTS

11. A. L. Burlingame, and B. R. Simoneit, "High Resolution Mass Spectrometry of Green River Formation Kerogen Oxidations"

12. A. L. Burlingame, D. H. Smith, T. O. Merren, and R. W. Olsen, "Real-Time High-Resolution Mass Spectrometry: The Measurement of Accurate Molecular and Fragment Mass and Relative Ionic Abundance: The Detection and Identification of Unresolved Isobaric Species"

Offprints from
Topics in Organic Mass Spectrometry, Volume 3
Edited by A. L. Burlingame
Published by John Wiley & Sons, Inc., 19

Applications of Mass Spectrometry to Organic Geochemistry*

H. K. SCHNOES† and A. L. BURLINGAME
Space Sciences Laboratory, University of California, Berkeley, California

I. INTRODUCTION

Mass spectrometry has become an important physical technique in the elucidation of the molecular structure of organic compounds. As an analytical instrument the mass spectrometer has had a relatively long history of usage in geochemical and petroleum research and is still employed routinely for compound type analyses of petroleum samples, as well as for the quantitative determination of components of such

* The authors acknowledge financial support from the National Aeronautics and Space Administration, Grants NsG 101, NGR 05-003-134 and NAS9-7889.

† Present address: Department of Biochemistry, University of Wisconsin, Madison, Wisconsin.

mixtures which represent fractions containing mainly saturated, unsaturated, and aromatic hydrocarbons. The speed of analysis, the relative ease of computer treatment of the various analytical steps and calculations, and the excellent quality of the data obtained make this area of application of mass spectrometry still one of the most important in geochemical research, although other analytical techniques (e.g., high resolution and gas chromatography) are receiving prominent attention. The application of mass spectrometry to detailed structural studies in organic chemistry is of more recent origin, but is now a flourishing field, particularly since instruments specifically designed for these purposes have become available in recent years. The considerable number of books addressing themselves to organic mass spectrometry (1–10) attest to the popularity of the technique and its significance in current chemical researches; they furnish, as well, a broad introduction into mass spectroscopic techniques and applications.

This chapter is intended to be a review of the results thus far available from geochemical research. Emphasis will be placed on the contribution of mass spectrometric data to the solution of specific structural problems, rather than on the exploitation of such data for the quantitative analysis of mixtures. Problems and techniques of type analysis will be of minor concern to us here. Also, the application of isotope ratio mass spectrometry for the determination of $^{12}C/^{13}C$ ratios in carbonaceous sediments is not reviewed. The reader is referred to the chapter by Hoering for an introduction to this important area of research (10a). Information on the mass spectrometric behavior of compounds of geochemical interest is to be reviewed, however, and currently available techniques of particular importance to geochemistry, such as gas chromatograph–mass spectrometer coupling, modern sample introduction methods, and computer application in high resolution mass spectrometry, will receive particular attention. An earlier review by Hood (11) discusses the literature up to about 1960, and therefore this chapter will concentrate on the developments in this field in the intervening years. For a current review of researches in organic geochemistry the reader is referred to the volumes *Advances in Organic Geochemistry* (12) and the forthcoming work by Eglinton and Murphy (13).

We believe it will become apparent that mass spectrometry is one of the basic physical tools available to the organic geochemist. Often, due to limitation of sample size, it furnishes the *only reliable structural* information on isolated compounds, and, when used in conjunction with other spectroscopic methods, it will provide crucial complementary data. We shall stress the type of structural information most readily available from a mass spectrum, as well as the interpretative ambiguities in such data.

II. INSTRUMENTATION AND TECHNIQUES

A. Conventional Instrumentation

Most studies in organic geochemistry thus far have utilized single-focusing (low resolution) mass spectrometers. Double-focusing (high resolution) instruments are now available in many laboratories which are active in geochemical research and have already contributed considerable important data to the field.

It is not necessary here to discuss the general design and performance characteristics of mass spectrometers, since a number of books deal with this subject in varying degrees of sophistication (1,10,14–17): however, a brief summary of some of the important and desirable features of mass spectrometers used in geochemistry may be set forth:

1. High sensitivity (nanogram sample range)
2. Resolution $M/\Delta M$ of the order of 1:2000 (10% valley definition) and a mass range of approximately 2000 mass units
3. Fast scanning capabilities and correspondingly fast recording systems
4. Direct sample introduction into the ion source
5. Coupling of a gas chromatograph to the mass spectrometer
6. Combination electron bombardment–field ionization source

This list needs little elaboration, since most of the mass spectrometers currently utilized in organic structural work incorporate these features in their basic design. Furthermore, not all parameters need to be that strictly defined. For many applications, for instance, much lower resolution and mass range would be quite satisfactory. Mass spectrometers are inherently very sensitive instruments and for the typical commercially available instruments using electron multipliers as detectors samples of $< 10^{-8}$ g will suffice for excellent spectra—a performance quite adequate for geochemical applications. Fast scanning (i.e., 0.1–2.0 sec per decade in mass), GLC coupling (see below) and direct insertion probe (18) are very important aspects but, again, these are fairly standard features of modern instruments. The above list, then, simply describes a typical mass spectrometer equally useful for either organic geochemical or routine structural organic analysis. Mass spectra are recorded usually via a recording oscillograph utilizing 2–5 kcps response galvanometers. Very rapid scanning requires correspondingly fast (≥ 5 kcps) galvanometers, which introduce problems in the accurate measurement of relative ionic abundances since these display a full deflection of only 2 in. as compared to the 5–10 in. deflection of slower galvanometers. In the near future, the best

solution to the problem of very fast recording of mass spectra, while retaining both good resolution and accuracy of intensity measurement, will involve the exploitation of digital data acquisition techniques (19,20). Digital techniques for recording of low resolution mass spectra have been described (21); this approach appears valuable also for computer searching and comparison of unknowns with a library of standard spectra stored on rapid-access magnetic disks in the computer system.

The appearance of a mass spectrum may depend somewhat on the particular instrument used* (see, for example, the discussion in reference 3) and various source parameters. For example, the temperature of the ion source has a pronounced effect on the fragmentation pattern (23–25) and, of course, the pattern is critically dependent upon the ionization methods used. Most analytical applications involve ionization of the sample by electron bombardment. For a number of compound types (normal or branched alkanes, amines, alcohols, etc.) electron bombardment ionization results in molecular ions of relatively low abundance. While this is not necessarily a serious shortcoming, alternative ionization methods—such as field ionization (26) and chemical ionization (27), which repress fragmentation and produce relatively intense molecular ion peaks or $M - 1$ peaks—may be of distinct advantage for some applications, i.e., mixture analysis. Different ionization methods are discussed thoroughly by Beckey and Comes in their chapter in this volume, and chemical ionization techniques and applications are reviewed by Field (28). Chemical ionization source modification kits are now commercially available.†

A combination electron bombardment–field ionization source (29) should be of particular advantage in geochemical studies. Both a field ion and electron bombardment spectrum can be obtained on the same sample, simplifying both mixture analysis and structural studies on isolated samples. For a discussion of the use of combination sources for structural investigation, see a recent paper by Beckey and Hey (30).

Such a combination has been utilized in the characterization of mixtures of free fatty acids isolated from the kerogen of the Green River Formation by Schulze, Simoneit, and Burlingame (29b).

The electron energy in an electron bombardment ion source can be varied continuously from 3 to about 100 eV and for routine analytical applications is usually set at 70 eV. At low electron energies in the neighborhood of the appearance potential of molecular ions (i.e., 5–15 eV), fragmentation is often repressed drastically, such that only molecular ions

* This is particularly true of the quadrupole-type mass analyzer (17,22) and for magnetic deflection instruments which may be scanned electrostatically employing ion multiplier detection.

† Scientific Research Instruments Corporation, Baltimore, Md. 21207.

appear in the spectrum. This fact can be exploited for mixture analysis (31), and it is particularly useful in high resolution work, permitting the composition of all detectable molecular species to be determined readily. A number of papers describing this technique will be discussed in some more detail later.

B. Sample Handling and Introduction Systems

Geochemical applications do not actually require any special handling or introduction techniques, but, of course, it must be kept in mind that often only extremely small quantities of samples are available for analysis.

Beynon (1) and Biemann (2) discuss in some detail general sample handling techniques and introduction systems as applied to routine organic chemical analysis. New developments in this area, since the appearance of these monographs, include primarily the use of direct insertion probes and cooled probes (also cooled ion sources) and the advent of GLC—mass spectrometer coupling techniques.

Geochemical samples of pure compounds destined for mass spectrometric analysis are usually obtained directly from the effluent of a gas chromatographic column. It is, then, most convenient to collect such samples in an ordinary melting point capillary which can be introduced directly into the ion source inlet system of the mass spectrometer. This straightforward collection technique avoids the necessity of further transferral of sample into a special introduction tube fitted for the mass spectrometer. Samples collected in devices from which they cannot be introduced into the mass spectrometer (for instance, some of the GLC traps commercially available) can be transferred in solution (e.g., dichloromethane) to a melting point capillary sealed at one end, with subsequent removal of solvent under a stream of pure nitrogen. At dry ice–acetone temperature, dichloromethane can be quantitatively removed from volatile samples using the inlet system vacuum (32). It is often most convenient in such cases to reinject the sample and recollect it in a capillary. Compounds of high volatility must be trapped in U-tube capillaries with appropriate cooling; the section of tubing containing the condensed sample can then be cut and introduced into the instrument. For geochemical samples obtained in microgram quantities or less, the common methods of sample introduction into the mass spectrometer by means of a reservoir (0.5–3 liter) and valve system are unsatisfactory. The sample reaches the mass spectrometer ion source as a stream of gas through a pinhole leak designed such that at any given time very little of the gas will be in the ionizing chamber. For such samples direct introduction is mandatory. Most commercial mass spectrometers are now fitted with

"direct introduction probes" as standard instrument accessories. The probe arrangement utilized in the authors' laboratory for geochemical analysis is illustrated in Figure 1. A melting point capillary containing the sample fits into the probe tip, which is inserted directly (through the valve arrangement shown and without breaking the instrument vacuum) into the ion source region. Upon volatilization (accomplished by the ion source and/or auxiliary probe heater), all of the sample passes through the region of the ionizing electron beam. Intense spectra can thus be obtained on very small quantities of material. A further advantage of the direct inlet is the possibility of partial fractionation of multiple-component samples upon carefully controlled heating.*

This implies, of course, that the direct inlet system is not useful for quantitative mixture analysis, since such analyses assume a constant partial pressure of each component (24). The direct proble inlet system is an absolute necessity for very nonvolatile and heat-sensitive samples, since the pressure in the ion source region (order of 10^{-6} to 10^{-7} mm Hg) is considerably lower than in a reservoir system and the lower temperatures

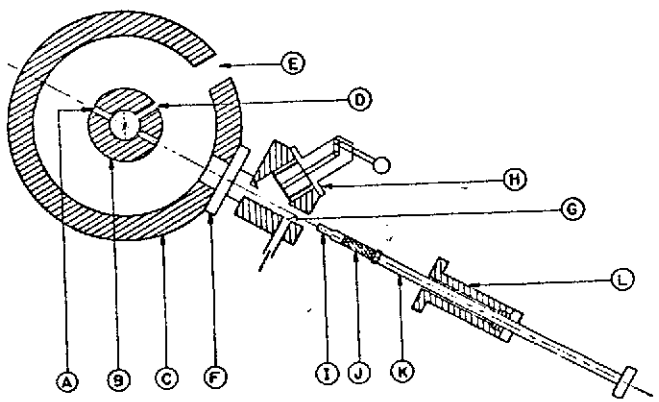

Fig. 1. Direct inlet system (CEC 21-110B mass spectrometer) (20). (*A*) pump-out port, (*B*) ion source block, (*C*) source housing, (*D*) gas inlet port, (*E*) heated cover plate port, (*F*) direct inlet attached to source housing, (*G*) pump-out line to rough pump and diffusion pump, (*H*) inline valve, (*I*) silver sample tip, (*J*) ceramic insulator, (*K*) probe shaft, (*L*) Quick disconnect shaft holder.

* For example, preparation of volatile derivatives (e.g., silyl ethers of hydroxy functions and acetylation or methylation of amino functions) often yields mixtures of the starting material and product, differing sufficiently in volatility to make at least partial fractionation possible in the direct inlet.

are sufficient for the sublimination of such compounds. The lower temperature and the fact that collisions with reservoir walls after volatilization are avoided minimize the decomposition of labile molecules.

The direct probe poses some difficulties for the analysis of volatile samples (e.g., small hydrocarbons and esters), since volatilization may occur very rapidly, even at the lowest operating temperatures of the ion source (approximately 70–100°C). To overcome this problem a liquid nitrogen cooled probe may be used (Fig. 2 illustrates such a probe constructed in the authors' laboratory). Spectra of hydrocarbons in the range from C_{10} to C_{18} have been obtained successfully using this technique. The operation and use of such a probe is, however, somewhat more cumbersome and time consuming. An alternative method, in which volatile samples are absorbed on molecular sieves, has been described (33). The desorption process from the sieve in the source chamber is sufficiently slow to permit the determination of mass spectra. Since it has been suggested (34) that liquid phase-coated solid support (GLC packing) may be used for efficient GLC fraction collection, it may also be useful for direct introduction of samples into the ion source of a mass spectrometer. The most convenient, although instrumentally most elaborate, system for introducing volatile samples directly into the ion source is the GLC-mass spectrometer coupling arrangement. This technique (described more fully below) is utilized ordinarily for the analysis of complex mixtures but would be of equal advantage for the introduction of individual samples. Wherever multiple-port construction of the ion source of the mass spectrometer permits the simultaneous connection of several inlet systems—a direct probe, all glass inlet, stainless steel inlet, and a GLC inlet—this latter method becomes routinely feasible and is to be recommended. Of course, this requires that the compound being investigated be thermally stable under the operating conditions and temperatures of the gas chromatograph and also that it will not be catalytically decomposed by the hot metal components of either the chromatograph or the mass spectrometer.

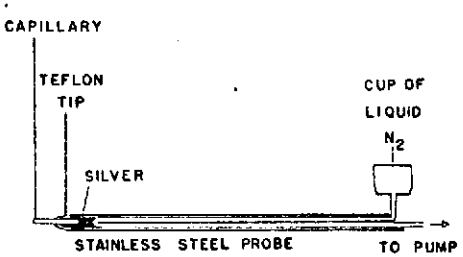

Fig. 2. Liquid nitrogen cooled direct inlet probe (35).

C. High Resolution Mass Spectrometers

The availability of instruments capable of resolution of the order of 1:30,000 or better and mass measurement with an accuracy of 5–10 ppm far extends the utility of mass spectrometry in structural studies. Such performance not only gives the typical fragmentation pattern of a compound, but also allows the unique* determination of elemental compositions of molecular and fragment ions. The interpretation of a spectrum is thus facilitated considerably and any conclusions drawn are derived from much firmer experimental bases.

High resolution and accuracy of mass measurement are achieved by a sequential arrangement of an electrical and magnetic field. Two basic geometries are used in commercial high resolution mass spectrometers. In the Nier-Johnson geometry, electric and magnetic fields achieve a point of double focus. Mass measurement is accomplished either by the "peak matching" technique or by scanning of the spectrum and recording onto either frequency modulated analog magnetic tape or digital magnetic tape. The Mattauch-Herzog geometry accomplishes the simultaneous focusing of all ions over a 30:1 mass range to be recorded on a photoplate. Peak matching or scanning is possible here, also, and the basic design is, in this sense, somewhat more versatile. The intricacies and problems of high resolution are covered in detail in other chapters of this volume. Applications of high resolution instruments are included in later sections with discussions of the compound classes, but more detailed consideration of high resolution mass spectrometric principles and application to geochemical problems have been discussed in another review (35).

The advantages of these instruments for geochemical work are great and obvious. In particular, application of high resolution equipment to mixture analysis yields much more information. The elemental composition of each component becomes available and compounds of the same nominal mass but different composition are readily distinguished. For pure samples composition data can be obtained on microgram quantities, and the coupling of a gas chromatograph to a high resolution mass spectrometer is certainly one of the most powerful and fastest methods for the analysis of complex mixtures. Pertinent applications will be mentioned in detail in later sections.

High resolution mass spectrometers can be exploited to the fullest potential only in combination with computer systems. The compositions

* With certain qualifications, since some combinations of elements result in mass doublets for which an unambiguous assignment of composition is not possible *a priori*; but see the chapter by Biemann for more thorough discussions of these problems.

of all ions in a mass spectrum can then be calculated rapidly and a partial interpretation of spectra can be attempted. Element mapping (36) and heteroatomic plotting (37) are practical and important results of this approach. The future will see the further development of sophisticated on-line mass spectrometer–computer operations (19,20,38,39).

D. Gas Chromatograph–Mass Spectrometer Coupling

The combination of gas chromatographic and mass spectrometric equipment results in analytical instrumentation of great power and versatility. In this section we shall discuss only those methods employing direct coupling of the two instruments without intermediate trapping of the gas chromatograph effluents. Trapping and collection of samples emerging from a gas chromatograph and subsequent mass spectral analysis can also, of course, be considered a "combination" technique; however, this is rather more unexceptional and has been discussed in a previous section. This latter approach has the advantage that the two analytical steps—separation of components in a mixture and mass spectral analysis—can be conducted separately in time and space, and the instrumental requirements for each operation are consequently also much less stringent. It does involve, however, one additional critical experimental step—the collection of each sample—which may cause problems and which is exactly the step the direct GC–MS combination technique is designed to circumvent.

The combination method, then, exhibits as its most characteristic features speed of analysis, sensitivity, and avoidance of an intermediate isolation step. We may consider these points in somewhat more detail here.

All the effluent of the gas chromatograph enters the mass spectrometer directly and, if the connection is suitably designed, very little loss of resolution results. Losses which are unavoidable when individual samples are isolated are thus very significantly reduced, and contamination, always a possibility when very small samples are to be trapped, is essentially avoided. The only source of contamination is the slow bleeding of column phase, but in most cases this will be easily recognized and distinguished from the components making up a given mixture. Very small quantities of samples are amenable to analysis and, thus, open tabular columns (capillary columns) possessing very high resolution but low capacity can be used to great advantage. Since individual collection of samples, a most time-consuming step, is avoided, a complete mass spectrometric analysis of all components can be obtained in essentially the time required for a

single gas chromatographic run. The direct combination approach is readily adaptable to routine analytical problems and perhaps to computer control of its operation and the interpretation of data (21c).

As mentioned above, the coupling puts relatively stringent requirements on the performance of the components. As far as the mass spectrometer is concerned, high sensitivity and very fast scan rates are the most important and necessary features. Scan rates of a decade in mass within fractions of seconds are desirable, since this would permit several consecutive scans as a component peak enters the ion chamber. Comparison of the spectra then provides a very good check on the homogeneity of each GLC band and significantly simplifies the task of interpretation of a given mass spectrum. The sensitivity requirement is equally crucial but need not be stressed particularly, since mass spectrometers are inherently very sensitive instruments; thus, a microgram of sample injected on a GLC column would be expected to yield a very intense spectrum, and most mass spectrometers will still produce an interpretable pattern on 1/1000 of this amount.

When double-focusing (high resolution) mass spectrometers are to be coupled to a gas chromatograph, some of the same considerations naturally apply. The object of a coupling arrangement would be the production of a complete high resolution mass spectrum of each component; both the Mattauch-Herzog type mass spectrograph and the Nier-Johnson mass spectrometer are suited for such purposes.

Gas chromatographs employing either capillary or packed columns have been coupled to mass spectrometers. Since the former use low flow rates of carrier gas of the order of 1–3 ml/min, it is possible to connect these columns directly to the mass spectrometers, permitting the total effluent to reach the ion source. The pumping system of the latter is fast enough to allow such operation without causing malfunction of the instrument. For packed columns, however, which operate under flow rates of up to 80 ml/min, an interface consisting of an enrichment device becomes essential. The function of this interface consists of selective removal of most of the carrier gas, permitting a stream heavily enriched in compound molecules to enter the mass spectrometer. Several such interfaces or "separators" have been described within the last few years. Two of them, the "molecular separator" of Ryhage (40) and the fritted glass tube of Watson and Biemann (41), are now being used quite routinely, whereas others, the semipermeable silicone membrane (42,43) and the Teflon membrane (44), do not seem to have found general acceptance as yet. The efficiency [defined as the ratio of the amount of sample entering the mass spectrometer to the amount entering the separator (45)] of the Ryhage and Watson-Biemann type separators (45) is of the order of 50%

and losses of sample are consequently quite significant, although these depend somewhat on the types of compounds studied [perhaps due to chemisorption on the walls of the separator (46)]. The low efficiency [the Teflon membrane seems to be superior in this respect with efficiencies of 50–90% (45); however, a detailed comparison of all separators appears desirable] is usually not a severe handicap, however, because of the high sensitivity of the mass spectrometer. The use of these separators permits flow rates up to 60 ml/min, while maintaining source pressures of 10^{-5} mm Hg or less.

If the gas chromatograph is equipped with an effluent splitter, part of the effluent can be diverted to an ionization detector to produce a conventional gas chromatogram. Alternatively, or in addition, the mass spectrometer total ion current monitor can be used as detector by connecting its output to a pen-and-ink recorder. In the author's laboratory a dual-pen recorder simultaneously produces gas chromatograms from both the output of the chromatograph ionization detector and the total ion monitor, providing a convenient and immediate check on the time lag between gas chromatograph and mass spectrometer and possible loss of resolution.

Several complete mass spectra (from three to ten) are usually obtained from a single GLC peak emerging from the column. Extremely rapid mass scanning (in the order of 0.1 sec to several seconds) is thus a necessity. Accurate identification of mass number (by simple counting) may be quite difficult under these circumstances, and the simultaneous recording of the spectrum of a marker compound—bled in from a reservoir or by the technique of Leemans and McCloskey (47)—is usually necessary. Consecutive runs both with and without a marker can be used to eliminate any uncertainties or ambiguities in the interpretation of the spectrum. On-line computer techniques would be the best solution to these problems (see also reference 21c).

The first attempts to couple a gas chromatograph to a mass spectrometer were described as early as 1957 (48), and since then the technique has found considerable application in a variety of fields. The chapter by Stenhagen and Ställberg-Stenhagen in this volume, as well as several other excellent review papers (47,49–52) should be consulted for detailed accounts of the technical aspects and applications of the method. In particular, the review by Saalfeld (50) and the *Proceedings of the Chromatography-Mass Spectrometry Symposium* (51) provide a very extensive bibliography of past researches.

A potentially important development not covered in these reviews is termed interrupted-elution gas chromatography (53,54). A gas chromatograph is automated to control the carrier gas flow such that individual

bands (peaks) may be removed at will and fed into either a mass spectrometer or an infrared spectrometer while preserving the chromatographic resolution of bands remaining on the column.

Applications to geochemical problems are by now quite numerous and relatively routine. Some examples include the separation on a capillary column of saturated hydrocarbons up to C_{11} and their mass spectrometric identification (55), and the analysis of olefinic compounds (56) and hydrocarbons in the C_8 to C_9 range. Sixteen C_9 hydrocarbons from petroleum were identified by the combination of a cycloidal focusing mass spectrometer (equipped with Wien filter and ion multiplier) and a capillary gas chromatograph (57). The combination of a gas chromatograph with a time-of-flight mass spectrometer was used in the experiments of Anders and co-workers (58–61). A study of volatile, odoriferous components in polypropylenebenzene sulfonate which occur as saturated ketones and conjugated diolefins has been reported. This work made use of coupled GLC–mass spectrometric techniques in addition to chemical transformations for preliminary separation (61a). The approach described could be applied to the volatile, lower molecular weight components of organic geochemical samples.

Since the introduction of separators, several interesting applications to geochemical work have been described using these enrichment devices. For example, Oró and collaborators reported the identification of pristane and phytane in the Precambrian Gunflint Chert (62) and the Precambrian Fig Tree Shale (63). Isoprenoid alkanes ranging from C_{15} to C_{20} have been identified in Little Osage Shale extract (64), and a novel series of 2,6-dimethylalkanes isolated from a Cretaceous shale (65) was characterized by the interesting new technique of coupling a two-stage gas–liquid chromatograph (in which the second stage separates isomeric branched alkanes, resolved according to molecular weight by the first stage) in series to a mass spectrometer (66). Isoprenoid fatty acids (67–69) from extracts of the oil shale from the Green River Formation and aromatic acids which produced ozonization of coal (70) have been similarly analyzed.

The work of Oro and collaborators (71) provides data on the analysis of extraterrestrial samples (e.g., Murray, Orgueil, Makoia, and other carbonaceous meteorites) procured by such combination methods. In general, the technique appears to yield quite excellent data, and there can be no doubt that it will become one of the most important and routine approaches to organic geochemical analysis.

A very important extension of the basic technique is the combination of gas chromatography and high resolution mass spectrometry (40,41,52, 72–75). An example of the results obtained by Hayes and Biemann (76) is illustrated in Figures 3 and 4, showing the GLC–high resolution mass

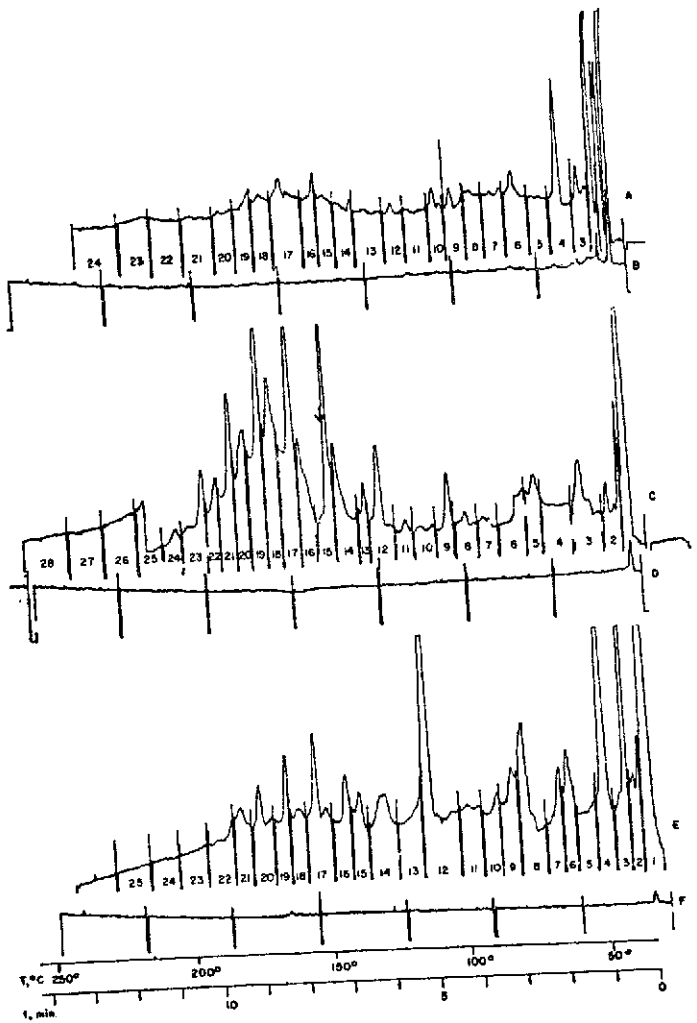

Fig. 3. Gas–liquid chromatogram of Murray meteorite (76).

Fig. 4. Element map of peak 15 in Figure 3 (76).

spectrometer analysis of the organic constituents of the Murray meteorite. The analytical method involves the pyrolysis of a sample of the meteorite, the condensation of the evolved organic matter in a cold trap, and subsequent flash evaporation of the condensate into a gas chromatograph connected to a mass spectrometer. The gas chromatograms illustrated in Figure 3 are the traces obtained when a sample of Murray chondrite was heated over a temperature range of 25–146° (A), 146–254° (*C*), and 255–409° (after admixture of zinc dust; *E*). Traces *B*, *D*, and *F* represent

blanks. High resolution spectra recorded on a photoplate were obtained for each peak; the vertical lines in each chromatogram indicate successive exposures. The photoplate data are subsequently reduced by computer techniques.

The end result of these manipulations is illustrated in Figure 4, the element map (see the chapter by Biemann on high resolution) of peak 15 in chromatogram *C*. It will be noted that compositions of ions are plotted in vertical columns labeled CH-aliphatic, CH-aromatic, CHS, CHO, CHO_2. In the case at hand, the element map permits the conclusion that the major component of GLC peak 15 is tridecane (*m/e* 184, $C_{13}H_{28}$; the asterisks indicate abundance on a semilogarithmic scale*) and that minor components are a methylnaphthalene ($C_{11}H_{10}$), a C_7alkyl benzene ($C_{13}H_{20}$), and a monounsaturated or monocyclic aliphatic compound of composition $C_{14}H_{28}$ (*m/e* 196). Furthermore, trace amounts of methylbenzothiophene (C_9H_6S) are seen to be present, but there are no oxygen-containing molecules or ions.

This one example may suffice to illustrate the wealth of information that can be obtained from high resolution mass spectra of mixtures of GLC fractions. The review articles quoted give many more examples of the coupling of high resolution equipment to gas chromatography using both packed and capillary columns. The routine use of high resolution instruments and the necessary analysis of the data requires the extensive utilization of computer methods. The work of Hayes (75) should be consulted for more details on the analysis of carbonaceous chondrites by GLC–high resolution and computer techniques.

III. STUDIES ON ORGANIC MATTER FROM GEOLOGICAL SOURCES

The application of mass spectrometry to the analysis of hydrocarbon fractions obtained from petroleum represents the earliest exploitation of the technique for the solution of organic chemical problems. Compound type analysis of petroleum fractions as first demonstrated by Brown (77) in 1951 was one of the major achievements, which since then has developed into a sophisticated method of instrumental analysis, used routinely in all laboratories involved in petroleum chemistry. Type analysis constitutes necessarily a preliminary investigation of complex mixtures since its objective is solely the recognition of compound classes in a sample, rather than the determination of individual components; such studies also

* The numbers immediately preceding them indicate error in measurement to the nearest millimass unit (mmu).

provide no information on structural detail of any compound or compound class. The success of the technique is based on the principle that any given compound type can be recognized by a set of specific peaks and that the spectrum of a mixture of types is simply the composite of the spectra of the individual compounds making up the mixture. If suitable calibration data on known compounds are available the mixture can then be analyzed quantitatively. In practice, only a limited number of types in a mixture can be analyzed by medium resolution mass spectrometers. Complex mixtures must either be prefractionated or several classes must be grouped and treated analytically as a single type. The technique of type analysis has seen many modifications and improvements in the last 25 years. The availability of computers has considerably facilitated the vast calculations necessary for these analyses. The technique of low voltage analysis of Field and Hastings (78) was a further modification. Whereas the former methods made use of characteristic mass summation to determine compound types, the low voltage technique employs only the molecular ions for analysis, thereby simplifying the calculations required. However, it has the shortcoming of distinguishing only seven compound types, thus necessitating extensive preseparation of mixtures for a complete analysis.

The utilization of high resolution mass spectrometers for such analyses, first demonstrated by Carlson et al. (79), presents a further significant advance, since these instruments, even at the moderate resolving powers of the early work, can readily distinguish between isomers of the same nominal mass (i.e., between saturated alkanes and napthalene derivatives, ^{12}C vs. $^{1}H_{12}$). We shall consider some of these applications under the pertinent sections below. However, a review of compound type analyses will not be attempted here. Dibeler (31) and Reed (80) provide general introduction and reviews of this field and leading literature references, and a detailed treatment of this subject is available (81).

In the following we shall consider mainly the contribution of mass spectrometry to the solution of specific structural problems and the identification of isolated compounds from all geological sources. We shall discuss separately each of several broad compound classes of importance to geochemical studies. Before doing so, a few general remarks may be appropriate, however. Organic compounds thus far obtained from geological sources represent actually fairly straightforward structural problems; that is to say, very few of them are structurally of a complexity that an organic chemist would ordinarily be confronted with were he to study other natural products. The vast majority represent simple hydrocarbons, acids, or aromatic bases which, were they available in quantity, would represent relatively simple identification problems. However, organic matter obtained from either petroleum or sediments usually represents extremely

complex mixtures from which any given substance can be isolated only in very low yield. This is particularly true for work on ancient sediments, the organic content of which is very low and from which a specific substance may be obtainable only in microgram or nanogram amounts. At this level most physical methods of characterization are no longer very useful and other spectroscopic data which may be obtained are severely limited. For hydrocarbons, mass spectrometry and gas–liquid chromatography are the only available methods for structural investigation, and since GLC is useful only when (*a*) the authentic compound is available for comparison and (*b*) very high efficiency columns are utilized which can distinguish between isomers exhibiting minor structural differences, mass spectrometry remains the only method capable of giving reliable data on an unknown. Gas chromatography and mass spectrometry should, of course, both be used for a characterization, but it perhaps should be stressed that whereas mass spectrometry alone may often suffice to characterize a compound, GLC alone is entirely insufficient and identifications based solely on this technique should be rejected.

The advantages of mass spectrometry are fairly self-evident. In the case of a completely unknown compound, it provides at least some basic and certain information, i.e., molecular weight, composition, and often also some specific structural information. Its shortcomings are equally important, however. It is commonly recognized that stereoisomers usually present very similar spectra, although positional isomers are sometimes equally difficult to distinguish; we will have occasion to comment on such cases below. Furthermore, each interpretation of a spectrum involves a judgment as to the purity of the sample. Does a peak which differs in intensity in the spectrum of the unknown from that of the standard imply a different structure or can it be ascribed to an impurity? Often a detailed analysis of the spectrum will provide the answer, but caution is obviously necessary, as demonstrated by an interesting case cited below. In this connection it perhaps should be stressed that a comparison of standard and unknown whose spectra have been obtained on different instruments may be quite misleading.

Finally, the interpretation of the spectrum of the unknown is only as good as our current understanding of the fragmentation behavior of the various compound classes. Ideally one would like to match the spectrum of the unknown with that of an authentic compound, but in practice this is not always feasible.

By the standards of classical organic chemistry very few structures of compounds isolated from sediments have been conclusively established. This does not necessarily detract from the usefulness of these studies since our knowledge of the organic constituents of sediments in particular

is so limited that almost any new information appears welcome. For relatively simple hydrocarbons the combination of gas chromatography and mass spectrometry will suffice for the definition of gross molecular structure. In the future, no doubt, more physical data such as infrared, ultraviolet, and NMR spectroscopy will become a necessity for the elucidation of structures of more complex material.

A. Hydrocarbons

Hydrocarbons, the major constituents in petroleum, have been most actively investigated. Primarily, due to this fact, an extensive collection of hydrocarbon mass spectra is available in various catalogs of mass spectral data (82), and detailed discussions of aliphatic, cyclic, and aromatic hydrocarbons and their type analysis in petroleum fraction can be found in the older literature (77,83–88). For a general survey and leading references to the mechanistic aspects of hydrocarbon mass spectrometry the volume of Budzikiewicz et al. (3) should be consulted.

In the following we shall discuss the data available on the identification of specific hydrocarbons by considering them in various categories roughly corresponding to normal, branched, cyclic, unsaturated, polycyclic and aromatic substances, including among the last also compounds possessing heteroatoms.

1. Normal Alkanes

Normal saturated hydrocarbons appear to occur in all carbonaceous geological environments, as well as being present in a wide variety of biological systems (89). Their mass spectra exhibit a very simple pattern (which has, no doubt, a complex mechanistic genesis) consisting of major peaks at intervals of 14 mass units, with a maximum usually around C_3 or C_4.

The identification of a normal alkane, then, depends essentially upon the correct recognition of the molecular ion. Impurities could, of course, obscure the simple pattern, particularly if they should give rise to intense peaks which might be taken as indications of branching in the chain. Since, however, normals are readily separable from branched alkanes by occlusion in molecular sieves, such problems rarely arise and the interpretation of the mass spectra of isolated compounds is thus a fairly trivial task. Indeed, most often in the published literature normal alkanes have been identified simply on the basis of their regular GLC elution pattern, which permits prediction of the carbon number of a normal alkane with a high degree of certainty.

2. Branched Alkanes

Mass spectrometry represents the best single method for the identification of branched saturated hydrocarbons since, in theory at least, the site of branching (and the size of the substituent at that site) can be deduced from the appearance of intense peaks (relative to their neighbors 14 mass units above and below) corresponding in mass to the fragment including the branching point. This type of structural information is not readily available from other physical methods, unless they involve direct comparison of unknown and standard.

This general statement is well illustrated for simple branched alkanes by the appearance of the spectra of *anteiso*-alkanes (Fig. 5), which show intense peaks resulting from loss of ethyl grouping ($M - 29$), whereas peaks due to ions of C_1 or C_3 fragments are almost completely absent. Similarly, *iso*-alkanes (Fig. 6) show prominent peaks of $M - 15$ and $M - 43$, and 4-methyl alkanes would be expected to exhibit an intense fragment peak at $M - 43$ (Fig. 7).

By analogy, more complex alkanes, as represented, for example, by the isoprenoidal hydrocarbons, should exhibit a series of such intensified peaks corresponding to the number of branching points in the molecule. In structures **1** and **2** the expected peaks for a C_{16} and C_{18} regular isoprenoid are graphically represented, and structure **3** shows the differences resulting from a slight modification of, for example, the C_{16} isoprenoid structure. This straightforward prediction is borne out by the spectra of these compounds, a few representative examples of which are given in Figures 8–10 [the C_{16}, C_{18}, and C_{20} isoprenoidal alkanes (structures **1**, **2** and **3a**, respectively), isolated from various geologic sources].

In theory, then, the mass spectrometric characterization of a relatively complex unknown alkane represents no particular difficulties; in practice, however, such identifications may not be easy. The most obvious and common problem is contamination by another compound, which sometimes may be quite evident because the contaminant exhibits a distinct molecular ion of its own but often may give the illusion of homogeneity when the contaminant is a simple isomer of the major component. If the contaminant contributes several intense peaks to the spectrum, the fragmentation pattern of the unknown may be sufficiently obscured to make definite characterization impossible or, in the worst case, present a totally misleading fragmentation pattern, which with great ingenuity can often be reconciled with a single, but incorrect, structure. The spectrum of Figure 11 illustrates such a case. A C_{18} alkane (MW = 254) isolated from the blue-green alga *Nostoc* (90), appearing homogeneous upon capillary GLC, showed enhanced peaks at *m/e* 113, 127, 155,

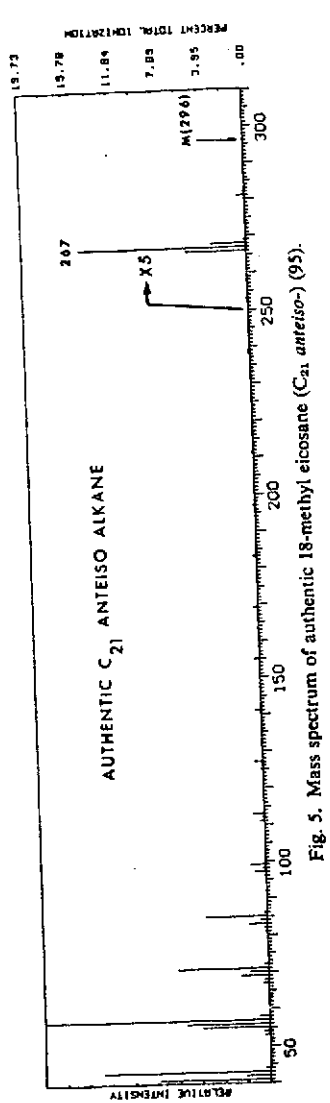

Fig. 5. Mass spectrum of authentic 18-methyl eicosane (C_{21} *anteiso*-) (95).

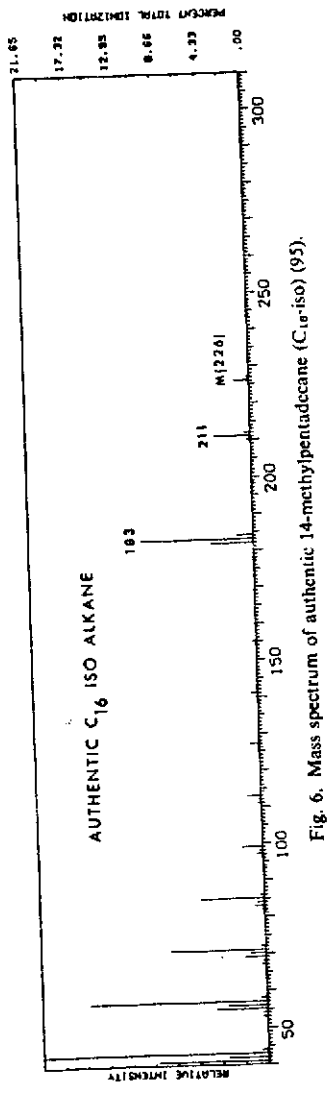

Fig. 6. Mass spectrum of authentic 14-methylpentadecane (C_{16}-iso) (95).

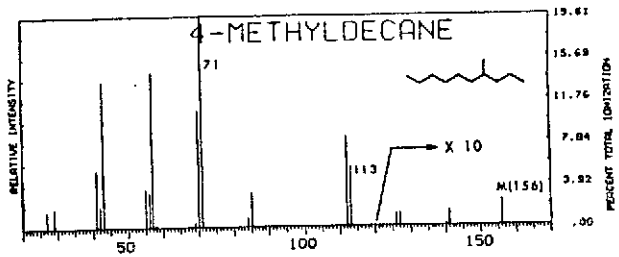

Fig. 7. Mass spectrum of 4-methyldecane.

and 169 in its mass spectrum. As shown in structure **4**, the hypothesis of 7,9-dimethylhexadecane (MW–254) would fit these data quite convincingly.

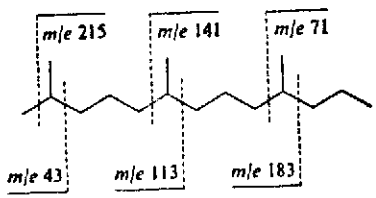

(1) MW = 226

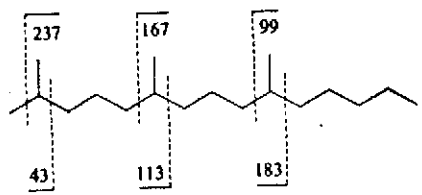

(2)

Synthesis of this compound quickly established that this could not be the structure and subsequently it was demonstrated that the apparently homogeneous substance was a mixture of 7-methyl and 8-methyl heptadecanes (91), which could not be separated by gas–liquid chromatography. Such problems are not too uncommon, since the purity of a hydrocarbon sample isolated from a very complex mixture which might contain many of the theoretically possible structural isomers is always subject to some doubt.

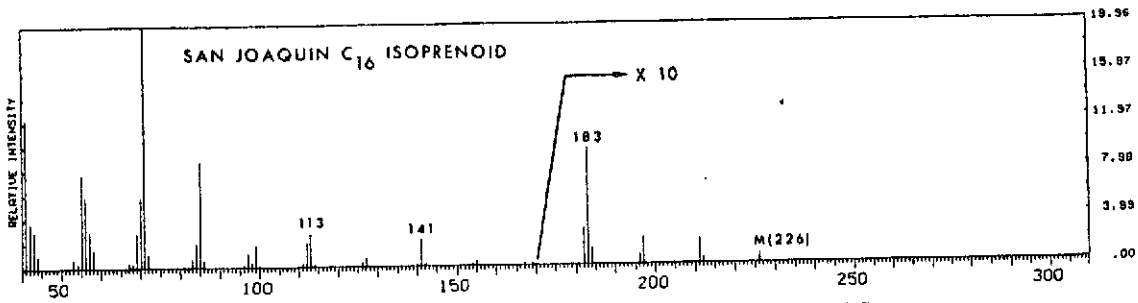

Fig. 8. Mass spectrum of C_{16} isoprenoid alkane (San Joaquin oil) (95).

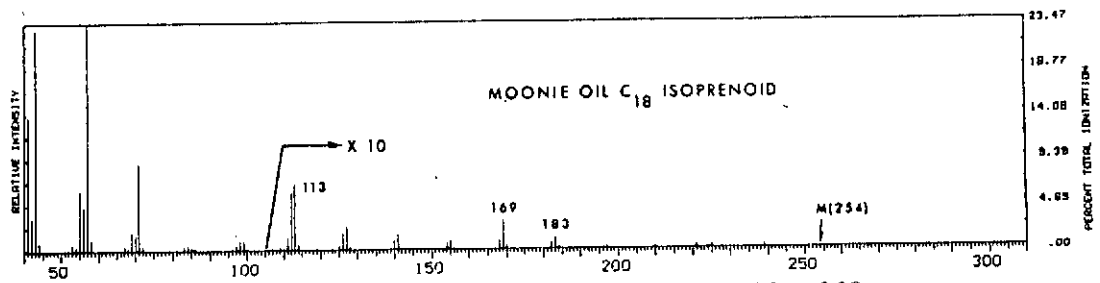

Fig. 9. Mass spectrum of C_{18} isoprenoid alkane (Moonie oil) (after ref. 96).

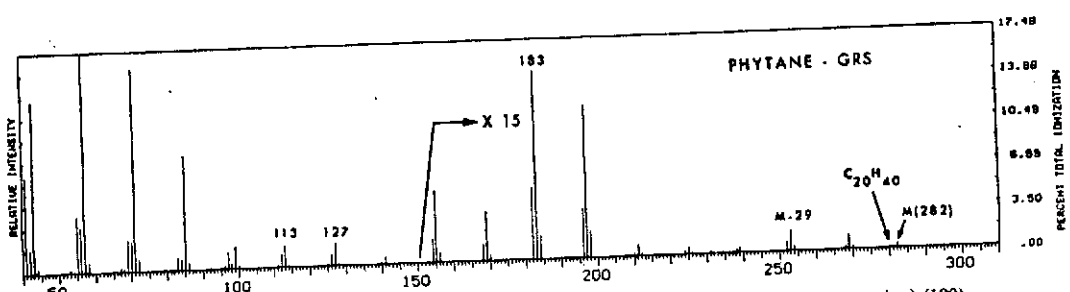

Fig. 10. Mass spectrum of C_{20} isoprenoid alkane, phytane (Colorado Green River Formation) (100).

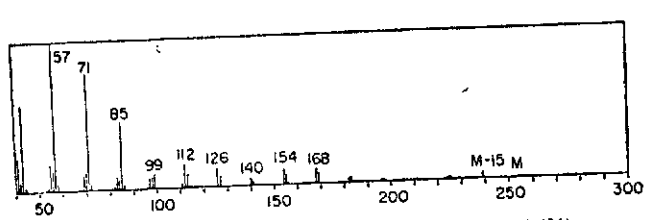

Fig. 11. Mass spectrum of C_{18} branched alkane (*Nostoc*) (91).

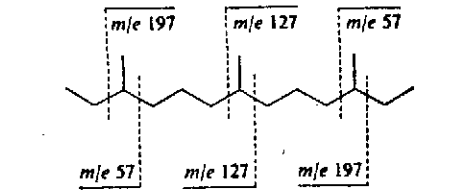

(3) MW = 226

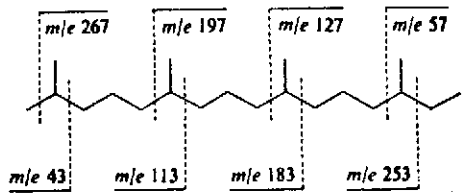

(3a) MW = 282

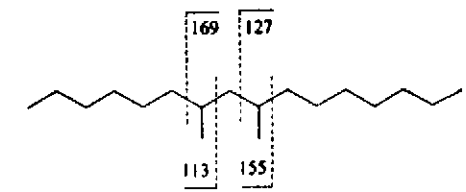

(4)

When the purity of an unknown is assured, identification can be made with reasonable confidence, but there are, unfortunately, still many cases where the mass spectra of structurally quite different alkanes can be distinguished only by relatively subtle differences in their fragmentation pattern. Inspection of the spectra of 2-methyloctane and 2,6-dimethylheptane (Figs. 12 and 13), differing essentially in the intensity of the ion at *m/e* 84, illustrates this point quite forcefully. Similarly, the spectra of 2,6,10-trimethylhexadecane, 2,6,10,13-tetramethylpentadecane, and 2,6,10,14-tetramethylpentadecane (pristane), shown in Figures 14–16 (92), exhibit a fairly uniform fragmentation pattern; the same is true for several C_{21} isoprenoidal isomers (93). In these cases, of course, the nonidentity of the isomers is readily demonstrated by their separation on capillary columns, but comparisons of retention times necessitate the synthesis of each suspected structural variation, a laborious undertaking, to say the least. The ambiguities inherent in mass spectral data are by no

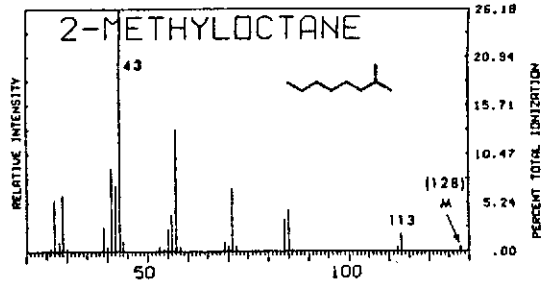

Fig. 12. Mass spectrum of 2-methyloctane (C_9 *iso*-alkane) (82).

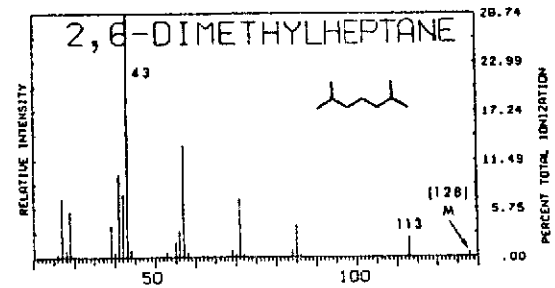

Fig. 13. Mass spectrum of 2,6-dimethylheptane (C_9 isoprenoid) (91).

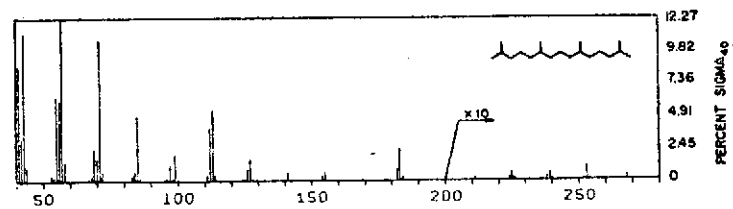

Fig. 14. Mass spectrum of pristane vs. $\%\Sigma_{40}$.

means unique to this particular method, but when mass spectrometry represents the only source of structural information, as it often must, its limitations should be clearly understood.

Henneberg and Schomburg (94) and Han et al. (91) have recently presented an analysis of the fragmentation pattern of branched alkanes which indicates that the ratio of even to odd peaks resulting from cleavages

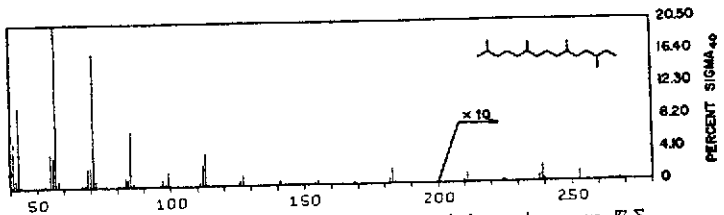

Fig. 15. Mass spectrum of 2,6,10,13-tetramethylpentadecane vs. $\%\Sigma_{40}$.

at branch points depends on the structure of the ion formed. This finding may be of considerable diagnostic value, but only in cases where purity is rigorously established, since these changes in intensity ratios are by no means striking.

Within the last few years mass spectrometry has contributed many data to the characterization of branched alkanes. *Iso*- and *anteiso*-alkanes have been shown to occur in a wide variety of sediments (95,96). The presence of 2-, 3-, 4-, and 5-methylalkanes has been reported in paraffin wax (97,98) on the basis of mass spectra of crude GLC cuts. Detailed mass spectrometric data on isolated, as well as authentic, *iso*- and *anteiso*-alkanes are presented in several papers (95,96,99–101). The fragmentation of these monoalkyl-substituted hydrocarbons is so unambiguous that the interpretation of their mass spectra is hardly subject to doubt.

Numerous reports are concerned with the isolation of isoprenoidal alkanes from sediments or petroleum and their—usually mass spectrometric—structural elucidation. Pristane (C_{19}; 2,6,10,14-tetramethylpentadecane) and phytane (C_{20}; 2,6,10,14-tetramethylhexadecane), the two most important members of this class, were first reported by Bendoraitis et al. (102) and Dean and Whitehead (103), respectively, and have since been isolated from a number of Precambrian sediments, such as the Soudan Formation (95,104), Fig Tree Shale (63), Gunflint Chert (62), and Nonesuch Formation (100,105,106) as well as from many younger sources

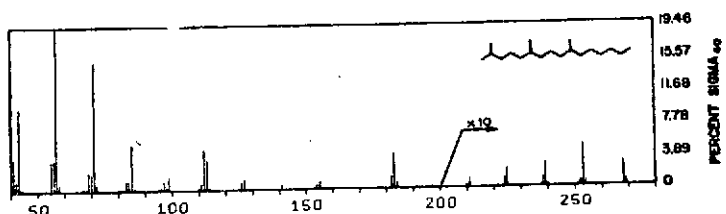

Fig. 16. Mass spectrum of 2,6,10-trimethylhexadecane vs. $\%\Sigma_{40}$.

(64,95,96,100,107,108). However, isoprenoids in the range of C_{14}–C_{18} (with the exception of the C_{17} compound) are also quite common. For example, the series C_{14}, C_{15}, C_{16}, and C_{18} occurs in Texas gas oil (107), the C_{15}, C_{16}, C_{18} hydrocarbons have been reported for the Green River Formation (100,108), and all or some members of this group have been shown to occur in a variety of different sediments and oils (65,95,96,109) The regular (i.e., branching at C-2, C-6, C-10, etc.) C_{21} isoprenoid has been identified in Texas gas oil by Bendoraitis et al. (107) and later Johns et al. (95) reported this compound from such sources as the Soudan Shale, Antrim Shale, and Nonesuch seep oil. Their characterization, based solely on the mass spectra of isolated compounds without comparison with authentic material, was tentative, since the spectra showed varying contributions from other hydrocarbon material. More recently, however, the structure of the C_{21} compound from the Soudan and Nonesuch has been more firmly established as 2,6,10,14-tetramethylheptadecane by comparing GLC retention times and mass spectra with synthetic material (93). The alternative possibility, 2,6,10,15-tetramethylheptadecane, a structure which could be derived by thermal cracking of squalane, was definitely ruled out. As mentioned, however, the mass spectra of these two isomers are rather similar. Göhring et al. (65) have characterized a novel class of isoprenoidal-type compounds, a homologous series of 2,6-dimethylalkanes (from C_8 to C_{14}) isolated from a Cretaceous shale and Nigerian crude oil. In this case, structural assignments appear firmly established, even though the mass spectra of the corresponding authentic hydrocarbons were not available for direct comparison.

A number of perdeuterio hydrocarbons up to C_{14} have been synthesized from carbon monoxide and deuterium gas using an iron meteorite catalyst and have been identified as isoprenoids on the basis of their mass spectra and GLC retention times (60).

A comparison of the chemical ionization and electron bombardment spectra of pristane (110) shows promise that the former technique might be useful for the characterization of branched alkanes. Limited data do not allow an estimation of the usefulness of the chemical ionization technique for structural determinations. For the case of pristane, its major advantage appears to be the greatly enhanced ($M - 1$) ion intensity; its major disadvantage is the large sample dose required (1–2 μl of pure pristane), although the authors suggest that the sensitivity could be improved by three orders of magnitude. Other hydrocarbons have been studied by chemical ionization techniques (111), including a number of branched compounds and squalane, and a comparison of field ionization and chemical ionization mass spectra of ten decane isomers has recently been presented (112).

There exists a report of the occurrence of the C_{17} isoprenane (2,6,10-trimethyltetradecane) (92). Its identification in the Antrim Shale based on coinjection of the authentic compound with hydrocarbon extract and mass spectrometry appears relatively secure, although the published mass spectrum by itself could certainly not be taken as very convincing evidence; the agreement of the spectra of isolated compound and authentic material is somewhat less than excellent, probably due to impurities in the natural product.

Papers by Mair (113), Meinschein (114), Ponnamperuma and Pering (115), and Blumer et al. (116) contain further references to mass spectral applications. Quite extensive mass spectral data on isolated and some authentic isoprenoid hydrocarbons have been presented and discussed in the papers by Eglinton et al. (100), Johns et al. (95), and van Hoeven et al. (96) and in the theses of Haug (117), Maxwell (69), and McCarthy (118).

Identification of larger isoprenoidal hydrocarbons is limited thus far to the report of carotane from the Green River Formation (119) and carotenes from the algal ooze of a Florida lake (90,118).

Only regular isoprenoids have been obtained from geological sources thus far; the frequency of their occurrence and the mass spectral and GLC data documented in the literature make their identification appear relatively certain, even though some of the original mass spectra, because of the presence of impurities, require cautious interpretation.

Isoprenoid alkanes with different substitution patterns (e.g., degradation products of squalane) are conceivable, as well as hydrocarbons which, though nonisoprenoidal, might be derived from more complex biological precursors. The finding (120) of 2-methyl-3-ethylheptane, for which limonene is suggested as precursor, is an illustrative example. The correct identification of the carbon skeleton of these compounds is thus crucial for any speculation concerning their biological precursors (121) and diagenetic history, and, since mass spectrometry does and will continue to play a major role in these efforts, the fairly complete documentation of data on novel compounds would be desirable, a plea not always fulfilled by the published literature.

3. *Cyclic Hydrocarbons*

The mass spectra of cyclic hydrocarbons are not as readily interpretable in structural terms as those of the corresponding acyclic compounds. The information provided by the mass spectrum of an unknown may thus be limited to the exact molecular weight, and perhaps size and number of substituents. Quite frequently, however, the occurrence of intense fragment ions in the spectra of alicyclic compounds may be misleading, and precise

structural deductions should be made with great caution, unless authentic compounds are available for comparison. Studies on the mechanisms of fragmentation of simple cyclic hydrocarbons are reviewed by Budzikiewicz et al. (3), who also provide a listing of the pertinent literature. McFadden and Buttery in a chapter in this volume present data on the application of mass spectrometry to structural studies in the monoterpene field, and a good summary of the mass spectra of lower terpene hydrocarbons is available (5). Meyerson et al. (122) have discussed the mass spectra of cyclohexane and substituted cyclohexanes.

Simple cycloalkyl compounds have been shown to occur in a variety of sediments and oils. Johns et al. (95) and van Hoeven et al. (96) have reported the occurrence of cyclohexyl alkanes of general structure 5 in Nonesuch seep oil (C_{16} to C_{19} compounds) and Moonie oil. In this case, the interpretation seems relatively straightforward, since these spectra show an intense ion at *m/e* 83 which corresponds to the cyclohexyl ion,

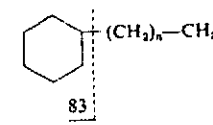

(5)

while the rest of the spectrum is reminiscent of straight-chain alkanes. The question as to whether some of these compounds could not be represented by methylcyclopentyl alkanes, which should show rather similar spectra, has not yet been resolved unambiguously. Cyclohexyl and cyclopentyl alkanes have been reported also as constituents of various petroleum fractions, usually on the basis of compound type analysis (see references 97, 98, and 123). With the aid of a gas chromatograph–mass spectrometer combination, Lindemann and Le Tourneau (124) were able to identify 14 monocyclic and bicyclic hydrocarbons, including several methylbicycloheptanes, bicyclooctanes, and bicylononanes, as well as methyl-substituted cyclohexane and cycloheptane derivatives. Mass and infrared spectra of most of these compounds isolated are presented in their paper. The isolation of carotane from the Green River Formation—a bicyclic isoprenoidal system—has already been mentioned (119).

4. *Steranes and Triterpanes*

Steranes and triterpanes represent some of the most complex compounds isolated from sediments or petroleum to date. The earliest reports were based on the recognition of molecular ions and certain fragment peaks suggestive of sterane-like compounds in the mass spectra of complex

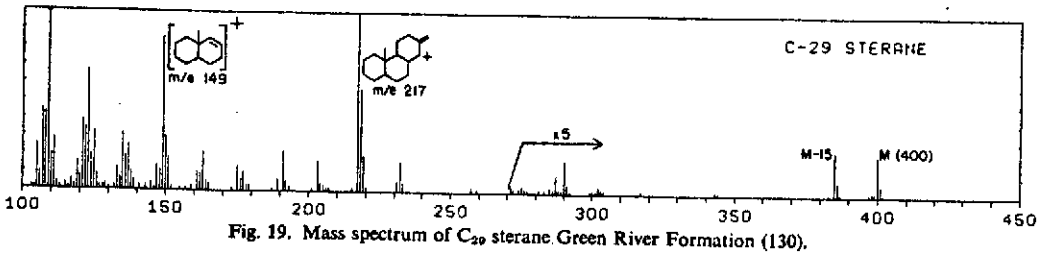

Fig. 19. Mass spectrum of C_{29} sterane Green River Formation (130).

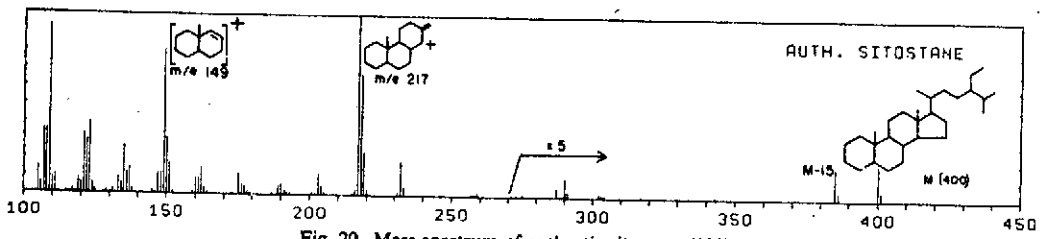

Fig. 20. Mass spectrum of authentic sitostane (130).

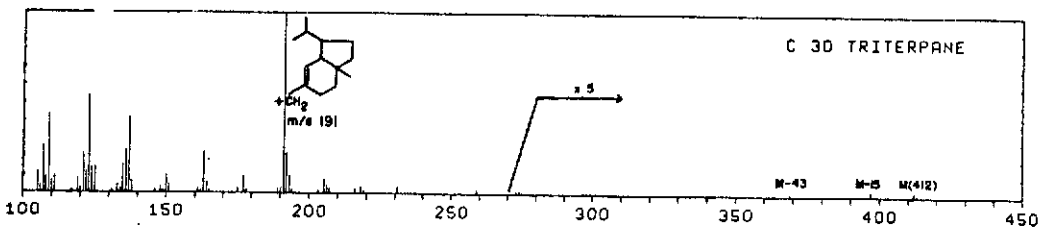

Fig. 21. Mass spectrum of C_{30} triterpane (130).

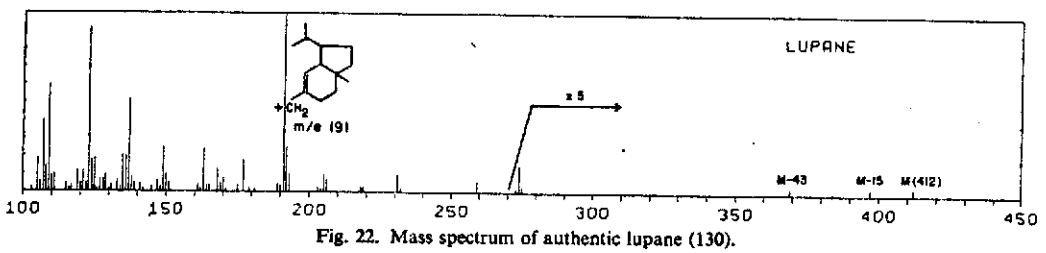

Fig. 22. Mass spectrum of authentic lupane (130).

data consisting of the mass spectrum of moretane (9b) demonstrate that such a skeleton may not be excluded on the basis of mass spectral data alone.* Recently, the capillary gas chromatographic behavior of authentic lupane has been compared with a branched cyclic hydrocarbon extract of a 10-g sample of the Green River Shale (132). These data indicate that the major triterpane is eluted somewhat later than lupane, and the skeleton of hopane (9c) has been suggested, although authentic hopane was apparently not available for confirmation. The peaks at *m/e* 191, 149, and 137 are quite typical for this type of pentacyclic skeleton, although simple positional isomers of the basic ring system (cf. lupane, hopane, moretane) could not be expected to give easily distinguishable fragmentation patterns. Detailed discussions and data bearing on the mass spectrometry of triterpenoid hydrocarbons may be found in the papers of Djerassi and co-workers (5,133,134).

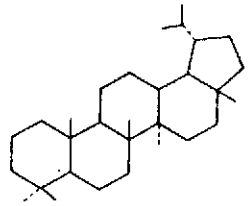

(9a)

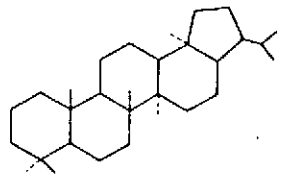

(9b)

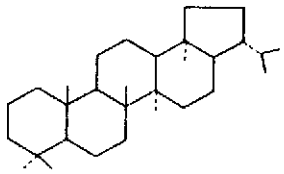

(9c)

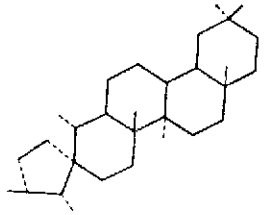

(9d)

Some mass spectrometric evidence for the presence of tetracyclic and pentacyclic hydrocarbons in a Precambrian sediment is illustrated in Figure 23. The data can be interpreted in terms of a mixture of C_{27} (MW = 372), C_{28} (MW = 386), and C_{29} (MW = 400) steranes and C_{30} triterpanes (MW = 412), but since a relatively complex mixture is at hand, these assignments must be considered to be quite tentative.

* Unpublished data from the authors' laboratory on a sample provided by Dr. Richie, University of Sydney, Sydney, Australia.

The identification of gammacerane (135) (10), the isolation of four new, as yet unidentified, triterpanes from Nigerian crude oil (136a) and of three (C_{27}–C_{30}) unknown triterpanes from the Westwood Shale (69), and the demonstration of apparently pentacyclic hydrocarbons of the triterpenoidal-type (peaks at 191 and 205) ranging in mass from 370 (C_{27}) to 454 (C_{33}) (137) represent more recent studies which employed mass spectrometry quite extensively. The tricyclic hydrocarbon fichtelite (11)

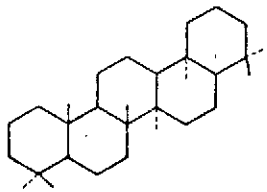

(10)

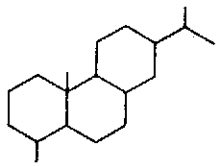

(11)

has been reported recently by Maxwell (69). Fairly extensive mass spectral data on other unidentified triterpenoidal substances have been obtained by Haug (117) and Maxwell (69). Mention should be made also of the identification of 1,2,3,4-tetracyclo-2,2,9-trimethylpicene (138) and cyclopentano- and methylcyclopentanophenanthrene (139) (which, though not sterane hydrocarbons, may represent their degradation products), although mass spectrometry was used only peripherally here.

It is evident from the above discussion that mass spectrometry, although rarely capable of defining a complex structure unambiguously, provides crucial information as to structural type and molecular size and can yield precise information on the gross structure of unknown compounds even when no suitable authentic material is available for comparison. The ability to recognize at least the structural type with relative certainty is of profound importance to geochemical studies, considering the minute quantities of substance usually available, since even such a partial characterization would be a rather tedious enterprise with other techniques and would depend mostly on fortunate speculation. It is to be remembered,

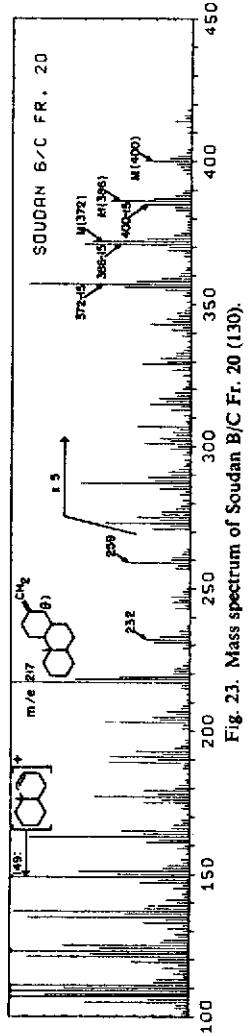

Fig. 23. Mass spectrum of Soudan B/C Fr. 20 (130).

however, that the mass spectrometric information available on authentic compounds is based solely on substances derived from natural products, and whether a substantially modified structure of a triterpenoid and steroid hydrocarbon derived from geologic sources could be recognized from its mass spectrum is then open to some question. High resolution data would be desirable for unknown compounds to exclude the possibility of oxygen substituents (a ketone would, of course, be isomeric with the hydrocarbon with one more methylene unit; see discussion in section on aromatic compounds). Complete identification may, in any event, prove to be a rather difficult and tedious problem, particularly if any of these compounds [consider, for example, the existence of "triterpane E" (9d) (136b) and of C_{27} or C_{31}–C_{33} triterpenoidal hydrocarbons] had undergone substantial structural modification.

5. *Olefins*

Mass spectrometric studies on olefins derived from geological material are not common, although compound type analyses, including determination of olefins in petroleum fractions, have been performed frequently. Field and Hastings (78), Frisque et al. (140), and Mikkelsen et al. (141) describe the methods and problems involved in quantitative analysis of fractions containing olefins.

The gas chromatograph–mass spectrometer combination with the addition of a "microreactor" has been utilized successfully for the analysis of olefinic mixtures and determination of individual compounds (56). The microreactor (installed either before or after the gas chromatograph) reduces olefinic compounds to the respective saturated substances, the structures of which are then characterized by mass spectrometry. The structure (often including stereochemistry) of the original olefin is then deduced from data of different runs (i.e., microreactor before and after the gas chromatograph) and retention values. This approach resulted in the identification of a considerable number of individual olefins from a cracked gasoline olefin–paraffin mixture (56), and of a series of α-olefins ranging from C_{11} to C_{14} (142). Olefins derived directly from sediments have not received much attention thus far except for some reports of olefins in shale oil (143,144).

An analysis of olefins from zooplankton is illustrative of the methodology appropriate for characterization of microgram quantities of individual alkenes. The carbon skeleton of four isomeric phytadienes (**12–15**) isolated by Blumer and Thomas (145) was established by mass spectrometry after hydrogenation to the saturated compounds, and the position of the double bonds was established by infrared spectroscopy and

ozonolysis of the dienes to an acid (for **12**) and aldehydes (from **12**, **14**, and **15**), respectively. Dienes **14** and **15** were found to differ only in double bond geometry. A similar approach was used to deduce the structure of three isomeric alkenes with the pristane carbon skeleton (146).

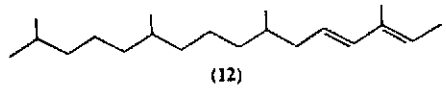

(12)

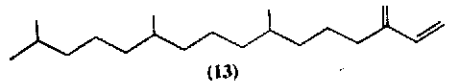

(13)

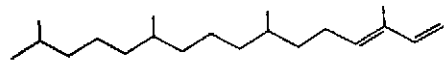

(14) (15)

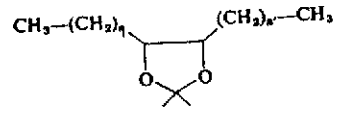

(16)

Complete characterization of olefins by mass spectrometry is usually not possible since double bond isomers tend to give rather similar, if not identical, spectra. Several methods, all involving derivatization of double bonds, have been devised recently for the determination of double bond positions. One of these depends on the characteristic fragmentation of isomeric ketones derived from the olefin by epoxidation and rearrangement (147). Epoxides formed from olefins can be used as such (148). Conversion of an alkene to an amino alcohol is also useful (149), and isopropylidene derivatives (150) such as **16** have been shown to be excellent derivatives for this purpose. Hydroxylation of the double bond and formation of *cis*-methyl ethers (151) or trimethylsilyl ethers (152) are other attractive methods. All methods are based on the fact that appropriate functionalization will yield compounds whose mass spectra display relatively intense peaks which are characteristic of the position of the double bond. The methods work best for one double bond, but methyl ether derivatives appear to give interpretable spectra for polyunsaturated structures, at least as far as carboxylic acid esters are concerned. The isopropylidene procedure seems to permit distinction between geometrical isomers, if both are available for direct comparison. The utility of any of these methods for the analysis of microgram samples or less has yet to be

demonstrated. The ozonolysis experiments of Blumer and Thomas (145,146) would appear to constitute another excellent approach for very small samples, particularly when used in connection with GLC–mass spectrometer instrumentation. Techniques have been described for the routine application of degradation by ozonolysis to microgram quantities of an olefin (153). However, for mixtures of alkenes an interpretation of the results in terms of structures of individual olefins might prove difficult. For geochemical use, a good method should be applicable to the analysis of very small quantities of relatively complex mixtures (olefin–paraffin), yielding suitable volatile derivatives for analysis by GLC–mass spectrometric techniques. Hydroxylation–silylation procedures would appear to have potential in this respect.

6. *Aromatic Compounds*

Aromatic hydrocarbons which, in general, exhibit rather well-defined mass spectra with relatively prominent molecular ion peaks and intense fragment peaks corresponding to the series *m/e* 91, 105, 119, 133, etc. (for alkyl-substituted benzenes; *m/e* 141, 155, etc., for alkylnaphthalenes, for example) have been actively subjected to mass spectrometric investigation. Discussions of results derived mainly from type analysis of petroleum fractions have been presented previously (11,154). O'Neal and Wier (83) have presented data on individual aromatics, a very comprehensive review (155) on the mass spectra of alkylbenzenes is available, and mechanistic problems are treated in some detail by Budzikiewicz et al. (3).

An example of identification of individual aromatic hydrocarbons in petroleum fractions is provided by the work of Mair and co-workers, whose analyses of the mononuclear (156,157), dinuclear (158,159), and trinuclear (139) aromatic fractions of petroleum have led to the characterization of a considerable number of aromatic compounds. Most effort has been devoted, however, to compound-type analyses of aromatic petroleum fractions, a reflection of the interests of petroleum chemists who were concerned with devising fast and reliable analytical methods to determine the overall composition of crude petroleum or distillate fractions rather than with the detailed characterization of isolated components. Low voltage mass spectrometry introduced by Field and Hastings (78) has been used with considerable success in this area (160–163). Since the ionization potential of aromatics is lower than that of aliphatic compounds, the analysis of the former in mixtures of olefins and saturated hydrocarbons becomes possible.

Low voltage techniques using single-focusing mass spectrometers distinguish between a limited number of compound classes. Ambiguities

arise particularly when heteroatomic compounds are present in the mixture, usually necessitating relatively elaborate preseparation. High resolution mass spectrometers, therefore, represent a very significant advance in instrumentation for studies in this area, since the resolving power and mass measurement accuracy of such equipment readily distinguishes between isobaric substances differing in elemental composition.

Carlson and co-workers (79) first applied high resolution mass spectrometry to geochemical investigations. Utilizing an instrument of relatively low resolution by current standards, they were able to achieve the separation of peaks due to saturated hydrocarbons from naphthalene homologs of the same nominal mass (^{12}C vs. H_{12}) and of alkylbenzenes from alkyl benzothiophenes (^{32}S vs. $^{12}C_2H_8$). Alkyl thiophenes could be identified also. Lumpkin (164), who obtained spectra of a trinuclear aromatic petroleum fraction at high and low resolution and high and low electron voltages, was able to distinguish series of acenaphthenothiophenes dibenzofurans, acenaphthenes, dibenzothiophenes, phenanthrenes, fluorenes and carbazoles. Accurate mass determination at a resolution of about 10,000 was accomplished by peak matching. Figure 24 is illustrative of some of Lumpkin's data, showing the effect of low ionizing voltage on the appearance of the mass spectrum. At 8 eV only the molecular ion of carbazole ($C_{14}H_{13}N$) appears at mass 195; as the electron energy is raised, various fragment ions of hydrocarbon, oxygen, and sulfur compounds become important contributors.

Johnson and Aczel (165) have described a technique for recording mixture spectra at a resolution of 10,000 and low ionizing voltages on chart paper from which compositions are calculated by linear distance measurements between peaks of known and unknown masses. The method is reasonably rapid and quite adequate for mixtures of homologous series

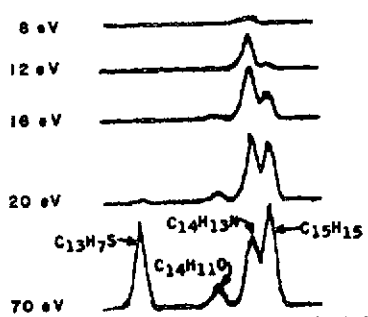

Fig. 24. Low voltage, high resolution mass spectrum of *m/e* 195 (after ref. 164).

of compounds containing N, S, or O as heteroatoms. Mead et al. (166) reported on hydrocarbon and sulfur compound types in petroleum utilizing a similar approach. A study of petroleum waxes, microcrystalline waxes, and ozokerite (167) at high resolution (5000–10,000) discussed the distribution of hydrocarbon-, oxygen-, and sulfur-containing constituents. An interesting finding of this work is the presence of the series $C_nH_{2n}O$ (n = 16–25) and $C_nH_{2n-2}O$ (n = 17–24), which could represent aliphatic and cyclic ketones, respectively.

A group type analysis of petroleum fractions by high resolution mass spectrometry (resolution about 5000) which determines 19 compound types has recently been reported by Gallegos et al. (168). Data from their paper are presented in Figure 25. Field ionization combined with high resolution instruments as reported by Mead and co-workers (169,170) will no doubt develop into another important technique for the analysis of complex mixtures. An analysis (170) for paraffins, (mono-, di-, and tricyclic paraffins), alkylbenzenes, and indane-tetralines gave quantitative data in good agreement with those obtained by more conventional mass spectrometric methods. The simplicity of the calculations makes field ionization an attractive alternative analytical technique, particularly for paraffin–cycloparaffin mixtures.

In these studies, high resolution spectra were either recorded on chart paper, or accurate masses were determined by the peak-matching technique, but in the future digital data acquisition and processing techniques and high resolution mass spectrometers coupled on-line to a fast computer will no doubt be applied routinely. This would then be an extraordinarily rapid method for the detailed analysis of any petroleum fraction. In the authors' laboratory such an on-line mass spectrometer–computer system is currently employed for preliminary analyses of organic fractions obtained from ancient sediments. The example of Figure 26 shows the spectrum of the carboxylic acid-free extract obtained from the demineralized (previously exhaustively extracted) Green River Shale (171). The spectrum was determined in real time (20) at a resolution of 10,000 using 70-eV electron bombarding energy. A detailed analysis is not appropriate here, but particularly noteworthy are several high mass ions. For example, the ion of composition $C_{40}H_{78}$ would correspond to the molecular ion of perhydro-β-carotene. Below that peak several ions, $C_{40}H_{70}$, $C_{40}H_{68}$, $C_{40}H_{66}$, and $C_{40}H_{62}$, might be taken to indicate polycyclic tetraterpenes. Triterpenoid carbon skeletons are indicated by the appearance of ions calculating for $C_{30}H_{52}$, $C_{29}H_{48}$; the intense fragment peak at m/e 191 ($C_{14}H_{23}$) would support this conclusion. Two very interesting oxygen-containing species are apparent from the C/HO plot: compositions of $C_{30}H_{50}O$ and $C_{29}H_{48}O$ are suggestive of terpenoidal ketones.

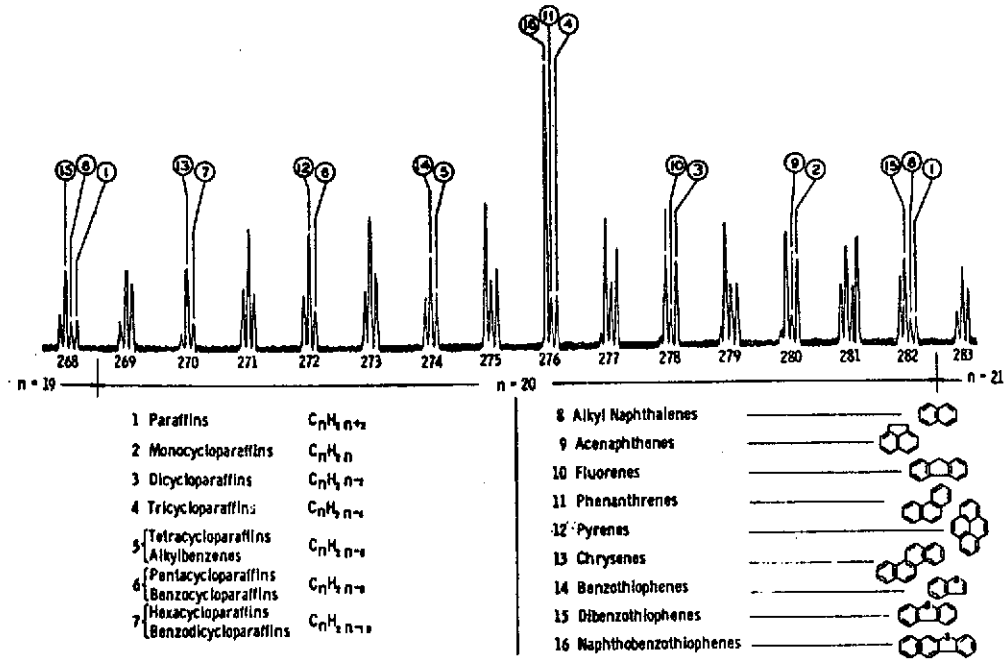

Fig. 25. Segment of a high resolution mass spectrum of the 800–950°F fraction of an Arabian crude oil (after ref. 168).

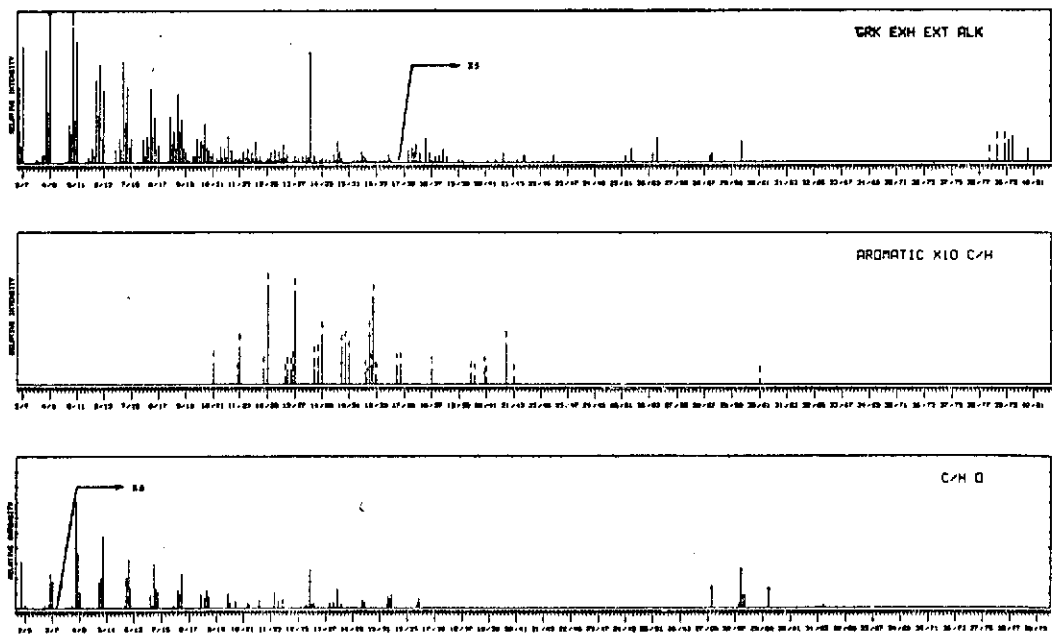

Fig. 26. High resolution mass spectrum of neutral and basic components of Green River Formation exhaustive extract.

The suggestion, if substantiated by the actual isolation of these ketones, is significant because a recent study by Eglinton and co-workers (132) employing a GLC low resolution mass spectrometry study of a similar fraction from the same shale failed to reveal the presence of functionalized components.

Such high resolution analyses of complex mixtures are no substitutes for the rigorous characterization of individual compounds, but they are extremely valuable as preliminary investigations to discover the range and class of compounds present in a mixture. The method can reveal minor, but potentially very interesting, components and provides excellent, although not necessarily unambiguous, initial data for more extensive and detailed investigations.

B. Carboxylic Acids

Studies on the fatty acid content of petroleum and shale oil have been reviewed by several authors (144,172–174). In the early work, mass spectrometry was utilized only infrequently, but in more recent publications, particularly those on the characterization of acidic constituents of shales, it has furnished very important structural data. For normal, branched, and oxyacids, mass spectrometry no doubt represents the single most useful physical method of identification, particularly since extensive mechanistic studies on these classes of carboxylic acids have been undertaken [for leading references, see the review by Ryhage and Stenhagen (175)]. Acids are commonly analyzed as their methyl esters, which exhibit very well-defined fragmentation patterns. For a normal acid methyl ester, for example, the ion at *m/e* 74 (resulting from McLafferty rearrangement of the gamma hydrogen) and the series of even-electron peaks at *m/e* 87, 101, 115, etc. (resulting from cleavage of the alkyl chain, presumably with multiple hydrogen rearrangements) are the dominant ionic species. Structures of more complex acids, such as isoprenoidal acids, are defined by both the possible shift of the peak at *m/e* 74 (if the substance carries an α-substituent) and the enhancement of certain peaks corresponding to cleavages at the site of branching. For norphytanic acid methyl ester (C_{19}), the pattern indicated roughly in **17** would be expected and, as Figure 27 shows, is indeed observed. Mixtures of normal fatty acids (which can be separated from a total acid extract by occlusion in molecular sieves) are most frequently characterized simply on the basis of the GLC elution pattern, and mass spectrometry has been used sparingly for their identification, providing mainly a further check on previous assignments. The isolation of normal acids from marine (176), recent and ancient sediments (177–181) and from shale kerogen (181,182) provides examples of this approach. By contrast, for the identification of isoprenoidal acids,

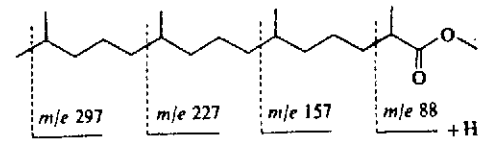

(17) MW = 312

mass spectrometry becomes much more important and, indeed, essential. Cason and Graham (183), using GLC and mass spectrometry, reported the occurrence of the C_{14}, C_{15}, C_{19}, and C_{20} isoprenoid acids in California petroleum; comparison with synthetic samples established the identity of these compounds conclusively. Most other studies on acids relied on mass spectral data more extensively to define the structures of compounds or to advance structural postulates. Eglinton and co-workers (67), employing a gas chromatograph–mass spectrometer combination, identified phytanic (C_{20}) and norphytanic (C_{19}) acids (see Figs. 27 and 28) in Green River extracts (67) and later also the series ranging from C_{14} to C_{17} and the C_{21} acid (68,186). Their reports contain complete mass spectral data on all isoprenoidal acids isolated. Isoprenoidal acids from the same shale have also been reported by Haug et al. (187), and Cason and Khodair (188) identified the C_{11} acid in petroleum. Studies on the kerogen of the Green River Formation (182,189) have revealed the presence of several isoprenoid acids; the mass spectra of the C_{19} and C_{20} acid esters from this work are shown in Figures 27 and 28.

When mass spectrometry supplies the only physical data on the structure of an unknown isoprenoidal acid, some caution should be exercised in the interpretation of the spectra since the enhancement of the peaks due to fragmentation at the site of branching is not very pronounced. Fortunately, the literature contains fairly complete documentation of the spectra of isolated isoprenoidal acids such that comparison with the older data is always possible. This is particularly important should acids with irregular branching be found in geologic materials. In this connection, it should be pointed out that isoacids are difficult to distinguish from normal acids by the mass spectrum alone (101). Isoacids do not appear to be common constituents of the carbonaceous sediments examined thus far. A report of their occurrence in the Green River Formation needs confirmation (190).

Unsaturated acids from Scottish shale oil (68,186) have been partially characterized by mass spectrometry. Distinction between olefinic esters and their cyclic isomers by mass spectrometry presents little difficulty, since the former exhibit rather pronounced $M - 32$ and $M - 74$ peaks, but the position of the double bonds can usually not be specified. The spectra

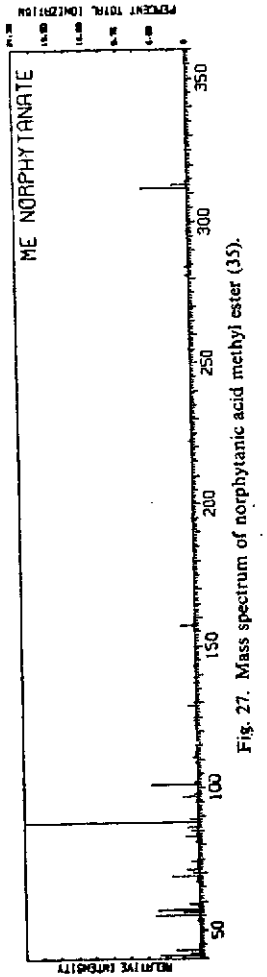

Fig. 27. Mass spectrum of norphytanic acid methyl ester (35).

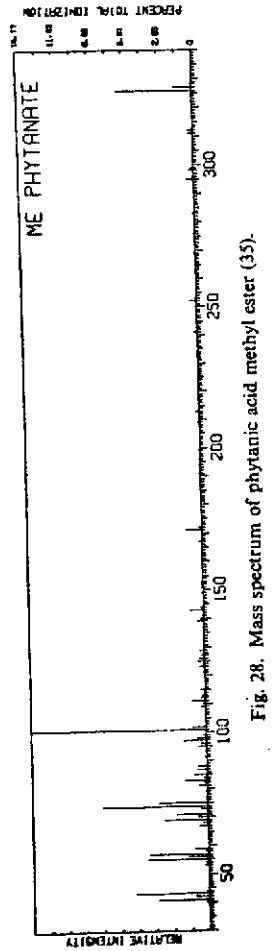

Fig. 28. Mass spectrum of phytanic acid methyl ester (35).

of α,β-unsaturated esters are an exception to this rule since they are readily distinguished from other unsaturated acids (175). Recently, a method has been developed which enables definition of the geometry of the α,β-unsaturated acids in question (191). This involves the esterfication of the α,β-unsaturated acid with a long-chain alcohol, such as hexanol. The fragment due to the diprotonated acid, common to these esters, occurs one mass unit lower in the *cis* isomer than in the *trans* isomer. An attractive feature of the method is that both isomers are not needed to define the stereochemistry of the double bond since the mass spectra of these derivatives are predictably different. For complete characterization of other than α,β-unsaturated acids, however, derivatization of the double bond by the methods described in the section on olefins is a prerequisite. McCloskey et al. (192) have reported on the mass spectra of isopropylidine derivatives of unsaturated esters, and the formation of methoxy derivatives (151) appears to be the best method currently for determining double bond positions of polyunsaturated esters.

Mass spectrometric identification of α,ω-dicarboxylic acid esters isolated from the Green River Formation (187) and from Scottish Torbanite have been reported (186). Based on the work of Ryhage and Stenhagen (175) such identifications appear relatively secure, since the mass spectra of acid esters of this type are distinguished by intense peaks at $M - 31$, $M - 73$ and *m/e* 98 and 74. Two examples, both acids isolated from the Green River Formation (187), illustrate this pattern (Figs. 29 and 30). The spectrum of Figure 29 is that of dimethyl tridecane-1,13-dioate, while that of Figure 30 would suggest an α-methyl substituent, i.e., dimethyl 2-methyltetradecane-1,14-dioate.

Haug, Schnoes, and Burlingame (193) reported the occurrence of methyl ketoacids in Green River Formation extracts and presented fairly conclusive mass spectral data in support of their structural assignments. Figure 31 shows the spectrum of methyl 10-oxoundecanoate. The fragmentation pattern is in excellent agreement with this structure, but the presence of impurities in the sample as well as the rarity of this class of compounds in sediments make further confirmation desirable. High resolution data suggesting an extended series of keto acids in the same formation have been presented recently (171,194) and are discussed in detail below (171).

Hydroxy and fatty acids have not been detected in sediments thus far, but the results of Eglinton et al. (195) on hydroxy acids from apple cutin have bearing on future geochemical investigations of these compounds. The acid esters were converted to trimethylsilyl ether derivatives (cf. structure **18**), which facilitates both their gas chromatographic and mass spectrometric analyses, as shown in Figure 32. The characteristic

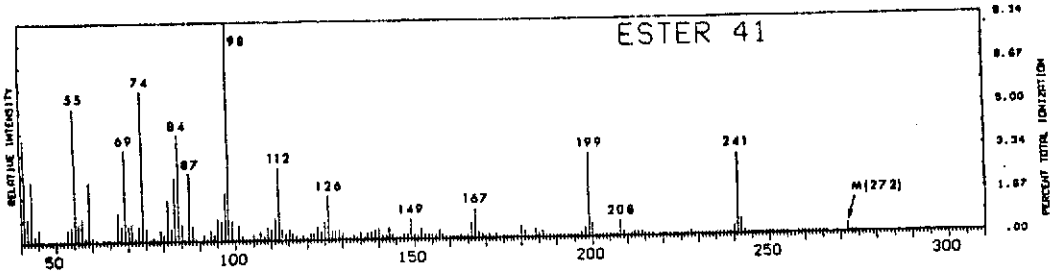

Fig. 29. Mass spectrum of dimethyl tridecane-1,13-dioate (187).

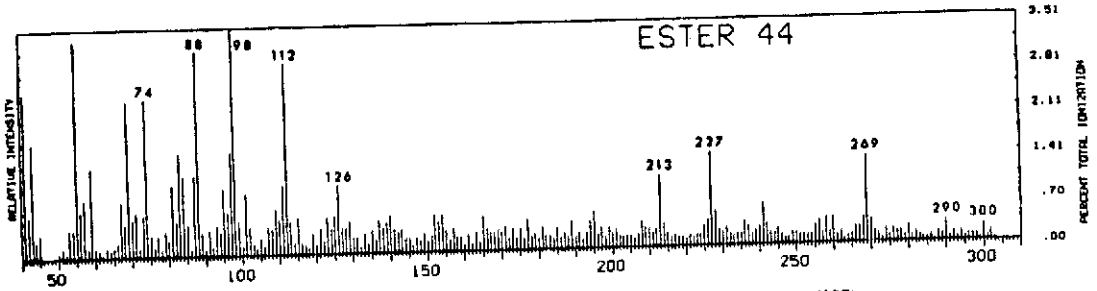

Fig. 30. Mass spectrum of dimethyl 2-methyltetradecane-1,14-dioate (187).

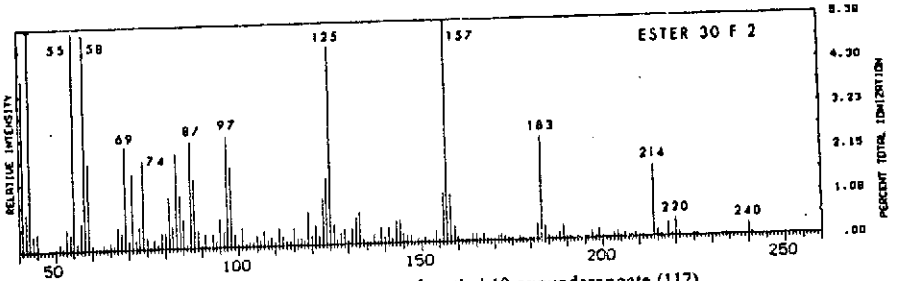

Fig. 31. Mass spectrum of methyl 10-oxoundecanoate (117).

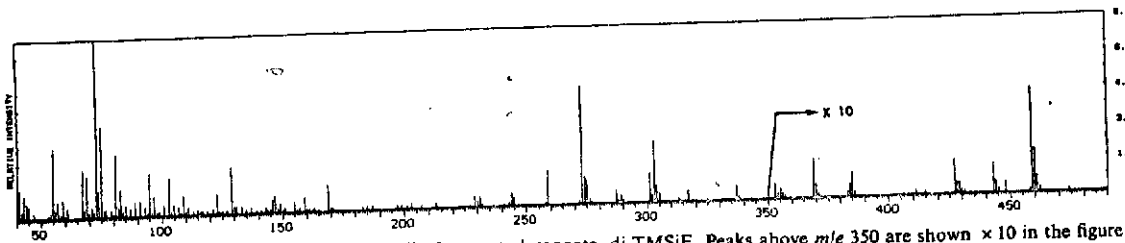

Fig. 32. Mass spectrum of methyl 10,18-dihydroxyoctadecanoate, di-TMSiE. Peaks above *m/e* 350 are shown × 10 in the figure [G. Eglinton, unpublished]

fragmentation of silyl ethers defines the position of the hydroxyl function (see **18** for *m/e* 273 and 303 and peaks in Fig. 32) and probably constitutes

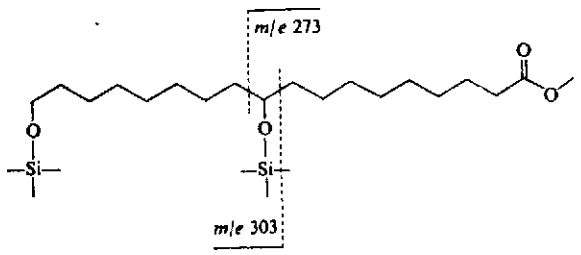

(18)

the best method of analysis for such compounds. The mass spectra of trimethylsilyl compounds exhibit "anomalous" peaks which have been shown to arise by transfer of the TMS grouping (185,196).

Aromatic acids from shales have been reported in one study (197), in which a considerable number of compounds were isolated but few could be rigorously identified, since the substitution pattern on the aromatic nucleus is difficult or impossible to establish from the mass spectrum itself and since relatively few compounds in this class have been subjected to any detailed mass spectrometric analysis (184,198–200).

Some general structural features are often quite apparent, however; for example, the size of the aromatic nucleus (number of substituents) and the length of the acid side chain can be deduced from the mass of fragments arising by benzylic cleavage common to these compounds. The spectra of Figures 33–35 from this work provide some examples. The first is clearly that of a methyl benzoic acid ester, whereby the lack of an appreciable $M - 32$ peak excludes the *ortho* isomer. The spectrum of Figure 34 is nicely accommodated by a structure of type **19**, which, if correct, would be of considerable biogenetic interest, and the spectrum of Figure 35 represents one of the possible isomers of a methyl naphthylcarboxylic acid. Di-, tri-, and tetracarboxylic acids have been obtained by

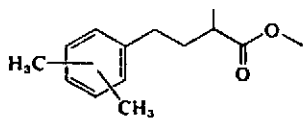

(19)

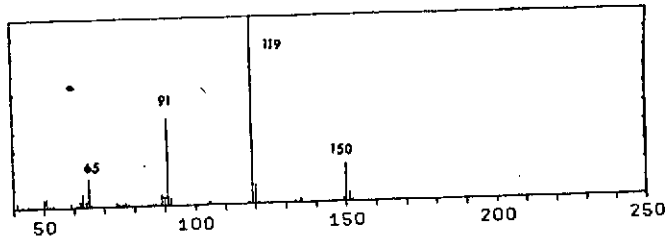

Fig. 33. Mass spectrum of methyl methylbenzoate (197).

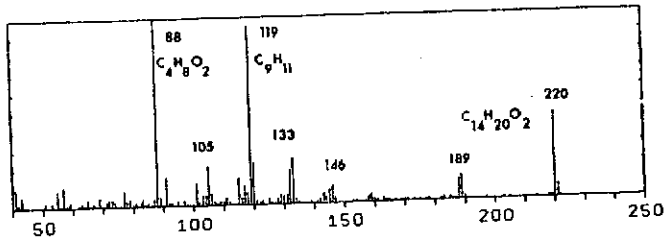

Fig. 34. Mass spectrum of methyl 2-methyl-4-(dimethylphenyl)-propionate (197).

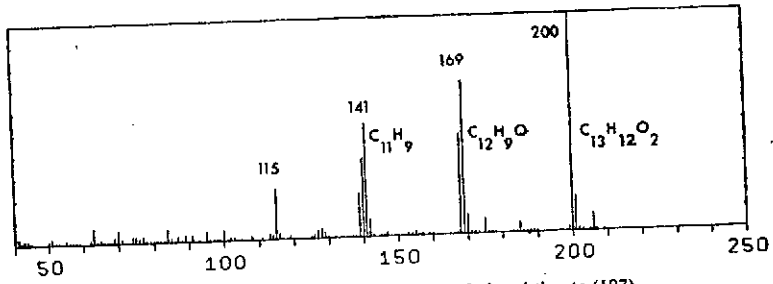

Fig. 35. Mass spectrum of methyl methylnaphthoate (197).

the ozonolysis of coal and some of their mass spectra are documented (46). More extensive collection and interpretation of the mass spectra of authentic compounds quite obviously should be the prelude to further detailed studies of this class of geochemicals, and NMR and infrared data will no doubt be necessary for any really rigorous characterization.

The mass spectra of cyclic acids and their esters are yet more complex, and the information they provide can only be described as ambiguous at this stage. The nature of the ring (cyclopentyl vs. cyclohexyl) and, therefore,

the number and/or size of substituents are not necessarily apparent from the mass spectral pattern. In at least some cases, stereochemistry introduces a further complicating feature, often drastically affecting the intensity of important peaks (201,202). Cason and Khodair (202) have published a discussion of the mass spectra of several cyclopentyl acetic acids and cyclopentenylacetic acids, and Cason's group has utilized mass spectrometry quite extensively for the characterization of monocyclic acids. However, the identification of a C_{11} cyclic acid (20) (203) and of acid **21**

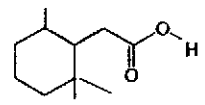

(20)

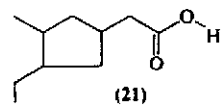

(21)

(201,204) in a California petroleum are examples where definite structural assignments depended on synthesis of presumed carbon skeletons guided by the evidence available from the mass spectra of the methyl esters and amides of the isolated acids. Monocyclic acids ranging in the molecular weight of their methyl esters from 156 (cyclopentylacetic) to 212 (C_{11} monocyclic acid) have been obtained in the authors' laboratory also from the Green River Oil Shale (117). In this case, mass spectrometric analysis allowed only tentative structural assignments for several relatively simple cases. Much more detailed mass spectrometric studies on a variety of cyclic acids are quite obviously needed here, but even at present mass spectrometry can provide invaluable structural leads and serve as a guide to more elaborate approaches (degradation, synthesis) to the determination of the structure of unknowns.

Finally, in this section, we wish to discuss an example taken from work in the authors' laboratory of the role which high resolution mass spectrometry combined with rather quantitative chemical transformations can play in providing precise information about the structural composition of complex mixtures of acids.* This mixture of acids was obtained by extraction of the 24-hr oxidation of Green River Formation kerogen with ether (171). The gas–liquid chromatogram of the methyl esters of this total ether extract is presented in Figure 36. It was known to contain

* W. J. Richter, B. R. Simoneit, D. H. Smith, and A. L. Burlingame, *Anal. Chem.*, 41, 1392 (1969).

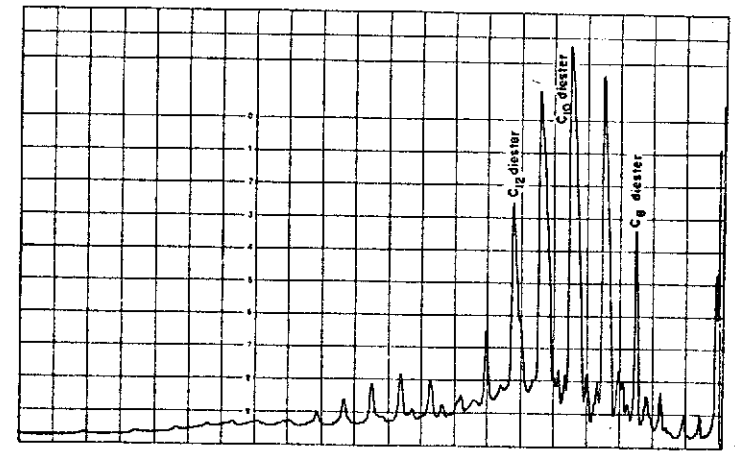

Fig. 36. Gas-liquid chromatogram of the total ether extract esters from the 24-hr. oxidation (Green River Formation).

dicarboxylic acids (C_8–C_{12}) as major components from capillary GLC–MS determinations, in addition to many other minor components. Examination of the high resolution mass spectrum (shown partially in Fig. 37) of this mixture of esters revealed a series (from C_5 to C_{14}) of low abundance ions corresponding to the molecular ions of dicarboxylic acid esters (peaks labeled *b* in C/H O_4 plot of Fig. 37). However, since the major peaks occur in the C/H O_3 plot due to the known loss of methoxyl radical from the molecular ion of the dibasic ester to give intense $C_nH_{2n-3}O_3$ type ions (*b'*), the molecular ions of oxo-carboxylic acid esters (*a*) were somewhat obscured by the ^{13}C isotope peaks of these $C_nH_{2n-3}O_3$ ions, although the peaks are too large to be accounted for solely by isotopes.

The suspected molecular ions, *a*, of the oxo-esters range from C_5 to C_{13}, as may be seen in the C/H O_3 plot of Figure 37. This ester mixture was then reduced with sodium borohydride and treated with silylating reagent to yield a mixture of dibasic esters and hydroxy esters–TMS ethers. The salient high resolution mass spectral data on this mixture are presented in Figure 38. It should be noted that the oxo-ester molecular ions present in Figure 37 (C/H O_3) are now absent in the C/H O_3, while the dibasic ester M—CH_3O· peaks are present. The reduced, silylated oxo-ester components now appear as hydroxyester–TMS ethers in the C/H SiO_3 plot of Figure 38. The fragments containing the TMS ether and ester functions (**22**) now range from C_5 to C_{13}, e.g., n = 1–9 in **22**, labeled *a'* in

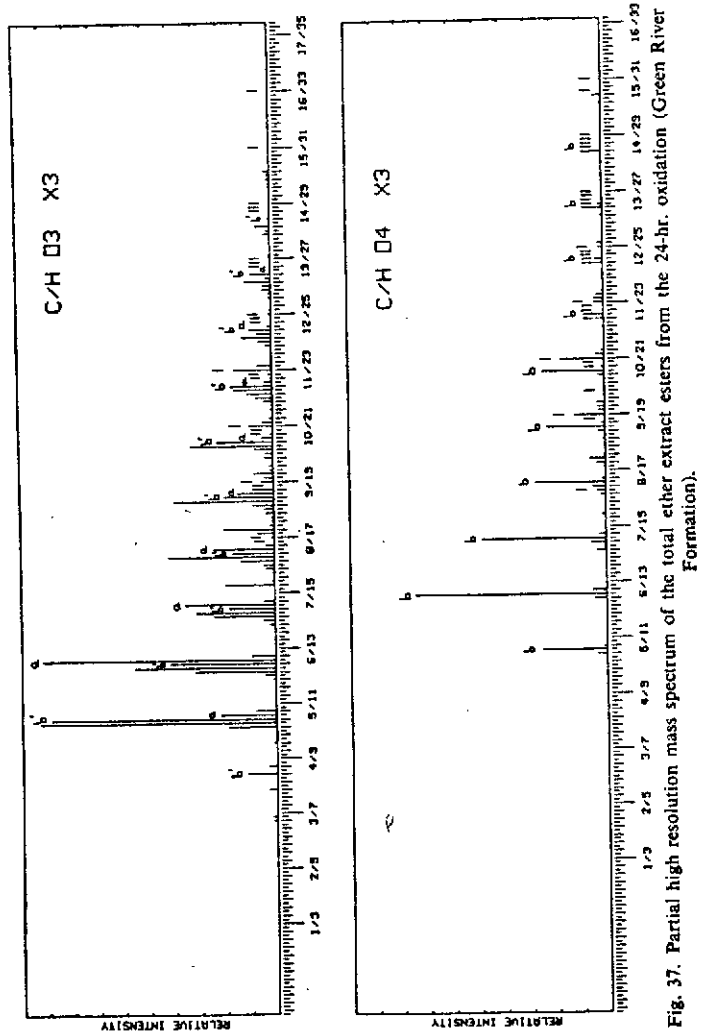

Fig. 37. Partial high resolution mass spectrum of the total ether extract esters from the 24-hr. oxidation (Green River Formation).

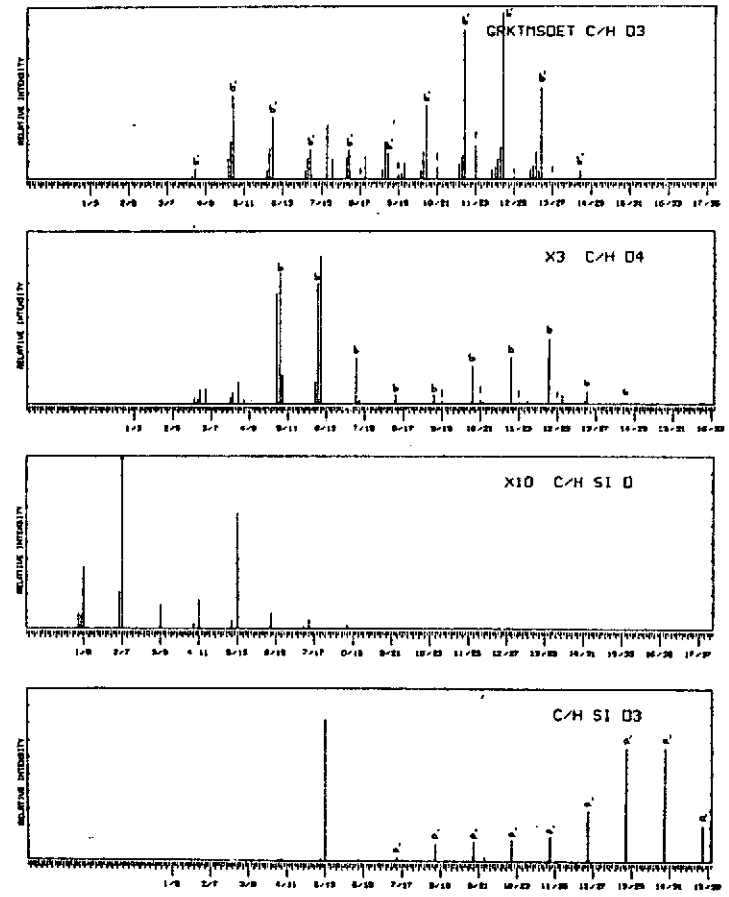

Fig. 38. Partial high resolution mass spectrum of the total ether extract esters after reduction and silylation (Green River Formation).

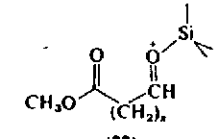

(22)

Figure 38. Examination of the C/H SiO plot in Figure 38 reveals only one peak of structure **23** with $m = 0$, thereby confirming that the original acids are, indeed, ($\omega - 1$)-oxo-carboxylic acids.

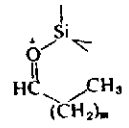

(23)

C. Nitrogen Compounds

Although a considerable number of individual nitrogen compounds have been isolated from petroleum and shale oil, mass spectrometry has been used primarily for compound type analyses rather than for detailed structural work. Several reviews (172,173,205–207) may be consulted for an introduction to the results of analyses on nitrogen compounds in petroleum. Type analyses of mixtures of nitrogen compounds are based on the "z-number concept," that is, a given nitrogen heterocyclic ring system of general composition $C_nH_{2n+z}N$ can be recognized by the value of z (i.e., hydrogen deficiency); for example, the "z-numbers" of alkylpyridines, indoles, or quinolines would be -5, -9, -11, respectively. A given skeleton is usually not, however, unambiguously defined by the z-number alone, since the value need not be unique for a given structural type; for example, both tetrahydroquinolines and cycloalkylpyridines have $z = -7$. Thus, prefractionation of nitrogen compound mixtures is usually a prerequisite for any detailed analytical study. High resolution mass spectrometry, while not distinguishing compositional isomers, would be of considerable advantage since compounds containing different heteroatomic combinations could be distinguished readily. Extensive fractionations of crude mixtures could thus be avoided in many cases.

Numerous compound classes have been shown to occur in oils and petroleum fractions by a combination of mass spectral, ultraviolet, and infrared data. The papers of Sauer and collaborators (208), La Lau (209), Jewell and Hartung (210,211), Snyder and Buell (212), and Dinneen et al. (213) are representative of these investigations. Recently, high resolution mass spectrometry has been utilized (214).

For the routine application of mass spectrometry to structural elucidation of individual compounds much more extensive mass spectral data on the various nitrogen-heterocyclic types would be desirable. Biemann (215) has discussed the fragmentation of several ethylpyridines; the mass spectra of a number of other substituted pyridines have recently been published (216,217). Discussions of quinolines, isoquinolines, and

tetrahydroquinolines have recently become available (218–220), as well as those of oxygenated quinolines (221,222). Two reviews summarize pertinent data on the mass spectra of *N*-heterocyclic compounds (3,223), particularly from the mechanistic viewpoint.

The unambiguous structural definition of aromatic nitrogen compounds, in contrast to aliphatic bases, is usually not possible by mass spectrometry alone, and ultraviolet and infrared spectroscopy, as well as NMR, have been used routinely in detailed investigations. In shale oil naphtha, substituted pyridines and pyrroles have been identified (144,224). Carbazole and alkylcarbazoles (C-1 → C-10) have been reported in Wilmington petroleum (225). Carbazole was purified by gas chromatography and identified from its mass spectrum (MW = 167) and other spectral data. Alkylpyridines, -pyrindines, and -indoles have been isolated and identified in petroleum (226).

Benzonitrile occurs in shale oil naphtha (144), and a number of other nitriles have been identified in hydrogenated furnace oils, such as dicyanobenzene, cyano-2,3-dihydroindene, cyanonaphthalene, dicyanonaphthalene, and dicyano-2,3-dihydroindene. Aliphatic nitriles (C-12 to C-15) have been reported in Colorado shale oil (143). A preliminary report of a very detailed analysis of Wilmington petroleum has been made (227). Nitrogen compounds of the cyclohexylpyridine, pyridine, and quinoline type were isolated by repeated gas chromatographic separation on different columns and were identified on the basis of NMR, ultraviolet, infrared, and mass spectral data. For example, 2-(2′,2′,6′-trimethylcyclohexyl)-4,6-dimethylpyridine and 2,3,7*a*,8,9-pentamethyl-*trans*-cyclopenta-(*f*)-pyrindane are mentioned, but no detailed mass spectral data were presented. The cyclohexylpyridine is a known constituent of petroleum (172,205). There appear to be no reports of bases extracted from shales directly, although a preliminary study utilizing both high and low resolution mass spectrometry of the bases from the Colorado Green River Formation has been undertaken in the authors' laboratory (117). Figure 39 illustrates part of

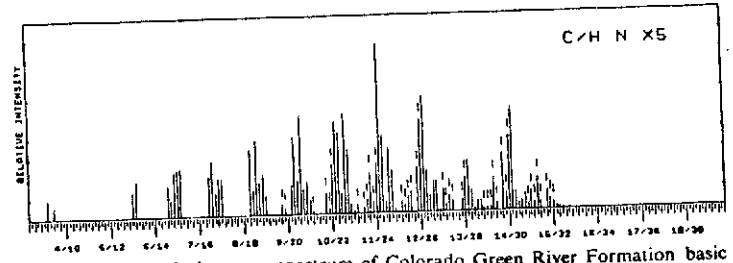

Fig. 39. High resolution mass spectrum of Colorado Green River Formation basic fraction, C/H N.

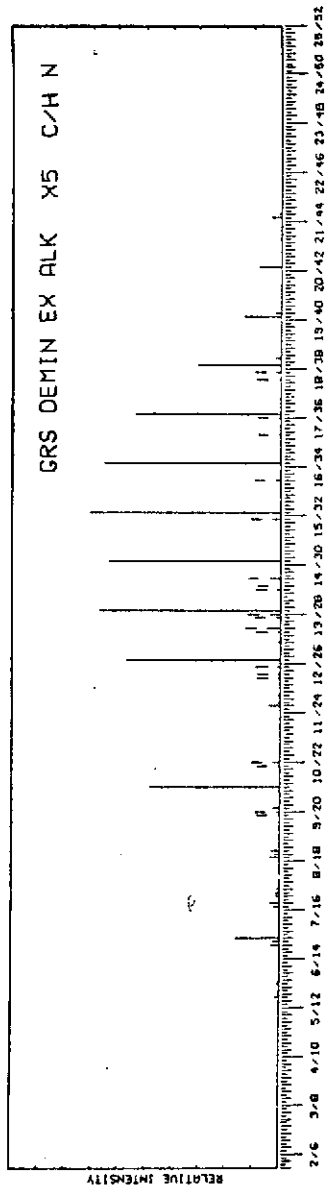

Fig. 40. Partial high resolution mass spectrum of a base extract from demineralized Green River Shale.

this data, a high resolution spectrum of the total bases isolated from a benzene–methanol extract of this oil shale. The spectrum, obtained at 70 eV, contains both molecular and fragment ions, and an interpretation in terms of the molecular species present can only be tentative. Ions of composition C_7H_9N, $C_8H_{11}N$, and $C_9H_{13}N$, for example, would correspond to molecular ions of simple alkylpyridines and the series C_7H_8N, $C_9H_{12}N$, $C_{10}H_{14}N$ would fit for fragment ions of this class of compounds. Alkylquinolines (with alkyl substituents ranging from C_1 to C_6) are indicated by the homologous series $C_{10}H_9N$ to $C_{15}H_{13}N$, whereby the C_3, C_4, and C_6 alkylquinolines appear to be present in greatest abundance. These quinolines appear as major base constituents among the nitrogen compounds in the total extract of this shale after demineralization (Fig. 40). The homologous series extends from the C_4 alkylquinoline ($C_{13}H_{15}N$) to the C_{13} alkylquinoline ($C_{22}H_{33}N$). Other nitrogen compounds are minor contributors, except for the C_3 alkylpyridine ($C_{10}H_{15}N$). A third series of compounds is apparent in Figure 39, commencing with the ion of composition $C_9H_{11}N$ up to $C_{15}H_{23}N$. Alkyltetrahydroquinolines would fit these compositions, but other compound types, e.g., cycloalkylpyridines, are equally possible. For each molecular ion series a corresponding group of peaks at even mass is present which can be ascribed to fragment ions. Alkylpyrroles may be present; the peaks at $C_{15}H_{13}N$ and $C_{14}H_{17}N$ would correspond to the C_{10} and C_9 alkylpyrrole molecular ions, respectively.

D. Porphyrins

Porphyrins represent a special class of nitrogen-containing compounds, considered here as a separate topic. The mass spectrometry of porphyrins and related cyclic tetrapyrroles has presented difficulties which could be overcome only with the availability of direct introduction systems. Since then, the sparse literature on porphyrin mass spectrometry, which included nickel etioporphyrin (228) and vanadyl etioporphyrin (229), has been enriched by a quick succession of fairly detailed papers on mass spectra of porphyrin, chlorin, and related tetrapyrrole compounds (230–237).

The results leave no doubt that mass spectrometry is an excellent tool for the study of fossil porphyrins. The tetrapyrrole system is quite stable and molecular ions are easily recognizable. If the basic ring skeleton can be defined by absorption spectroscopy, then the mass of the molecular ion, its composition, and the elimination of certain fragments allow postulation of at least tentative conclusions concerning the number and type of substituents. Preliminary analyses to determine the molecular weight range of porphyrins (and elemental composition) by high resolution mass spectrometry in a complex mixture are easily carried out and the

distribution of porphyrins in different geologic environments can be quickly and routinely determined. Not surprisingly, then, mass spectrometry has assumed increasing importance in recent work on geoporphyrins. For example, a pigment mixture isolated from the Serpiano Oil Shale (238) was analyzed by absorption spectroscopy and mass spectrometry. Homologous series of porphyrins of the etio- and deoxyphylloerythro ring skeleton were indicated. Chlorins could also be recognized, although these tended to degrade partially to the corresponding porphyrin skeleton. Two series of vanadium complexes were identified—a homologous etio group, exhibiting a molecular weight range from 436 to 492, and a deoxyphylloerythro group with molecular ions ranging from 438 to 504. The mass spectra of another fraction indicated two series of compounds, one comprising the homologs of molecular weight from 430 to 500, the other those from 456 to 498. These data could be rationalized by the assumption of trivinyletioporphyrins, but chromatographic data and ultraviolet spectra were consistent with hydroxyetioporphyrins; the vinyl groupings could then be explained by the elimination of water in the mass spectrometer inlet systems. Later work on the Serpiano Oil Shale pigments (239) using Sephadex columns for fractionation indicated high molecular weight constituents (up to 20,000). Porphyrin fractions of molecular weight up to 700 were obtained also; their mass spectra indicated alkyl substitution on the ring system including from 7 to 23 methylene units.

Porphyrin constituents of the Green River Formation, its shale oil, and of Wilmington Crude Oil have been compared (240). The ultraviolet spectra of the oil shale porphyrins indicated structures of the phyllo type; the mass spectra showed two series; one, homologs of etioporphyrin, the other, homologs of etioporphyrin with one additional degree of unsaturation; their molecular weights ranged from 420 to 534 for one series and from 422 to 536 for the other. The shale oil porphyrins were generally of lower molecular weight (ranging from 366 to 522 as the indium monochloride complexes formed by introduction of the sample through an indium valve) and belonged to the etio spectral type. The petroleum porphyrins showed the phyllo-type absorption spectrum and a series of molecular ions from 438 to 550. For the shale and petroleum porphyrins, tetrapyrrole nuclei substituted by alkyl and carbalkoxy groupings are suggested. The porphyrin distribution in petroleums has been studied using low-voltage mass spectrometry (241), and more recently high resolution mass spectrometry was employed for an extensive investigation into the porphyrin constituents of about ten petroleums, as well as of gilsonite, the Athabasca tar sands, and the Colorado Green River Formation Oil Shale (242). Two major and one minor series of petroporphyrins were detected: a series of alkyl etioporphyrins, whose visible spectra

suggested either incomplete substitution or bridge substituents, and a monocycloalkano series, whose visible spectra suggested the deoxyphylloerythroporphyrin skeleton. For the minor series, homologs of alkylbenzoporphyrin (**24**) are suggested from the available mass spectral and absorption data.

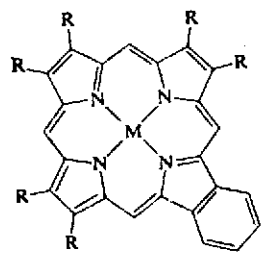

(24)

The complexity of porphyrin mixtures has thus far prevented the isolation of individual components. Gas chromatography would be an excellent method for the isolation of pure fossil porphyrins in microgram amounts if sufficiently volatile derivatives of the porphyrins could be prepared. Recently, Boylan and Calvin (243) reported the preparation of relatively volatile silicon complexes of etioporphyrin, a potentially very useful approach to the detailed study of geoporphyrins. Mass spectral data and retention times of silicon porphyrins of type **25** are listed in their preliminary study. It is not yet clear from available data whether this method will be suitable for complex mixtures of geoporphyrins, since the preparation of the silicon complexes requires relatively severe reaction conditions; however, the approach appears worthy of continued study and refinement.

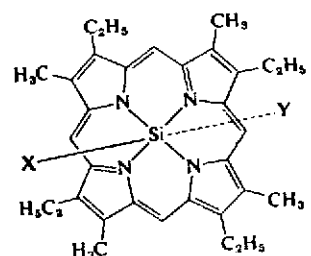

(25)

E. Sulfur-Containing and Other Compounds

Sulfur-containing compounds of petroleum have been quite actively investigated, since the properties of a particular crude oil or distillate fraction depend to some extent on the nature and concentration of these compounds. Information on the sulfur compound types in petroleum has been reviewed (174); summaries of thiols and sulfides in petroleum (173) and of sulfur compounds in shale oil naphtha have been presented (144). Mass spectrometry has been utilized quite extensively in this area, and the literature contains extensive tabulation and discussion of the mass spectra of different compound classes. This subject, particularly the mechanistic aspects of sulfur compound mass spectrometry, is well summarized in the work of Budzikiewicz, Djerassi, and Williams (3). Thiols, sulfides, disulfides, sulfones, and thiophenes are some of the important classes considered by them. Extensive tabulations of mass spectra of thiols and sulfides (244,245), disulfides (245), and thiophenes (245–252) may be consulted for some of the original data. Compound type analyses for both aromatics and sulfur compound types have been described (253) which distinguish nine aromatic hydrocarbon classes as well as benzothiophenes, dibenzothiophenes, and naphthobenzothiophenes. An application (254) of this method showed that condensed thiophenes and their homologs were major constituents of the sulfur compounds in Wasson petroleum. Mass spectrometric data, bearing either on compound type analysis or on identification of individual components have been presented in a number of investigations (123,255,256). The identification of a series of thiophenes in shale oil, including mass spectrometric results on isolated and authentic compounds, has been reported (144).

More recently, high resolution mass spectrometry has been utilized for the determination of sulfur-containing compounds in mixtures with hydrocarbon material. The early work of Carlson et al. (79) as well as more recent contributions by Reid (167), Drushel and Sommers (257), Mead et al. (166), Lumpkin (164), and Gallegos et al. (168), are representative of this work. An example of such a group type analysis (168) at high resolution which determines benzothiophenes, dibenzothiophenes, and naphthobenzothiophenes has been presented in an earlier section.

Oxygen-containing heterocyclic compounds—for example, benzofuran and related structural types—have been detected in petroleum (79,164,211, 224). A recent investigation utilizing high resolution mass spectrometry reported quantitative data on benzofuran, dibenzofuranes, and benzonaphthofuranes (214). Alkyl-substituted fluorenones (C-1 to C-4) have been identified in Wilmington Petroleum (258) by ultraviolet spectroscopy and the mass spectrum of a mixture exhibiting peaks at *m/e* 194, 208, 222, 236. The partial identification of an alicyclic ketone, as acetyl-isopropylmethylcyclopentane, based on mass spectral and NMR data has been reported (259). Camphor and borneol (!) have been identified in a 2-billion-year old sediment for Greenland (260). Comparison of the mass spectra of isolated and authentic samples leaves no doubt about the correctness of identification. Phenyl alkyl ketones have been detected in petroleum by high resolution group type analysis (214). Phenols have been identified in shale oil (144), and a recent group type analysis gives a quantitative estimate of their occurrence in petroleum (214). As this summary shows, very few compounds, other than those of the hydrocarbon, acid, nitrogen- and sulfur-containing classes, have been identified. Since, however, some of these substances may be of great biological and diagnostic interest, they will undoubtedly receive more prominent attention in the future.

References

1. (a) J. H. Beynon, *Mass Spectrometry and Its Application to Organic Chemistry*, Elsevier, Amsterdam, 1960; (b) J. H. Beynon, R. A. Saunders, and A. E. Williams, *Mass Spectrometry of Organic Molecules*, Elsevier, Amsterdam, 1968.
2. K. Biemann, *Mass Spectrometry: Organic Chemical Applications*, McGraw-Hill, New York, 1962.
3. H. Budzikiewicz, C. Djerassi, and D. H. Williams, *Mass Spectrometry of Organic Compounds*, Holden-Day, San Francisco, 1967.
4. H. Budzikiewicz, C. Djerassi, and D. H. Williams, *Structural Elucidation of Natural Products by Mass Spectrometry*, Vol. 1, *Alkaloids*, Holden-Day, San Francisco, 1964.
5. H. Budzikiewicz, C. Djerassi, and D. H. Williams, *Structural Elucidation of Natural Products by Mass Spectrometry*, Vol. 2, *Steroids, Terpenoids and Sugars*, Holden-Day, San Francisco, 1964.
6. G. Spiteller, *Massenspektrometrische Strukturanalyse organischer Verbindungen*, Verlag Chemie, Weinheim, 1966.
7. F. W. McLafferty, Ed., *Mass Spectrometry of Organic Ions*, Academic Press, New York, 1963.
8. See also the series, *Advances in Mass Spectrometry*, (a) J. D. Waldron, Ed., Vol. 1, Pergamon Press, London, 1959; (b) R. M. Elliott, Ed., Vol. 2, Macmillan New York, 1963; (c) W. L. Mead, Ed., Vol. 3, The Institute of Petroleum, London, 1966; (d) E. Kendrick, Ed., Vol. 4, The Institute of Petroleum, London, 1968.
9. (a) F. W. McLafferty and J. Pinzelik, *Index and Bibliography of Mass Spectrometry 1963–1965*, Wiley, New York, 1967; (b) J. Capellen, H. J. Svec, and C. R. Sage, *Bibliography of Mass Spectroscopy Literature, Compiled by Computer Method*, U.S.A.E.C., Div. Tech. Information, March 1966, No. IS-1335; (c) J. Capellen, H. J. Svec, and C. R. Sage, *ibid.*, July 1967 No. IS-1611.
10. H. Kienitz, *The Mass Spectra of Organic Molecules*, Elsevier, Amsterdam, 1968.

10a. T. C. Hoering, in *Researches in Geochemistry*, Vol. 2, P. H. Abelson, Ed., Wiley, New York, 1967, pp. 87–111.

11. A. Hood, "The Molecular Structure of Petroleum," in F. W. McLafferty, Ed., *Mass Spectrometry of Organic Ions*, Academic Press, New York, 1963, Chap. 12.
12. U. Colombo and G. D. Hobson, Eds., *Advan. Org. Geochem.*, Macmillan, New York, 1964; G. D. Hobson and M. C. Louis, Eds., *Advances in Organic Geochemistry 1964*, Pergamon Press, London, 1966; G. D. Hobson and G. C. Spears, Eds., *Advances in Organic Geochemistry 1966*, Pergamon Press, London, 1969.
13. G. Eglinton and M. T. J. Murphy, Eds., *Organic Geochemistry: Methods and Results*, Springer-Verlag, New York, in press.
14. H. Ewald and H. Hintenberger, *Methoden und Anwendungen der Massenspektroskopie*, Verlag Chemie, Weinheim, 1953.
15. C. A. McDowell, Ed., *Mass Spectrometry*, McGraw-Hill, New York, 1963.
16. R. W. Kiser, *Introduction to Mass Spectrometry and Its Applications*, Prentice-Hall, Englewood Cliffs, N. J., 1965.
17. C. Brunnée and H. Voshage, *Massenspektrometrie*, Verlag Karl Thiemig KG, Munich, 1964.
18. (a) A. L. Burlingame, *Advan. Mass Spectrometry*, 3, 701 (1966); (b) J. A. McCloskey, Ph.D. Thesis, Massachusetts Institute of Technology, Cambridge, Mass., 1963; (c) W. F. Haddon, E. M. Chait, and F. W. McLafferty, *Anal. Chem.*, 38, 1968 (1966); (d) G. A. Junk and H. J. Svec, *ibid.*, 37, 1629 (1965); (e) G. L. Kearns, *ibid.*, 36, 1402 (1964); (f) C. Brunnée, *Z. Anal. Chem.*, 217, 333 (1966).
19. A. L. Burlingame, D. H. Smith, and R. W. Olsen, *Anal. Chem.*, 40, 13 (1968).
20. A. L. Burlingame, *Advan. Mass Spectrometry*, 4, 15 (1968); see also A. L. Burlingame: paper presented at International Chromato-Mass Spectrometry Symposium, Moscow, May 21–28, 1968.
21. (a) R. Hites and K. Biemann, *Anal. Chem.*, 39, 965 (1967); (b) R. Hites and K. Biemann, *Advan. Mass Spectrometry*, 4, 37 (1968); (c) R. Hites and K. Biemann, *Anal. Chem.*, 40, 1217 (1968).
22. W. M. Brubaker, *Advan. Mass Spectrometry*, 4, 293 (1968).
23. A. Cassuto, in *Mass Spectrometry*, R. I. Reed, Ed., Academic Press, New York, 1965, p. 283.
24. J. H. Beynon, *Mass Spectrometry and Its Applications to Organic Chemistry*, Elsevier, Amsterdam, 1960, pp. 428–431.
25. G. Remberg, E. Remberg, M. Spiteller-Friedmann, and G. Spiteller, *Org. Mass Spectrometry*, 1, 87 (1968) and earlier papers of this series.
26. (a) H. D. Beckey, in *Mass Spectrometry*, R. I. Reed, Ed., Academic Press, London, 1965, p. 93; (b) H. D. Beckey, H. Knöppel, G. Metzinger, and P. Schulze, *Advan. Mass Spectrometry*, 3, 35 (1966); (c) A. J. B. Robertson, and B. W. Viney, *Advan. Mass Spectrometry*, 3, 23 (1966).
27. (a) M. S. B. Munson and F. H. Field, *J. Am. Chem. Soc.*, 88, 2621 (1966) and subsequent papers; (b) F. H. Field, *Advan. Mass Spectrometry*, 4, 645 (1968).
28. F. H. Field, *Accounts Chem. Res.*, 1, 42 (1968).
29. (a) H. D. Beckey, U.S. Pat. No. 3,313,934 (1967); (b) P. Schulze, B. R. Simoneit, and A. L. Burlingame, *J. Mass Spectrometry Ion Phys.*, 1, 183 (1969); (c) E. M. Chait, T. W. Shannon, J. W. Amy, and F. W. McLafferty, *Anal. Chem.*, 40, 835 (1968).
30. H. D. Beckey and H. Hey, *Org. Mass Spectrometry*, 1, 47 (1968).

31. V. H. Dibeler, in *Mass Spectrometry*, C. A. McDowell, Ed., McGraw-Hill, New York, 1963, p. 334.
32. K. Biemann, *Mass Spectrometry: Organic Chemical Applications*, McGraw-Hill, New York, 1962, pp. 28–30.
33. E. Schumacher and R. Taubenest, *Helv. Chim. Acta*, 49, 1439 (1966).
34. J. W. Amy, E. M. Chait, W. E. Baitenger, and F. W. McLafferty, *Anal. Chem.*, 37, 1265 (1965).
35. A. L. Burlingame and H. K. Schnoes, in *Organic Geochemistry: Methods and Results*, G. Eglinton and M. T. J. Murphy, Eds., Springer-Verlag, New York, 1969, pp. 89–149.
36. K. Biemann, P. Bommer, and D. M. Desiderio, *Tetrahedron Letters*, 1964 [26], 1725.
37. A. L. Burlingame and D. H. Smith, *Tetrahedron*, 24, 5749 (1968).
38. D. H. Smith, R. W. Olsen, and A. L. Burlingame, Annual Conference on Mass Spectrometry and Allied Topics, 16th, Pittsburgh, Pa., May 13–17, 1968, p. 101.
39. A. L. Burlingame, D. H. Smith, R. W. Olsen, and T. O. Merren, Annual Conference on Mass Spectrometry and Allied Topics, 16th, Pittsburgh, Pa., May 13-17, 1968, p. 109.
40. R. Ryhage, *Anal. Chem.*, 36, 759 (1964).
41. J. T. Watson and K. Biemann, *Anal. Chem.*, 36, 1135 (1964).
42. E. D. Engelhardt, private communication, January 1967.
43. P. Llewellyn and D. Littlejohn, Conference on Analytical Chemistry and Applied Spectroscopy, Pittsburgh, February 1966.
44. S. R. Lipsky, C. G. Harworth, and W. J. McMurray, *Anal. Chem.*, 38, 1585 (1966).
45. M. A. Grayson and J. C. Wolf, *Anal. Chem.*, 39, 1438 (1967).
46. W. D. MacLeod and B. Nagy, *Anal. Chem.*, 40, 841 (1968).
47. F. A. J. M. Leemans and J. A. McCloskey, *J. Am. Oil Chem. Soc.*, 44, 11 (1967).
48. J. C. Holmes and F. A. Morrell, *Appl. Spectry.*, 11, 86 (1957).
49. (a) W. H. McFadden, *Separation Sci.*, 1, 723 (1966); (b) W. H. McFadden, *Advan. Chromatog.*, 4, 265 (1967).
50. F. E. Saalfeld, Naval Research Laboratory Report No. 6525, 1967.
51. International Chromato-Mass Spectrometry Symposium, Moscow, May 21–28, 1968.
52. D. Henneberg, *Z. Anal. Chem.*, 229, 355 (1967).
53. R. P. W. Scott, I. A. Fowles, D. Welti, and T. Wilkins, *Gas Chromatography, 1966*, A. B. Littlewood, Ed., The Institute of Petroleum, London, 1967, p. 318.
54. R. M. Elliott and W. J. Richardson, *Ann. Conf. Mass Spectr. and Allied Topics, 15th*, Denver, Colorado, May 14–19, 1967, p. 351.
55. L. P. Lindemann and J. L. Annis, *Anal. Chem.*, 32, 1742 (1960).
56. L. P. Lindemann, *Abstracts*, Am. Chem. Soc., Div. Petrol. Chem., Atlantic City, N.J., 7 [3] 15 (1962).
57. J. A. Dorsey, R. N. Hunt, and M. J. O'Neal, *Anal. Chem.*, 35, 511 (1963).
58. M. H. Studier, R. Hayatsu, and E. Anders, *Science*, 149, 1455 (1965).
59. M. H. Studier, and R. Hayatsu, *Anal. Chem.*, 40, 1011 (1968).
60. M. H. Studier R. Hayatsu, and E. Anders, *Geochim. Cosmochim. Acta*, 32, 151 (1968).
61. R. Hayatsu and M. H. Studier, *Geochim. Cosmochim. Acta*, 32, 175 (1968).

61a. W. K. Seifert, *Intern. Congr. Surface Active Substances, 4th, 1964*, 1, 471–485 (1967); *Tenside*, 2, 150, 182, 216 (1965).

62. J. Oró, D. W. Nooner, A. Zlatkis, S. A. Wikstrom, and E. S. Barghoorn, *Science*, **148**, 77 (1965).
63. J. Oró and D. W. Nooner, *Nature*, **213**, 1082 (1967).
64. V. E. Modzeleski, W. D. McLeod, Jr., and B. Nagy, *Anal. Chem.*, **40**, 987 (1968).
65. K. E. H. Göhring, P. A. Schenck, and E. D. Englehardt, *Nature*, **215**, 503 (1967).
66. P. A. Schenck and C. H. Hall, *Anal. Chim. Acta*, **38**, 65 (1967).
67. G. Eglinton, A. G. Douglas, J. R. Maxwell, J. N. Ramsay, and S. Ställberg-Stenhagen, *Science*, **153**, 1133 (1966).
68. J. N. Ramsay, M.S. Thesis, University of Glasgow, Scotland (1966).
69. J. R. Maxwell, Ph.D. Thesis, University of Glasgow, Scotland (1967).
70. M. C. Bitz and B. Nagy, *Anal. Chem.*, **39**, 1310 (1967).
71. (a) J. Oró, E. Gelpi, and D. W. Nooner, *J. Brit. Interplanet. Soc.*, **21**, 83 (1968); (b) R. J. Olson, J. Oró, and A. Zlatkis, *Geochim. Cosmochim. Acta*, **31**, 1935 (1967).
72. D. Henneberg, *Anal. Chem.*, **38**, 495 (1966).
73. J. T. Watson and K. Biemann, *Anal. Chem.*, **37**, 844 (1965).
74. J. T. Watson, Ph.D. Thesis, Massachusetts Institute of Technology, Cambridge, Massachusetts (June 1965).
75. J. M. Hayes, Ph.D. Thesis, Massachusetts Institute of Technology, Cambridge, Mass. (1966).
76. J. Hayes and K. Biemann, *Geochim. Cosmochim. Acta.*, **32**, 239 (1968).
77. R. A. Brown, *Anal. Chem.*, **23**, 430 (1951).
78. E. H. Field and S. H. Hastings, *Anal. Chem.*, **28**, 1248 (1956).
79. E. G. Carlson, G. T. Paulissen, R. H. Hunt, and M. J. O'Neal, Jr., *Anal. Chem.*, **32**, 1489 (1960).
80. R. I. Reed, *Application of Mass Spectrometry to Organic Chemistry*, Academic Press, New York, 1966, p. 128.
81. ASTM Manual of Hydrocarbon Analysis, American Society for Testing and Materials Special Tech. Publ. 332A, 2nd ed., Philadelphia, 1968.
82. *Catalog of Mass Spectral Data*, American Petroleum Institute, Research Project 44, Carnegie Institute of Technology, Pittsburgh, Pa.
83. M. J. O'Neal, Jr., and T. P. Wier, Jr., *Anal. Chem.*, **23**, 830 (1951).
84. R. J. Clerc, A. Hood, and M. J. O'Neal, Jr., *Anal. Chem.*, **27**, 868 (1955).
85. H. E. Lumpkin, B. W. Thomas, and A. Elliott, *Anal. Chem.*, **24**, 1389 (1952).
86. R. A. Brown, R. C. Taylor, F. W. Melpolder, and W. S. Young, *Anal. Chem.*, **20**, 5 (1948).
87. R. A. Friedel, A. F. Logar, Jr., and J. L. Staultz, *Appl. Spectry.*, **6**, 24 (1952).
88. H. E. Lumpkin, *Anal. Chem.*, **28**, 1946 (1956).
89. R. C. Clark, Jr., Woods Hole Oceanographic Institution, Woods Hole, Mass., Ref. No. 66-34, July 1966.
90. J. Han, E. D. McCarthy, W. van Hoeven, M. Calvin, and W. H. Bradley, *Proc. Natl. Acad. Sci. U.S.*, **57**, 29 (1968).
91. J. Han, E. D. McCarthy, and M. Calvin, *Anal. Chem.*, **40**, 1475 (1968).
92. E. D. McCarthy and M. Calvin, *Tetrahedron*, **23**, 2609 (1967).
93. E. D. McCarthy, W. van Hoeven, and M. Calvin, *Tetrahedron Letters*, **1967** [45], 4437.
94. D. Henneberg and G. Schomburg, *Advan. Mass Spectrometry*, **4**, 333 (1968).

95. R. B. Johns, T. Belsky, E. D. McCarthy, A. L. Burlingame, P. Haug, H. K. Schnoes, W. J. Richter, and M. Calvin, *Geochim. Cosmochim. Acta*, 30, 1191 (1966).
96. W. van Hoeven, P. Haug, A. L. Burlingame, and M. Calvin, *Nature*, **211**, 1361 (1966).
97. E. J. Levy, E. J. Galbraith, and F. W. Melpolder, *Advan. Mass Spectrometry*, **2**, 395 (1963).
98. E. J. Levy, R. R. Doyle, R. A. Brown, and F. W. Melpolder, *Anal. Chem.*, 33, 698 (1961).
99. J. D. Mold, R. K. Stevens, R. E. Means, and J. M. Ruth, *Biochemistry*, **2**, 605 (1963).
100. G. Eglinton, P. M. Scott, T. Belsky, A. L. Burlingame, W. J. Richter, and M. Calvin, *Advan. Org. Geochem. 1964*, Pergamon Press, London, 1966, p. 41.
101. T. G. Tornabene, E. Gelpi, and J. Oró, *J. Bacteriol.*, **94**, 333 (1967).
102. J. G. Bendoraitis, B. L. Brown, and L. S. Hepner, *Anal. Chem.*, **34**, 49 (1962).
103. R. A. Dean and E. V. Whitehead, *Tetrahedron Letters*, **1961**, [21], 768.
104. T. Belsky, R. B. Johns, E. D. McCarthy, A. L. Burlingame, W. J. Richter, and M. Calvin, *Nature*, 206, 446 (1965).
105. G. Eglinton, P. M. Scott, T. Belsky, A. L. Burlingame, W. J. Richter, and M. Calvin, *Science*, **145**, 263 (1964).
106. W. G. Meinschein, E. S. Barghoorn, and J. W. Schopf, *Science*, **145**, 262 (1964).
107. J. G. Bendoraitis, B. L. Brown, and L. S. Hepner, *World Petroleum Congr., 5th*, New York, 1963, Sect. V-15.
108. J. J. Cummins and W. E. Robinson, *J. Chem. Eng. Data*, **9**, 304 (1964).
109. B. J. Mair, N. C. Drouskop, and T. J. Mayer, *J. Chem. Eng. Data*, **7**, 420 (1962).
110. E. Gelpi and J. Oró, *Anal. Chem.*, **39**, 388 (1967).
111. F. H. Field, M. S. B. Munson, and D. A. Becker, *Advan. Chem.*, **58**, 167 (1966).
112. H. D. Beckey, *J. Am. Chem. Soc.*, **88**, 5333 (1966).
113. B. J. Mair, *Geochim. Cosmochim. Acta*, **28**, 1303 (1964).
114. W. G. Meinschein, *Science*, **145**, 262 (1964).
115. C. Ponnamperuma and K. L. Pering, *Nature*, **209**, 979 (1966).
116. M. Blumer, M. M. Mullin, and D. W. Thomas, *Science*, **140**, 974 (1963).
117. P. A. Haug, Ph.D. Thesis, University of California, Berkeley, Calif., (1967).
118. E. D. McCarthy, Ph.D. Thesis, University of California, Berkeley, Calif. (1967).
119. M. T. J. Murphy, A. McCormick, and G. Eglinton, *Science*, **157**, 1040 (1967).
120. B. J. Mair, Z. Rouen, E. J. Eisenbrown, and A. G. Harodysky, *Science*, **154**, 1339 (1966).
121. E. D. McCarthy and M. Calvin, *Nature*, **216**, 642 (1967).
122. S. Meyerson, T. D. Nevitt, and P. N. Rylander, *Advan. Mass Spectrometry*, **2**, 313 (1963).
123. B. Nagy and G. C. Gagnon, *Geochim. Cosmochim. Acta*, **23**, 155 (1961).
124. L. P. Lindemann and R. L. Tourneau, paper presented at World Petroleum Congr., 6th, Frankfurt, Germany, June 19–26, 1963.
125. M. J. O'Neal and A. Hood, *Am. Chem. Soc., Symp. Polycyclic Hydrocarbons*, Div. Petrol. Chem., **1965**, 127.
126. D. O. Schissler, D. P. Stevenson, R. J. Moore, G. J. O'Donnell, and R. E. Thorpe, Ann. Conf. on Mass Spectrometry and Allied Topics, 5th, New York, 1957.

127. W. G. Meinschein, *Bull. Am. Assoc. Petrol. Geologists*, **43**, 925 (1959).
128. W. G. Meinschein, *Geochim. Cosmochim. Acta*, **22**, 58 (1961).
129. E. G. Carlson, M. L. Andre, and M. J. O'Neal, *Advan. Mass Spectrometry*, **2**, 377 (1963).
130. A. L. Burlingame, P. Haug, T. Belsky, and M. Calvin, *Proc. Natl. Acad. Sci. U.S.*, **54**, 1406 (1966).
131. C. Djerassi, *Advan. Mass Spectrometry*, **4**, 199 (1968).
132. W. Henderson, V. Wollrabe, and G. Eglinton, *Chem. Commun.*, **1968**, 710.
133. H. Budzikiewicz, J. M. Wilson, and C. Djerassi, *J. Am. Chem. Soc.*, **85**, 3688 (1963).
134. J. Karliner and C. Djerassi, *J. Org. Chem.*, **31**, 1945 (1966).
135. I. R. Hills, E. V. Whitehead, D. E. Anders, J. J. Cummins, and W. E. Robinson, *Chem. Commun.*, **1966**, 752.
136. (a) J. R. Hills and E. V. Whitehead, *Nature*, **209**, 977 (1966). (b). I. R. Hills, G. W. Smith, and E. V. Whitehead, *Nature*, **219**, 243 (1968).
137. N. Danieli, E. Gil-Av, and M. Louis, *Nature*, **217**, 730 (1968).
138. W. Carruthers and D. A. M. Watkin, *J. Chem. Soc.*, **1964**, 724; W. Carruthers and D. A. M. Watkin, *Chem. Ind. (London)*, **1963**, 1433.
139. B. J. Mair and J. L. Martinez-Pico, *Proc. Am. Petrol. Inst.*, **45**, 173 (1962).
140. A. J. Frisque, H. M. Grubb, C. H. Ehrhardt, and R. W. van der Haar. *Anal. Chem.*, **33**, 389 (1961).
141. L. Mikkelsen, R. L. Hopkins, and D. Y. Yee, *Anal. Chem.*, **30**, 317 (1958).
142. R. M. Teeter, C. F. Spencer, J. W. Green, and L. H. Smithson, *J. Am. Oil Chem. Soc.*, **43**, 82 (1966).
143. T. Iida, E. Yoshii, and E. Kitatsuji, *Anal. Chem.*, **38**, 1224 (1966).
144. G. U. Dinneen, R. A. Van Meter, J. R. Smith, C. W. Bailey, G. L. Cook, C. S. Allbright, and J. S. Ball, *Bur. Mines Bull.*, **593**, (1961).
145. M. Blumer and D. W. Thomas, *Science*, **147**, 1148 (1965).
146. M. Blumer and D. W. Thomas, *Science*, **148**, 370 (1965).
147. G. W. Kenner and E. Stenhagen, *Acta Chem. Scand.*, **18**, 155 (1964).
148. R. T. Aplin and L. Coles, *Chem. Commun.*, **1967**, 858.
149. H. Audier, S. Bory, M. Fetizon, P. Longevialle, and R. Toubiana, *Bull. Soc. Chim. France*, **1964**, 3034.
150. R. E. Wolff, G. Wolff, and J. A. McCloskey, *Tetrahedron*, **22**, 3093 (1966).
151. W. G. Nichaus and R. Ryhage, *Tetrahedron Letters*, **1967**, [49], 5021.
152. G. Eglinton, D. H. Hunneman, and A. McCormick, *Org. Mass Spectrometry*, **1**, 593 (1968).
153. M. Beroza and B. A. Bierl, *Anal. Chem.*, **39**, 1131 (1967).
154. R. A. Dean and E. V. Whitehead, World Petroleum Congress, 6th, Frankfurt, Germany, 1963, Section V, Paper 9.
155. H. M. Grubb and S. Meyerson, in *Mass Spectrometry of Organic Ions*, F. W. McLafferty, Ed., Academic Press, New York, 1963, p. 453.
156. B. J. Mair and J. M. Barnewall, *J. Chem. Eng. Data*, **9**, 282 (1964).
157. B. J. Mair, *J. Chem. Eng. Data*, **12**, 126 (1967).
158. B. J. Mair and T. J. Mayer, *Anal. Chem.*, **36**, 351 (1964).
159. F. F. Yew, and B. J. Mair, *Anal. Chem.*, **38**, 231 (1966).
160. H. E. Lumpkin and T. Aczel, *Anal. Chem.*, **30**, 321 (1958).
161. H. E. Lumpkin and T. Aczel, *Anal. Chem.*, **36**, 181 (1964).
162. R. J. Gordon, R. J. Moore, and C. E. Muller, *Anal. Chem.*, **30**, 1221 (1958).
163. G. F. Crable, G. L. Kearns, and M. S. Norris, *Anal. Chem.*, **32**, 13 (1960).

164. H. E. Lumpkin, *Anal. Chem.*, **36**, 2399 (1964).
165. B. H. Johnson and T. Aczel, *Anal. Chem.*, **39**, 682 (1967).
166. W. K. Mead, W. L. Mead, and K. M. Bowen, *Advan. Mass Spectrometry*, **3**, 731 (1966).
167. W. K. Reid, *Anal. Chem.*, **38**, 445 (1966).
168. E. J. Gallegos, J. W. Green, L. P. Lindeman, R. L. LeTourneau, and R. M. Teeter, *Anal. Chem.*, **39**, 1833 (1967).
169. W. L. Mead and W. K. Reid, International Mass Spectrometry Conference, Berlin, Sept. 25–29, 1967.
170. W. L. Mead, *Anal. Chem.*, **40**, 743 (1968).
171. A. L. Burlingame, P. A. Haug, H. K. Schnoes, and B. R. Simoneit, in *Advances in Organic Geochemistry 1968*; I. Havenaar and P. A. Schenck, Eds., Pergamon-Vieweg, Braunschweig, 1969, p. 85.
172. (a) H. L. Lochte and E. R. Littman, *The Petroleum Acids and Bases*, Chemical Publishing Company, New York, 1955. (b) H. Prinzler, *Naphthensäuren*, VEB Deutscher Verlag für Grundstaffindustrie, Leipzig, 1963.
173. J. S. Ball, W. F. Haines, and R. V. Helm, World Petroleum Congress, 5th New York, 1959, Sect. V-14.
174. G. Costantinides and G. Arich, in *Fundamental Aspects of Petroleum Geochemistry*, B. Nagy and U. Colombo, Eds., Elsevier, Amsterdam, 1967, p. 109.
175. R. Ryhage and E. Stenhagen, in *Mass Spectrometry of Organic Ions*, F. W. McLafferty, Ed., Academic Press, New York, 1963, Chap. 9.
176. J. E. Cooper and E. E. Bray, *Geochim. Cosmochim. Acta*, **27**, 1113 (1963).
177. J. E. Cooper, *Nature*, **193**, 744 (1962).
178. K. A. Kvenvolden, *Nature*, **209**, 573 (1966).
179. P. H. Abelson and P. L. Parker, *Carnegie Inst. Wash. Yearbook*, **61**, 181 (1961).
180. D. L. Lawlor and W. E. Robinson, paper presented at the Detroit Meeting, American Chemical Society, Division Petroleum Chemistry, May 9, 1965.
181. T. C. Hoering and P. H. Abelson, *Carnegie Inst. Wash. Yearbook*, **64**, 218 (1965).
182. A. L. Burlingame and B. R. Simoneit, *Science*, **160**, 531 (1968).
183. J. Cason and D. W. Graham, *Tetrahedron*, **21**, 471 (1965).
184. S. Meyerson and L. C. Leitch, *J. Am. Chem. Soc.* **88**, 56 (1966).
185. G. H. Draffan, R. N. Stillwell, and J. A. McCloskey, *Org. Mass Spectrometry*, **1**, 669 (1968).
186. A. G. Douglas, K. Douraghi-Zadeh, G. Eglinton, J. R. Maxwell, and J. N. Ramsay, *Advances in Organic Geochemistry 1966*, G. D. Hobson and G. C. Spears, Eds., Pergamon, London, in press.
187. P. Haug, H. K. Schnoes, and A. L. Burlingame, *Science*, **158**, 772 (1967).
188. J. Cason and A. I. A. Khodair, *J. Org. Chem.*, **32**, 3430 (1967).
189. A. L. Burlingame and B. R. Simoneit, *Nature*, **218**, 252 (1968).
190. P. L. Parker and R. F. Leo, *Science*, **152**, 649 (1966).
191. W. J. Richter and A. L. Burlingame, paper presented at International Conference on Mass Spectroscopy, Kyoto, September 8–12, 1969.
192. J. A. McCloskey and M. J. McClelland, *J. Am. Chem. Soc.*, **87**, 5090 (1965).
193. P. Haug, H. K. Schnoes, and A. L. Burlingame, *Chem. Commun.*, **1967**, 1130.
194. A. L. Burlingame and B. R. Simoneit, *Nature*, **222**, 741 (1969).
195. G. Eglinton and D. H. Hunneman, *Phytochemistry*, **7**, 313 (1968).
196. W. J. Richter and A. L. Burlingame, *Chem. Commun.*, **1968**, 1158.

197. P. Haug, H. K. Schnoes, and A. L. Burlingame, *Geochim. Cosmochim. Acta*, **32**, 358 (1968).
198. F. W. McLafferty and R. S. Gohlke, *Anal. Chem.*, **31**, 2076 (1959).
199. T. Aczel and H. E. Lumpkin, *Anal. Chem.*, **34**, 33 (1962).
200. R. D. Grigsby, M. C. Hamming, E. J. Eisenbraun, D. V. Hertzler, and N. Bradley, Abstracts, Ann. Conf. on Mass Spectrometry and Allied Topics, 14th, Dallas, Tex., May 22–27, 1966, p. 574.
201. A. I. A. Khodair, Ph.D. Thesis, University of California, Berkeley (1965).
202. J. Cason and A. I. A. Khodair, *J. Org. Chem.*, **32**, 575 (1967).
203. J. Cason and K. L. Liauw, *J. Org. Chem.*, **30**, 1763 (1965).
204. J. Cason and A. I. A. Khodair, *J. Org. Chem.*, **31**, 3618 (1966).
205. H. L. Lochte, *Ind. Eng. Chem.*, **44**, 2597 (1952).
206. V. A. Deal, F. T. Weiss, and T. T. White, *Anal. Chem.*, **25**, 426 (1953).
207. L. R. Snyder and B. E. Buell, *J. Chem. Eng. Data*, **11**, 545 (1966).
208. R. W. Sauer, F. W. Melpolder, and R. A. Brown, *Ind. Eng. Chem.*, **44**, 2606 (1952).
209. C. LaLau, *Anal. Chim. Acta*, **22**, 239 (1960).
210. D. M. Jewell and G. K. Hartung, *J. Chem. Eng. Data*, **9**, 297 (1964).
211. G. K. Hartung and D. M. Jewell, *Anal. Chim. Acta*, **26**, 514 (1962).
212. L. R. Snyder and B. E. Buell, *Anal. Chem.*, **36**, 767 (1964).
213. G. U. Dinneen, G. L. Cook, and H. B. Jensen, *Anal. Chem.*, **30**, 2026 (1958).
214. H. Snyder, B. E. Buell, and H. E. Howard, *Anal. Chem.*, **40**, 1303 (1968).
215. K. Biemann, *Mass Spectrometry: Organic Chemical Applications*, McGraw-Hill, New York, 1962, pp. 130–136.
216. R. A. Khnernitz, A. A. Polyakov, A. A. Petrov, and F. A. Medvedev, *Dokl. Acad. Nauk. SSSR*, **167**, 1066 (1966).
217. J. H. Beynon, R. A. Saunders, and A. E. Williams, *Mass Spectrometry of Organic Molecules*, Elsevier, Amsterdam, 1968, p. 299.
218. S. D. Sample, D. A. Lightner, O. Buchardt, and C. Djerassi, *J. Org. Chem.*, **32**, 997 (1967).
219. P. M. Draper and D. B. MacLean, *Can. J. Chem.*, **48**, 1487 (1968).
220. P. M. Draper and D. B. MacLean, *Can. J. Chem.*, **48**, 1498 (1968).
221. D. M. Clugston and D. B. MacLean, *Can. J. Chem.*, **44**, 781 (1966).
222. R. L. Stevenson and M. E. Wacks, Abstracts, 14th Ann. Conf. on Mass Spectrometry and Allied Topics, Dallas, Tex., May 22–27, 1967, p. 581.
223. G. Spiteller, *Advan. Heterocyclic Chem.*, **7**, 301 (1966).
224. R. A. Van Meter, C. W. Bailey, J. R. Smith, R. T. Moore, C. S. Allbright, I. A. Jacobson, Jr., V. M. Hylton, and J. S. Ball, *Anal. Chem.*, **24**, 1758 (1952).
225. R. V. Helm, D. R. Latham, C. R. Ferrin, and J. S. Ball, *Anal. Chem.*, **32**, 1765 (1960).
226. H. V. Drushel and A. L. Sommers, *Anal. Chem.*, **38**, 19 (1966).
227. (a) C. F. Brandenburg and D. R. Latham, National Meeting, Society for Applied Spectroscopy, 4th, Denver, Colorado, 1965. (b) *J. Chem. Eng. Data*, **13**, 391 (1968).
228. A. Hood, E. G. Carlson, and M. J. O'Neal, in *Encyclopedia of Spectroscopy*, G. L. Clark, Ed., Reinhold, New York, 1960, p. 613.
229. W. L. Mead and A. J. Wilde, *Chem. Ind. (London)*, **1961**, 1315.
230. D. R. Hoffman, *J. Org. Chem.*, **30**, 3512 (1965).
231. A. H. Jackson, G. W. Kenner, K. M. Smith, R. T. Aplin, H. Budzikiewicz, and C. Djerassi, *Tetrahedron*, **21**, 2913 (1965).

232. J. Seibl, *Advan. Mass Spectrometry*, **4**, 317 (1968).
233. H. Budzikiewicz, *Advan. Mass Spectrometry*, **4**, 313 (1968).
234. J. Seibl, *Org. Mass Spectry.*, **1**, 215 (1968).
235. H. Budzikiewicz and F. G. van der Haar, *Org. Mass Spectrometry*, **1**, 223 (1968).
236. A. H. Jackson, G. H. Kenner, H. Budzikiewicz, C. Djerassi, and J. M. Wilson, *Tetrahedron*, **23**, 603 (1967).
237. H. Budzikiewicz, F. G. van der Haar, and H. H. Inhoffen, *Ann. Chem.*, **701**, 23 (1967).
238. D. W. Thomas and M. Blumer, *Geochim. Cosmochim. Acta*, **28**, 1147 (1964).
239. M. Blumer and W. D. Snyder, *Chem. Geol.*, **2**, 35 (1967).
240. J. R. Morandi and H. B. Jensen, *J. Chem. Eng. Data*, **11**, 81 (1966).
241. E. W. Baker, *J. Am. Chem. Soc.*, **88**, 2311 (1966).
242. E. W. Baker, T. F. Yen, J. P. Dickie, R. E. Rhodes, and L. F. Clark, *J. Am. Chem. Soc.*, **89**, 3631 (1967).
243. D. B. Boylan and M. Calvin, *J. Am. Chem. Soc.*, **89**, 5472 (1967).
244. E. J. Levy and W. A. Stahl, *Anal. Chem.*, **33**, 707 (1961).
245. G. L. Cook and G. U. Dinneen, Bureau of Mines Report No. 6698 (1965).
246. I. W. Kinney, Jr., and G. L. Cook, *Anal. Chem.*, **24**, 1391 (1952).
247. N. G. Foster, D. E. Hirsch, R. E. Kendall, and B. H. Eccleston, Bureau of Mines Report No. 6433 (1964).
248. N. G. Foster, D. E. Hirsch, R. E. Kendall, and B. H. Eccleston, Bureau of Mines Report, No. 6671 (1965).
249. N. G. Foster, Bureau of Mines Report No. 6741 (1966).
250. G. L. Cook and N. G. Foster, *Proc. Am. Pet. Inst.*, **41**, III, 199 (1961).
251. V. Hanus and V. Cermak., *Coll. Czech. Chem. Commun.*, **24**, 1602 (1959)
252. N. G. Foster and R. W. Higgins, Abstracts, 14th Ann. Conf. on Mass Spectrometry and Allied Topics, Dallas, Tex., May 22–27, 1966, p. 463.
253. S. H. Hastings, B. H. Johnson, and H. E. Lumpkin, *Anal. Chem.*, **28**, 1243 (1956).
254. H. E. Lumpkin and B. H. Johnson, *Anal. Chem.*, **26**, 1719 (1954).
255. C. J. Thompson, N. G. Foster, H. J. Coleman, and H. T. Rall., Bureau of Mines Report No. 6879 (1966).
256. (a) C. J. Thompson, H. J. Coleman, H. T. Rall, and H. M. Smith, *Anal. Chem.*, **27**, 175 (1955). (b) *Anal. Chem.*, **38**, 1562 (1966). (c) *J. Chem. Eng. Data*, **9**, 473 (1964).
257. H. V. Drushel and A. L. Sommers, *Anal. Chem.*, **39**, 1819 (1967).
258. D. R. Latham, C. R. Ferrin, and J. S. Ball, *Anal. Chem.*, **34**, 311 (1962).
259. C. F. Brandenburg, D. R. Latham, G. L. Cook, and W. E. Haines, *J. Chem. Eng. Data*, **9**, 463 (1964).
260. K. R. Pedersen and J. Lam, *Medd. Groenland*, **185**, [5], 1–16 (1968).

[Reprinted from the Journal of the American Chemical Society, 90, 3284 (1968).]

Enzymic Cyclization of 15-Norsqualene 2,3-Oxide

Sir:

In mechanistic studies of lanosterol (II) biosynthesis we have selectively modified the normal precursor, squalene 2,3-oxide (I), in the central and terminal zones in order to gauge the effect on cyclization and thereby become informed as to the initiation,[1] sequential,[2] and side-chain[3] aspects of the normal annulation. In experiments designed to increase understanding of the factors controlling the later stages of lanosterol formation, especially the methyl-hydrogen migrations, we now find that 15-norsqualene 2,3-oxide (III) is enzymically transformed without incorporation of a proton from the medium to a lanosterol analog of the gross structure IV.

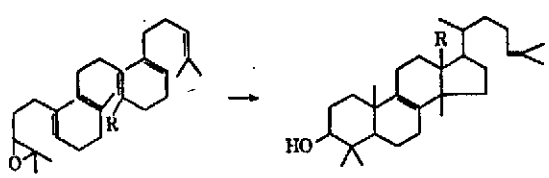

I, R = CH_3
III, R = H

II, R = CH_3
IV, R = H

Synthesis of the radiolabeled substrate III was achieved by employing in the critical stage cross-coupling of the *trans,trans*-acetal dienol V[5] and *trans,trans*-3-norfarnesol

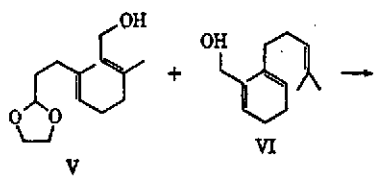

V VI

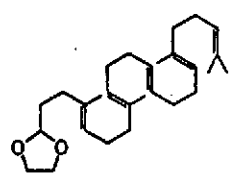

VII

(1) R. B. Clayton, E. E. van Tamelen, and R. G. Nadeau, *J. Am Chem. Soc.*, 90, 820 (1968).
(2) E. E. van Tamelen, K. B. Sharpless, R. Hanzlik, R. B. Clayton, A. L. Burlingame, and P. C. Wszolek, *ibid.*, 89, 7150 (1967).
(3) E. E. van Tamelen, K. B. Sharpless, J. D. Willett, R. B. Clayton, and A. L. Burlingame, *ibid.*, 89, 3920 (1967).
(4) The 22,23-dihydro case described herein was subsequently also reported by E. J. Corey and S. K. Gross, *ibid.*, 89, 4561 (1967).
(5) K. B. Sharpless, R. P. Hanzlik, and E. E. van Tamelen, *ibid.*, 90, 209 (1968).

(VI)[6] to pentaene VII, carried out by treatment with $TiCl_3$ and MeLi.[5] After purification as the thiourea adduct and introduction of tritium by exchange with T_2O on the free aldehyde corresponding to V, conversion to the epoxide III was effected by means previously described.[5] The oily, all-*trans* epoxide III exhibited spectral properties, including nmr (60 Mc in $CDCl_3$; TMS internal standard: *trans*-HC=CH, τ 4.58; four >C=CH–, 4.88; >CHO–, 7.30; $10CH_2$, 8.00; 5>C=C(CH_3), 8.31 and 8.40; $(CH_3)_2C$–O–, 8.71 and 8.75) entirely in accord with the assigned structure.

Using methods previously summarized,[2] we incubated 2.46 mg of radiolabeled epoxide III with 120 ml of a clarified microsomal squalene oxide–lanosterol cyclase preparation equivalent to 80 g of rat liver and obtained, after tlc of the nonsaponifiable fraction, 0.680 mg (27% yield based on *dl*-III) of a crystalline compound (A) with the same tlc mobility as that of lanosterol (VIII) (R_f 0.46 in 25% EtOAc–hexane). Both A and its catalytic reduction product (AH_2) were convertible to monoacetate (A-Ac and AH_2-Ac) and trimethylsilyl ethers (A-TMSE and AH_2-TMSE), mass spectra of which indicated the composition $C_{29}H_{48}O$ and $C_{29}H_{50}O$ and AH_2, respectively. More vigorous reduction[8] afforded AH_4-Ac.

A time-averaged 100-MHz nmr spectrum of A in $CDCl_3$–TMS solution (Varian HA-100 instrument) exhibited the following resonances: one vinyl proton (triplet, τ 4.88), one hydroxyl (broad peak, τ 6.52), one proton under oxygen (triplet, τ 6.78), two olefinic methyls (τ 8.31 and 8.40), saturated methyls (τ 9.00, one CH_3; τ 9.03, one CH_3; τ 9.20, two CH_3). Lanosterol (VIII) displayed an essentially identical spectrum except that saturated methyl resonances appeared at τ 8.99 (C_{19}), 9.01 (4α), 9.11 (14α), 9.18 (4β), and 9.30 (C_{18}). Lanosteryl acetate and A-Ac were also found to be very similar with respect to nmr behavior, except in the methyl region (lanosteryl acetate: C_{19}, τ 8.99; $C_{4\alpha,4\beta,14\alpha}$, 9.11; C_{18}, 9.30; and A-acetate: 9.00, one CH_3; 9.11, two CH_3; 9.19, one CH_3).

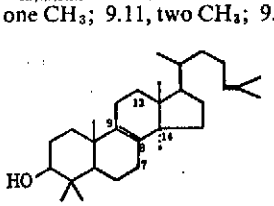

VIII

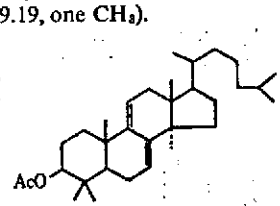

IX

When AH_2-Ac was treated under conditions (HCl–$CHCl_3$ for 48 hr) which equilibrate Δ^8- and Δ^7-dihydrolanosteryl acetate (LH_2-Ac), there was formed in good yield one new isomer (BH_2-Ac) with a longer glpc retention time than that of AH_2-Ac. In contrast to the mass spectrum of AH_2-TMSE,[9] that of its isomer BH_2-TMSE exhibited an intense even-mass peak at *m/e* 274 which can be attributed to a retro-Diels–Alder cleavage of ring B with charge retention by the diene fragment. This structurally highly specific behavior is reconcilable only with a Δ^7 position of the isomerized double bond. An analogous prominent peak is observed at *m/e* 288 in the mass spectrum of the Δ^7 isomer of LH_2-TMSE. The mass spectrum of AH_4-Ac exhibited peaks indicating loss of side chain and C_{15-17} of ring D, with and without associated loss of acetic acid, at *m/e* 243 and 303, respectively.

In order to probe chemically for the position of the nuclear double bond in A, AH_2-Ac was treated for 24 hr with *m*-chloroperbenzoic acid in CH_2Cl_2 over solid Na_2HPO_4 buffer.[10] When the epoxide product (R_f 0.47 in 15% ETOAc–hexane) was exposed for 2 hr to a trace of $HClO_4$ in C_6H_6–HOAc (1:1), a new product (C) formed (R_f 0.63, 15% ETOAc–hexane) which exhibited λ_{max}^{EtOH} 235, 243, and 252 mμ (ϵ ratio 1.00:1.12:0.75, respectively). These data compare favorably with those of dihydroagnosteryl acetate (IX) (R_f 0.63 in 15% EtOAc–hexane) (λ_{max}^{EtOH} 237, 244, and 253 mμ (ϵ ratio 1.00:1.22:0.84, respectively)) and suggest the presence of a Δ^8 double bond in tetracycle A.

Direct structural confirmation of the Δ^8 double bond and C_{13} hydrogen features in isomer AH_2 was derived mainly from the high-resolution mass spectrum of a derivative in which the original double bond position had been marked by suitable functionalization, *viz.*, a seco-diketone acetate ($C_{31}H_{52}O_4$; observed mass 488.3842, calculated mass 488.3865) obtained by treatment of AH_2-Ac with RuO_4. The high-resolution mass spectral fragmentation pattern was compatible with the expected structure X and corresponded well with the spectral data of the homologous seco product XI resulting from LH_2-Ac upon treatment with the same reagent.[11] Major fragmentation processes which furnish evidence for the position of the carbonyl functions are denoted in X as over-all cleavages, not including associated hydrogen-transfer reactions. Thus, for instance, the fragment *m/e* 305 represents the rather characteristic behavior of a cyclic ketone and limits, together with the highly saturated $C_{14}H_{25}$ fragment at *m/e* 193, the possible positions of the carbonyl groups to the original rings B and C.

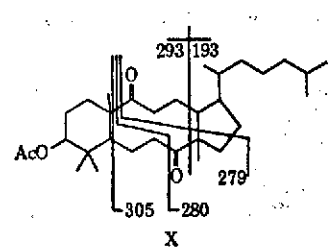

X

(6) The synthesis of trienol VI involved conversion of the known dienyne i[7] with methyllithium and formaldehyde to the acetylenic alcohol

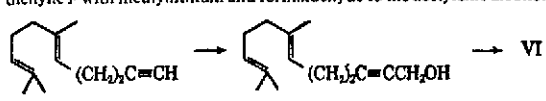

i ii

ii, which was reduced by means of lithium aluminum hydride at 65° in THF.

(7) P. A. Stadler, A. Nechvatal, A. J. Frey, and A. Eschenmoser, *Helv. Chim. Acta*, 40, 1373 (1957).

(8) J. D. Chanley and T. Mezzetti, *J. Org. Chem.*, 29, 228 (1964).

(9) Notably absent in the mass spectrum of AH_2-TMSE was a peak due to loss of the side chain which would be expected for a tetracyclic structure with a $\Delta^{12(14)}$ double bond. Such loss from a $\Delta^{12(14)}$ case was observed by F. Cohen, R. A. Mallory, and I. Scheer, *Chem. Commun.*, 1019 (1967).

(10) J. Fried, J. Brown, and M. Applebaum, *Tetrahedron Letters*, 13, 849 (1965).

(11) G. Snatzke and H. Fehlhaber, *Ann.*, 663, 112 (1963). Transannular aldolization was avoided by careful handling, and mass spectra of the intact diketones were obtained *via* direct sample introduction.

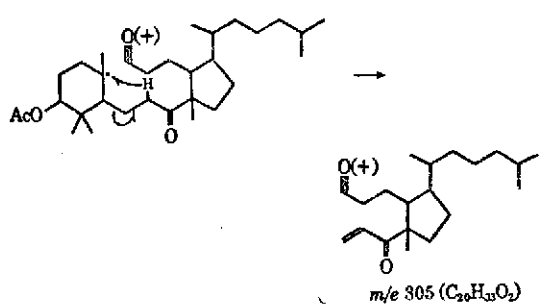

m/e 305 ($C_{20}H_{33}O_2$)

Corresponding fragments occur at *m/e* 319 and 207 in the spectrum of the higher homolog, XI. Another prominent fragment of the composition $C_{18}H_{32}O_3$ at *m/e* 280 (*m/e* 294 in seco-diketolanosterol-Ac) confines the possible carbonyl locations to a sufficiently small area of the B–C ring moiety to permit exclusion of alternative positions based on possible chemical structures of the olefinic precursor. Finally, an abundant fragment recorded at *m/e* 279 ($C_{17}H_{27}O_3$) obviously comprises such a portion of the molecule as to include C_{14} and C_{15}, since it appears unshifted at the same mass in the spectrum of the lanosterol derivative XI. An alternative formation of this fragment ion would have to include C_{17} in the latter case and thus require the highly unlikely rupture of two bonds attached to the same carbon atom (XI). Genesis of this important ion may be initiated by cleavage α to the carbonyl

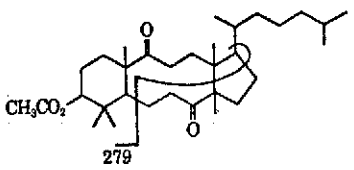

XI

group with reverse charge distribution, followed by radical-induced fragmentation of the 15,16 and 13,14 bonds.

(12) National Science Foundation Predoctoral Fellow, 1966–present.
(13) National Institutes of Health Predoctoral Fellow, 1965–1967.

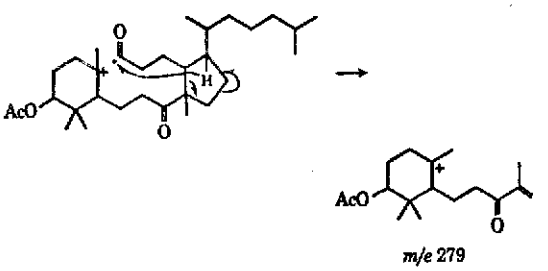

m/e 279

From the abundant fragment at *m/e* 279 and associated high-resolution data it is also apparent that C_{14} bears the methyl group which migrated during biosynthesis of IV.

That the cyclization of III is mechanistically analogous to that of the normal substrate I follows from the nonincorporation of ^3H into IV on cyclization of unlabeled III in a medium containing ^3H_2O (0.235 Ci ml).

Acknowledgments. The authors are indebted to Dr. D. H. Smith for the determination of real-time high-resolution mass spectra (Model AEI MS-902 on line to SDS Sigma 7), to Miss P. C. Wszolek for the low-resolution spectra of the TMSE double bond isomers (AEI MS-12) (University of California at Berkeley), and to Dr. T. Nishida (Stanford University) for the time-averaged nmr spectra. Financial support was provided by the National Aeronautics and Space Administration (Grants NsG 101 and NGR 05-0030134 to A. L. B.), National Institutes of Health (GM 10421 to E. E. v. T. and GM 12493 to R. B. C.), and the American Heart Association (to R. B. C.).

Eugene E. van Tamelen, R. P. Hanzlik,[12] K. B. Sharpless[13]
Department of Chemistry, Stanford University
Stanford, California 94305

Raymond B. Clayton
Department of Psychiatry, Stanford University
Stanford, California 94305

W. J. Richter, A. L. Burlingame
Department of Chemistry and Space Sciences Laboratory
University of California, Berkeley, California 94720
Received February 26, 1968

Tetrahedron. Vol 24, pp. 2825 to 2837. Pergamon Press 1968. Printed in Great Britain

MASS SPECTRA OF AMARYLLIDACEAE ALKALOIDS

THE LYCORENINE SERIES[1]

H. K. SCHNOES, D. H. SMITH,[2] A. L. BURLINGAME

Department of Chemistry and Space Sciences Laboratory, University of California, Berkeley, California 94720

P. W. JEFFS

Department of Chemistry, Duke University, Durham, North Carolina

and

W. DÖPKE

Department of Chemistry, Humboldt University, Berlin, Germany

(*Received in USA* 5 *April* 1967; *accepted for publication* 13 *June* 1967)

Abstract—The mass spectra of alkaloids belonging to the benzopyrano[3.4g]indole series are presented and discussed. It is shown that the fragmentation pattern for this particular carbon skeleton is quite characteristic and can be rationalized in terms of simple mechanisms. This permits the identification and location of various substituents within different parts of the molecule.

ALKALOIDS of the Amaryllidaceae family have enjoyed much active investigation,[3] resulting in the complete characterization of many bases of considerable structural variety. A mass spectrometric study at this time, based on a great number of different systems would appear desirable, since it should yield a set of independent data of advantage to future structural work.

Our interest in the chemistry and biochemistry of these alkaloids led us to undertake a relatively broad and detailed study[4] of all structural types. We wish to present here the results obtained for one group of these bases—the benzopyrano[3.4g]indole series—represented by structures I–XV.

In an earlier paper,[4a] some characteristic features of the decomposition patterns of alkaloids of the crinine class were commented upon and Duffield *et al.*,[5] surveying the mass spectrometric behavior of several types of Amaryllidaceae alkaloids, have presented mechanistic interpretations of some of the dominant fragmentation modes. Very recently, a brief note[6] discussed, in part, the salient points of the mass spectra of several lactone alkaloids also included in the present report. A few applications to structural problems[4b, 7] indicate the potential utility of the technique. It would appear from this study that future chemical investigation of these lactone alkaloids should derive great benefit from the application of mass spectral methods, since the dominant modes of fragmentation of these compounds is readily interpretable in terms of skeletal type and substitution pattern. Furthermore, the generalizations derived from the mass spectra of such lactones appear equally applicable to relatively more complex structures, as has been demonstrated recently by confirmation of the structure of the alkaloid clivimine.[8]

Both low and high resolution* mass spectra of the following substances have been obtained: the $\Delta^{3a,4}$-5-hydroxy compounds, hippeastrine (I), neronine (II) and krigeine (III) the corresponding 3a,4-dihydro derivatives, α-dihydrohippeastrine (IV), α-dihydroneronine (V), clivonine (VI), 0-acetylclivonine (VII) and α-dihydrocandimine (VIII), as well as the 5-desoxy derivatives, masonine (IX), dehydrokrigenamine (X), krigenamine (XI), homolycorine (XII), albomaculine (XIII), lycorenine (XIV) and deoxylycorenine (XV).

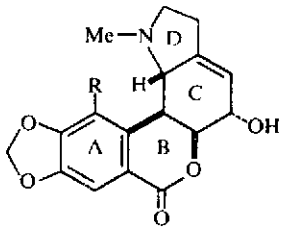

I R = H
II R = OMe

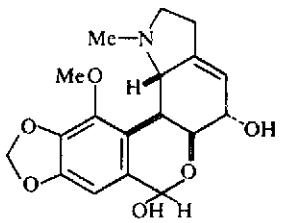

III

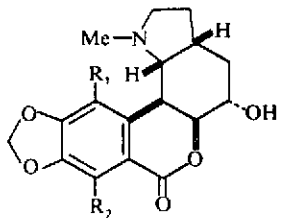

IV $R_1 = R_2 = H$
V R_1 = OMe; R_2 = H
VIII R_1 = H; R_2 = OMe

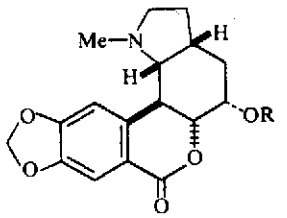

VI R = H
VII R = COMe

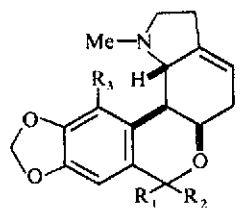

IX R_1, R_2 = O; R_3 = H
X R_1, R_2 = O; R_3 = OMe
XI R_1 = H; R_2 = OH; R_3 = OMe

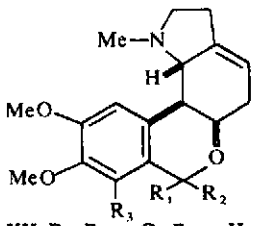

XII R_1, R_2 = O; R_3 = H
XIII R_1, R_2 = O; R_3 = OMe
XIV R_1 = H; R_2 = OH; R_3 = H
XV $R_1 = R_2 = R_3 = H$

* In the high resolution mass spectra presented here, peaks are plotted in separate graphs according to their iso-heteroatomic content. The number of heteroatoms is indicated on each individual plot and the carbon-hydrogen ratio is given by the abscissa. The major divisions indicated on the abscissa correspond to the composition of saturated fragments. A fragment containing fewer hydrogens than the saturated ions thus appears *below* the major divisions and its composition is determined by counting down from the saturated position. For example, peak *b* in Fig. 10, drawn in the C/H NO plot five units to the left of the division corresponding to the saturated mononitrogen-containing fragment, $C_nH_{2n+2}NO$, $C_7H_{16}NO$, has the composition $C_7H_{11}NO$. A peak marked by a short vertical line above it indicates more than seven degrees of unsaturation. Its true composition is determined by adding one carbon and substracting two hydrogens from the composition indicated by its position on the graph. A detailed description of this method is in preparation (D. H. Smith and A. L. Burlingame, *Tetrahedron Letters* in preparation).

All lactone alkaloids of the Amaryllidaceae conform to the gross structural pattern illustrated by formulae I–XV (except for macronine[9] which, although a lactone, exhibits the skeletal arrangement of the tazettine class of alkaloids) and the compounds thus differ only in substitution pattern, degree of oxygenation and unsaturation. The mass spectra reflect these differences only in the mass-shift of peaks and not in the fundamental modes of fragmentation, which appear notably indifferent to peripheral structural modifications. One mode of decomposition dominates: cleavage of the labile bonds in ring C with fragmentation of the molecule into two parts, one representing the pyrrolidine ring (plus substituents), the other (a less abundant fragment) encompassing the aromatic lactone moiety. A further general and noteworthy feature is the low abundance of the molecular ion in the spectra of all $\Delta^{3a,4}$-compounds. Ions corresponding to loss of one, two and three hydrogen atoms are usually more intense than the molecular ion. This somewhat unusual elimination of hydrogen (partially thermal in nature) would generate $\Delta^{3a,4}$-conjugation (or aromatization of ring C). In addition, the $\Delta^{3a,4}$-bond is expected to enhance the lability of ring C, also resulting in molecular ions of low abundance. Such conclusions are corroborated by the mass spectra of the 3a,4-dihydro derivatives, all of which show quite prominent molecular ions.

The dominant fragmentation sequence of the $\Delta^{3a,4}$-compounds is conveniently illustrated by the spectrum of hippeastrine (I, Figs. 1 and 10). It shows very intense peaks at *m/e* 125 (**b**, $C_7H_{11}NO$) and 96 ($\mathbf{b_1}$, $C_6H_{10}N$). Such N-containing fragments, comprising the pyrrolidine nucleus, are the most characteristic feature of all alkaloids in the lycorenine series. All other ions are by comparison minor contributors, although the sequence of peaks **a** ($C_{10}H_6O_4$, *m/e* 190), $\mathbf{a_1}$ ($C_9H_6O_3$, *m/e* 162), $\mathbf{a_2}$ ($C_8H_6O_2$) and $\mathbf{a_3}$ ($C_8H_5O_2$) are significant because they convey important structural information. The peaks at *m/e* 125 and 190 completely account for the two parts of the molecule (i.e. $125 + 190 = 315 = M^+$), and an explanation for their genesis is reasonably apparent: a *retro*-Diels–Alder reaction would conveniently generate both fragment **a** ($C_8H_6O_4$, *m/e* 190) and **b** ($C_7H_{11}NO$, *m/e* 125). This fragmentation can be thought of as a concerted reaction of the *retro*-Diels–Alder type but, of course, a stepwise sequence, i.e. cleavage of the 11b,11c-bond following that of 5,5a, is equally feasible. In Scheme I, the fragmentation is illustrated as a concerted process, yielding either ion **a** or **b**.

Subsequent elimination of carbon monoxide from **a** is unexceptional and results in the benzofuranyl fragment $\mathbf{a_1}$ ($C_9H_6O_3$). Elimination of neutral carbon monoxide* and the formyl radical from ion $\mathbf{a_1}$ yields species $\mathbf{a_2}$ ($C_8H_6O_2$, *m/e* 134) and $\mathbf{a_3}$ ($C_8H_5O_2$, *m/e* 133), respectively. This process is best formulated as involving the ether oxygen of the benzofuranyl ion radical, since the methylenedioxy moiety does not appear to undergo this fragmentation† in analogous systems. The absence of metastable peaks does not permit a distinction between the possible pathways **a**-CO-H and **a**-CHO for the generation of ion $\mathbf{a_3}$.

The elimination of a formyl radical (·CHO) from fragment **b** may proceed by the pathway outlined in Scheme I. Transfer of the hydroxyl hydrogen atom is established

* Data from the literature [W. H. Pirkle, *J. Am. Chem. Soc.* **87**, 3022 (1967)] concerning the elimination of CO from 2-pyrone would suggest other possibilities for the formulation of fragment $\mathbf{a_1}$.

† A. L. Burlingame and B. R. Simoneit, unpublished results from this laboratory.

by the retention of a deuterium atom in fragment $\mathbf{b_1}$ ($C_6H_{10}N$) in the spectrum of hippeastrine-OD. A metastable ion at *m/e* 74·1 (calc. 73·7) confirms the transition from **b** to $\mathbf{b_1}$. The postulated sequences appear to be quite general and essentially invarient for all compounds of this type. The fragmentation pattern thus readily permits the location of substituents in both moieties of the molecule. For example, in the spectrum of neronine (II, Fig. 2) the peak corresponding to fragment **a** is shifted by 30 m.u. (*m/e* 220, $C_{11}H_8O_5$) due to the presence of an additional OMe substituent. Hydroxyl substitution at C-5 is immediately evident from the mass and composition of fragment **b**. In the case of the 5-desoxy derivatives (IX–XV), an ion

SCHEME I

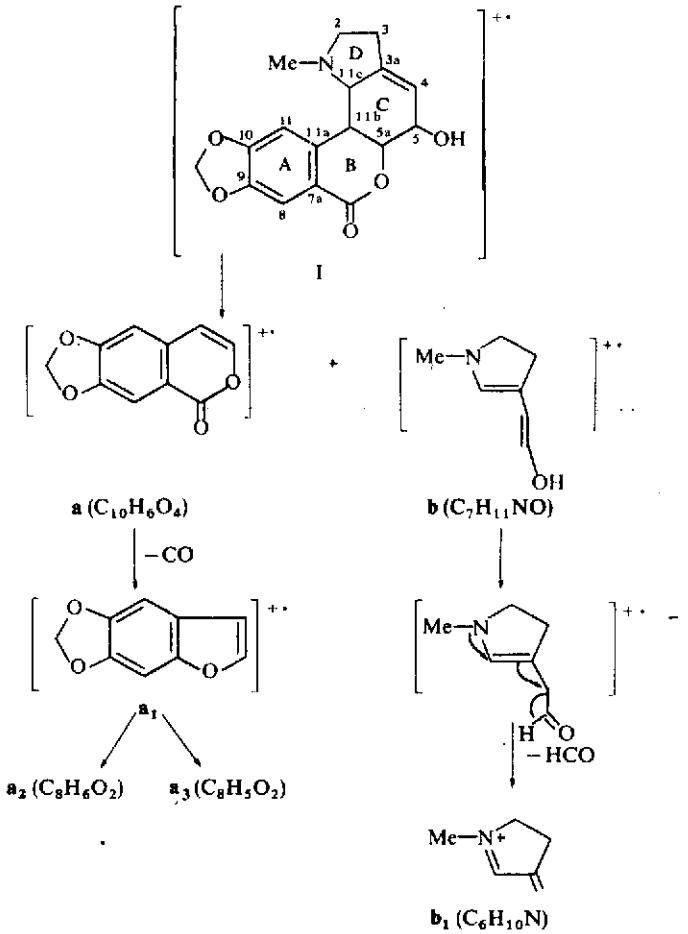

of type **b** gives rise to an intense peak at *m/e* 109, of the expected composition $C_7H_{11}N$ (cf. Figs 4, 5 and 6).

Substances with OMe substituents in the aromatic ring (cf. neronine, Fig. 2; albomaculine, Fig. 5) show some additional peaks, since now the loss of Me radicals is superimposed upon the general pathway. Such eliminations should, of course, be facile, since they contribute to the stability of the ions formed; for neronine (II, Fig. 2) one observes peaks corresponding to the sequence sketched in Scheme II.

It is to be noted that the loss of a Me radical generates another carbonyl oxygen function which might now partake in the expulsion of carbon monoxide.

While the significant features of the fragmentation pattern of the hemiacetyl members (cf. III, XI, XIV) of this series are readily ascertained in the light of the foregoing discussion, they are less suited to mass spectrometric analysis due to thermal lability toward elimination of water. The spectrum of krigeine (III, Fig. 3)

SCHEME II

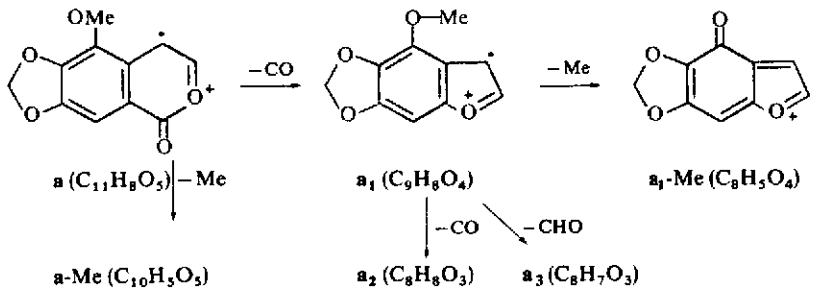

may serve as an example. In this case, two OH functions are available for the elimination of water. Since the loss of water in the case of the 5-hydroxy lactones is a minor process, the facile elimination of water in the hemiacetals can be ascribed to the hemiacetal OH function. Species resulting from elimination of the elements of water either upon electron impact or thermally would give rise to quite different fragmentation patterns. Fig. 3 illustrates this point. Most notably, the M-H_2O peak (*m/e* 329) is very intense and, while the usual and expected fragments are easily recognizable (e.g. the intense peaks **b**, *m/e* 125; $\mathbf{b_1}$, *m/e* 96, as well as **a**, *m/e* 222; **a**-OH, *m/e* 205; $\mathbf{a_1}$, *m/e* 194), other ions arising probably from the M-H_2O species are now also quite abundant.

The mass spectrum of the ether, deoxylycorenine, XV, Figs. 6 and 11, exhibits the usual fragmentation pattern leading to ions **a** ($C_{11}H_{12}O_3$) and **b** ($C_7H_{11}N$). The further decomposition of **a** is interesting, because elimination of the elements of carbon monoxide occurs even though no carbonyl function is originally present. Scheme III depicts formulation of the prominent fragments of the **a** group (cf. Fig. 11):

SCHEME III

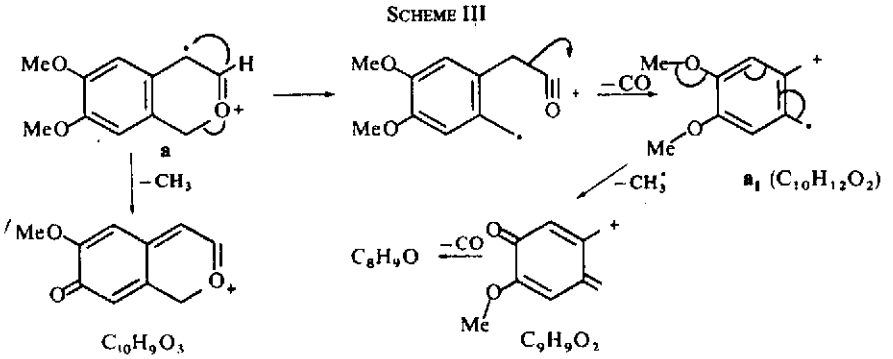

In the spectra of the saturated lactones, α-dihydrohippeastrine (IV, Fig. 7), α-dihydroneronine (V, Fig. 8), α-dihydrocandimine (VIII), clivonine (VI, Fig. 9) and O-acetylclivonine (VII), the more intense molecular ion peaks are notable. This feature, as suggested above, may reflect a greater stability of the molecular ion, both with respect to hydrogen atom loss and the tendency towards ring C cleavage reactions. The latter still predominate, however, as evidenced by the appearance of fragments of type **a** and **b**, which are readily accounted for by concerted or stepwise cleavages of ring C. The expected ionic products derived from decomposition of α-dihydrohippeastrine (IV, Fig. 7) are shown in Scheme IV. The depicted sequence results in the elimination of the 4,5-bridge and yields the abundant ion **b** (*m/e* 83, C_5H_9N), typical for all dihydro derivatives. Loss of a hydrogen atom leads to **b'**.

The spectra of the dihydro compounds furnish some evidence that a stepwise

SCHEME IV

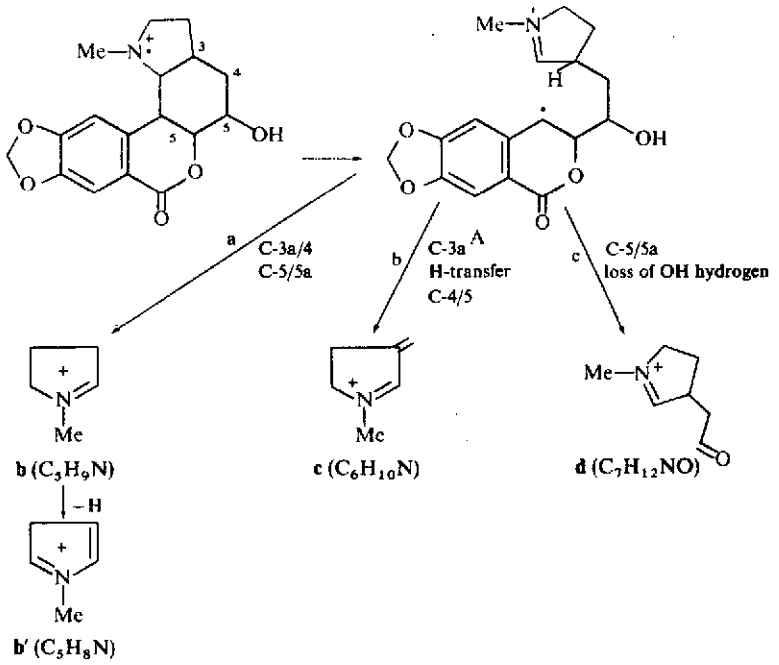

rather than concerted process should be considered for the decomposition of ring C. Peak **a**, ($C_{10}H_6O_4$), for example, is accompanied by a peak one mass unit higher (**a'**, $C_{10}H_7O_4$), indicating that fragmentation with hydrogen atom transfer does occur. In Scheme IV, intermediate A would provide the opportunity for such transfer reactions, and it is suggested that a hydrogen atom from C-3a is transferred to the radical site. Subsequent cleavage of the 4,5-bond would yield the nitrogen containing fragment **c** (*m/e* 96, $C_6H_{10}N$), a very abundant ion. Cleavage of the 5,5a-bond with subsequent loss of the hydroxyl hydrogen (path c) would yield peak **d** (*m/e* 126, $C_7H_{12}NO$), a sequence corroborated by the fact that in the spectrum of dihydrohippeastrine-OD, ion **d** does not retain the deuterium atom. The alternative decomposition, i.e. rupture of the 5,5a-bond followed by 3a,4-cleavage, results in the base peak **b** (C_5H_9N) already mentioned (path a). Of course, loss of an acetaldehyde radical from **d** would also account for the genesis of **b** and, likewise, a

"McLafferty" rearrangement involving the carbonyl function of **d** could be thought of as the source of **b'** (C_5H_8N). Unfortunately, metastable ions are not observed in these spectra and, therefore, a more precise delineation of pathways is not possible.

Only the alkaloid clivonine (VI, Fig. 9) differs in stereochemistry (*trans* B/C ring juncture) from the other compounds of this series, such that possible stereochemical effects on the fragmentation pattern could not be investigated extensively. The spectrum of clivonine is almost indistinguishable from that of its isomer dihydrohippeastrine (IV, Fig. 7), suggesting the absence of steric influence on the course of the decomposition. Such a result might be expected since all proposed pathways involve simple homolytic cleavages of labile bonds—reactions which should be unaffected by stereochemical detail.

The compounds appear, however, quite sensitive to instrument operating conditions. While the gross fragmentation pattern is unaffected, differences in detail can be noted between successive runs, implying that some of the fragmentation sequences discussed above (e.g. loss of hydrogen, H_2O) may represent partial thermal degradation.

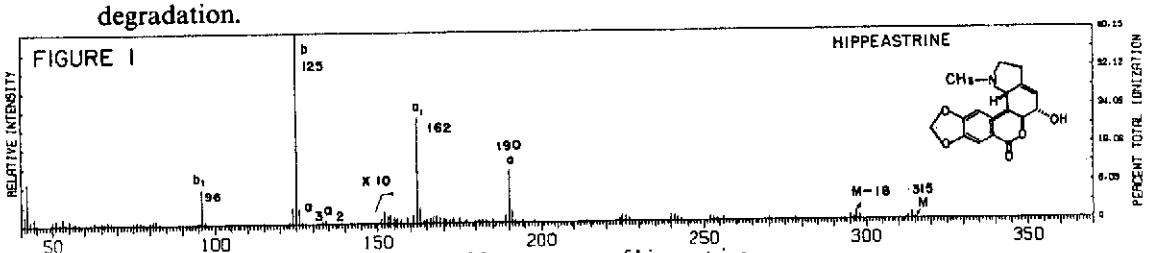

FIG. 1 Mass spectrum of hippeastrine.

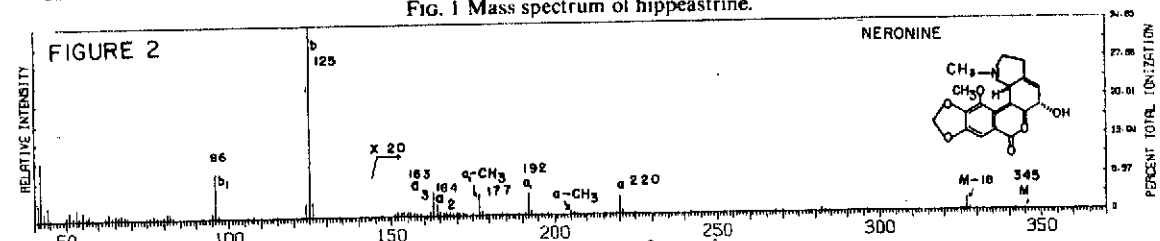

FIG. 2 Mass spectrum of neronine.

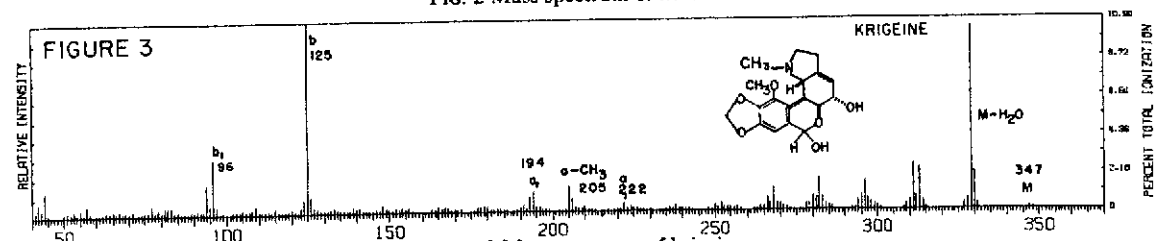

FIG. 3 Mass spectrum of krigeine.

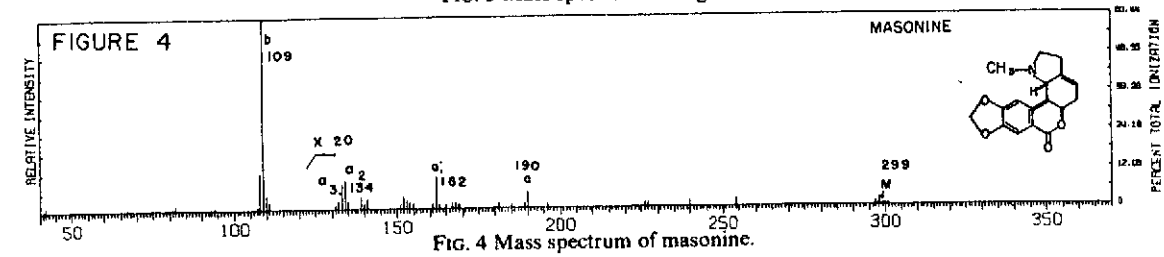

FIG. 4 Mass spectrum of masonine.

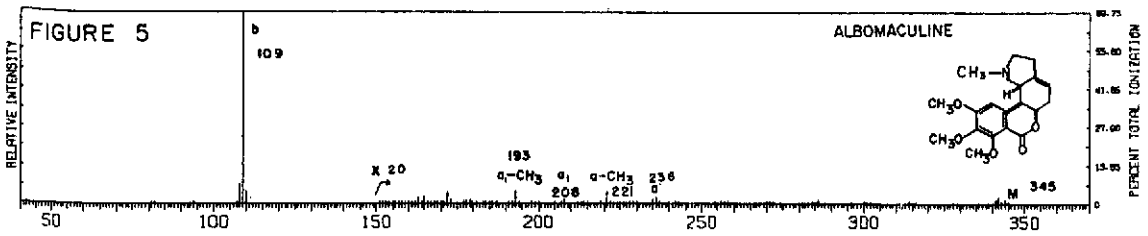

FIG. 5 Mass spectrum of albomaculine.

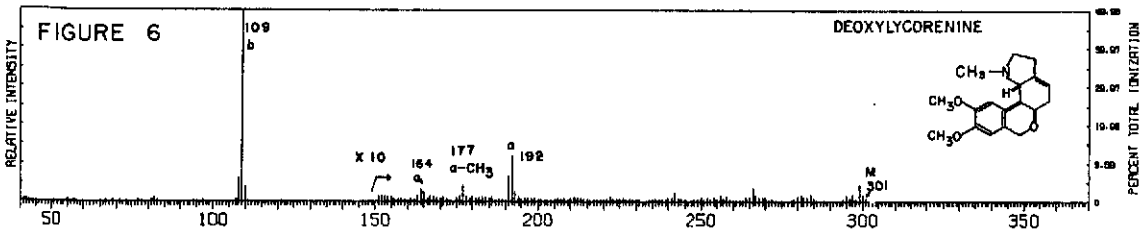

FIG. 6 Mass spectrum of deoxylycorenine.

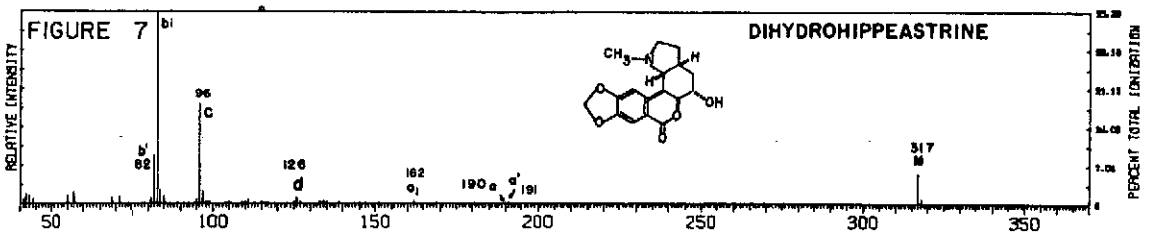

FIG. 7 Mass spectrum of α-dihydrohippeastrine.

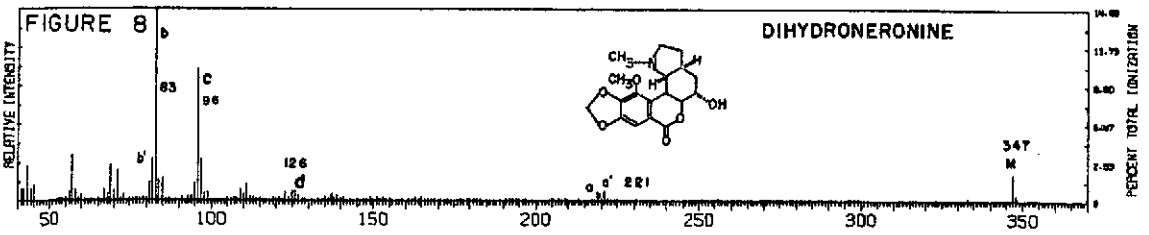

FIG. 8 Mass spectrum of α-dihydroneronine.

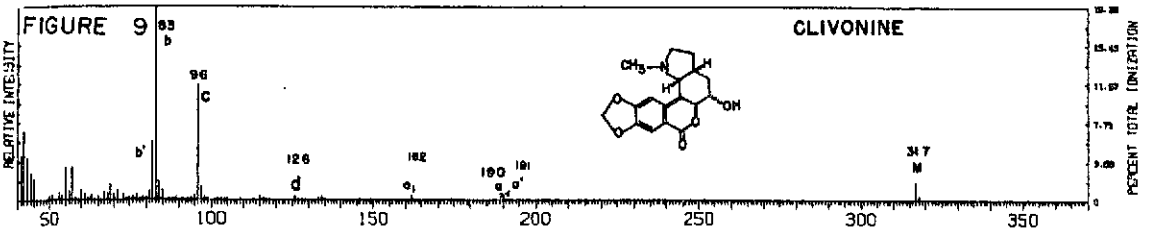

FIG. 9 Mass spectrum of clivonine.

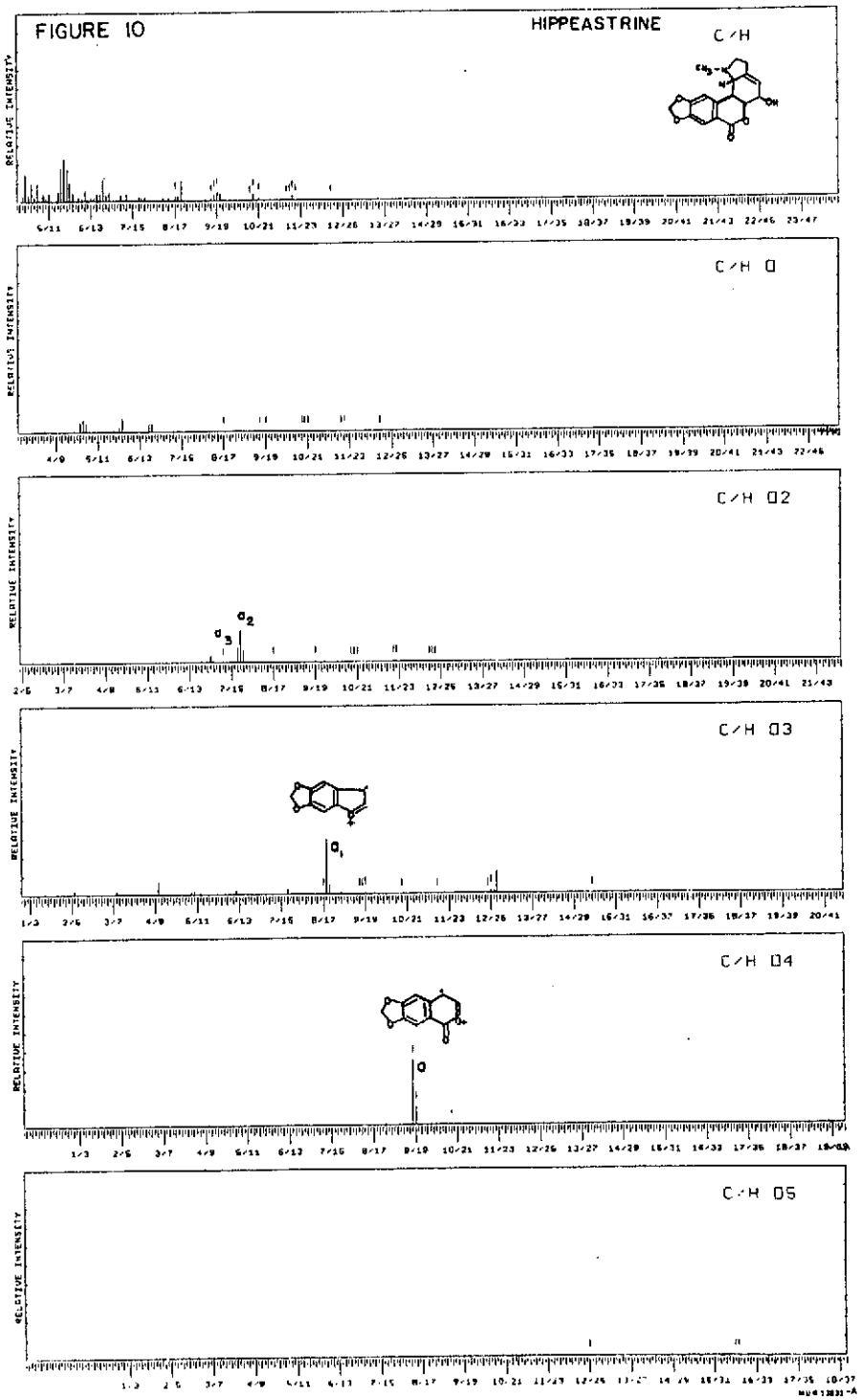

FIG. 10 High resolution mass spectrum of hippeastrine: Hydrocarbon and O-containing fragments.

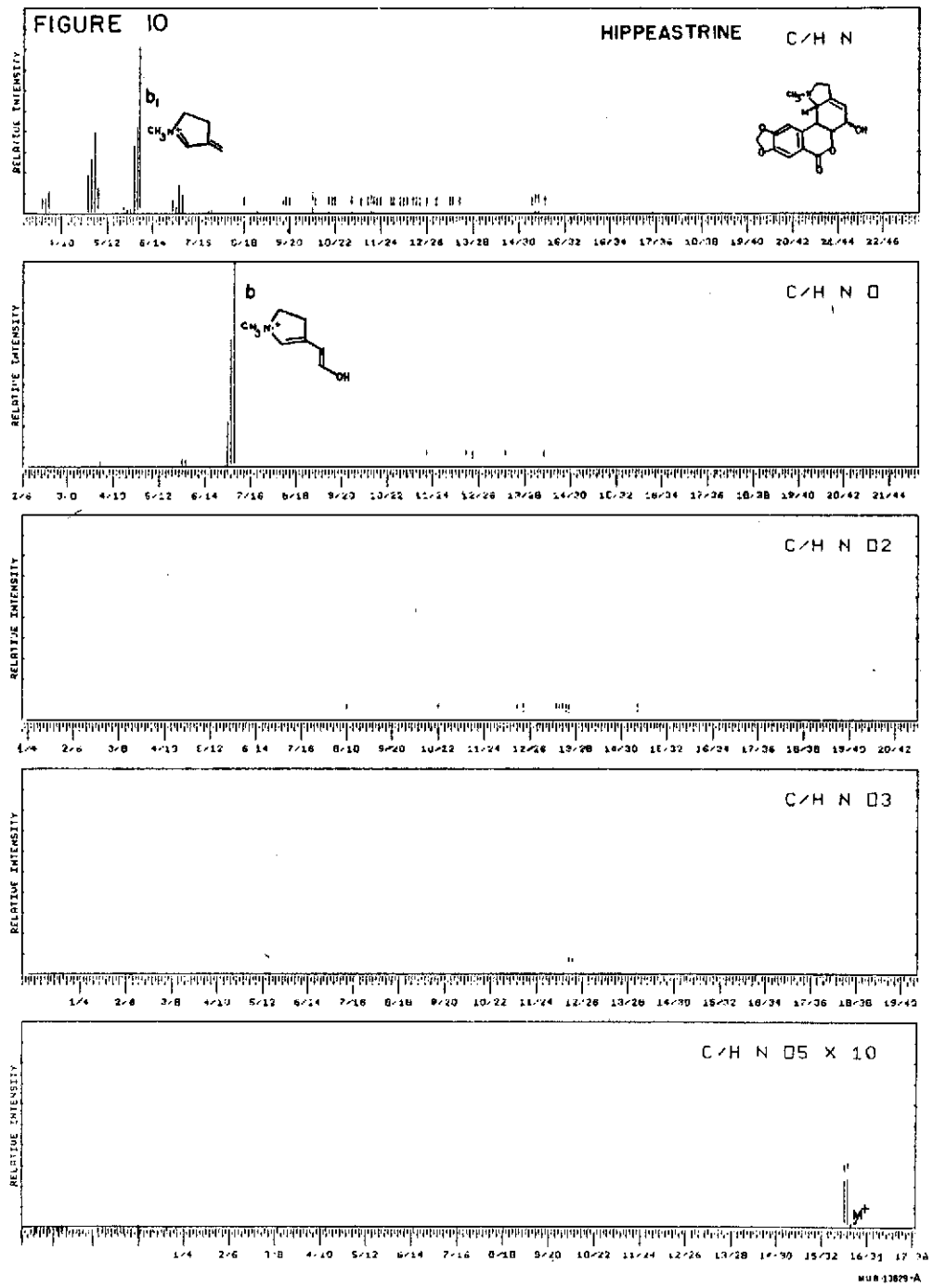

FIG. 10 High resolution mass spectrum of hippeastrine: N-containing fragments.

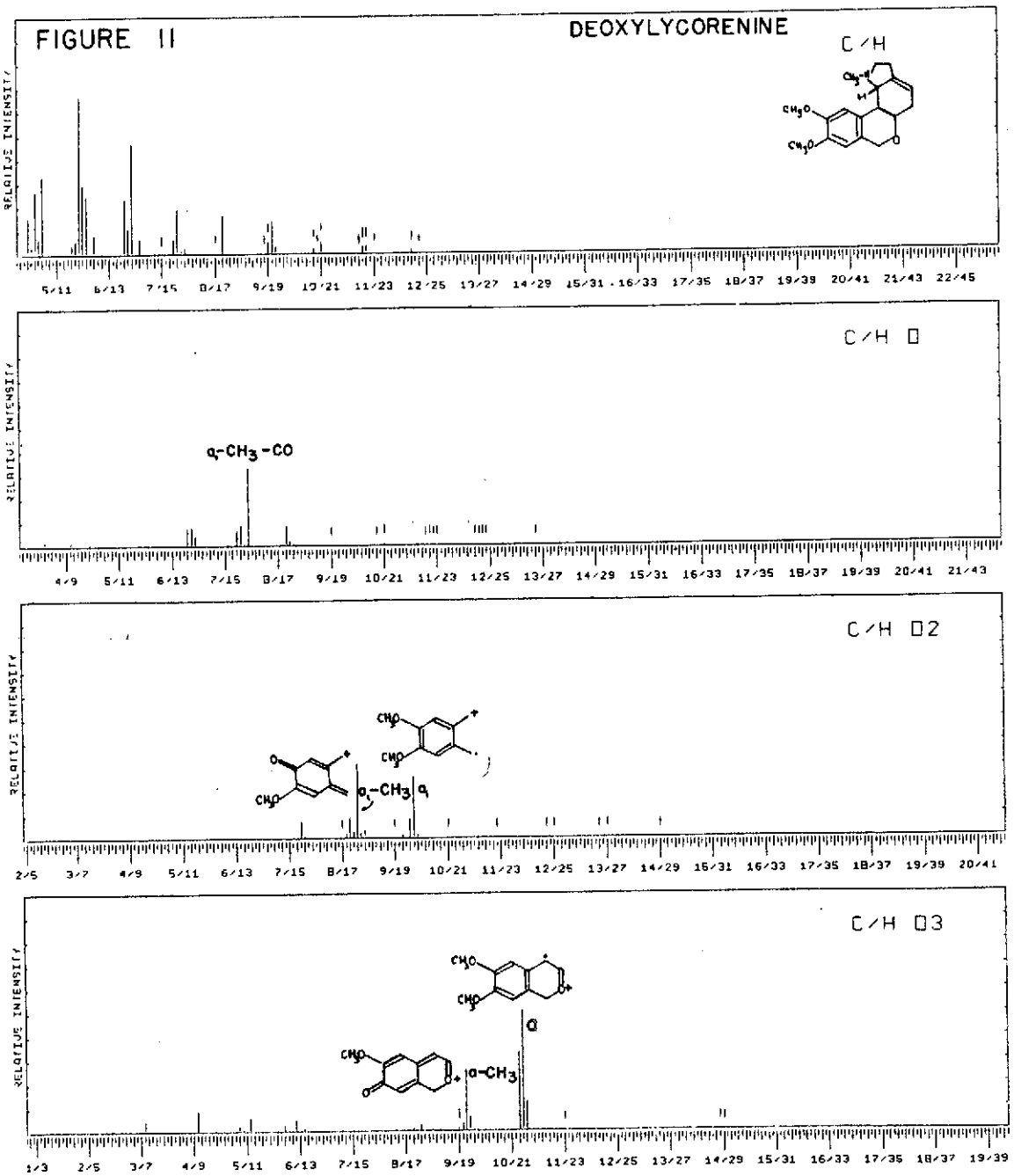

FIG. 11 High resolution mass spectrum of deoxylycorenine: Hydrocarbon and O-containing fragments.

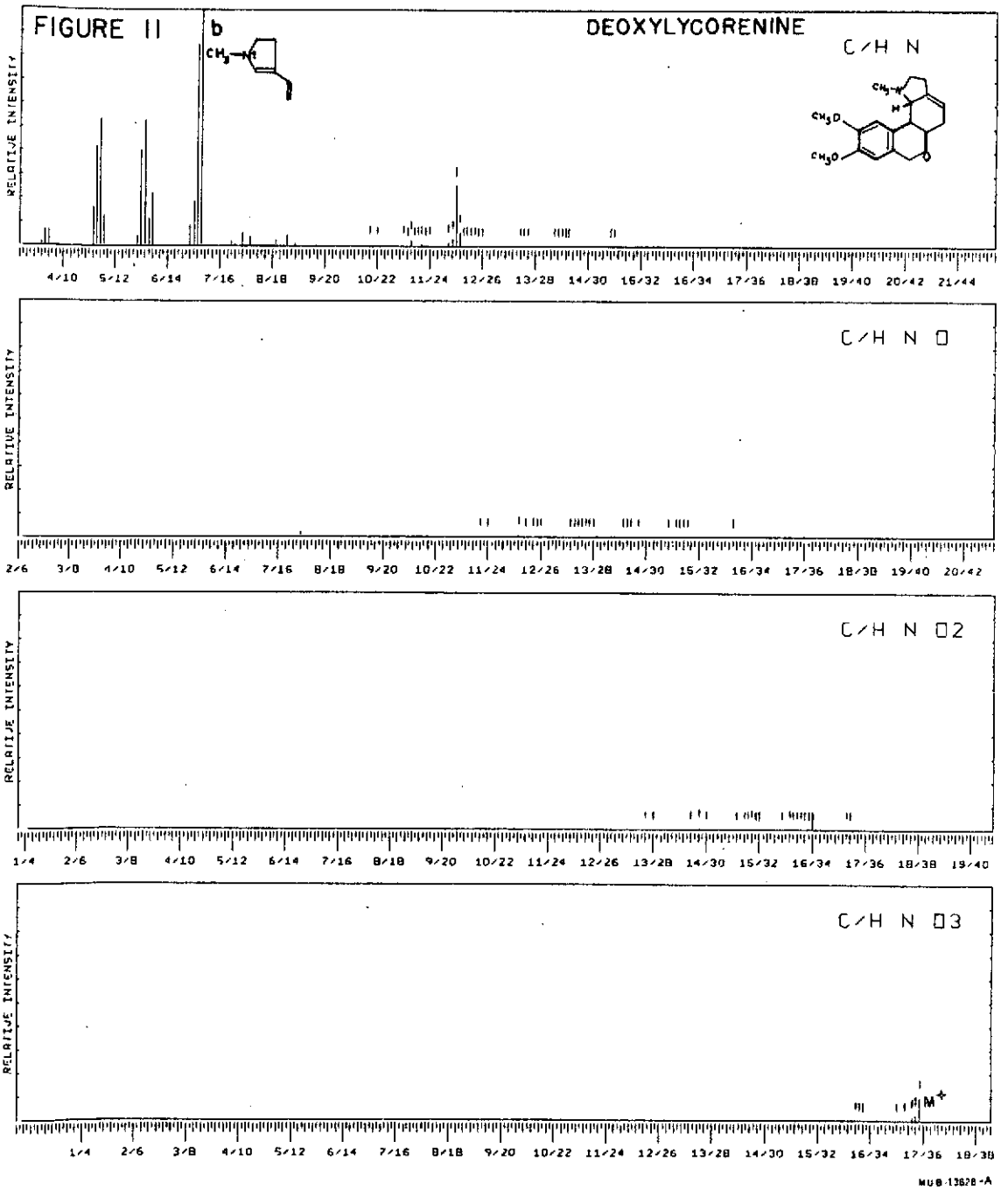
FIGURE II
b
DEOXYLYCORENINE
C/H N
C/H N O
C/H N O2
C/H N O3
RELATIVE INTENSITY
M+
MUB-13628-A

EXPERIMENTAL

Low resolution spectra were determined on a modified C.E.C. 21-103C mass spectrometer [ionizing voltage: 70 eV; ionizing current: 20 μa; ion source temp: 250°]. High resolution mass spectra were obtained with a double focussing mass spectrograph (C.E.C. 21-110B) [ionizing voltage: 70 eV; ionizing current: 150 μa; temp at minimum value necessary to obtain ion beam]. In both instruments samples were introduced directly into the ion source chamber.

REFERENCES

[1] This represents Part IX of the Berkeley series, *High Resolution Mass Spectrometry in Molecular Structure Studies*—VIII: S. M. Kupchan, J. M. Cassady, J. E. Kelsey, H. K. Schnoes, D. H. Smith and A. L. Burlingame, *J. Am. Chem. Soc.* **88**, 5292 (1966). The work at the University of California was supported by grants from the National Aeronautics and Space Administration (NsG 101 and NGR 05-003-134).

[2] NASA predoctoral trainee, 1965–67.

[3] Cf. W. C. Wildman, *The Alkaloids* (Edited by R. H. F. Manske) Vol. VI; p. 289. Academic Press, New York (1 54); H.-G. Boit, *Ergebnisse der Alkaloid Chemie bis* 1960. Chapt. 25. Akademie Verlag, Berlin (1961).

[4] [a] A. L. Burlingame in W. L. Mead, Ed., *Advances in Mass Spectrometry* Vol. III; p. 701. The Institute of Petroleum/ASTM Mass Spectrometry Symposium, London (1966);
[b] A. L. Burlingame, H. M. Fales and R. J. Highet, *J. Am. Chem. Soc.* **86**, 4976 (1964);
[c] A. L. Burlingame, P. Longevialle, R. W. Olsen, K. L. Pering, D. H. Smith, H. M. Fales and R. J. Highet, in preparation.

[5] A. M. Duffield, R. T. Aplin, H. Budzikiewicz, C. Djerassi, C. F. Murphy and W. C. Wildman, *J. Am. Chem. Soc.* **87**, 4902 (1965).

[6] T. Ibuka, H. Irie, A. Kato, S. Uyea, K. Kotera and Y. Nakagawa, *Tetrahedron Letters* 4745 (1966).

[7] T. H. Kinstle, W. C. Wildman and C. L. Brown, *Ibid.* 4659 (1966).

[8] W. Döpke, M. Bienert, A. L. Burlingame, H. K. Schnoes, P. W. Jeffs and D. S. Farrier, *Ibid.* 451 (1967).

[9] C. F. Murphy and W. C. Wildman, *Ibid.* 3857 (1964).

Geochimica et Cosmochimica Acta, 1968, Vol. 32, pp. 358 to 361. Pergamon Press. Printed in Northern Ireland

Aromatic carboxylic acids isolated from the Colorado Green River Formation (Eocene)

PAT HAUG, H. K. SCHNOES* and A. L. BURLINGAME

Department of Chemistry and Space Sciences Laboratory,
University of California, Berkeley, California 94720

(*Received* 25 *August* 1967; *accepted in revised form* 30 *October* 1967)

Abstract—Several series of aromatic carboxylic acids (including mono-, di-, and trimethyl benzoic; mono-, di-, and trimethyl propanoic; mono- and dimethyl butanoic; indanoic and tetrahydronaphthoic; and naphthoic acids) have been isolated from the extract of Colorado Green River Shale. Gas liquid chromatographic and both low and high resolution mass spectrometric techniques were utilized for separation and characterization respectively.

We wish to report on a mass spectrometric study of the carboxylic acids in the Green River Shale (Eocene), specifically on the occurrence and type of aromatic acids. Although normal *iso*, *anteiso* and isoprenoid acids have been reported in this sediment [ABELSON and PARKER (1962), LAWLOR and ROBINSON (1965), LEO and PARKER (1966), EGLINTON *et al.* (1966), RAMSAY (1966), DOUGLAS *et al.*, (1968) HAUG *et al.* (1967)], aromatic acids have received little attention thus far. In fact, from geological sources no individual aromatic acids appear to have been isolated [LOCHTE and LITTMANN (1955), WHITEHEAD and BREGER (1963)] with the exception of benzoic acid, which has been isolated from soil [KONONOVA (1961)]. The presence of aromatic hydrocarbons has been established and, of course, aromatic hydrocarbons have been studied extensively using mass spectrometry (BURLINGAME and SCHNOES, 1968; SCHNOES and BURLINGAME, 1968). We find that the Colorado sediment contains several series of aromatic acids whose methyl esters range in molecular weight from 150 (methyl substituted benzoate) to 242 (trimethyl naphthoate). For each mol. wt. a series of isomers is present. Although the mass spectrometric data do not completely define positions of aromatic substitution for individual acids they allow the recognition of structural types and provide a comprehensive picture of the range and nature of the acids present.

The oil shale (5.3 kg after removal of the outer layer; obtained from Parachute Creek, 8 miles northwest of Grand Valley Colorado latitude N 39°37′, longitude W 108°7′, elevation 7300′) was pulverised and extracted ultrasonically with 4:1 benzene/methanol. From 55 g of hexane soluble organic extract 0.4 g of free acids were extracted with aqueous sodium hydroxide (1 N). After extraction of the phenols from a saturated sodium bicarbonate solution, the acids remaining were esterified (BF_3 and MeOH). Final separation and purification were carried out on gas chromatography columns of 3% SE-30 on 80/100 mesh Aeropack (10 ft × 1/4 in.) and 3% HIEPF 8BP on 80/100 mesh Gas Chrom Q (Applied Science 6 ft × 1/4 in.) programmed at 4°/min with a flow rate of 50 ml/min. The collected G.L.C. fractions were then identified by mass spectrometry.

Figure 1 illustrates some of the data obtained for the aromatic esters. Figure 1a represents the mass spectrum of methyl *m*- or *p*-methylbenzoate. The peaks at M-31 (m/e 119) and M-31-28 (m/e 91) are characteristic of methyl benzoates, while the lack of an intense peak at M-32 eliminates the possibility of an *o*-methyl substituted methyl benzoate. Although the mass spectra of methyl *m*- and *p*-methylbenzoate are almost identical [MCLAFFERTY and GOHLKE (1959)], the presence of both isomers is indicated by the isolation of a second fraction with a slightly different gas chromatographic retention time giving a very similar mass spectrum. In addition, several other benzoate esters were isolated: four isomers of methyl dimethylbenzoate of mol. wt. 164 and three isomers of methyl trimethylbenzoate of mol. wt. 178 are present, as indicated by their mass spectral fragmentation patterns.

* Present address: Department of Biochemistry, University of Wisconsin, Madison, Wisconsin.

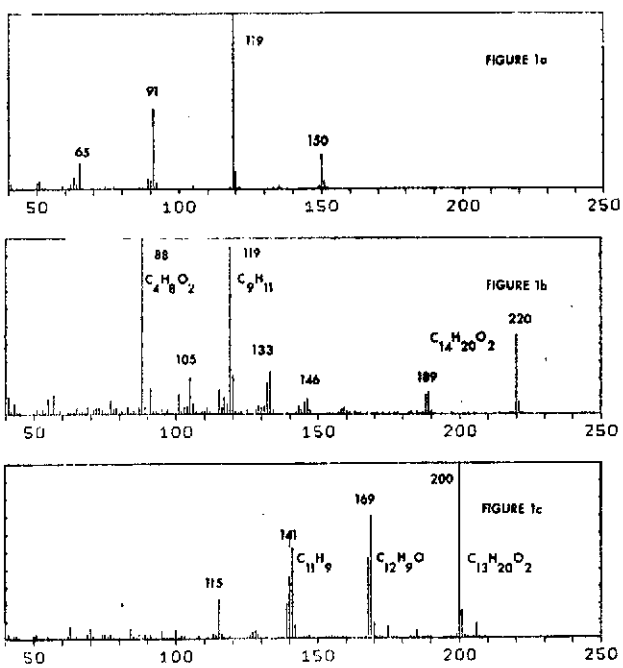

Fig. 1. Mass spectra of (a) methyl *m*- or *p*-methylbenzoate; (b) methyl 2-methyl-4-(dimethylphenyl) butanoate; (c) methyl methylnaphthoate.

For each of the higher homologues of phenylalkyl acids from mol. wt. 192 to 234 several isomers were found. Among these there do not appear to be more highly substituted methyl benzoates or appreciable amounts of phenyl acetic esters. Mass spectra indicate the presence of trimethyl, tetramethyl and pentamethyl substituted phenyl propanoic acid (mol. wt. 206-220 and 234, respectively), where isomers of the latter two bear one methyl group on C-2. Another interesting series corresponds to mono- and dimethyl substituted 4-phenyl butanoic acid esters. The degree to which structures can be established is well illustrated by the spectrum of Fig. 1b which is interpreted as methyl 2-methl-4-(dimethylphenyl) butanoate; the intense peak at m/e 88 requires an alpha methyl substituent and m/e 119 demands a dimethyl phenyl moiety. Structure I combines these features, although, of course, the positions of the methyl substituents on the aromatic ring are not determined. A di-*ortho* structure would be one of the possible isomers, which could be derived as the degradation product of monocyclic polyterpenoids (II), one methyl group being lost in aromatisation. The mass spectral interpretations were confirmed by accurate mass measurements, which in the case above gave m/e 220 as ($C_{14}H_{20}O_2$) m/e 119 (C_9H_{11}) m/e 88 ($C_4H_8O_2$). (Elemental compositions of other fractions were confirmed by high resolution mass spectrometry.)

Aside from these substituted phenylalkyl acids, several compounds (molecular weights 204, 218 and 232) were isolated which, in accordance with their mass spectral composition,

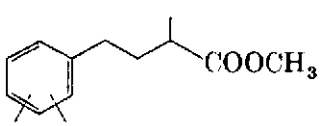

I

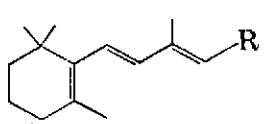

II

must be cycloaromatic esters. Indanoic and tetrahydronaphthoic acids appear as the most likely possibilities but details of their structures cannot be specified at this time. Another group of acids is represented by several naphthoic acids. Figure 1c shows the mass spectrum of methyl methylnaphthoate. Although these compounds have molecular ions of the same nominal mass as saturated carboxylic acids, their fragmentation pattern combined with high resolution mass spectra [for example, m/e 200 ($C_{13}H_{12}O_2$), m/e 169 ($C_{12}H_9O$), m/e 141 ($C_{11}H_9$)] leave no doubt about their condensed nature. Two isomers of mol. wt. 200 and one of mol. wt. 214 were isolated. High resolution mass spectra of several fractions indicate the presence of two higher homologues (mol. wt. 228, 242). These naphthoate esters could be derived from the corresponding cycloaromatic esters (mentioned above) by further dehydrogenation.

The aromatic acids identified from the Green River Shale indicate that some of them may be derived from cyclic terpenoid precursors. Aside from the desirability of more complete characterization of these substances, similar studies on cyclic and aromatic hydrocarbons appear necessary to provide a comparison which would permit some insight into both the origin and the diagenesis of these compounds in the sediment. A comprehensive report of our results on these aromatic acids is in preparation, as well as preliminary communications which are in press on the other types of acids present [dicarboxylic and keto acids (HAUG *et al.*, 1967), kerogen acids (BURLINGAME and SIMONEIT, 1968)] in this shale.

Acknowledgments—Financial support from the National Aeronautics and Space Administration (Grants NsG 101, NGR 05-003-134) is gratefully acknowledged. The authors wish to thank Mr. B. R. SIMONEIT for collection of the oil shale specimens.

REFERENCES

ABELSON P. H. and PARKER P. L. (1962) Fatty acids in sedimentry rocks. *Carnegie Inst. Wash. Year book* **61**, 181.

BURLINGAME A. L. and SCHNOES H. K. (1968) Analytical methods—Low and high resolution mass spectrometry. Combined gas-liquid chromatography-mass spectrometry. In *Organic Geochemistry: Methods and Results* (Editors G. Eglinton and Sister M. T. J. Murphy). Springer-Verlag, in preparation.

BURLINGAME A. L. and SIMONEIT B. R. (1968) Fatty acids liberated from chromic acid oxidation of Colorado Green River Formation kerogen (Eocene). *Nature*, in preparation.

DOUGLAS A. G., DOURAGHI-ZADEH K., EGLINTON G., MAXWELL J. R. and RAMSAY J. N. (1968) Fatty acids in sediments including the Green River Shale (Eocene) and Scottish Torbanite (Carboniferous). *Advances in Organic Geochemistry* (Editors G. D. Hobson and G. C. Speers). Pergamon Press, in press.

EGLINTON G., DOUGLAS A. G., MAXWELL J. R., RAMSAY J. N. and STÄLBERG-STENHAGEN S. (1966) Occurrence of isoprenoid fatty acids in the Green River Shale. *Science* **153**, 1133.

HAUG P., SCHNOES H. K. and BURLINGAME A. L. (1967) Isoprenoid and dicarboxylic acids isolated from the Colorado Green River Shale (Eocene). *Science*, **158**, 772; Keto-carboxylic acids isolated from the Colorado Green River Shale (Eocene). *Chem. Commun.*, No. 21, 1130.

KONONOVA M. M. (1961) *Soil Organic Matter*. p. 47. Pergamon.

LAWLOR D. L. and ROBINSON W. E. (1965) Fatty acids in Green River Formation oil shale. *Div. Pet. Chem. Amer. Chem. Soc.* Detroit, May 9.

LEO R. F. and PARKER P. L. (1966) Branched chain fatty acids in sediments. *Science* **152**, 649.

LOCHTE H. L. and LITTMANN E. R. (1955) *The Petroleum Acids and Bases*. Chemical Publishing Co.

MCLAFFERTY F. W. and GOHLKE R. S. (1959) Mass spectrometric analysis. Aromatic acids and esters. *Anal. Chem.* **31**, 2076.

RAMSAY J. N. (1966) The organic geochemistry of fatty acids. M.S. Thesis, University of Glasgow.

SCHNOES H. K. and BURLINGAME A. L. (1968) Application of mass spectrometry to organic geochemistry. *Topics in Organic Mass Spectrometry* (Editor A. L. Burlingame). Wiley–Interscience, in preparation.

WHITEHEAD W. L. and BREGER I. A. (1963) Geochemistry of petroleum. *Organic Geochemistry* (Editor I. A. Breger) Chap. 7. Macmillan.

Real-Time Data Acquisition, Display, and Subsequent Processing in High Resolution Mass Spectrometry[1]

A. L. Burlingame, D. H. Smith, and R. W. Olsen

Department of Chemistry and Space Sciences Laboratory, University of California, Berkeley, Calif. 94720

The technique of high resolution mass spectrometry has presented rather formidable data acquisition, reduction, and presentation problems. In our efforts to make the task more routine in terms of these problems, a prototype system for obtaining complete high resolution mass spectra has been developed. This system employs real-time recording of the mass spectra with a high speed digital computer. The electron multiplier output of the mass spectrometer is digitized during a high resolution magnetic scan of the spectrum. The digitized raw data are compressed by deletion of all intensities below a preset threshold and stored in the computer memory. The resulting data are then presented on a cathode ray tube (CRT) display, allowing convenient operator interaction with the system. The data may then be either rejected or stored on digital magnetic tape. Subsequent processing of the data yields accurate masses and intensities for all peaks in the spectrum. The system is designed to be flexible in terms of clock and scan rates and in the computer programming for the task of data acquisition. The results presented demonstrate the high quality mass and intensity determination that such a computer coupled mass spectrometer system can routinely provide.

THE PAST FEW YEARS have been marked by an extremely active interest in the high resolution mass spectrometry of organic compounds, since Beynon (*1*) triggered the application of accurate mass measurement to the determination of the atomic composition of organic compounds using a double-focusing instrument. The desirability of obtaining complete high resolution mass spectral data—i.e., where accurate masses of all peaks in the mass spectrum are determined—has been expressed by several workers (*2–4*). The ability to determine this information has proved essential to the mechanistic understanding of the fragmentation patterns of series of related, known compounds and the detailed correlation of spectra of unknown molecules with known carbon skeletal systems in structural and stereochemical studies (*3, 4*).

In the past, primarily two approaches have been utilized to obtain complete high resolution mass spectra in a semi-automated manner. The first of these approaches has concerned the recording of mass spectra on a photographic plate placed in the plane of double focus in an instrument of Mattauch-Herzog geometry. This technique suffers from the limitation of being rather time-consuming because the plate must be exposed, developed, and measured before any mass calculations can be accomplished (*4*). Another limitation has been the generally poor behavior of the photoplate in terms of routinely obtaining reproducible and accurate relative intensity measurements from exposure to exposure. Reproducible high resolution fragmentation patterns are very important in developing interpretative structural and stereochemical correlations among spectra and in studies of hydrogen rearrangements evidenced in peak shifts in the spectra of isotopically labeled molecules.

The second approach has involved analog magnetic tape recording of an exponential scan of a spectrum, using an instrument of Nier-Johnson geometry (*5*). This method appears to have some limitations also. Mass determinations reportedly yield accuracies of about 10 ppm, apparently limited by the performance of the recording system. Also, the low dynamic range of this analog tape system appears to affect adversely the intensity measurement accuracy.

Problems of this nature led us to consider development of a digital recording system, employing a high speed digital computer in real-time for data acquisition during a magnetic scan of a high resolution spectrum—i.e., a system where the data are collected, processed, and stored and/or displayed

[1] Part XIV in the Berkeley Series, High Resolution Mass Spectrometry in Molecular Structure Studies; for Part XIII, see A. L. Burlingame *et al.*, *J. Am. Chem. Soc.*, **89**, 3346 (1967).

(1) J. H. Beynon, "Advances in Mass Spectrometry", J. D. Waldron, Ed., Vol. I, Pergamon Press, London, 1959, p. 328.
(2) P. Bommer, W. McMurray, and K. Biemann, 12th Ann. Conf. on Mass Spectrometry and Allied Topics, Montreal, June 7-12, 1964, p. 428.
(3) K. Biemann, P. Bommer, D. M. Desiderio, and W. J. McMurray, "Advances in Mass Spectrometry," W. L. Mead, Ed., Elsevier, Vol. III, Amsterdam, 1966, p. 639.
(4) A. L. Burlingame, *Ibid.*, p. 701.
(5) W. J. McMurray, B. N. Green, and S. R. Lipsky, ANAL CHEM., 38, 1194 (1966).

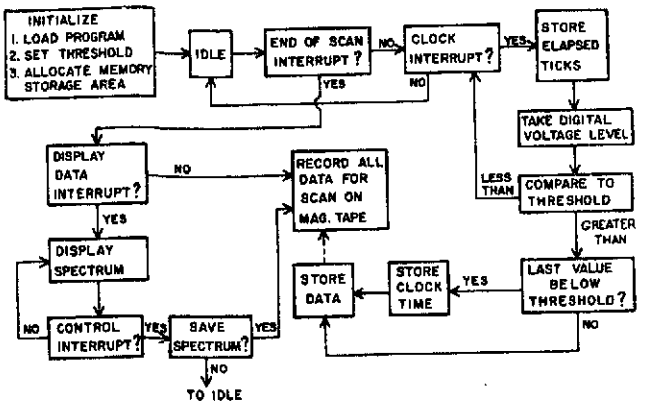

Figure 3. Data acquisition software

written on digital magnetic tape at the discretion of the operator.

A simplified flow chart of the software, or programming, used in the computer during data acquisition is presented in Figure 3. At the time the program is loaded into the computer, various parameters are set. The two most important are mentioned in Figure 3. A binary threshold is selected at this time for later comparison with a measured voltage level. Also selected at this time is the portion of the computer memory used to store the data. This is generally set to provide a 15,360 data point storage capacity. This represents 12 blocks of 1280 words each, which is the eventual magnetic tape format.

The computer then is set to an idle mode. A clock interrupt causes the computer to begin operation. The elapsed number of timing marks are stored by incrementing a clock register. When the A/D has finished conversion, the digital voltage level is read and compared to the preset threshold. (A more efficient approach under development in our laboratory consists of a circuit external to the control processing unit which determines whether each data point is greater than threshold, while simultaneously incrementing the clock count, and thereby transfers to the central processor memory only data points which are above threshold.) If it is less than the threshold, the computer waits for the next clock interrupt. If the voltage level is greater than the threshold, the program determines whether or not the previous level was above the threshold. If it was, the value is simply stored. If not, both the clock time and the voltage level are stored. This process results in a block of data in which up to approximately 500 peaks are separated by time flags at the beginning of each peak voltage profile.

The process is terminated by an end-of-scan interrupt. At this point, the operator may immediately record the data on magnetic tape or he may choose to display the data. The data may be displayed dynamically in a number of ways on the CRT. The whole spectrum may be presented at once, for example, as a display of the peak voltage envelope *vs.* time. In this mode the spectrum resembles a simple line drawing (or analog oscilloscope trace on a storage scope), as the peaks are very narrow compared to the elapsed scan time. Alternatively, the time scale may be expanded to any degree under program control and the peak profiles scanned across the CRT screen sequentially at any chosen rate. This display may be halted at any time by the operator to allow opportunity to study in greater detail peak profiles, dynamic instrument resolution, and relative intensities. When the display mode is complete, the spectrum may be either recorded on magnetic tape or aborted. If these data are chosen to be recorded, the blocks of data for the scan are read from the disk and written on digital magnetic tape. In either case, the computer is automatically reset to idle, at which point the next spectrum scan may be taken.

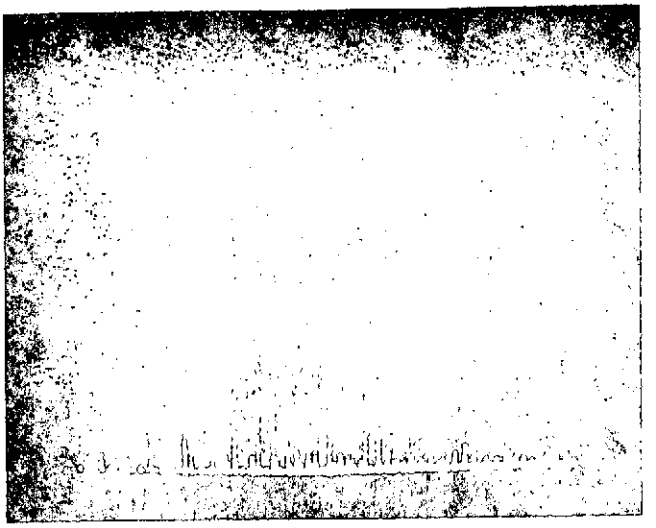

(*a*)

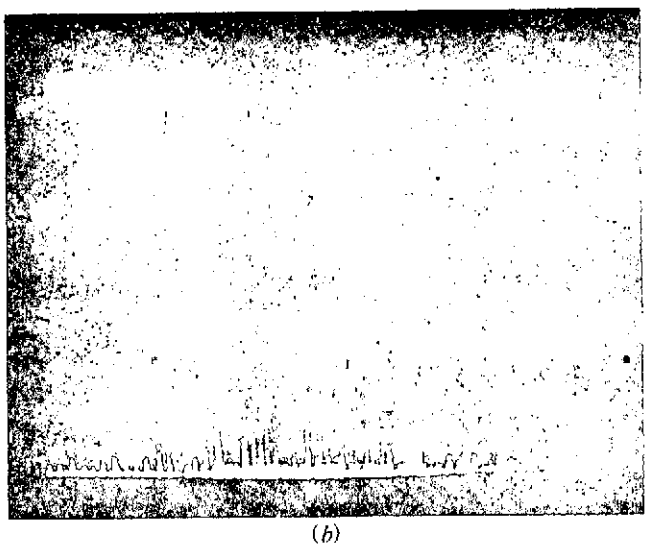

(*b*)

Figure 4. (*a*) CRT display of PFK spectrum; (*b*) CRT display of PFK and ambelline spectra

The CRT display [Digital resolution of CRT is 1024 × 1024 points], which is located adjacent to the mass spectrometer, has proved to be one of the most important parts of the system in terms of convenience. It provides a window whereby the operator can maximize adjustment of instrument parameters to obtain the optimum resolution and sensitivity and the proper beam of calibration compound. It is felt that this type of operator interaction with the system, involving not only the display mode but the degree of control possible in the general scanning procedure, represents a unique advantage of a real-time digital data acquisition and processing system. It is also felt that this interaction should be considered in any future system design because of the versatility and enhanced reliability in obtaining optimal spectral data, which this permits.

Figure 4 presents the CRT display in the complete spectrum mode. The top photograph is the spectrum of perfluorokerosine (PFK), the mass calibration standard, from *m/e* 500 to *m/e* 50. From this display the operator immediately knows that sufficient PFK is available for mass calibration. The bottom photograph presents the spectrum of PFK and ambelline, an alkaloid of *Amaryllidaceae* family, which has a nominal molecular weight of 331. This compound was introduced through the direct insertion lock of the mass spectrometer. It is seen from this display that the spectrum of the alkaloid is of sufficient intensity to permit mass determination of all significant peaks.

Table I. Representative Data for Saturated Ions from Six Successive Scans of *n*-Octadecane

Composition	Exact mass	Calcd mass[a]	Std dev[b]
C_3H_7	43.05477	43.05479	4.5
C_4H_9	57.07042	57.07060	3.7
C_5H_{11}	71.08607	71.08634	6.4
C_6H_{13}	85.10172	85.10209	5.2
C_7H_{15}	99.11737	99.11733	5.1
C_8H_{17}	113.13302	113.13291	6.5
C_9H_{19}	127.14867	127.14810	6.3
$C_{10}H_{21}$	141.16432	141.16450	4.2
$C_{11}H_{23}$	155.17997	155.18139	6.1
$C_{12}H_{25}$	169.19562	169.19741	2.7
$C_{13}H_{27}$	183.21126	183.21172	4.9
$C_{14}H_{29}$	197.22691	197.22717	4.1
$C_{15}H_{31}$	211.24256	211.24224	3.8
$C_{16}H_{33}$	225.25821	225.25876	3.1
$C_{17}H_{35}$	239.27386	239.27348	4.2
$C_{18}H_{38}(M+)$	254.29733	254.29810	5.6

[a] Mean of six determinations.
[b] Standard deviation of the mean, ppm.

The basic steps in the data reduction programming are summarized in Figure 5. As was mentioned previously, this procedure is closely related to that used in photoplate data reduction. The programming is designed to elicit the maximum amount of the available information in a high resolution mass spectrum. The procedure, which is handled entirely by a Control Data Corp. Model 6600 computer system, begins with the raw data tape generated by the data acquisition system. The tape, with any number of spectra, is read and the data are searched to identify the time flags at the beginning of each peak voltage profile. Peak positions may be determined by three methods currently under investigation: peak tops, centers of gravity, or curve fitting techniques.

Peak intensity data is determined according to the position criterion used. Maximum intensity is used for peak top data, peak areas or peak tops are used for center of gravity positions, and both peak maxima and areas are under evaluation for the curve fitting approach.

The exact masses and times of three calibration points at the low mass end of the data are then chosen from the output of the peak position and intensity determination procedure. The positions of the rest of the PFK peaks are determined by extrapolation using a three-term polynomial of the form $M = A + BT + CT^2$. [It is generally found that this polynomial approximates the mass *vs.* time dependence accurately enough to predict the time of the next PFK peak within the time width of the peak.] When this process is complete, masses of all remaining lines are calculated by interpolation using the calibration points four at a time in a polynomial of the form $M = A + BT + CT^2 + DT^3$.

PFK peaks are then removed from the data and possible elemental compositions for the remaining peaks are determined. This process is accomplished using an algarithm to determine generated compositions that may include any of the elements and their isotopes found in organic molecules. The resulting data are sorted according to the heteroatom content of each peak and presented in graphic form using the Cal-Comp Plotter. The details and advantages of this heteroatomic plotting technique, which has been developed specifically to aid in interpretation of high resolution mass spectral data, have been discussed previously (*10, 11*).

(10) A. L. Burlingame, Euchem Conference on Mass Spectrometry, Sarlât, France, Sept. 7–12, 1965.
(11) A. L. Burlingame and D. H. Smith, unpublished data.

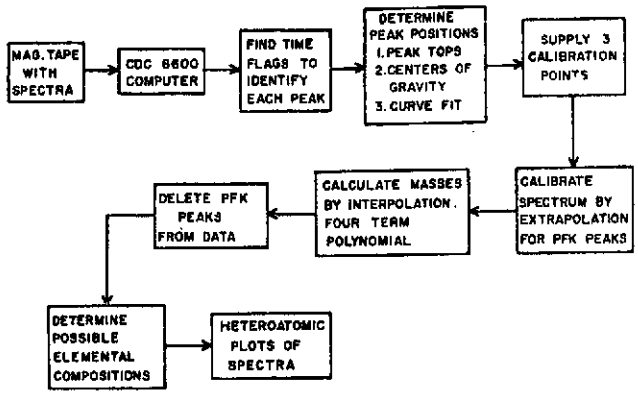

Figure 5. Data reduction programming

RESULTS

Mass Measurement. One of the primary investigations of interest was the degree of mass measurement precision and accuracy that could be attained with this system. This was evaluated at different scan and clock rates. Because of instrument sensitivity limitations at the high resolutions used (1:20,000), the fastest scan studied was one of 40 seconds duration for *m/e* 800 to *m/e* 15, or proportionately faster for a shorter mass range. At a clock rate of 15 kHz, mass measurement precision and accuracy is about 8 ppm. Of special interest, however, are results obtained in slower scans that are applicable to all situations, including a coupled interrupted-elution gas chromatograph–mass spectrometer system (R. P. W. Scott, Unilever Research Laboratory, personal communication, April 1967) and direct sample insertion systems. The particular set of system parameters studied in most detail utilized the spectrum of *n*-octadecane ($C_{18}H_{38}$). A hydrocarbon was chosen simply because there can be no doubt about the elemental composition and thus the mass of all fragment ions, which makes mass measurement accuracy easy to evaluate. The scan rate was 100 seconds from *m/e* 300 to *m/e* 30, at a clock rate of 12 kHz. This yields 30 to 50 data points per peak profile at a resolution of 1:20,000.

Six successive scans were recorded and analyzed. The difference in elapsed times between *m/e* 305 ($C_8F_{11}^+$, *m/e* 304.98242) and *m/e* 31 (CF^+, *m/e* 30.998402) for the six scans was a maximum of 300 clock pulses out of a total of 1.2 to 10^6 pulses. This sort of reproducibility is extremely promising. It indicates that future calibration of a spectrum can be simplified by use of expectation times to identify calibration peaks, rather than the more complex extrapolation procedure used at the present time, which requires that three peaks be specified from the raw data. Analysis of these data, using both peak tops and centers of gravity as peak position criteria, indicates that centers of gravity yield much more precise results. Centers of gravity were used in all calculations which are discussed below. The standard deviations of the determined masses in the six scans averaged about 4 ppm. Some representative data are included in Table I. The data in Table I are presented in Figure 6. The mean of the six determinations is indicated, and the brackets indicate the standard deviations, both of which are expressed in this case in millimass units rather than parts per million. In general, the greater errors are obtained for peaks of low intensity (less than 5% of base peak, *m/e* 57). This appears to be a result of the poorer definition of peak profile for these low intensity peaks, resulting probably in part from ion statistical considerations and in part from poorer signal to noise ratio.

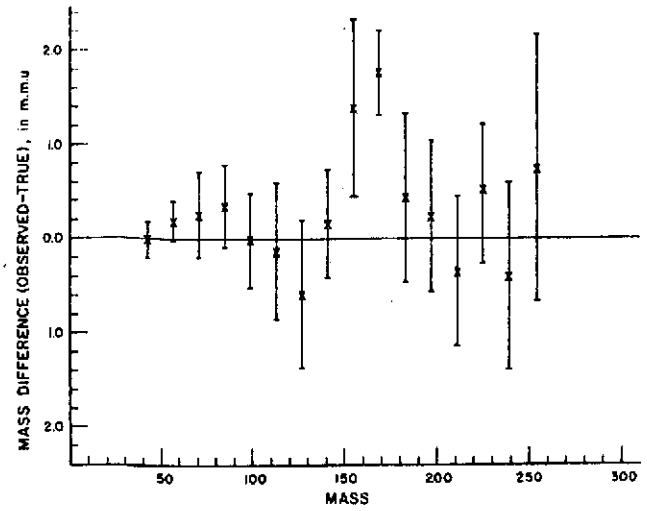

Figure 6. Data from Table I, presented as mass difference (average of the six scans), observed-true mass, in millimass units (mmu) *vs.* mass. Brackets indicate standard deviations

Mass measurement accuracy is of the order of mass measurement precision as reflected in the means listed in Table I. It is important to note that errors of this magnitude are sufficiently small to minimize determination of ambiguities in elemental compositions (*5*).

The smoothness of the mass *vs.* time function was evaluated in the following manner. Because the calibration points are used four at a time to calculate masses, masses of all peaks except those at the extremities of the calibration range can be calculated by interpolation three times, using three different sets of four calibration points. In no mass region did these three determinations differ significantly from one another, as compared to the standard deviations in Table I. This indicates that the function is very smooth and is being approximated adequately by the four-term polynominal in the present system.

What is most important, however, is that mass measurement errors are only slightly greater than the time resolution of the system. For example, at *m/e* 30, the time duration between two timing marks represents a mass difference of about 4 ppm (0.12 mmu). At *m/e* 300, this mass difference is about 1 ppm (0.3 mmu). (See error curve, Figure 2.) It is felt, then, that mass measurement accuracy may be substantially improved by implementation of higher clock rates.

Table II. Representative Data from Spectrum of 6-Hydroxycrinamine, Determined Both by Photoplate and Real-Time System

Composition[a]	Calculated Mass		Error[b]	
	Photoplate	Real-time	Photoplate	Real-time
$C_{17}H_{19}NO_5$	317.1293	317.1283	3.0	2.0
$C_{16}H_{15}NO_4$	285.0986	285.0995	−1.4	−0.5
$C_{16}H_{14}NO_3$	268.0985	268.0980	1.2	0.7
$C_{15}H_{14}NO_3$	256.0981	256.0967	0.7	−0.7
$C_{14}H_{11}O_3$	227.0713	227.0711	0.5	0.3
$C_{14}H_9O_2$	209.0616	209.0607	1.3	0.4
$C_{12}H_9O$	169.0642	169.0657	−1.1	0.3
$C_{11}H_9$	141.0700	141.0699	−0.4	−0.5
C_9H_7	115.0548	115.0540	0.0	0.8

[a] Assigned on basis of calculated mass for single measurement.
[b] Error in millimass units (mmu), calculated mass.

Intensity Measurement. Two criteria for relative ion beam intensities have been investigated in some detail—e.g., peak tops and peak areas. Generally speaking, intensities based on peak tops give good qualitative descriptions of the fragmentation pattern. This is illustrated in Figure 7, where both the low and high resolution spectra of *n*-octadecane are presented. From the high resolution data, there can be no doubt that one has the spectrum of a straight chain, saturated hydrocarbon ($C_{18}H_{38}$). From a quantitative standpoint, however, these determinations leave a great deal to be desired. In the above mentioned six scans, for example the standard deviations of relative intensities are about 10% of the peak height.

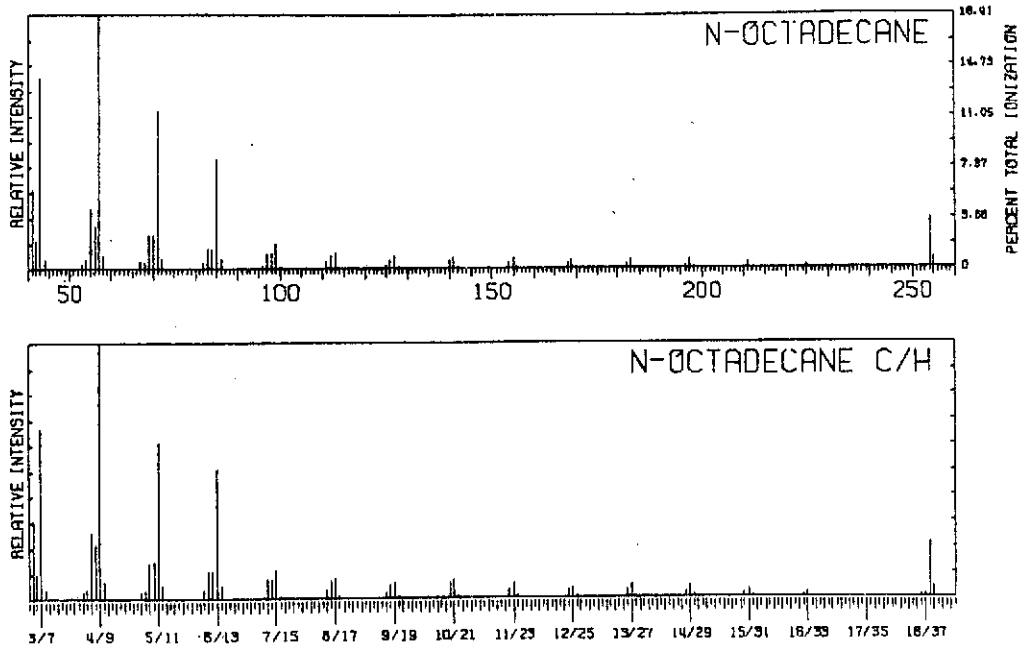

Figure 7. Low resolution spectrum and heteroatomic plot of high resolution data for *n*-octadecane

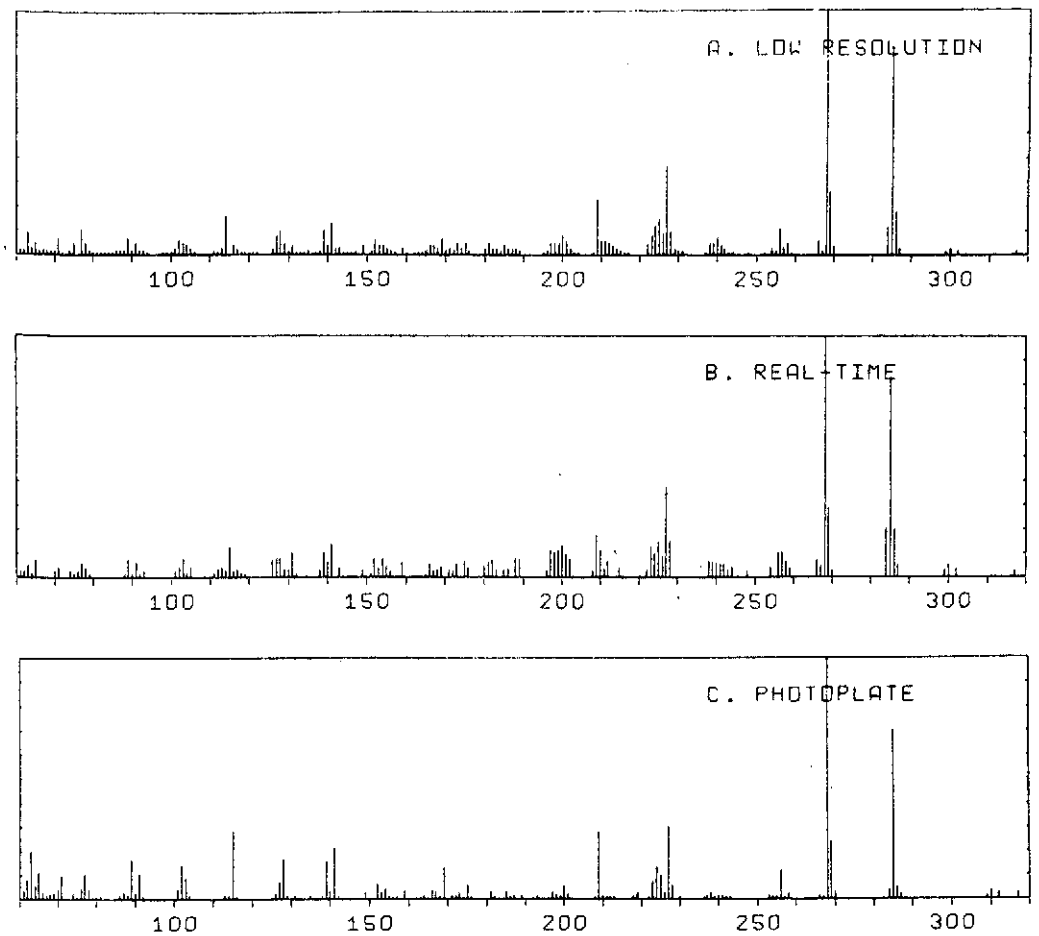

Figure 8. Comparison of data for 6-hydroxycrinamine: (*a*) low resolution spectrum; (*b*) summed intensities of high resolution, real-time data; and (*c*) summed intensities of high resolution photoplate data (antilog % transmission measurements, corrected for the emulsion H/D curve)

Peak areas yield better reproducibility. Standard deviations of relative intensities are 2 to 4% of peak height. If a scanning function other than exponential is used, the change in peak width with mass must be taken into account. In the case of the discussed function, peak widths vary as mass$^{1/2}$. When this correction is applied to the raw areas, quite good agreement with the low resolution spectrum is obtained. It is hoped that curve fitting techniques being developed will provide more quantitative results. This problem is receiving a great deal of attention at this time to further improve the worth of the technique for peak intensity determination.

Two specific applications of the above techniques will serve to indicate the quality of data that may be obtained with this system. One application involved the spectra of several alkaloids of the *Amaryllidaceae* (*12*) obtained by direct introduction of the samples into the ion source. These spectra had all previously been obtained by the photoplate technique, so that a comparison of the methods was possible. In terms of mass measurement, the real-time systems leads to much more consistent results. The word consistent refers to mass measurement errors, which in the real-time system are all of the same order as the time resolution of the system, as was mentioned above. The photoplate data generally exhibit a greater variation in differences between calculated and assigned masses. One must keep in mind that this is primarily a measuring system limitation (*4*). It is felt, however, that the very promising results obtained so far with the real-time system indicate that this method is capable of greater mass measuring accuracy. Some representative data are included in Table II.

As far as intensity measurements are concerned, the low resolution intensities obtained by summing the intensities (peak top) to each nominal mass in the real-time data yield much better agreement with the observed low resolution intensities than do the photoplate data. This is illustrated in Figure 8, where the top spectrum (*a*) is the low resolution data, (*b*) the summed real-time intensities, and (*c*) the summed photoplate intensities for the spectrum of 6-hydroxycrinamine.

A second application involves the spectra of tetrahydro-*N*-acetylpyrrole and three deuterated analogs. Although the mass spectrometer is not capable of resolving masses differing by two hydrogens *vs.* a deuterium atom, the inclusion of an internal mass standard permits mass measurement accuracies capable of distinguishing between the two possibilities. Indeed, it was found that the deuterium content of nearly every peak could be determined by a simple comparison of differences between observed mass and masses of compositions including any number of deuterium atoms. The lowest difference yields the correct deuterium content. In those few cases where there are significant contributions of both compositions (2 hydrogens *vs.* D) to an observed peak, the observed measured mass generally lies intermediate between the two masses calculated on the basis of elemental composition. Some representative data are included in Table III.

(12) A. L. Burlingame, P. Longevialle, H. M. Fales, and R. J. Highet, *J. Am. Chem. Soc.*, submitted.

Table III. Representative Data from Unlabeled and Labeled *N*-Acetyltetrahydropyrroles

Ion[a]	Calculated mass[b]	Possible composition[c]	Exact mass	Diff.[d]
M+(d_o)	113.08380	$C_6H_{11}NO$*	113.08406	0.2
		C_6H_9NO D_1	113.08242	−1.4
m/e 98 (d_o)	98.06106	C_5H_8NO D_1	98.05897	−2.1
		C_5H_8NO*	98.06058	−0.5
M+(d_{2a})	115.09600	C_6H_7NO D_3	115.09480	−1.2
		C_6H_9NO D_2*	115.09643	0.4
		$C_6H_{11}NO$ D_1	115.09807	2.0
m/e 100(d_{2a})	100.07263	C_5H_6NO D_2*	100.07296	0.3
		C_5H_8NO D_1	100.07460	2.0
M+(d_{2b})	115.09682	C_6H_7NO D_3	115.09480	−2.0
		C_6H_9NO D_2*	115.09643	−0.4
		$C_6H_{11}NO$ D_1	115.09807	1.2
m/e 100(d_{2b})	100.07280	C_5H_6NO D_2*	100.07296	0.1
		C_5H_8NO D_1	100.07460	1.8
M+(d_3)	116.10333	C_6H_8NO D_3*	116.10262	−0.7
		$C_6H_{10}NO$ D_2	116.10426	0.9
m/e 98(d_3)	98.06121	C_5H_5NO*	98.06058	−0.6
		C_5H_6NO D_1	98.05895	−2.2

[a] d_o indicates unlabeled molecule; d_{2a} indicates 2,2-d_2;

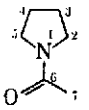

d_{2b} indicates 3,3-d_2;
d_3 indicates 7,7,7-d_3.
[b] From real-time data.
[c] * indicates assigned composition.
[d] Diff. in mmu.

Because these spectra exhibit multiplets at all important peaks below *m/e* 80 (CH_2 *vs.* N, CH_4 *vs.* O, or NH_2 *vs.* O), interpretation of peak shifts in the spectra of the deuterated compounds is an impossible task on the basis of the low resolution spectra only. Intensities (peak top) of the real-time data, where these multiplets are separated and deuterium content determined, are sufficiently quantitative to yield a clear formulation of the fragmentation process occurring in this system (*13*).

(13) A. L. Burlingame and J. Tesarek, Space Sciences Laboratory, University of California, Berkeley, unpublished data, 1967.

CONCLUSIONS

A system for acquiring high resolution mass spectral data in real-time employing a digital computer has been developed. At this stage of development, the real-time data acquisition system followed by data reduction provides extremely accurate mass measurements and reasonable intensity data. It is felt that this system offers several advantages over previous methods for determining this data, including not only present capabilities but future potentialities for enhancement of accuracy in mass and intensity determinations. The high quality data presented, coupled with the flexibility, rapidity, and ease of such digital data acquisition, represents a significant state of the art advance in high resolution mass spectrometry.

The use of a digital computer for techniques of this nature offers additional advantages. In a real-time system, the capability exists not only for data acquisition but also for a considerable amount of actual data reduction while the scan of the spectrum is taking place. An obvious goal is to provide the final output of masses, elemental composition, and intensities in suitable form for interpretation in a turn-around time of 2 or 3 minutes.

An additional advantage of the computer is its capability for interaction both with the operator and with the mass spectrometer in terms of control of the various instrument and scanning parameters.

It may be of some interest to note that the data reduction procedure discussed above requires, from raw data to final plotted output, 20–30 seconds of 6600 central processor time for the averge spectrum.

ACKNOWLEDGMENT

The authors wish to express their thanks to Jan Hauser for developing the data acquisition and CRT display programming; to Robert E. Furey and B. R. Simoneit for engineering and technical assistance; and to the Lawrence Radiation Laboratory (Berkeley) Computer Center.

RECEIVED for review July 28, 1967. Accepted October 16, 1967. Research presented in part at the 15th Annual Conference on Mass Spectrometry and Allied Topics, Denver, May 14–19, 1967 and the ACS Division of Physical Chemistry Special Conference on Computers in Chemistry, LaJolla, June 26–30, 1967. Financial support provided by the National Aeronautics and Space Administration (NsG 101; NGR 05-003-134; NsG 243, Suppl. 5). D. H. S. was the recipient of a NASA Predoctoral Fellowship during 1965–67.

Organic Mass Spectrometry, 1968, Vol. 1, pp. 139 to 149. Heyden & Son Limited. Printed in Northern Ireland

HIGH RESOLUTION MASS SPECTROMETRY IN MOLECULAR STUDIES. PART XVII[1].

EVIDENCE FOR RING CONTRACTIONS IN MOLECULAR IONS: THE FRAGMENTATION OF N-ACETYLMORPHOLINE*

J. M. TESAREK, W. J. RICHTER and A. L. BURLINGAME

Department of Chemistry and Space Sciences Laboratory, University of California, Berkeley, California 94720

(*Received* 23 *January* 1968)

Abstract—In comparing N-acetylmorpholine to closely related systems, two major differences in fragmentation are observed. M-15 and M-43 fragments, although quite common to such systems, are unusual with respect to their genesis. Formation of the M-15 fragment by loss of C-3 instead of the anticipitated loss of C-2 or C-8 is evident from shifts in the spectra of deuterated analogs. The M-43 species arises from total loss of the N-acyl substituent rather than the usual two-step loss of ketene plus a ring hydrogen. These data are presented in support of mechanistic rationale involving radical induced ring contraction to a common intermediate molecular ion. Techniques of high resolution mass spectrometry and isotope labeling have been employed to substantiate certain mechanistic details.

INTRODUCTION

IN CONTRAST to the well-established[2] energetically favorable hydrogen migration processes occurring upon electron bombardment of organic molecules, the frequent occurrence of skeletal rearrangement is only recently being recognized and subjected to mechanistic scrutiny.[3] The possibility of ring contraction as a type of more deep-seated skeletal rearrangement of molecular ions was first suggested as a rationale for the genesis of the intense *m/e* 69 fragment from *trans*-Δ^3-10-methyl-2-octalone.[4] Similarly, ring contraction was invoked to account for the ease of elimination of ketene from the molecular ions of 4,4-dimethylcyclohexan-2-one and related cyclic hexenones.[5]

While these ring contraction processes are probably best interpreted as proceeding *via* ionic reaction centers, this paper presents evidence that the unusual losses of methyl and acetyl moieties from the molecular ion of N-acetylmorpholine may proceed *via radical* induced ring contraction.

Even though several studies of saturated heterocyclic compounds containing only one heteroatom have been published,[6] investigations of analogues containing more heteroatoms are relatively rare. Certain aspects of the mass spectra of piperazines, their alkylated derivatives,[6b] and saturated ring systems bearing several oxygen[7a] and sulfur[7b] atoms have been presented.

The compounds dealt with in this report are mainly N-acetylmorpholine (I) and

* Financial support was provided by the National Aeronautics and Space Administration, Grants NsG 101 and NGR 05-003-134.

several labeled analogs. These include 2,2-d_2-N-acetylmorpholine (II), 3,3-d_2-N-acetylmorpholine (III), 2,2,3,3,d_4-N-acetylmorpholine (IV), and 8,8,8-d_3-N-acetylmorpholine (V):

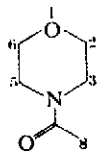

I

Fragmentation of N-acetylmorpholine

M^+ *and* M-1 *ions.* The mass spectrum of (I) displays a molecular ion M^+ at *m/e* 129 with an abundance of approximately 10% of the total ionization. The accompanying M-1 peak is of much lower intensity and is regarded as being due to a species formed by the loss of a hydrogen atom alpha to the nitrogen (C-3) in analogy to simple alicyclic amines[7c] and their acylated derivatives.[8] However, no direct evidence is available from these data for this assignment, since none of the deuterated analogs show corresponding shifts to M-2 to any major extent. The operation of an isotope effect which strongly discriminates against deuterium must therefore be inferred, as has in fact been observed in the case of pyrrolidine-2,2-d_2 and piperidine-2,2-d_2.[6c]

M-15 *ions.* The occurrence of M-15 peaks is quite common in the spectra of N-acetyl derivatives of simple aliphatic[9] and heterocyclic amines.[10] Loss of the methyl group from the N-acetate moiety is frequently observed for N-substituted acetamides,[10] but is generally not an important process except for the lowest members of this class, limited in the number of fragmentation pathways available. A rather prominent CH_3 loss of this type, however, is exhibited by a related heterocyclic system, N-acetylpyrrolidine:[8]

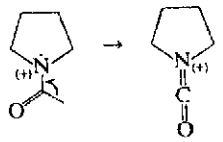

In contrast to this datum, the next higher homolog, N-acetylpiperidine, eliminates mainly the methylene group beta to nitrogen, together with an alpha hydrogen in the formation of a comparably abundant M-15 species.[11] The process may be considered to proceed in several steps:

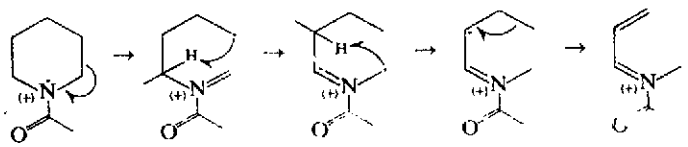

An analogous loss of the CH_2-group beta to nitrogen, together with a hydrogen atom from the opposite alpha position, has been reported for piperidine and its N-methylated derivative.[6c]

Surprisingly, the elimination of a methyl radical in N-acetylmorpholine (I) represents the loss of completely different atoms, namely of a carbon atom alpha to

nitrogen and a hydrogen atom from the adjacent beta position rather than the opposite side of the ring, depicted schematically:

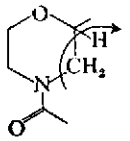

This is evident from the following mass shifts observed in the spectra of the labeled compounds II–V (see Table 1). In the spectrum of 8,8,8-d_3-N-acetylmorpholine (V), the peak is shifted almost completely from *m/e* 114 in the unlabeled compound to *m/e* 117 indicating that the methyl group of the acetate is almost totally retained.

TABLE 1. MAJOR PEAKS IN THE MASS SPECTRA OF N-ACETYLMORPHOLINE AND DEUTERIUM-LABELED ANALOGS

	M+	M-15	M-43	M-72	M-73	M-86
I 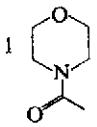	129	114	86	57	56	43
II 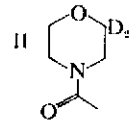	131 (87%)	116 (70%)	88*	57 (33%)	56 (16%)	43*
	130 (13%)	115 (32%)		59 (30%)	58 (15%)	
III 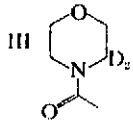	131 (99%)	116 (53%)	88*	59	58	43*
	130 (1%)	114 (35%)				
IV 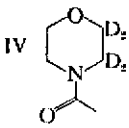	133 (83%)	115 (27%)	90*	59 (30%)	58 (?0–17%)	43*
	132 (17%)	118 (60%)		61 (31%)	60 (?0–15%)	
V 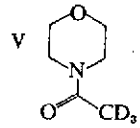	132 (93%)	117	86*	58	56 (27%)	46*
	131 (7%)				57 (?0–10%)	

* Main shift observed.

Positive evidence for the source of the carbon atom lost and the origin of the transferred hydrogen stems from the spectra of the 2,2-d_2- and 3,3-d_2-analogs, II and III, respectively. In these spectra the peak splits between *m/e* 115 and 116, and *m/e* 114 116, respectively. In addition, the peak in the spectrum of the 2,2,3,3-d_4-compound splits mainly between *m/e* 115 and 118, with small contributions observed at *m/e* 116 and 117.

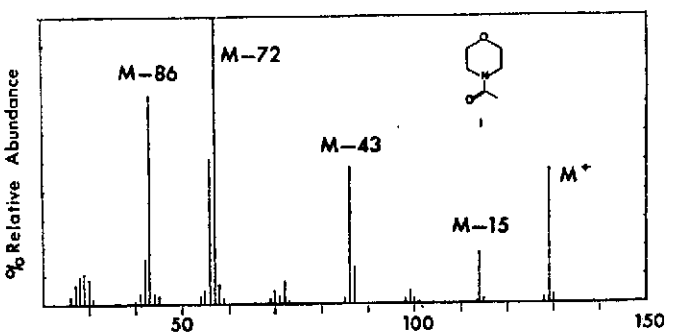

FIG. 1. Mass spectrum of N-acetylmorpholine.

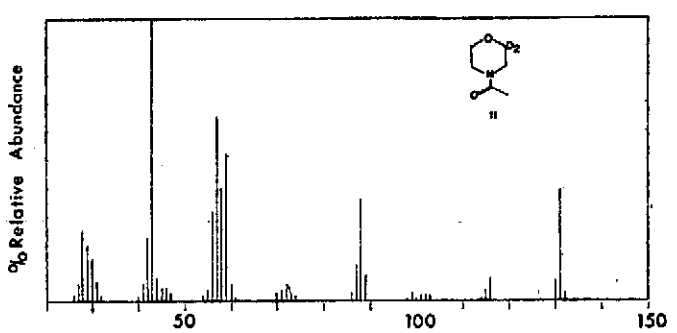

FIG. 2. Mass spectrum of 2,2-d_2-N-acetylmorpholine.

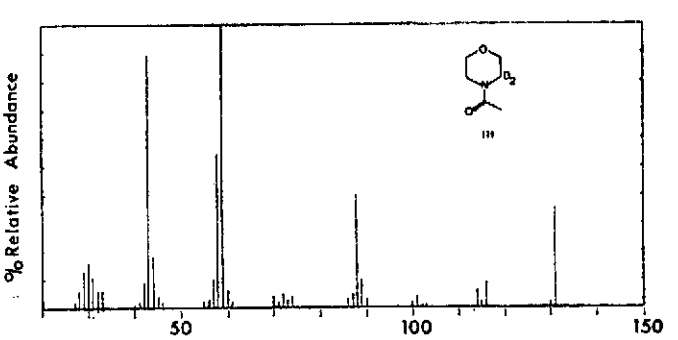

FIG. 3. Mass spectrum of 3,3-d_2-N-acetylmorpholine.

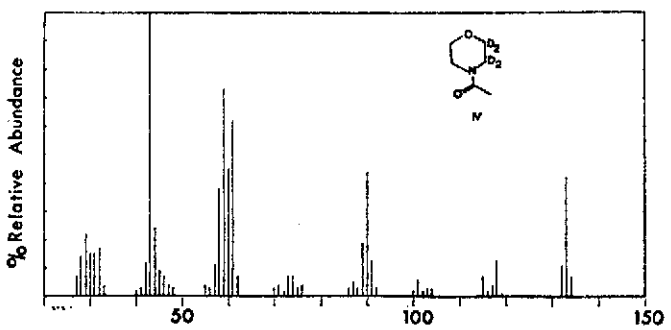

FIG. 4. Mass spectrum of 2,2,3,3-d_4-N-acetylmorpholine.

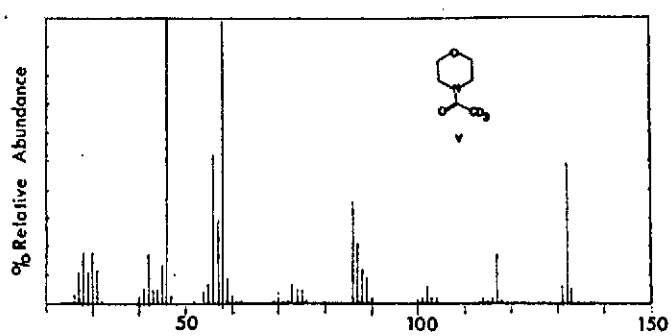

FIG. 5. Mass spectrum of 8,8,8-d_3-N-acetylmorpholine.

Formally, this methyl loss represents rupture of two bonds to C-3 as well as to C-2, one rupture even involving a C—N linkage, which is not believed to occur readily as a one-step process. Obviously, a sequence of several events is required to result in such a complex fragmentation process. A slow overall process may be reflected in the associated, unusually large metastable peak. It is interesting, however, to note that this process remains important (in contrast to most others) even at low ionizing voltages.

The genesis of the M-15 fragment itself appears rather plausible if normal alpha-cleavage, as exhibited by aliphatic amides, is assumed to be followed by an attack of the primary radical thus generated on the conjugated π-system of the acyl-immonium ion. This formation of a "new bond"[12] causing cyclization of the open molecular ion $M_{1(1)}$ to a rearranged molecular species $M_{1(2)}$ would reflect an alternative mode of radical reactivity which is probably much more general than now recognized and acknowledged,* and apparently capable of competing successfully with the commonly

* It may seem ironic that one of the few and earliest suggested cases of radical addition to double

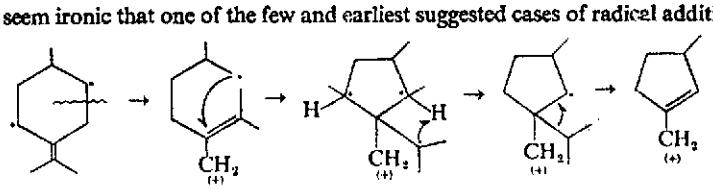

bonds, namely loss of C_3H_7 from $\Delta^{4(8)}$-Menthene[13] has been regarded invalid on grounds of demonstrated unsymmetrical hydrogen abstraction from the marked equivalent positions.[14]

observed hydrogen-abstraction cleavage type of fragmentation:

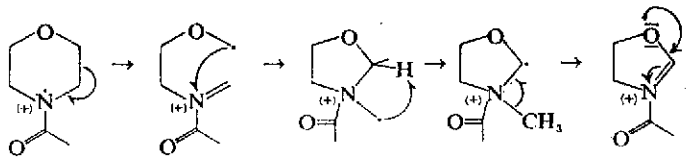

M_0 $M_{1(1)}$ $M_{1(2)}$ $M_{1(3)}$ M-15

The radical attack on the double bond would transfer the necessary reactivity required for the subsequent hydrogen abstraction to the alpha-carbon atom and, in addition, leave the originally adjacent hydrogen atoms in a unique position exactly as demanded by the established selectivity of the β-abstraction step. The preferential H-transfer in a four-membered transition state could be interpreted as a consequence of favorable product development control, since only a radical site flanked by both heteroatoms can trigger the loss of a methyl radical, resulting not only in regeneration of the original conjugated acyl-immonium structure, but also gaining additional stabilization by incorporating the second heteroatom into the resonance system. Thus, considerable overall driving force might be mobilized for a process possibly involving endothermic phases. Polar effects, which would facilitate the abstraction of a hydrogen atom from the particular environment, might be of additional importance.

M-43 *ions*. The commonly observed formation of an M-43 species in substituted acetamides involves a two-step process.[10] A sequence $M^+ \rightarrow M\text{-}1 \rightarrow M\text{-}43$, consisting of loss of a hydrogen atom alpha to nitrogen and the elimination of a neutral molecule of ketene is frequently indicated by the presence of proper metastable peaks. The reverse sequence of these steps might also function. Such behavior is shown, for instance, by N-acetylpyrrolidine[8] and, to a major extent by N-acetylpiperdidine[11] also.

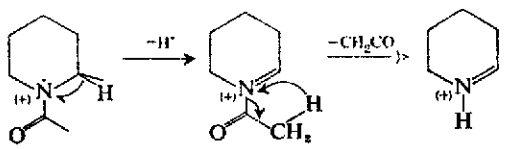

If such a two-step loss were operative in the case of N-acetylmorpholine, splitting of the *m/e* 86 peak in the unlabeled compound between the masses 87 and 88 would be expected for 3,3-d_2-N-acetylmorpholine (III) and a quantitative shift from 86 to 87 anticipated for 8,8,8-d_3-N-acetylmorpholine (V). The spectrum of 2,2,3,3-d_4-N-acetylmorpholine (IV) should also show a splitting between *m/e* 88 and 90.

As in the case of the previously discussed M-15 fragment, the expected shifts are not those observed, thus clearly establishing that this mode of fragmentation does not prevail as in closely related systems. Nevertheless, the high resolution spectrum shows the peak to consist of practically only one species of the composition C_4H_8NO, formally corresponding to the loss of CH_3CO from the molecular ion.

From the spectrum of the 8,8,8-d_3-N-acetylmorpholine (V) and the presence of a metastable peak at *m/e* 57·4, it can be deduced that the elimination of the acetyl group

proceeds in a single step with predominantly no hydrogen transfer between the ionic species and the CH_3CO radical eliminated. This deviation from the two-step H/CH_2CO elimination is again readily explained on the basis of the two rearranged molecular ions $M_{1(2)}$ and $M_{1(3)}$:

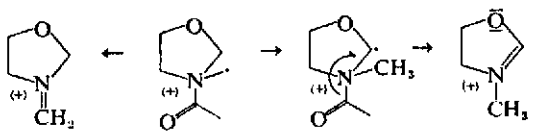

M-43 $M_{1(2)}$ $M_{1(3)}$ M-43

The elimination of CH_3CO as an integral unit would appear to be a process competing with the elimination of the CH_3-radical or at least to be related to the latter process by a common root in their formation. As might be expected in this case, the process remains of considerable significance at lower ionizing voltages.

The rather unambiguous shifts are accompanied, however, by minor contributions indicative of isotope scrambling between the positions 2 and 8, and even 3 to a lesser extent. This probably reflects some interaction of the radical reaction center with geometrically available positions of its environment prior to the terminating cleavage event[15]. Such relatively common processes, frequently of only secondary importance, are consistent with observations that radical-type hydrogen transfer is usually a more rapid reaction than the final cleavage step. The intermediate molecular ion $M_{1(2)}$, for example, would probably permit a rapid multistep exchange of hydrogen atoms leading to a certain loss of identity of hydrogen atoms at the positions affected and denoted for the sake of brevity by double fishhooks:

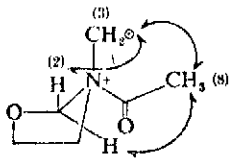

Evidence for isotopic interchange between these positions stems from the presence of the smaller satellite peaks at M-45, M-44 and M-43 in the spectrum of the 8,8,8-d_3-compound (V) accompanying the main loss of CD_3CO (M-46). Corresponding transfer in the opposite direction, namely interchange with C-8, is evident from the spectrum of 2,2-d_2-N-acetylmorpholine (II). The satellites are now observable for losses of increasing masses, (M-44 and M-45). The 3,3-d_2-analog (III) exhibits the same pattern with somewhat lower ion abundances. The decrease of intensity for contributions reflecting gain or loss of more than one label is expected from probability considerations.

M-30 *ions.* Although the loss of 30 mass units produces the base peak of the mass spectrum of morpholine,[11] the corresponding loss in N-acetylmorpholine represents only about 1% of the total ionization. From high resolution data, the M-30 ion is demonstrated to be homogeneous in composition, consisting of C_5H_9NO exclusively. This corresponds to the loss of a molecule of formaldehyde, and a consideration of the

mass spectra of the series of deuterated compounds shows unambiguously that the ether oxygen and the adjacent ring carbon atom are implicated in this loss. The low abundance of the ion as compared with morpholine itself is probably a consequence of further degradation pathways available for the acetylated species, particularly those leading to the most abundant fragments *m/e* 56 and 57.

m/e 56 *and* 57 *ions.* The very abundant ions of mass 57 and mass 56 (i.e., M-72 and M-73) have been shown by high resolution mass measurements to be predominantly C_3H_7N and C_3H_6N. These data indicate losses of $C_3H_4O_2$ and $C_3H_5O_2$ from the molecular ion, necessarily at least two-step processes since the parent molecule does not contain three adjacent carbon atoms. There is a certain ambiguity in the interpretation of their genesis, since these ions can arise from several sequences of steps. A peak group analysis reveals retention of the carbon atoms alpha to the nitrogen atom, as well as retention of the attached hydrogen atoms. Consideration of the mass spectrum of 8,8,8-d_3-N-acetylmorpholine suggests that the peak at *m/e* 56 results from the formal loss of the entire acetyl group with *all of its hydrogen atoms.* A smaller peak at *m/e* 57 in the mass spectrum of the d_3-compound implies that, to a lesser degree, one of the deuterium atoms from the tri-deuterio-acetate group is transferred to the charged fragment and retained. The 2,2-d_2- and 2,2,3,3-d_4-N-acetylmorpholine spectra show shifts and splits indicative of loss of one of the carbon atoms alpha to the ether oxygen, loss of the attached hydrogen atoms, and loss of the ether oxygen. These fragmentation patterns present several possibilities, of which the occurrence of at least two is indicated by the presence of metastable peaks:

$$\text{(a)}\ \text{M} \xrightarrow{m^*} \text{M-43} \xrightarrow{m^*} \text{M-73}$$

$$\text{(b)}\ \text{M} \xrightarrow{m^*} \text{M-42} \xrightarrow{m^*} \text{M-72} \xrightarrow{m^*} \text{M-73}$$

Analogously to the cyclization of the molecular ion, two alternative ways of new bond formation are conceivable for sequence (b), leading to three- and four-membered species of *m/e* 57.

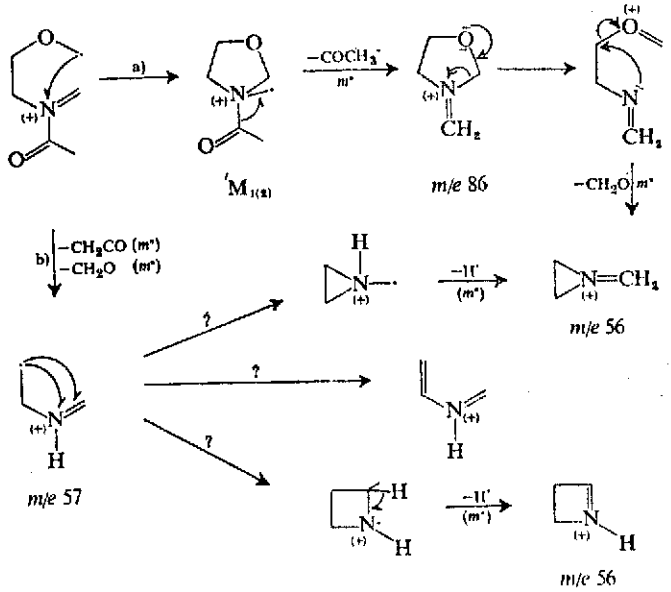

The final step, loss of a hydrogen radical from these species, would account for the observed split of the M-73 peak between the masses 56 (major component) and 57 (minor component) in the case of the 8,8,8-d_3-compound.

m/e 43 *ions*. The second largest peak (approximately 10% of the total ionization) of the mass spectrum of N-acetylmorpholine is recorded at *m/e* 43. The composition of this ion has been established by high resolution mass spectrometry to be mostly C_2H_3O, with only small contributions from C_2H_5N and C_3H_7. From the series of deuterated derivatives, it can readily be seen that this peak remains at *m/e* 43 for all compounds except for 8,8,8-d_3-N-acetylmorpholine, where it shifts quantitatively to *m/e* 46, showing that cleavage of the nitrogen-carbonyl bond with charge retention on the carbonyl fragment has occurred, either in the original or rearranged molecular ion or at some later stage of the fragmentation. A peak at *m/e* 43 of varying degrees of prominence is more or less ubiquitous in the mass spectra of primary, secondary, and tertiary acetamides.[10,11] This ion seems to become more important in alicyclic amides where the nitrogen is part of the ring system, probably because its formation would require only one bond cleavage, not (like other fragments) requiring cleavage or rearrangment in the ring. *m/e* 43, corresponding mainly to CH_3CO ions as shown by high resolution measurements and deuterium labeling, forms the base peak of the mass spectrum of N-acetylpyrrolidine,[8] N-acetylpiperidine,[11] and N-acetylhexamethyleneimine.[13]

DISCUSSION

The two unusual features of the fragmentation behavior of N-acetylmorpholine are the origins of the atoms expelled and the nature of the processes involved in the formation of M-15 and M-43 fragments. In order to ascertain the generality or scope of these modes of fragmentation, comparisons have been made with closely related systems.

As previously stated, this process involving alpha-carbon loss in I is absent in piperidine[6c] and its N-methylated derivative,[6c] since the carbon atom of the CH_3 radical eliminated stems mainly from the beta-position. Introduction of an oxygen atom into the ring system leading to morpholine[11] and N-methylmorpholine[11] still does not favor loss of the carbon atom alpha to nitrogen, in spite of its close relationship to N-acetylmorpholine. In fact, loss of methyl is now almost entirely suppressed. Absence of the nitrogen atom in the six-membered saturated ring does not change this behavior; tetrahydropyran exhibits only a negligible M-15 peak.[6c] For the sulfur analog, tetrahydrothiopyran, a substantial loss of CH_3 from the alpha position has been reported recently.[6g] The hydrogen atom transferred is abstracted in this case largely from one of the beta positions, possibly in analogy to N-acetylmorpholine (I). From these data obtained by symmetrical labeling it is unfortunately not obvious whether the adjacent position is involved specifically.[6g] In the absence of a second heteroatom any selectivity of the transfer step should be reduced, also allowing for the observed gamma-abstraction.

For acyclic amines, loss of alkyl radicals from the nitrogen atom not incorporated into the ring system does occur, but is of negligible extent. The well-documented elimination of C_2H_5 radicals in N-ethylcyclopentyl- and cyclohexylamines has been shown to arise from the ring portion of the molecule.[10] However, in the case of the corresponding N-acetyl derivatives, the M-29 peaks are produced to a predominant extent by loss of the N-ethyl substituents. This drastic difference in fragmentation

has been established by deuterium labeling for N-ethyl-N-acetylcyclopentylamine and an analogous behavior extrapolated for the higher homolog.[10] These data could also be accommodated by a mechanism closely analogous to the one outlined for the methyl elimination in N-acetylmorpholine:

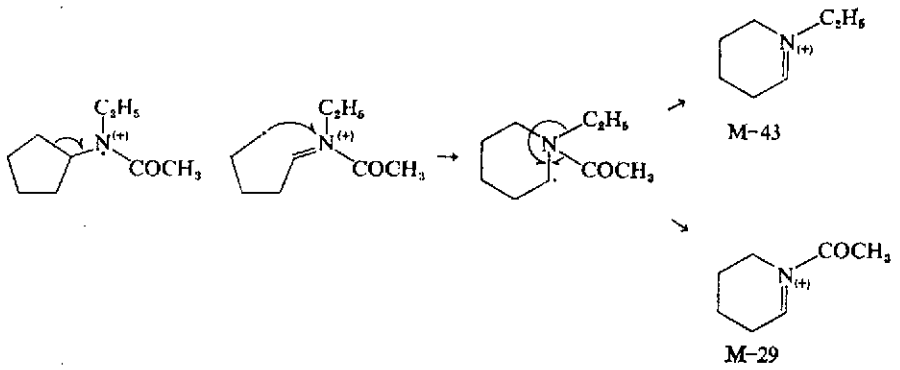

Such a mechanism would also account for the observed loss of CH_3CO as a mainly intact unit.

In addition, N-acetylpiperidine[11] shows an analogous loss of CH_3 and CH_3CO only to a smaller extent. The more important part of such fragmentation represents the losses of the beta carbon atom (as in piperidine), and the common two-step H/CH_2CO elimination.

Conceivably, a major prerequisite for the unusual fragmentation sequence outlined for the losses of 15 and 43 mass units in N-acetylmorpholine (I) is the presence of a sufficiently electron-deficient center as a site for new bond formation. Such conditions might easily exist at the charged nitrogen atom in the acyl-immonium species resulting from alpha-cleavage, i.e. $M_{1(1)}$. As a consequence, the behavior of amines and their acylated derivatives could be expected to display the observed differences. Also, product development control and possibly polar effects seem to be significant in the hydrogen transfer step, providing additional driving force and selectivity with respect to the site of abstraction. Lack of a second heteroatom in the ring might thus be responsible for the decidedly minor importance of both processes in the case of N-acetylpiperdine. Further investigation of the principles involved in the formation of the discussed fragments is in progress.

EXPERIMENTAL

The high and low resolution mass spectra were run on a Consolidated Electrodynamics Corporation mass spectrometer, model 21-110B (all-glass inlet system at 225°, source temperature 240°, ionizing energy 70 eV, ionizing current μa).* Vapour phase chromatography was conducted on a Varian Aerograph instrument (6′ × ¼″ SS column ,15% FFAP on Chromosorb W 100/120 mesh, helium flow rate approximately 30 cc/min, temperature 180°). Active hydrogen atoms were exchanged by vapor phase chromatography on a 15′ × ¼″ SS column, 10% potassium hydroxide, 5% Carbowax 20 M on 100/120 mesh-Chrom P which had been pre-treated with deuterium oxide by injection of approximately 30 microliter portions several times a day over a period of one week.[16]

3,3-d_2-N-*Acetylmorpholine.* A solution of 3-morpholone (0·7 g, K & K Laboratories, Inc.) in tetrahydrofuran (approximately 10 ml) distilled from lithium aluminum hydride (Metal Hydrides,

* We wish to thank Dr. D. H. Smith for high resolution mass spectra.

Inc.) was added to a stirred slurry of lithium aluminum deuteride (0·4 g, Metal Hydrides, Inc.) in 20 ml of distilled tetrahydrofuran. After heating under reflux for 12 hours, the reaction mixture was decomposed with a saturated sodium sulfate solution and the inorganic suspension filtered. The solution of deuterated morpholine in tetrahydrofuran was cooled in an ice bath and converted to the N-acetate by slow addition of excess acetic anhydride. After stirring for 15 minutes, the product was isolated for mass spectrometric analysis by vapor phase chromatography. The extent of deuterium incorporation as determined by mass spectrometric analysis was 99% d_2, 1% d_1.

2,2-d_2-N-*Acetylmorpholine;* 2,2,3,3-d_4-N-*Acetylmorpholine.* 3-Morpholone (5·3 g) was heated under reflux in deuterium oxide (42 ml) containing potassium carbonate (3 g) over a period of 10 days.[17] The solution was cooled, lyophilized, and the residue extracted with methylene chloride. The dideutero-morpholone was isolated by evaporation of the methylene chloride. The lactam was reduced with lithium aluminum hydride (or deuteride) and acetylated as described above. The isotopic purity as determined by mass spectrometric analysis was found to be: 2,2-d_2-N-acetylmorpholine, 87% d_2, 13% d_1; 2,2,3,3-d_4-N-acetylmorpholine, 83% d_4, 17% d_3.

8,8,8-d_3-N-*Acetylmorpholine.* The active hydrogen atoms of N-acetylmorpholine (Eastman Organic Chemicals) were exchanged by vapor phase chromatography on a deuterium oxide-pretreated column (column described above). With a column temperature of 225° and a helium flow rate of 30 cc/min, a retention time of approximately 12 minutes was observed. The extent of deuterium incorporation as determined by mass spectrometry was 93% d_3, 7% d_2.

REFERENCES

1. Part XVI, A. L. Burlingame, International Mass Spectrometry Conference, Berlin, Sept. 25–29, 1967 (*Advances in Mass Spectrometry*, Vol. 4, E. Kendrick, Ed., The Institute of Petroleum, London, in preparation).
2. C. Djerassi, *Pure and Applied Chemistry* **9**, 159 (1964).
3. P. Brown and C. Djerassi, *Angew. Chemie* **6**, 477 (1967).
4. W. J. Richter, see ref. 3.
5. A. L. Burlingame, C. C. Fenselau, W. J. Richter, W. G. Dauben, G. W. Shaffer and N. D. Vietmeyer, *J. Am. Chem. Soc.* **89**, 3346 (1967).
6. [a] J. Collin, *Bull. Soc. Chem. Belg.* **69**, 449 (1960); [b] R. A. Saunders and A. E. Williams, *Advances in Mass Spectrometry, Vol. 3*, Ed. W. L. Mead, The Institute of Petroleum, London, 1966, pp. 681–700; [c] A. M. Duffield, H. Budzikiewicz, D. H. Williams and C. Djerassi, *J. Am. Chem. Soc.* **87**, 810 (1965); [d] E. J. Gallegos and R. W. Kiser, *J. Phys. Chem.* **66**, 136 (1962); [e] A. M. Duffield, H. Budzikiewicz and C. Djerassi, *J. Am. Chem. Soc.* **87**, 2920 (1965); [f] J. H. Beynon, *Advances in Mass Spectrometry, Vol. 1*, Ed. J. D. Waldron, Pergamon Press, London, 1959, p. 328; [g] R. Smakman and T. J. DeBoer, International Mass Spectrometry Conference, Berlin, Sept. 25–29, 1967.
7. [a] J. Collin, *Bull. Soc. Chem. Belg.* **69**, 585 (1960); [b] R. H. Shapiro, T. E. McEntee, Jr. and D. L. Coffen, International Mass Spectrometry Conference, Berlin, Sept. 25–29, 1967.
8. A. M. Duffield and C. Djerassi, *J. Am. Chem. Soc.* **87**, 4554 (1965).
9. J. A. Gilpin, *Anal. Chem.* **31**, 935 (1959).
10. Z. Pelah, M. A. Kielczewski, J. M. Wilson, M. Ohashi, H. Budzikiewicz and C. Djerassi, *J. Am. Chem. Soc.* **85**, 2470 (1963).
11. J. M. Tesarek, unpublished results from this laboratory.
12. The term 'new bond formation' is used here mainly for describing steps in a less general meaning than implied by F. W. McLafferty in *Mass Spectrometry of Organic Ions*, Ed. F. W. McLafferty, Academic Press, New York, 1963, p. 309.
13. A. F. Thomas and B. Willhalm, *Helv. Chim. Acta* **47**, 475 (1964).
14. D. S. Weinberg and C. Djerassi, *J. Org. Chem.*, **31**, 115 (1966).
15. Radical centers as a primary source of isotope scrambling in the vicinity has been suggested, for example, for aromatic systems see footnote 14 in J. Ronayne, D. H. Williams and J. Bowie, *J. Am. Chem. Soc.* **88**, 4980 (1966).
16. M. Senn, W. J. Richter, and A. L. Burlingame, *J. Am. Chem. Soc.* **87**, 680 (1965).
17. A. M. Duffield, H. Budzikiewicz, and C. Djerassi, *J. Am. Chem. Soc.* **86**, 5536 (1964).

Reprinted from THE JOURNAL OF CHEMICAL PHYSICS, Vol. 49, No. 11, 4870–4876, 1 December 1968
Printed in U. S. A.

Formation and Detection of Metastable Ions in a Double-Focusing Mass Spectrometer*, †

PETER SCHULZE AND A. L. BURLINGAME
Department of Chemistry and Space Sciences Laboratory, University of California, Berkeley, California 94720
(Received 9 May 1968)

By changing the acceleration voltage independently from the voltage applied to the electrostatic analyzer of a double-focusing mass spectrometer, it is possible to detect "metastable" ions which are formed in the field-free drift region in front of the electrostatic analyzer. The parent and daughter ions of the decomposition can be determined unambiguously. Applying this technique to various compounds it was found that it is also possible to detect ions whose decomposition originates during acceleration by the ion gun as well as during flight through the electrostatic analyzer. Theoretical calculations are presented which verify these assumptions and show the location of decomposition in the electrostatic analyzer. Using this technique, it was also possible to show that doubly charged ions may undergo a metastable transition which leads to another doubly charged ion.

INTRODUCTION

Metastable ions have received considerable attention in single-focusing mass spectrometry since their original description by Hipple.[1] Such considerations have led to their widespread use in the interpretation of the mass spectra of rather complex organic molecules, since they provide insight into the sequence of unimolecular decompositions by relating two peaks in a mass spectrum. Based upon relationships which Beynon *et al.*[2] have derived, which describe a correlation between the width of a flat-topped metastable peak and the amount of kinetic energy released during fragmentation, McLafferty and co-workers[3] have used the shape of metastable peaks to postulate gas-phase structures of fragment ions by comparing the abundance and energy release of metastable ions in classes of compounds. Literature dealing with the more physical and instrumental aspects of metastable ion formation has been reviewed by Beynon and Fontaine.[4]

These authors have suggested that metastable transitions can occur at each point of the ion path for both single- and double-focusing instruments. This is in agreement with earlier postulations and the results of Ottinger,[5] who has shown that molecular ions formed by electron impact undergo unimolecular decompositions with a series of rate constants ranging from at least 10^{-8}–10^{-6} sec^{-1}.

Beynon and Fontaine,[4] on the other hand, present only suggestive evidence for ion decompositions occurring during the acceleration of the ions. For decompositions during the flight through the electric sector, reference is made to an older paper,[6] in which only a qualitative description of such decompositions in the electric sector is given.

In the case of double-focusing mass spectrometers,

* The results reported here were presented in part at the 155th National American Chemical Society Meeting, 31 March–5 April 1968, San Francisco, Calif., Div. of Physical Chemistry, Abstracts, p. S268.

† Generous financial support was provided by the National Aeronautics and Space Administration, Grant NGR 05-003-134.

[1] J. A. Hipple and E. U. Condon, Phys. Rev. 68, 54 (1945).

[2] J. H. Beyon, R. A. Saunders, and A. E. Williams, Z. Naturforsch. 20a, 180 (1965).

[3] T. W. Shannon and F. W. McLafferty, J. Am. Chem. Soc. 88, 5021 (1966); F. W. McLafferty and W. T. Pike, *ibid.* 89, 5951 (1967).

[4] J. H. Beyon and A. E. Fontaine, Z. Naturforsch. 22a, 334 (1967).

[5] C. Ottinger, Z. Naturforsch. 22a, 20 (1967); I. Herthel and C. Ottinger, *ibid.* 22a, 1141 (1967).

[6] J. H. Beynon, R. A. Saunders, and A. E. Williams, Nature 204, 67 (1964).

only metastable ions which are formed between the boundaries of the electric and magnetic sectors are observed under normal operating conditions. However Jennings[7] and Futrell *et al.*[8] have developed a method whereby metastable ions formed in the field-free drift region before the electric sector may be brought into focus by proper adjustment of the accelerating potential with respect to that of the electric sector.

Using this technique, this paper describes results observed during studies of metastable transitions in the field-free drift region between the source and electric sector. It is shown that it is possible to observe ions which result from decompositions during the period of acceleration. Also, certain metastable peaks were observed to "move," as noted by Beynon[6] who suggested that they represent decompositions occurring during the flight of the ions through the electric sector itself. The term "moving metastable peaks" is used for those peaks in the mass spectrum which have the broad shape of a normal metastable peak and which change their position on the mass scale with changing accelerating voltage, while the voltage across the electric analyzer is kept constant. Shannon *et al.*[9] mentioned such a "moving" metastable peak for the loss of water from the molecular ion of 2,3-dihydroxy-2,3-diphenylindanone, but these authors do not give any explanation as to where the ions are formed. In order to understand the instrument conditions which led to the observation of these "moving" metastable peaks, theoretical calculations have been carried out in order to determine the point of decomposition of the ions in the instrument more clearly.

Application of these studies may be found in the detection of metastable peaks coincident with the normal mass spectrum by shifting the metastable peaks from under intense peaks.

THEORY

All ions which are accelerated in the ion source by a potential of $U_{acc}=U_0$ volts have an energy of eU_0 regardless of their mass, assuming zero initial kinetic energy. Under normal conditions the voltage of the electrostatic sector is adjusted so that these ions pass through and a normal mass spectrum is recorded. If the transition $m_1^+ \rightarrow m_2^+ + (m_1-m_2)$ occurs in the field-free region where no additional acceleration is imposed to the ion m_2^+, this ion has only an energy of $E=(m_2/m_1)eU_{acc}=(m_2/m_1)eU_0$, which is not enough to pass through the electric sector under normal conditions.

If one increases the acceleration voltage to $U_{acc}=(m_1/m_2)U_0$, the loss of energy is compensated and the ions of mass m_2 arising from the transition have just the energy eU_0 necessary to pass the electric sector. Since the voltage of the electric sector is not changed, the mass scale remains unchanged also, and the ions still occur at mass m_2 at the detector. All other ions which do not arise from a metastable transition, in which the ratio of the masses is equal to m_1/m_2, will not be observed because they have an energy too high or too low to be transmitted by the electric sector.

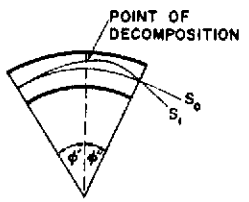

FIG. 1. Ion path for decomposition inside the electric sector (schematic.)

Employing this method, the mass m_2 of the transition is recorded and, because the voltage U_{acc} determines the mass m_1, the whole decomposition is known. Jennings and co-workers[10] used this method successfully to determine fragmentation paths in various molecules.

If the decomposition takes place during the acceleration, the ion m_2^+ will be accelerated further and its final energy is given by

$$E=(m_2/m_1)eU_1+e(U_{acc}-U_1), \tag{1}$$

where U_{acc} is the total applied acceleration voltage and U_1 the voltage by which the ion m_1^+ was accelerated before the decomposition took place.

If this energy E is equal to the energy eU_0, which such ions must have in order to pass the electric sector, the ions will be detected at mass m_2 and the result is given by

$$eU_0=(m_2/m_1)eU_1+e(U_{acc}-U_1)$$

or

$$U_1=[m_1/(m_1-m_2)](U_{acc}-U_0). \tag{2}$$

That means that, if one is able to detect ions at mass m_2 while scanning the high voltage between $U_{acc}=U_0$ (normal mass spectrum, $U_1=0$) and $U_{acc}=(m_1/m_2)U_0$ [$U_1=(m_1/m_2)U_0=U_{acc}$, i.e., ions from decompositions in the field-free region], these ions result from decompositions taking place in the accelerating region.

For decompositions inside the electric sector, the following considerations apply. Ions of mass m_1 may be accelerated by a voltage U_{acc} whose value should lie between

$$U_0 \leq U_{acc} \leq (m_1/m_2)U_0. \tag{3}$$

These ions have an energy which is higher than the permissible energy, eU_0, by an amount, β' percent, where

$$\beta'=[(U_{acc}-U_0)/U_0]100. \tag{4a}$$

These ions will enter the electric sector at the center

[7] K. R. Jennings, J. Chem. Phys. 43, 4176 (1965).
[8] J. H. Futrell, K. R. Ryan, and L. W. Sieck, J. Chem. Phys. 43, 1832 (1965).
[9] T. W. Shannon, T. E. Mead, C. G. Warner, and F. W. McLafferty, Anal. Chem. 39, 1748 (1967).
[10] M. Barber, W. A. Wolstenholme, and K. R. Jennings, Nature 214, 664 (1967).

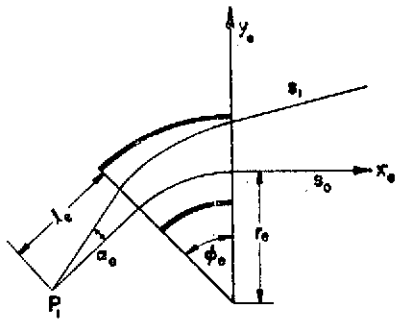

FIG. 2. Coordinate system for calculation of the ion path after leaving the electric sector.

line between the sector plates (Fig. 1), but will deviate (because of the higher energy) from the center pathway by an amount which depends on the energy deviation β' and the distance the ions travel inside the electric sector before the decomposition takes place. This distance may be represented by an angle ϕ'. The energy deviation after decomposition at this point for the ions m_2^+ is given by

$$\beta''=\frac{(m_2/m_1)(U_{acc}-U_0)}{U_0}\,100. \tag{4b}$$

This expression will be negative as long as $U_{acc}<(m_1/m_2)U_0$. Therefore, the ions will move back towards the center line of the electric sector and may be able, after passing through an angle ϕ'', where $\phi'+\phi''=\phi_e$ represents the angle of the electric sector, to pass through the exit slit of the electric sector and enter the magnetic sector to be mass analyzed.

According to Hintenberger and Koenig,[11] it is possible to find the equation of motion for ions leaving the electric sector if their trajectory, when entering the electric sector, describes an angle α with respect to the optic axis and displays an energy deviation β (Fig. 2). The equation is given by

$$y_e=r_e\sum_{i,j=0}^{2}A_{ij}\alpha_e^i\beta^j+x_e\sum_{i,j=0}^{2}B_{ij}\alpha_e^i\beta^j \tag{5}$$

if one considers only up to second-order terms. The coefficients A_{ij} and B_{ij} depend only on the geometry of the electric sector (angle and radius) and the distance l_e between that point in front of the electric sector where the ions seem to leave the optic axis and the electric-sector boundary.

This equation was used to find the trajectory of the ions decomposing inside the electric sector. Prior to decomposition, the distance the ions travel inside the electric sector is represented by the angle ϕ'. The initial energy deviation is given by β' in Eq. (4a). The initial angular deviation from the theoretical ion optical path may be considered to be zero because of the small slitwidth of the entrance slit of the electric sector and the relatively long distance between source slit and electric-sector entrance slit. The equation of motion at the point of decomposition is given by

$$y_e'=A'+B'x_e', \tag{5a}$$

where both A' and B' are dependent in a complicated way upon ϕ'. From these expressions for A' and B', it is possible to calculate the angle which the ion path forms with the optic axis at the point of decomposition and to calculate the apparent distance l_e. If one applies Eq. 5 once more, the remaining path inside the electric sector after decomposition may be determined. Now α and l_e are no longer zero and the distance through the electric sector which the ions have to pass is given by $\phi''=\phi_e-\phi'$. Thus, one obtains an equation which may be represented by

$$y_e=A+Bx_e. \tag{5b}$$

A and B are still dependent on ϕ' and on β' and β''. β' and β'' may be determined from the applied high voltage and the known values for m_1 and m_2. Since the ions must be able to leave the electric sector, the condition for A is given by

$$-\tfrac{1}{2}W_e\leq A\leq+\tfrac{1}{2}W_e, \tag{6}$$

where W_e is the width of the exit slit of the electric sector. Thus, for a given set of β', β'' values, one will obtain a small range of ϕ' values which represent that path length during which a metastable transition $m_1^+\rightarrow m_2^++(m_1-m_2)$ must take place if the resulting ions are able to reach the magnetic sector.

EXPERIMENTAL

The mass spectrometer used in these experiments was a standard C.E.C. Model 21-110B. It was normally used with wide-open slits in order to get sufficient sensitivity. The mass spectrometer normally is equipped with a high-voltage supply, the high voltage of which is not continuously variable over wide ranges. To permit this capability it was necessary to replace the high-voltage supply (ion accelerator) by an external, highly stable, high-voltage power supply, the voltage of which was adjustable continuously from 0–10 kV. Normally, however, the voltage was adjusted in steps of 10 V in the voltage range of interest. The voltage divider of the ion accelerator was still used in order to obtain easily the appropriate focus and repeller potentials. These potentials were set at the beginning of the experiments for maximum beam intensity in the normal operation mode, i.e., $U_{acc}=U_0$. During the experiments the focus and repeller potentials were not changed externally, but changed only commensurate with the changes in high voltage. It was assumed that this would not unduly affect the intensity of the resulting ions.

The experiments were carried out in two different ways, depending upon the results which were sought.

[11] H. Hintenberger and L. A. Koenig, Z. Naturforsch. **12a**, 140 (1957).

Since the metastable ions in the field-free region had to be observed in order to establish as many metastable transitions as possible, the instrument was set up for operation at nominal 4 kV. The actual acceleration voltage was about 3700 V. The voltage difference between both plates of the electric sector was 370 V and was maintained at this value throughout the entire experiment. The mass in question was tuned to the collector by adjusting the magnet and, after this, the high voltage was scanned from about 3600 V up to the highest possible $U_{acc}=(m_1/m_2)U_0$ but not higher than 8 kV. Thus, under these conditions it would be possible to detect all precursor ions m_1 for a specific product ion m_2 up to about $m_1=2m_2$. If one wishes to detect parent ions of more than twice the mass of the daughter ion, the instrument's electric sector voltage would have to be set to 185 V which corresponds to operation at nominal 2 kV for the acceleration voltage.

If one attempts to look only for small mass changes as, for instance, decompositions in which the loss of hydrogen radicals or hydrogen molecules are involved, the instrument is set for an operation at 7500 V (electric-sector voltage constant at 750 V) and the high voltage is scanned up to maximum 8 kV. It is, of course, possible also to look not only for a single mass while scanning the high-voltage U_{acc}, but to scan magnetically either a part of or the whole mass spectrum while the voltage U_{acc} is incremented each time by a certain small amount. This procedure is consuming of both time and sample, but it is the only way to detect the "moving" metastable peaks.

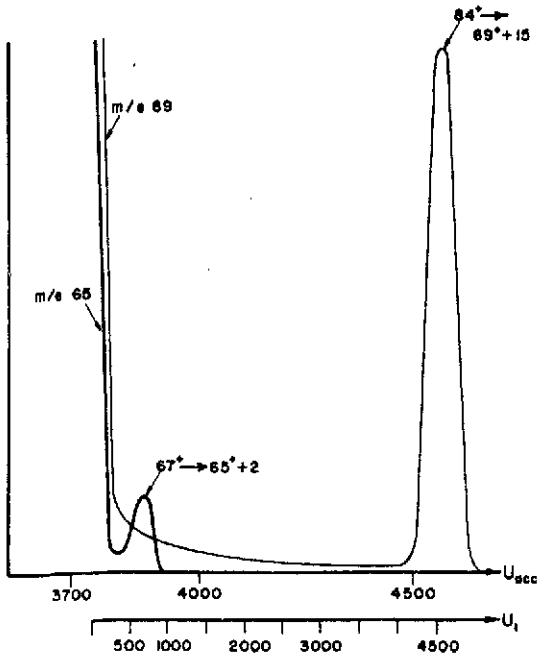

FIG. 3. Voltage dependency of m/e 65 and m/e 69 in 1-octene.

RESULTS

During these investigations it was found that nearly every peak in a given mass spectrum has at least one metastable precursor ion and often two or more. This is in agreement with results published by Jennings *et al.*[7,10] and Shannon *et al.*[9] By scanning the high voltage up from 3700 V while keeping the voltage across the electric sector constant, one obtains, of course, a very high signal at any mass m_2 for $U_{acc}=U_0=3750$ V. (This is the voltage at which an ordinary mass spectrum would be recorded by scanning the magnetic field.) Upon scanning the accelerating voltage further up, the signal at m_2 vanishes until another peak at m_2 is found at a voltage $U_{acc}=(m_1/m_2)U_0$, indicating that the fragment ion m_2 coming from the decomposition of the ion m_1 in the field-free region has now enough energy to pass the electric sector. In the mass spectrum of 1-octene the voltage dependence of the ion intensity at m/e 69 and m/e 65 is recorded and shown in Fig. 3. With increasing voltage a second signal appears at m/e 65 at a voltage $U_{acc}=3870$ V, which corresponds to the transition $67^+\rightarrow 65^++2$. After this, the signal drops to the base line and no other precursor ion for m/e 65 is recorded. For m/e 69 one observes a maximum at $U_{acc}=4565$ V, which indicates the transition of $84^+\rightarrow 69^++15$. The continuum in between indicates, according to Eq. (2), that these are transitions which occur during acceleration and that their product ions are able to reach the collector. The U_1 scale for this decomposition is plotted in Fig. 3 and, as might be expected, the abundance of these transitions increases as one approaches the ionization chamber. Ottinger[8] has also detected such a tailing between the main peak and that for the first transition. As, in this case, the tail represents much shorter times, and due to the special design of his ion source, Ottinger was able to draw conclusions about how a mass spectrum would look if one were able to record it only 10^{-8} sec after ionization. Such tailing due to decompositions during acceleration was found for many molecular ions as well as for fragment ions.

Instead of scanning the high voltage and keeping the magnetic field constant in order to get all the transitions to a specific mass m_2, it is, of course, possible to increase the voltage stepwise by a suitable amount while each time scanning magnetically the mass range in question. There is certain difficulty in establishing a mass scale, however, since the ions normally recorded are absent. However, it is possible to establish a mass scale from one mass spectrum to the next since small peaks still occur at certain masses due to the above mentioned transitions during acceleration even over wide voltage ranges, e.g., m/e 69 in the example of 1-octene.

Scanning the whole spectrum each time is advantageous in that all metastable transitions which involve a certain relative change of mass are recorded simul-

TABLE I. Decomposition of $C_2H_5OH^+$ ions in the electrostatic analyzer. $C_2H_5OH^+ \rightarrow C_2H_5O^+ + H (46^+ \rightarrow 45^+ + 1)$.

				m^* (calc)			ϕ' (calc)		
U_{acc} (V)	β' (%)	β'' (%)	m^* (obs)	$A=-3\times10^{-3}$	$A=0$	$A=+3\times10^{-3}$	$A=-3\times10^{-3}$	$A=0$	$A=+3\times10^{-3}$
7500	0	−2.17	44.4–44.0	43.85	43.11	...	19°02′	31°49′	...
7540	0.53	−1.65	44.6–44.0	44.31	44.03	43.56	11°40′	16°54′	24°57′
7580	1.07	−1.13	44.9–44.2	44.64	44.45	44.17	6°08′	10°09′	14°57′
7620	1.60	−0.61	45.0–44.4	44.9	44.75	44.53	1°36′	5°00′	8°48′
7660	2.13	−0.09	45.0–44.7	...	44.97	44.80	...	0°42′	3°57′

taneously. Using this method, it is also possible to see peaks which are broad, like ordinary metastable peaks. They do not occur at integer mass numbers but do change their position with the changing high voltage. Beynon[2,4] reports such peaks for decompositions which involve the loss of hydrogen radicals from the molecular ions of toluene and ethanol. In this work "moving" metastable peaks were also detected for transitions in which a larger neutral entity is lost,

$94^+ \rightarrow 66^+ + 28$ in phenetole,

$84^+ \rightarrow 69^+ + 15$ in 1-octene.

The point where these transitions could occur was thought, at first, to be during acceleration. It was assumed that the resulting ions should have just a little less energy than was required by the electric sector, but that they should still be able to pass the electric sector. This assumption would contradict the double-focusing principle, since ions of a certain mass, but with differing energy, should still be focused at one point if they pass the entire electric and magnetic sectors.[12] Therefore, a verification of Beynon's[2,4] assumption that the decompositions leading to those "moving" metastables occur inside the electric sector was attempted. The equations derived by Hintenberger and Koenig[11] were applied as explained in the theoretical part. The results are shown in Tables I–III for the transitions,

$C_2H_5OH^+ \rightarrow C_2H_5O^+ + H$ $(46^+ \rightarrow 45^+ + 1)$ in ethanol,

$C_8H_7^+ \rightarrow C_8H_5^+ + H_2$ $(43^+ \rightarrow 41^+ + 2)$ in 1-octene,

$C_6H_6O^+ \rightarrow C_5H_6^+ + CO$ $(94^+ \rightarrow 66^+ + 28)$ in phenetole.

The first column shows the values for U_{acc}; the second and third columns show the calculated values for β' and β'', according to Eqs. (4a) and (4b). The fourth column shows the experimental values m^* for the position of the metastable peak. Values of ϕ' were calculated (eighth and ninth columns) for those ions which leave the electric sector at both sides of its exit slit. This defines, according to Eq. (6), the value of A

TABLE II. Decomposition of $C_8H_7^+$ ions in the electrostatic analyzer. $C_8H_7^+ \rightarrow C_8H_5^+ + H_2 (43^+ \rightarrow 41^+ + 2)$.

				m^* (calc)			ϕ' (calc)	
U_{acc} (V)	β' (%)	β'' (%)	m^* (obs)	$A=-3\times10^{-3}$	$A=0$	$A=+3\times10^{-3}$	$A=-3\times10^{-3}$	$A=+3\times10^{-3}$
7560	0.8	−3.89	39.75	...	38.7	...	17°4′	23°56′
7580	1.07	−3.63	39.9	...	38.95	38.6	15°15′	21°9′
7600	1.33	−3.38	40.1	39.4	39.2	38.9	13°38′	18°55′
7620	1.60	−3.13	40.2	39.6	39.4	39.1	12°6′	16°55′
7640	1.87	−2.87	40.3	39.8	39.6	39.3	10°39′	15°8′
7660	2.13	−2.62	40.35	39.9	39.7	39.5	9°20′	13°31′
7680	2.40	−2.36	40.4	40.1	39.9	39.7	8°2′	12°00′
7700	2.67	−2.11	40.5	40.2	40.0	40.0	6°50′	10°35′
7720	2.93	−1.86	40.6	40.35	40.2	40.15	5°42′	9°18′
7740	3.20	−1.60	40.7	40.5	40.3	40.3	4°35′	8°1′
7760	3.47	−1.34	40.75	40.6	40.45	40.4	3°31′	6°49′
7780	3.73	−1.09	40.8	40.7	40.6	40.5	2°31′	5°43′
7800	4.00	−0.84	40.85	40.8	40.7	40.6	1°33′	4°39′
7820	4.27	−0.58	40.9	40.9	40.8	40.7	0°37′	3°36′
7840	4.53	−0.33	41.0	...	40.9	40.8	...	2°38′
7860	4.80	−0.07	41.0	...	41.0	40.9	...	1°40′
7880	5.07	+0.18	41.0	...	...	...	...	0°47′
7900	5.33	+0.43	41.0	...	...	...	...	...

[12] We wish to thank Dr. J. H. Beynon, Imperial Chemical Industries, Manchester, for a helpful discussion of this point.

TABLE III. Decomposition of $C_6H_6O^+$ ions in the electrostatic analyzer. $C_6H_6O^+ \rightarrow C_5H_5^+ + CO$ ($94^+ \rightarrow 66^+ + 28$).

				m^* (calc)			ϕ' (calc)	
U_{acc} (V)	β' (%)	β'' (%)	m^* (obs)	$A=-3\times10^{-2}$	$A=0$	$A=+3\times10^{-2}$	$A=-3\times10^{-2}$	$A=+3\times10^{-2}$
5100	35.64	−4.76	64.8	62.7	62.5	62.4	2°03′	2°25′
5130	36.44	−4.20	65.0	63.2	63.0	62.9	1°44′	2°07′
5160	37.23	−3.64	65.0	63.7	63.5	63.35	1°27′	1°49′
5190	38.03	−3.09	65.4	64.1	63.95	63.8	1°11′	1°32′
5220	38.83	−2.53	65.6	64.55	64.4	64.2	0°55′	1°16′
5250	39.62	−1.97	65.7	65.0	64.8	64.6	0°40′	1°0′
5280	40.43	−1.41	65.8	65.35	65.2	65.0	0°25′	0°45′
5310	41.22	−0.85	65.9	65.7	65.5	65.3	0°11′	0°31′
5340	42.02	−0.29	66.0	···	65.8	65.6	···	0°16′

in Eq. (5) to be

$$A=\pm\tfrac{1}{2}W_e.$$

The width of the electric-sector exit slit in the C.E.C. 21-110B is approximately 0.060 in. (1.5 mm). [For the transition $46^+ \rightarrow 45^+ + 1$ in ethanol, it was difficult to determine the center of the metastable peak. Therefore, the range in which it occurs is given and a value for ϕ' is calculated also for ions passing the center of the electric-sector exit slit ($A=0$).] From these data it can be seen that, as the accelerating voltage is increased, the metastable ions detected are formed closer to the entrance of the electric sector. As may be expected, those decompositions which involve only a relatively small mass change—and, thus, a small energy change—can be observed throughout the entire electric sector, as in the case of ethanol; whereas, the decompositions in phenetole can be observed only at the very front end of the electric sector. Such a decomposition is accompanied by an energy change of nearly 30%, but it is still possible to show that the decomposition leading to the moving metastable peak occurs definitely inside the electric sector.

In order to prove whether metastable transitions do indeed take place as indicated from the calculated values of ϕ' in the electric sector giving rise to metastable peaks occurring at the experimentally determined positions on the mass scale (values of the fourth column), the apparent mass of these ions was calculated. Hintenberger and Koenig[11] give an equation for the deflection of an ion by a magnetic sector field. The values for A and B in Eq. (5b), using the values of ϕ' in Tables II–IV, were used to calculate the point and the angle where the ions enter the magnetic field. The constants of the magnetic field are $\phi_m=90°$ and $r_m=12$ in.

By doing this, the values for m^* in the fifth, sixth, and seventh columns for the ions which leave the electric sector at both edges and the center of the exit slit were obtained. It was not expected that these values would be exactly the same as those found experimentally, but the agreement is good and demonstrates that the assumptions regarding the region of decomposition are correct.

The main reasons for the remaining discrepancies are that the calculations do not consider: (1) An initial angle distribution of the ions entering the electric sector as α_e has been assumed to be zero; (2) any initial energy distribution of the ions entering the electric sector due to the potential distribution inside the ion source and the different points of ionization because of the finite width of the electron beam; (3) the deceleration or acceleration which the ions get inside the electric sector when leaving or coming back to the center line because of having more or less of the required energy; (4) the fact that, in our case, the potential in the middle of both electric-sector plates was not on zero potential but was approximately at −9.5 V; (5) any stray fields; and (6) the fact that the magnet in the Mattauch–Herzog–Robinson geometry, as used in the C.E.C. 21-110B, has a curved field boundary and not a straight line, as is implied in the above calculations.

It should be possible to use these "moving" metastable peaks to detect transitions which involve only a very small mass difference, as, for example, the loss of a hydrogen atom. The corresponding metastable peak in these cases is always hidden by a normal ion peak,

TABLE IV. Metastable transitions of doubly charged ions in phenetole.

$121^{++} \rightarrow 93^{++} + 28$
$120^{++} \rightarrow 92^{++} + 28$
$118^{++} \rightarrow 90^{++} + 28$
$94^{++} \rightarrow 66^{++} + 28$
$93^{++} \rightarrow 65^{++} + 28$
$92^{++} \rightarrow 64^{++} + 28$
$107^{++} \rightarrow 79^{++} + 28$
$79^{++} \rightarrow 77^{++} + 2$

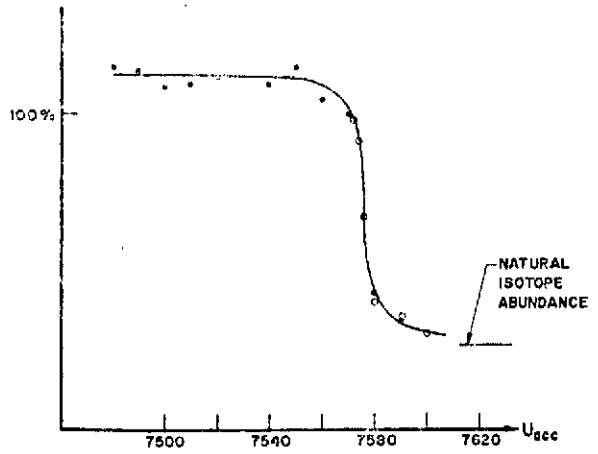

FIG. 4. Percent of m/e 162 compared to m/e 161 in nicotine.

and it should be possible to "move" the metastable peak from under the normal peak. Instrumental conditions, however, make this difficult. The C.E.C. 21-110B mass spectrometer has an energy bandpass of about 1%. The normal mass spectrum, therefore, is still present and unchanged as long as the acceleration voltage is changed by less than 1%. For decompositions which involve less than 1% of mass difference (loss of a hydrogen atom from ions with $m/e > 100$) part of the metastable peak due to decomposition of ions in the electric sector has moved during the high voltage change from (m_2^2/m_1) to m_2. Since this represents only very few ions at the time, the "moving" metastable peak is almost indistinguishable from the ordinary background. If, on the other hand, the intensity at mass m_2 is plotted vs the high voltage, one would expect to see a small shoulder or a tailing at the high-voltage side of the peak, but this, too, is very difficult to detect.

One possible way to circumvent these difficulties is to record the intensity of the assumed parent ion m_1 *and* the daughter ion m_2 together as a function of the high voltage. The ratio of both intensities should change during a 1%–2% change of the high voltage only, if they are connected by a metastable decomposition. Otherwise, the ratio should be constant until both peaks disappear.

As an example, the decomposition of the parent ion of nicotine, mass 162, to the M-1 peak is given. There is no doubt about the transition. The abundance of mass 161 is slightly smaller than m/e 162 in the normal mass spectrum and the metastable peak for this decomposition can be seen at m/e 160. The "moving" metastable peak is not readily detectable, but if one plots the ratio of both peaks vs the voltage, the ratio drops down to the natural isotope abundance as soon as ions coming from the ionizing region are no longer able to pass the electric sector (U_{acc} = about 1% above U_0) (Fig. 4). Ions of m/e 161 are able to pass at this acceleration voltage only if they come from decompositions of the parent ion occuring in front of the electric sector.

DOUBLE-CHARGED METASTABLE IONS

Jennings[13] has discussed consecutive metastable transitions where the first transition occurs in the first field-free region of a double-focusing mass spectrometer and the second one in the second field-free region. The molecule studied was toluene and the transition sequence was $C_7H_7^+ \rightarrow C_5H_5^+ \rightarrow C_3H_3^+$. An attempt was made to verify this result on phenetole for the sequence $C_6H_5OC_2H_5^+ \rightarrow C_6H_6O^+ \rightarrow C_5H_6^+$. The masses involved are $122^+ \rightarrow 94^+ \rightarrow 66^+$. This is accomplished by tuning in the "metastable" peak for the last transition in the normal mass spectrum, which is $m_2^2/m_1 = 66^2/94 = 46.34$. If one then raises the acceleration voltage to $U_{acc} = (122/94)U_0$, only those ions of mass 94 which result from a decomposition in front of the electric sector can pass it and decompose further. Trying this, a small signal was found. However, by scanning the mass spectrum around m/e 45 magnetically, some peaks were noted which occurred at just half-mass values. Upon further investigation it was found that the signal obtained was due to the transition,

$$C_6H_5OC_2H_4^{+\cdot} \rightarrow C_6H_6O^{+\cdot} + C_2H_4,$$

which gives a signal at m/e 93/2 = 46.5 and at a voltage of $U_{acc} = (122/93)U_0$, which is nearly the same as $(122/94)U_0$ (4879 vs 4868 V). By investigating this further, some more metastable transitions of this kind were found in phenetole, where doubly charged ions decompose to yield other doubly charged ions (Table IV). Such decompositions have been reported by Meyerson and Vander Haar[14] for a few compounds, but all of their observations concerned ions of even mass number. In addition to even mass ions, this study has shown that doubly charged ions of odd mass may also undergo such transitions. The observed intensities were too high to be attributed to isotope-containing species.

A more common decomposition of this type is the loss of hydrogen molecules from doubly charged ions. This has been observed to some extent in cyclic amines. Doubly charged parent ions, as well as fragment ions which have one or more hydrogen atoms less than the molecular ion, undergo such decompositions.[15]

---

[13] K. R. Jennings, Chem. Commun. **1966**, 283.

[14] S. Meyerson and W. Vander Haar, J. Chem. Phys. **37**, 2458 (1962).

[15] P. Schulze and A. L. Burlingame (unpublished results).

Data Acquisition, Processing, and Interpretation via Coupled High-Speed Real-time Digital Computer and High Resolution Mass Spectrometer Systems*

By A. L. BURLINGAME

(Department of Chemistry and Space Sciences Laboratory, University of California, Berkeley, California)

SUMMARY

The development of techniques for the acquisition, processing, and presentation of high resolution mass spectra is reviewed with particular emphasis on the use of real-time digital computers coupled to high resolution mass spectrometers.

A discussion of results obtained in our laboratory with instruments employing both the Mattauch-Herzog and Nier-Johnson geometry is presented.

INTRODUCTION

AFTER wrestling for 20 years in conception, the potentialities held by computers for the alleviation of routine tasks and the logical extension of the human mind are now approaching a stage of infancy,[1] destined to carry off a revolution in modern society unparalleled in the technological revolution of a century ago. The plummeting drop in cost accompanied by significant increases in performance (high speed, multiplexed input-output, interrupt priority, time sharing, feedback and control, etc.) and reliability have endowed this third generation of digital computers with a nearly ubiquitous market of users in all scientific disciplines. In addition, the versatility inherent in a programmable device over hardware designed for a single task need hardly be mentioned. These features bring the modest investment for a formidable computer system well within the reach of organizations with sufficient resources to afford a research programme in high resolution mass spectrometry.

REVIEW

Since the last conference in this series, the proliferation of the applications of mass spectrometry pervades the entire scope of organic chemistry, as may be seen in numerous ways. This has most currently been brought into focus by

* This review represents Part XVI in the series "High Resolution Mass Spectrometry in Molecular Structure Studies". For Part XV, see Kupchan, S. M., Davis, A. P., Barboutis, S. J., Schnoes, H. K., and Burlingame, A. L. *J. Am. chem. Soc.*, 1967, **89**, 5718.

Budzikiewicz, Djerassi, and Williams in their volume entitled "Mass Spectrometry of Organic Compounds."[2] This volume makes no claim to review the scope of instrumental and physicochemical techniques now becoming available which will facilitate routine availability of high-quality mass spectral data.

Expedience almost always dictates a path of least resistance to the actual utilization of information by a wide population of research workers, and hence iterative solutions are milestones in the history of formidable technical problems, such as our topic of data acquisition, processing, and presentation in high resolution mass spectrometry.

In this survey, I wish to review these milestones as I see them, describe the current trends and their successes, and suggest the path of least resistance for the next three years—a forecast strewn with potential pitfalls.

In the ten years since Beynon[3] triggered the application of accurate mass measurement to the determination of the atomic composition of organic compounds using a double-focusing instrument, scientists have yearned to bring the full potentialities of high resolution mass spectrometry to their respective disciplines. Such an atmosphere has encouraged the development by commercial manufacturers of instruments with routinely usable resolutions in excess of 30,000—an increase of more than a factor of three in the past three years. Current physical dimensions appear capable of about another factor of two with usable sensitivity and, of course, higher performance instruments are under development.

While instrument groups were concerned with upgrading spectrometer performance, techniques for data acquisition, processing, and presentation became academic problems. The technique of "peak-matching", first used by Nier,[4] allowed accurate measurement of selected, relatively intense peaks under double-focusing conditions. Demand for ascertaining the accurate mass of all peaks in the spectra of complex organic molecules[5(a), (b)] prompted the development of routine methods for measurement of high resolution mass spectrograms. Automated high precision microphotometers have been developed to such a state via data acquisition on to IBM punch cards,[5(c)] incremental magnetic tape,[6] and on-line to small digital computers.[6] While the accuracy of mass measurement has been within usable tolerances ($\pm$ 3–5 mmμ), the photo-plate technique suffers from the limitations of being rather time-consuming, while at the same time providing sources of error due to the fact that the plate must be exposed, developed, and measured before any mass calculations can be accomplished. Another limitation is the historically poor behaviour of photographic emulsions in terms of routinely obtaining reproducible relative ion intensity measurements.[7] Techniques for the deconvolution of partially resolved multiplets in spectrograms, which would improve the virtual resolution of the spectrograph, have been used.[8]

To facilitate the mental assessment and comprehension of the vast amount of information contained in a high resolution mass spectrum, several modes of computer presentation have been utilized, all of which first sort the data according to hetero-atomic content and then present hetero-atomic groups as a two-dimensional array, *e.g.* "element mapping",[9] series of plots, *e.g.* "hetero-atomic plotting",[10] or as three-dimensional plots designated "topographical element mapping"[11]—a combination of the principles in the first two methods.

Concurrently, the task of acquisition of high resolution mass spectral data

from spectrometer instrumentation without use of the feature of a plane of double-focus (spectrograph), has stimulated the development of fast magnetic scanning and concomitant fast response recording systems. Habfast and Maurer[12] have cautioned against passing premature judgment on the relative merits of photographic *v.* exponential electrical recording of high resolution mass spectral data prior to an understanding of the fundamental differences and trade-offs involved.

Various workers[13] have considered problems associated with fast scanning under high resolution conditions (M/ΔM 10,000; 10 per cent valley). The instrumental resolving power and sensitivity experienced with fast scanning are generally degraded over their optimum values obtainable under static operating conditions. These problems are inherent in the ion optical aberrations, as well as in the amplification and recording systems employed. Theoretical relationships between number of ions per peak and mass measurement precision have been presented.[14] It is shown that for exponential scanning the ion statistics are independent of mass and scan rate (not the case for other scan functions, see later discussion).

Thus far, two approaches have been investigated which are capable of operating at the high data rates encountered in rapid scanning at actual instrument resolutions in excess of 10,000.

The first approach has involved analogue magnetic tape recording of an exponential magnetic scan of a spectrum, using an instrument of Nier-Johnson geometry.[15] Exponential scans from an AEI MS-9 at 10- and 32-sec per decade in mass have been recorded on analogue magnetic tape from a 10 KHz band pass ion multiplier–amplifier system. This method reportedly yields mass measurement accuracies of about 10 ppm, apparently limited by the performance of the tape recording system. Data presented suggest that the low dynamic range of this analogue tape system appears to affect adversely the intensity measurement accuracy. A system employing an FM tape recorder coupled to a PDP-4* computer has been described[16] for digitization of raw data which is subsequently reduced by batch processing.

Problems of the nature outlined above have concentrated current effort on the second approach, namely, the development of digital recording systems aimed at sufficient capacity and flexibility to perform the many tasks associated with research in high resolution mass spectrometry.

Initial studies on recording the electron multiplier-amplifier output directly on gapless digital magnetic tape during a magnetic scan indicated the feasibility of the digital technique[17] for high resolution instrumentation.[18] Several groups have discussed systems employing on-line computers utilizing analogue-to-digital converters for direct digitization of multiplier-amplifier output and data acquisition during exponential magnetic scans using AEI MS-9 mass spectrometers.[19] Work from this laboratory,[20] employing direct digitization of the multiplier-amplifier output from a CEC 21-110B mass spectrometer and on-line data transfer to a high-speed digital computer, has been described in some detail. This system differs from others in that a high precision quadratic (in mass) magnetic scan was utilized as a scanning function instead of the conventional exponential. This system included a digital, dynamic CRT display of the raw data.

* Digital Equipment Corporation, Boston, Mass.

This brings my presentation to focus upon a discussion of current techniques and results from our laboratory.

EXPERIMENTAL

The system currently in use for this work involves the hardware, or instruments, outlined in Fig 1. The mass spectrometers used were the Consolidated Electrodynamics Corporation 21-110B mass spectrometer and the Associated Electrical Industries MS-9 (modified). The CEC instrument is of the Mattauch-Herzog geometry and is used also for our photographic plate work. A magnetic scan function is supplied to the magnet control circuitry to vary the magnetic field in an approximately known manner. The function presently in use changes the field approximately linearly with respect to time, from high mass to low mass.

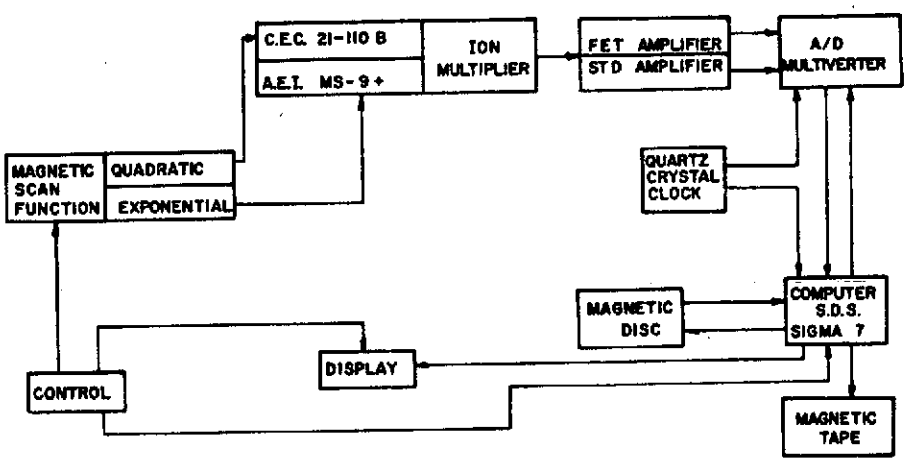

FIG 1. Data acquisition hardware.

This means that mass is proportional to time squared. This scan function enjoys two primary advantages over an exponential dependence of mass with time ($m \propto e^T$). The first advantage is that the high mass region, where mass measurement accuracy is most important, is passed through more slowly in a linear as opposed to an exponential magnet current scan. In other words, the interval between two timing marks represents a smaller mass difference. The second advantage is that data reduction is simplified because an equation of $m \propto T^2$ is easy to approximate with a four- to five-term polynomial. An exponential must, however, be determined in a computer by evaluating a power series until the series converges to the required precision, a slower process. In our particular case, the calculation of accurate masses from real-time data required only minor modifications in our extensive programme for photo-plate data reduction, since the mass-time dependence is quite similar to the mass-distance function on the photo-plate. Fig 2 presents the general form of the mass *v.* time function.

Scanning rates from a few seconds to several minutes for m/e 800 to m/e 20 may be chosen.

The output of the electron multiplier during the scan is fed to a field effect transistor amplifier system. The amplified signal is supplied to a high-speed analogue to digital (A/D) converter that is also capable of multiplexing up to 128 separate inputs (Raytheon Computer Corporation Multiverter). With a cycle time of 40 μsec, the maximum digitization rate for a single input (mode for current operation) is 25 KHz. The voltage level input (0–10 v) is converted to a 15 bit (14 bit plus sign) binary number, representing a usable dynamic range of more than 10,000 to 1.

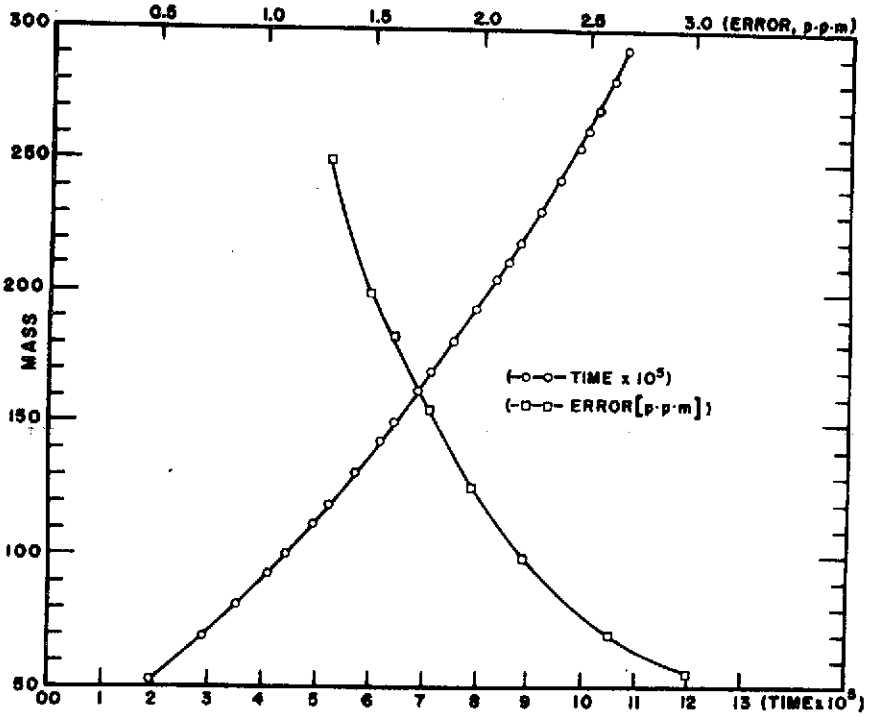

FIG 2. Mass-time relationship.

A pulse from a temperature-controlled quartz crystal clock* determines the initialization of the A/D conversion. This pulse also prepares the computer to accept the converted data. The digitized voltage is transferred to a Scientific Data Systems Sigma 7 computer. The programming involved in handling the input data will be discussed below.

The control system both initializes and terminates the clock count and the scan of the spectrum. Upon termination, the digitized data may be displayed on a CRT display system (Conrac Character Display Monitor, Model CDF) and/or written on digital magnetic tape at the discretion of the operator.

A simplified flow chart of the software, or programming, used in the computer during data acquisition is presented in Fig 3. At the time the programme is loaded into the computer various parameters are set. The two most important

* Subsequent digital circuits allow a choice of clock rates from 2 to 25 KHz in stops of 1 KHz.

are: (*a*) a binary threshold is selected at this time for later comparison with a measured voltage level; (*b*) priority interrupts are set.

Upon receiving an interrupt (external command), the programme enters the control phase. This phase processes the interrupt by checking to see that the command is allowed; if allowed, a branch occurs to the particular sub-routine requested by the interrupt. These sub-routines include those mentioned in the second line of Fig 3, *i.e.* start scan, stop scan, record and/or display data, and abort.

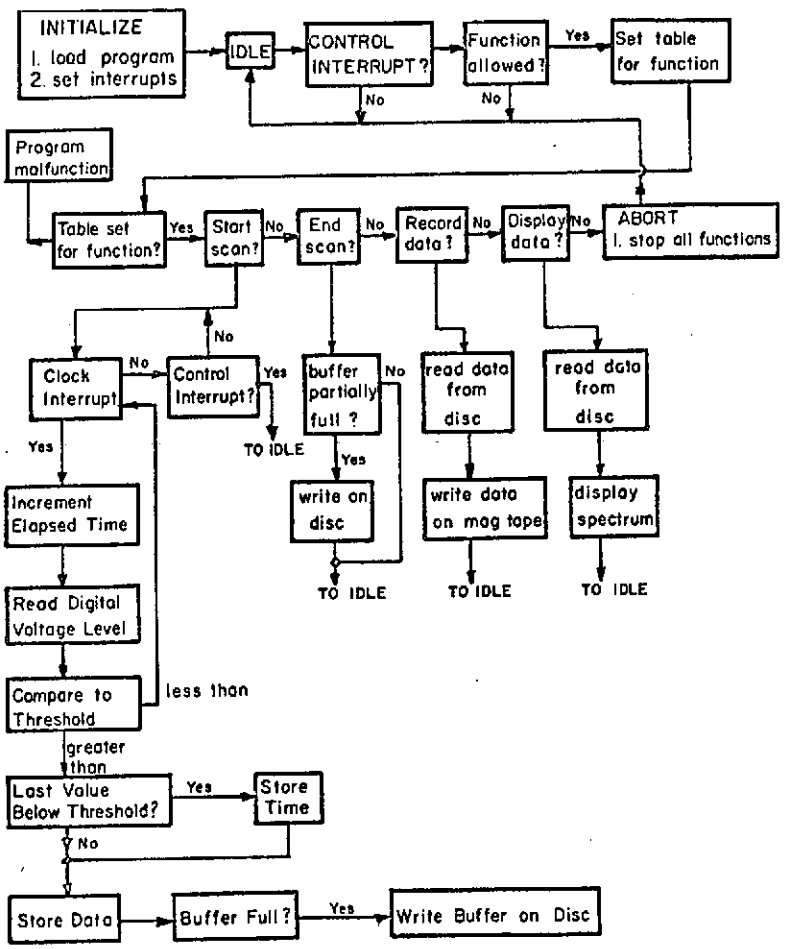

FIG 3. Data acquisition software.

If the control interrupt requests a start scan function, the programme transfers to the data acquisition sub-routine. A clock interrupt begins the data cycle. The elapsed number of clock ticks is stored by incrementing a clock register. When the A/D has finished conversion, the digital voltage level is read and compared to the pre-set threshold. (A more efficient approach under development in our laboratory consists of a circuit external to the central processing

unit which determines whether each data point is greater than threshold, while simultaneously incrementing the clock count, and thereby transfers to the central processor memory only data points which are above threshold.) If it is less than the threshold, the computer waits for the next clock interrupt. If the voltage level is greater than the threshold, the programme determines whether or not the previous level was below the threshold. If it was not, the value is simply stored. If it was, both the clock time and the voltage level are stored. The data are stored in one of two buffers. After each datum is stored, the programme checks to see whether the buffer is full. If it is, this buffer is written on the magnetic disc of the Sigma 7, while subsequent data are stored in the second buffer. This process results in blocks of data in which peaks are separated by time flags at the beginning of each peak voltage profile.

The process is terminated by an end-of-scan interrupt. At this point, the operator may immediately record the data on magnetic tape or may choose to display the data. The data may be displayed in a number of ways. The entire spectrum may be presented at once, for example, as a display of peak envelope *v.* time. In this mode the spectrum resembles a simple line drawing (or analogue oscilloscopic trace on a storage scope) since the peaks are very narrow compared to the elapsed scan time. Alternatively, the time scale may be expanded to any degree under programme control and the peak profiles scanned across the CRT screen sequentially at any chosen rate. This display may be halted at any time by the operator to allow opportunity to study in greater detail peak profiles, dynamic instrument resolution, and relative intensities. When the display mode is complete, the spectrum may be either recorded on magnetic tape or aborted. If these data are chosen to be recorded, the blocks of data for the scan are read from the disc and written on digital magnetic tape. In either case, the computer is automatically reset to idle, at which point the next spectrum scan may be taken.

The CRT display, which is located adjacent to the mass spectrometer, has proved to be one of the most important parts of the system in terms of convenience. It provides a "window" whereby the operator can maximize adjustment of instrument parameters to obtain the optimum resolution and sensitivity and the proper beam of calibration compound. It is felt that this type of operator interaction with the system, involving not only the display mode but the degree of control possible in the general scanning procedure, represents a unique advantage of a real-time digital data acquisition and processing system. It is also felt that this interaction should be considered in any future system design because of the versatility and enhanced reliability in obtaining optimal quality spectral data, which this permits.

Fig 4(*a*) and (*b*) presents the CRT display in the complete spectrum mode. Fig 4(*a*) is the spectrum of perfluorokerosine (PFK), the mass calibration standard, from m/e 500 to m/e 50. From this display the operator immediately knows that sufficient PFK is available for mass calibration. Fig 4(*b*) presents the spectrum of PFK and ambelline, an alkaloid of *Amaryllidaceae* family, which has a nominal molecular weight of 331. This compound was introduced through the direct insertion lock of the CEC mass spectrometer. It is seen from this display that the spectrum of the alkaloid is of sufficient intensity to permit mass determination of all significant peaks.

Returning to the AEI MS-9 (modified), exponential magnetic scanning was employed utilizing their standard 10 KHz band width amplifier in conjunction

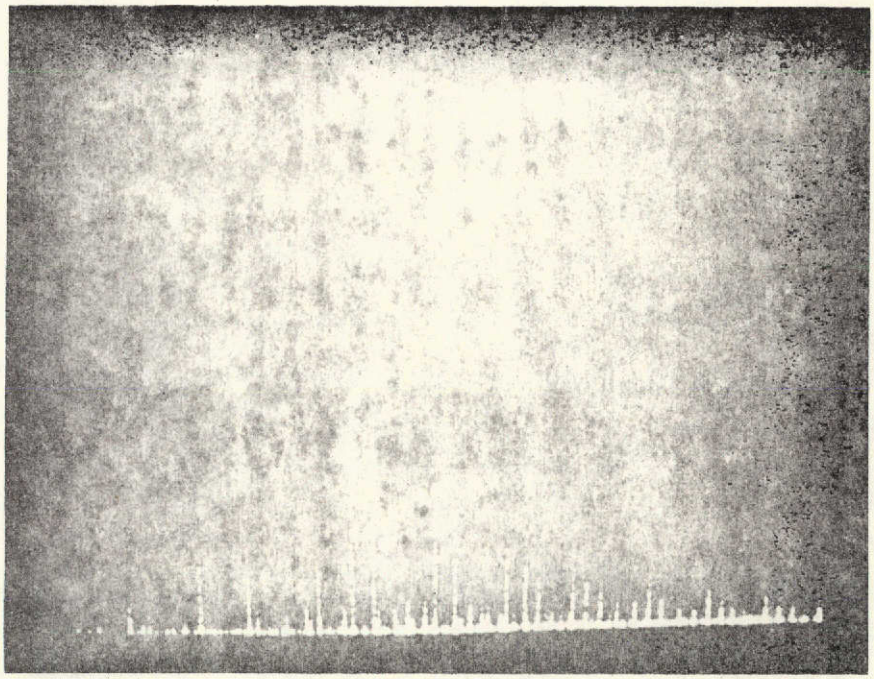

FIG 4(*a*). CRT display of PFK.

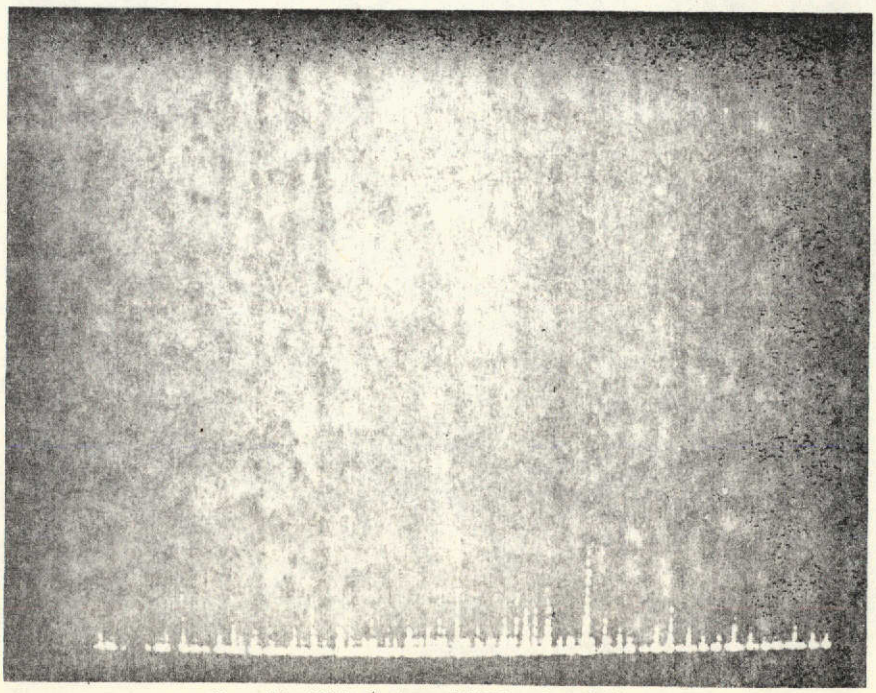

FIG 4(*b*). CRT display of PFK and ambelline.

with a voltage divider circuit which matches the voltage output of the MS-9 to the 0–10 v range of the A/D.

The basic steps in the data reduction programming are summarized in Fig 5. As was mentioned previously, this procedure is closely related to that used in photo-plate data reduction. The programming is designed to elicit the maximum amount of the available information in a high resolution mass spectrum. The procedure, which is handled entirely by a Control Data Corporation Model 6600 computer system, begins with the raw data tape generated by the Sigma 7 data acquisition system. The tape, with any number of spectra, is read and the data are searched to identify the time flags at the beginning of each peak voltage profile. Peak positions may be determined by two methods currently under investigation: peak tops and centres of gravity.

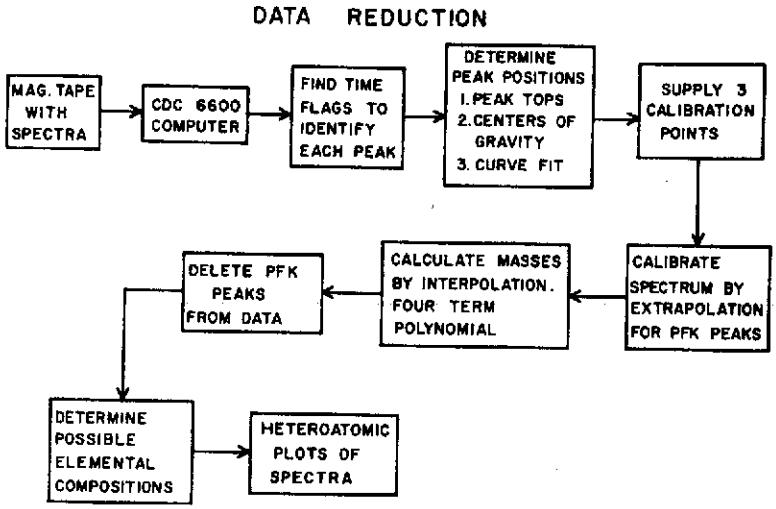

FIG 5. Data reduction.

Peak intensity data may be determined in two different ways, either that given by the maximum peak intensity or the areas, respectively.

The positions and masses of three calibration points at the low mass end of the data are then chosen from the output of the peak position and intensity determination procedure. In the case of quadratic scan spectra (CEC 21-110B), the position of the rest of the PFK peaks are determined by extrapolation using a three-term polynomial of the form $M = A + BT + CT^2$.* When this process is complete, masses of all remaining lines are calculated by interpolation using the calibration points four at a time in a polynomial of the form

$$M = A + BT + CT^2 + DT^3.$$

In the case of exponential magnetic scan data (AEI MS-9 modified), the basic equations† discussed briefly by McMurray and Lipsky[15] for the exponential

* It is generally found that this polynomial approximates the mass *vs.* time dependence accurately enough to predict the time of the next PFK peak within the time width of the peak.

† We wish to thank G. L. Kearns (Picker-Nuclear, White Plains, N. Y.) for providing this information.

dependence of mass and time were incorporated in our programme logic utilized for quadratic real-time and photo-plate data.

PFK peaks are then removed from the data and possible elemental compositions for the remaining peaks are determined within error tolerances. This process is accomplished using a computer programme outlined here for CHON that may include any of the elements and their isotopes found in organic molecules, such as chlorine, sulphur, etc.

LOGIC FOR RAPID DETERMINATION OF POSSIBLE ELEMENTAL COMPOSITIONS

1. Specify maximum numbers of atoms wished to be considered: MAX_C, MAX_H, MAX_O, MAX_N.

2. Find fractional weights of elements and fractional part of measured mass by subtraction of nominal mass:

e.g. $FW_H = \cdot0078+$; $FW_O \cdot0051+$; $FW_N = \cdot0030+$, FWT (measured mass)

3. Find limits for possible numbers of H:

$$CMAX_H = \frac{FWT^+ + FW_O \cdot MAX_O}{FW_H}$$

$$CMIN_H = \frac{FWT^- - FW_N \cdot MAX_N}{FW_H}$$

Note: MAX_H denotes the maximum specified, while $CMAX_H$ is the calculated maximum.

Where $FWT^+ = FWT +$ measurement error tolerance, and $FWT^- = FWT -$ measurement error tolerance, *e.g.* 0·00500 mass units.

At this point, certain restrictions can be applied: $CMAX_H$ cannot exceed MAX_H; if it does, set it to MAX_H; if it is negative, there is no composition to be found.

$CMIN_H$ must be at least zero.

Further, considering only CHON, the number of Hs in the composition is even or odd as the measured mass is even or odd* so this correction is applied to $CMIN_H$ and $CMAX_H$.

Finally, if $CMIN_H > CMAX_H$, there is no composition.

At this stage, there are generally only two or three possibilities for the actual number of hydrogens and the programme proceeds with hetero-atoms O, N.

4. Using the calculated possibilities for number of hydrogens one at a time, the possible numbers of oxygens are calculated:

$$CMAX_O = \frac{(FWT^- - FW_H \cdot {}^{\#}H - FW_N \cdot MAX_N)}{FW_O}$$

$$CMIN_O = \frac{(FWT^+ - FW_H \cdot {}^{\#}H)}{FW_O}$$

Again, the minimum must be at least zero and the maximum cannot exceed MAX_O.

If the maximum is negative or exceeded by the minimum, there is no composition using the present #Hs.

* The programme accounts for measured masses that are either slightly below nominal mass or have fractions greater than 0·5.

5. For each possible combination of the possible numbers of H and O, the possible numbers of N are calculated:

$$CMAX_N = \frac{(FWT^+ + FW_O \cdot {}^{\#}O - FW_H \cdot {}^{\#}H)}{FW_N}.$$

$$CMIN_N = \frac{(FWT^- - FW_H \cdot {}^{\#}H + FW_O \cdot {}^{\#}O)}{FW_N}.$$

(These two equations are the same, but in actual practice two different values for FWT are used, taking the input tolerances into account.)

As in the case of O, if $MAX_N < O$ or if $MIN_N > MAX_N$, there is no composition for the present values of H and O.

6. At this point (if there is a possible composition), we have a value for ${}^{\#}H$, ${}^{\#}O$, ${}^{\#}N$.

The programme then subtracts:

${}^{\#}H \cdot WT_H + {}^{\#}O \cdot WT_O + {}^{\#}N \cdot WT_N$ from the sample mass and determines whether the remainder is an integral multiple of 12. If this is the case, a composition has been found and it is printed.* The programme then tries another combination of ${}^{\#}H$, ${}^{\#}O$, ${}^{\#}N$, thus finding all possible compositions for the sample given mass.

These resulting composition data are sorted according to the hetero-atom content of each peak and presented in graphic form using the Cal-Comp Plotter. The details and advantages of this hetero-atomic plotting technique, which has been developed specifically to aid in interpretation of high resolution mass spectral data, have been discussed previously.[5]

RESULTS

Mass measurement

One of the primary investigations of interest was the degree of mass measurement precision and accuracy that could be attained with these systems. This was evaluated at different resolutions, scan, and clock rates.

CEC 21-110—Due to instrument sensitivity limitations at the high resolutions used (1 : 20,000), our studies were concentrated on results obtainable in relatively slow scans that are nevertheless applicable to all situations, including a coupled interrupted-elution gas chromatograph — mass spectrometer system,† and direct sample insertion systems. The particular set of system parameters studied in most detail utilized the spectrum of *n*-octadecane ($C_{18}H_{38}$). A hydrocarbon was chosen simply because there can be no doubt about the elemental composition and thus the mass of all fragment ions, which makes mass measurement accuracy easy to evaluate. The scan rate was 100 sec from m/e 300 to m/e 30, at clock rates of 12 and 24 KHz. This yields 30 to 100 data points per peak profile, depending on clock rate and mass at a resolution of 1 : 20,000.

Six successive scans at 12 KHz were recorded and analysed. The difference in elapsed times between m/e 305 ($C_8F_{11}^+$, m/e 304·98242) and m/e 31 (CF^+, m/e 30·998402) for the six scans was a maximum of 300 clock ticks out of a total of 1·2 to 10^6 ticks. This sort of reproducibility is extremely promising. It

* The programme rejects all combinations in which ${}^{\#}H > 2 \cdot {}^{\#}C + {}^{\#}N + 3$ or ${}^{\#}C > MAX_C$.

† Scott, R. P. W., Unilever Research Laboratory, personal communication, April 1967.

indicates that future calibration of a spectrum can be simplified by use of expectation times to identify calibration peaks, rather than the more complex extrapolation procedure used at the present time, which requires that three peaks be specified from the raw data. Analysis of this data, using both peak tops and centres of gravity as peak position criteria, indicates that centres of gravity yield much more precise results. Centres of gravity were used in all calculations which are discussed below. The standard deviations of the determined masses in the six scans averaged about 4 ppm, with a worst case of 6·5 ppm and a best case of 2·5 ppm. Some representative data are included in Table I. The data in Table I are presented in Fig 6. The mean of the six determinations is indicated, and the brackets indicate the standard deviations, both of which are expressed

TABLE I

Representative data for saturated ions from six successive scans of *n*-octadecane

Composition	Exact mass	Calculated mass*	Standard deviation†
C_3H_7	43·05477	43·05479	4·5
C_4H_9	57·07042	57·07060	3·7
C_5H_{11}	71·08607	71·08634	6·4
C_6H_{13}	85·10172	85·10209	5·2
C_7H_{15}	99·11737	99·11733	5·1
C_8H_{17}	113·13302	113·13291	6·5
C_9H_{19}	127·14867	127·14810	6·3
$C_{10}H_{21}$	141·16432	141·16450	4·2
$C_{11}H_{23}$	155·17997	155·18139	6·1
$C_{12}H_{25}$	169·19562	169·19741	2·7
$C_{13}H_{27}$	183·21126	183·21172	4·9
$C_{14}H_{29}$	197·22691	197·22717	4·1
$C_{15}H_{31}$	211·24256	211·24224	3·8
$C_{16}H_{33}$	225·25821	225·25876	3·1
$C_{17}H_{35}$	239·27386	239·27348	4·2
$C_{18}H_{38}(M^+)$	254·29733	254·29810	5·6

* Mean of six determinations.
† Standard deviation of the mean, ppm

in this case in millimass units rather than parts per million. In general, the greater errors are obtained for peaks of low intensity (less than 5 per cent of base peak, m/e 57). This appears to be a result of the poorer definition of peak profile for these low intensity peaks, resulting probably in part from ion statistical considerations and in part from poorer signal-to-noise ratio. Mass measurement accuracy is of the order of mass measurement precision as reflected in the means listed in Table I. It is important to note that errors of this magnitude are sufficiently small to reduce to a considerable degree ambiguities in the determination of elemental compositions.

The smoothness of the mass *v.* time function was evaluated in the following manner. Because the calibration points are used four at a time to calculate masses, masses of all peaks except those at the extremities of the calibration range can be calculated by interpolation three times, using three different sets of four calibration points. In no mass region did these three determinations differ significantly from one another, as compared to the standard deviations in Table I.

peak tops give good qualitative descriptions of the fragmentation pattern. This is illustrated in Fig 7, where both the low and high resolution spectra of *n*-octadecane are presented. From the high resolution data there can be no doubt that one has the spectrum of a straight chain, saturated hydrocarbon ($C_{18}H_{38}$). From a quantitative standpoint, however, these determinations leave a great deal to be desired. In the above-mentioned six scans, for example, the standard deviations of relative intensities are about 10 per cent of the peak height.

Current results indicate that peak areas also provide semi-quantitative description of the fragmentation pattern. In addition to this, however, they yield better reproducibility. Standard deviations of relative intensities in successive scans under the same conditions are 2–4 per cent of peak height.

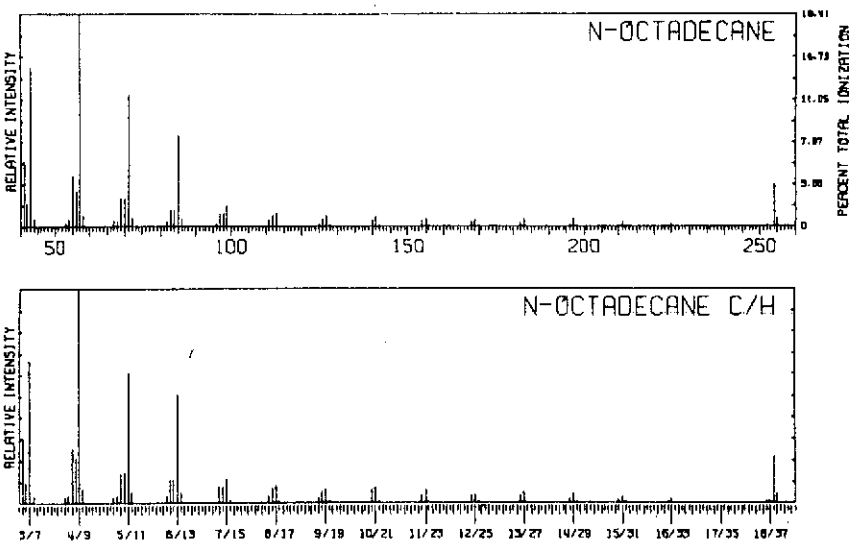

FIG 7. Low and high resolution spectrum of *n*-octadecane.

In relation to discussion in "Experimental" above, it should be pointed out that in a linear magnet current scan (used in CEC 21-110) peak time widths increase as a function of $M^{1/2}$. Therefore the measured peak area must be normalized, taking this function into account. Of course, such normalization procedures for the exponential scan are theoretically not necessary, assuming constant instrument resolution over the entire mass range.

Three specific examples of the above techniques will serve to indicate the quality and type of data that may be obtained with these systems. One application involved the spectra of several alkaloids of the *Amaryllidaceae*,* obtained by direct introduction of the samples into the ion source. These spectra had all previously been obtained by the photo-plate technique, so that a comparison of the methods was possible. In terms of mass measurement, the real-time system leads to much more consistent results. The word "consistent" refers to mass

* Burlingame, A. L., Longevialle, P., Fales, H. M., and Highet, R. J. *J. Am. chem. Soc.*, in preparation.

measurement errors, which in the real-time system are all of the same order as the time resolution of the system, as was mentioned above. The photo-plate data generally exhibit a greater variation in differences between calculated and assigned masses. One must keep in mind that this is primarily a measuring system limitation. It is felt, however, that the very promising results obtained so far with the real-time system indicate that this method is capable of greater mass measuring accuracy. Some representative data are included in Table II.

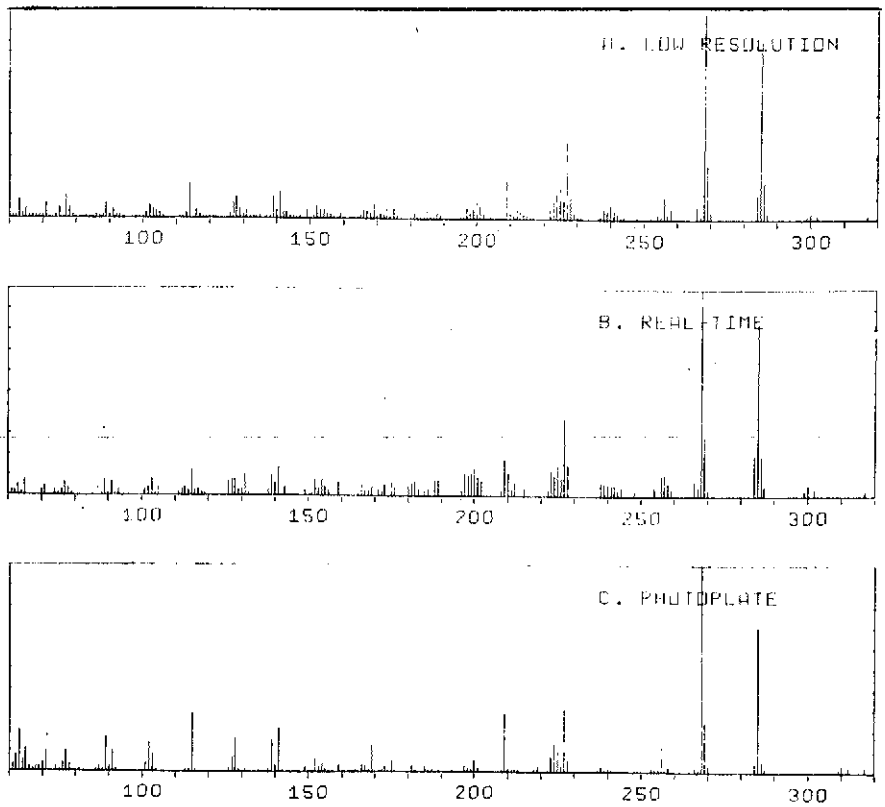

FIG 8. Comparison of 6-hydroxycrinamine a b c.

As far as intensity measurements are concerned, the "low resolution" intensities obtained by summing the intensities (peak top) at each nominal mass in the real-time data yield much better agreement with the observed low resolution intensities than do the photo-plate data. This is illustrated in Fig 8, where the top spectrum (*a*) is the low resolution data, (*b*) the summed real-time intensities, and (*c*) the summed photo-plate intensities for the spectrum of 6-hydroxycrinamine.

A second application involves the spectra of tetrahydro-*N*-acetyl pyrrole and three deuterated analogues. Although current mass spectrometers are not capable of resolving masses differing by two hydrogens *v.* a deuterium atom, the inclusion of an internal mass standard permits mass measurement accuracies

TABLE II

Representative data from the spectrum of 6-hydroxycrinamine, determined both by photo-plate and real-time system

	Calculated mass		Error†	
Composition*	Photo-plate	Real-time	Photo-plate	Real-time
$C_{17}H_{19}NO_5$	317·1293	317·1283	3·0	2·0
$C_{16}H_{15}NO_4$	285·0986	285·0995	−1·4	−0·5
$C_{16}H_{14}NO_3$	268·0985	268·0980	1·2	0·7
$C_{15}H_{14}NO_2$	256·0981	256·0967	0·7	−0·7
$C_{14}H_{11}O_3$	227·0713	227·0711	0·5	0·3
$C_{14}H_9O_2$	209·0616	209·0607	1·3	0·4
$C_{12}H_9O$	169·0642	169·0657	−1·1	0·3
$C_{11}H_9$	141·0700	141·0699	−0·4	−0·5
C_9H_7	115·0548	115·0540	0·0	0·8

* Assigned on the basis of calculated mass.
† Error in millimass units (mmμ), calculated-exact mass.

TABLE III

Representative data from unlabelled and labelled *N*-acetyl-tetrahydro-pyrroles

Ion**	Calculated mass†	Possible composition‡	Exact mass	Diff.¶
M+(d_0)	113·08380	$C_6H_{11}NO$*	113·08406	0·2
		$C_6H_9NO\ D_1$	113·082421	−1·4
M+(d_{2a})	115·09600	$C_6H_7NO\ D_3$	115·09480	−1·2
		$C_6H_9NO\ D_2$*	115·09643	0·4
		$C_6H_{11}NO\ D_1$	115·09807	2·0
M+(d_{2b})	115·09682	$C_6H_7NO\ D_3$	115·09480	−2·0
		$C_6H_9NO\ D_2$*	115·09643	−0·4
		$C_6H_{11}NO\ D_1$	115·09807	1·2
M+(d_3)	116·10333	$C_6H_8NO\ D_3$*	116·10262	−0·7
		$C_6H_{10}NO\ D_2$	116·10426	0·9
m/e 98(d_0)	98·06106	$C_5H_6NO\ D_1$	98·05897	−2·1
		C_5H_8NO*	98·06058	−0·5
m/e 100(d_{2a})	100·07263	$C_5H_6NO\ D_2$*	100·07296	0·3
		$C_5H_8NO\ D_1$	100·07460	2·0
m/e 100(d_{2b})	100·07280	$C_5H_6NO\ D_2$*	100·07296	0·1
		$C_5H_8NO\ D_1$	100·07460	1·8
m/e 98(d_3)	98·06121	C_5H_8NO*	98·06058	−0·6
		$C_5H_6NO\ D_1$	98·05895	−2·2

** d_0 indicates unlabelled molecule,
d_{2a} indicates 2,2-d_2;
d_{2b} indicates 3,3-d_2;
d_3 indicates 7,7,7-d_3.
† From real-time data.
‡* Indicates assigned composition.
¶ Difference in mmμ

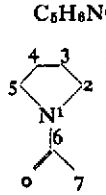

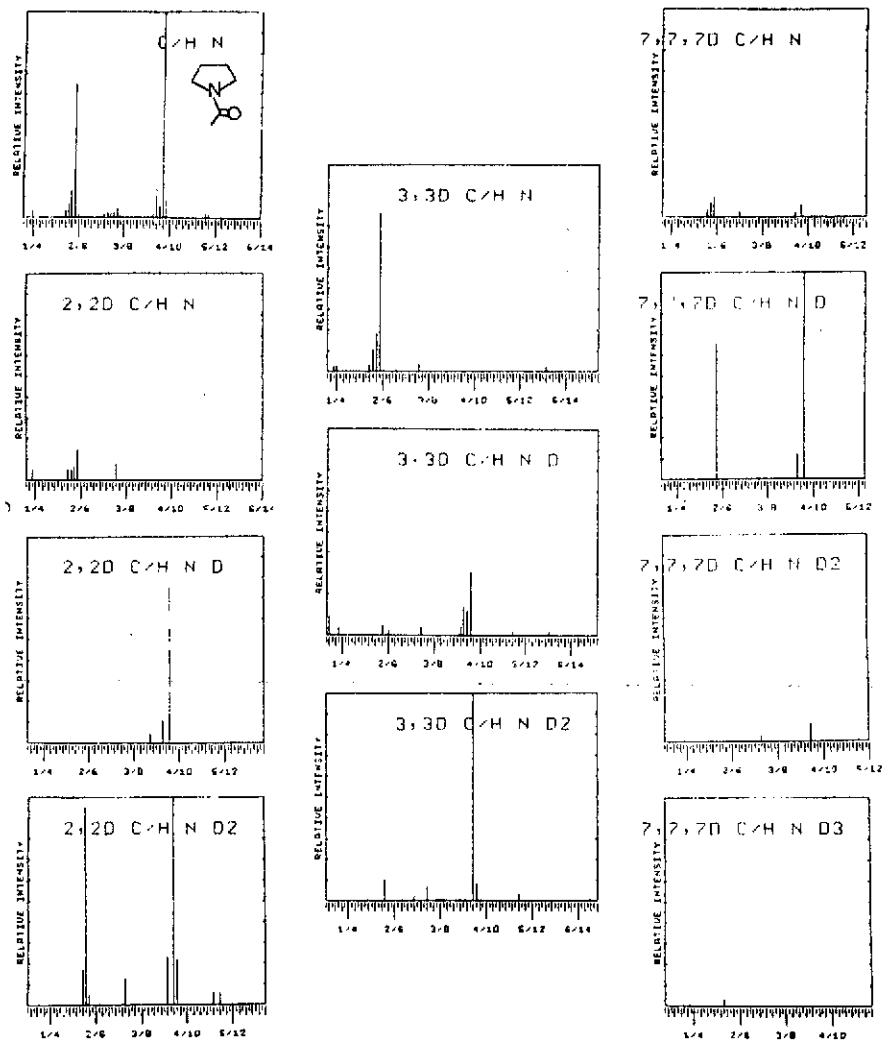

FIG 9. Deuterium data on *N*-acetyl tetrahydropyrrole.

capable of distinguishing between the two possibilities. Indeed, it was found that the deuterium content of nearly every peak could be determined by a simple comparison of differences between observed mass and masses of compositions including any number of deuterium atoms. The lowest difference yields the correct deuterium content. In those few cases where there are significant contributions of both compositions (2 hydrogens *v.* D) to an observed peak, the observed measured mass generally lies intermediate between the two masses calculated on the basis of elemental composition. Some representative accurate mass data are included in Table III and the nitrogen-containing fragments and their respective deuterium contents are shown in Fig 9. Because these spectra

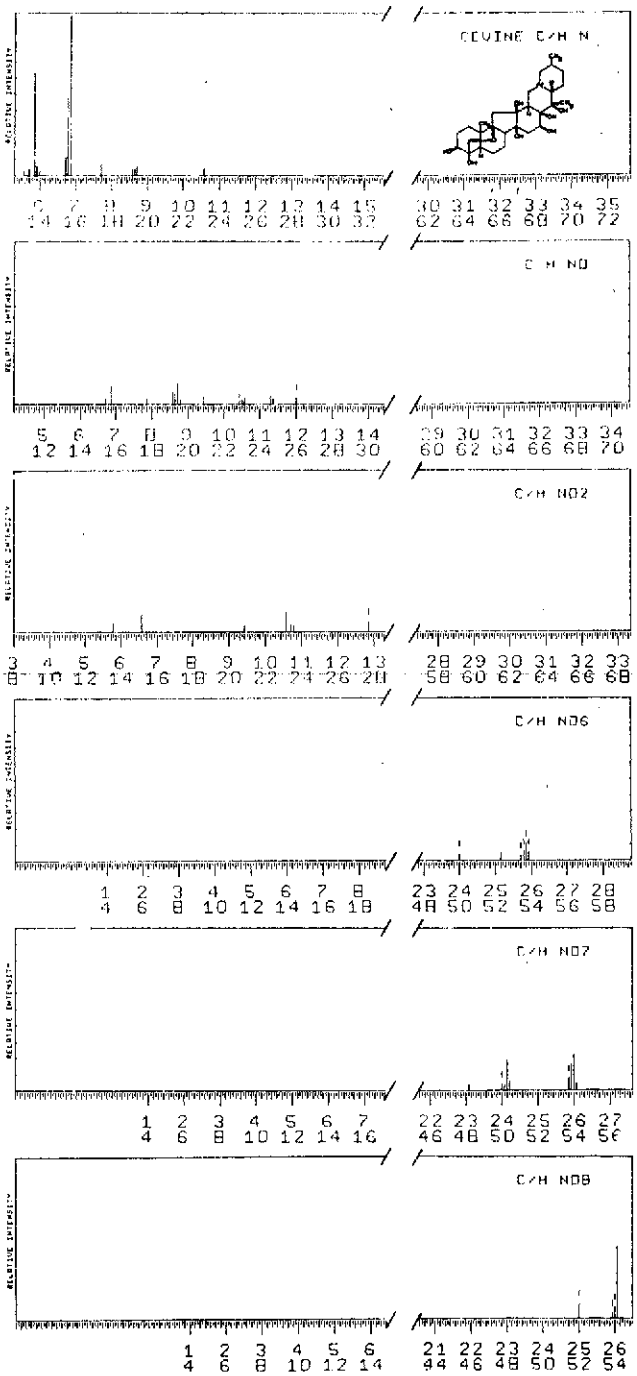

FIG 10. High resolution mass spectrum of cevine.

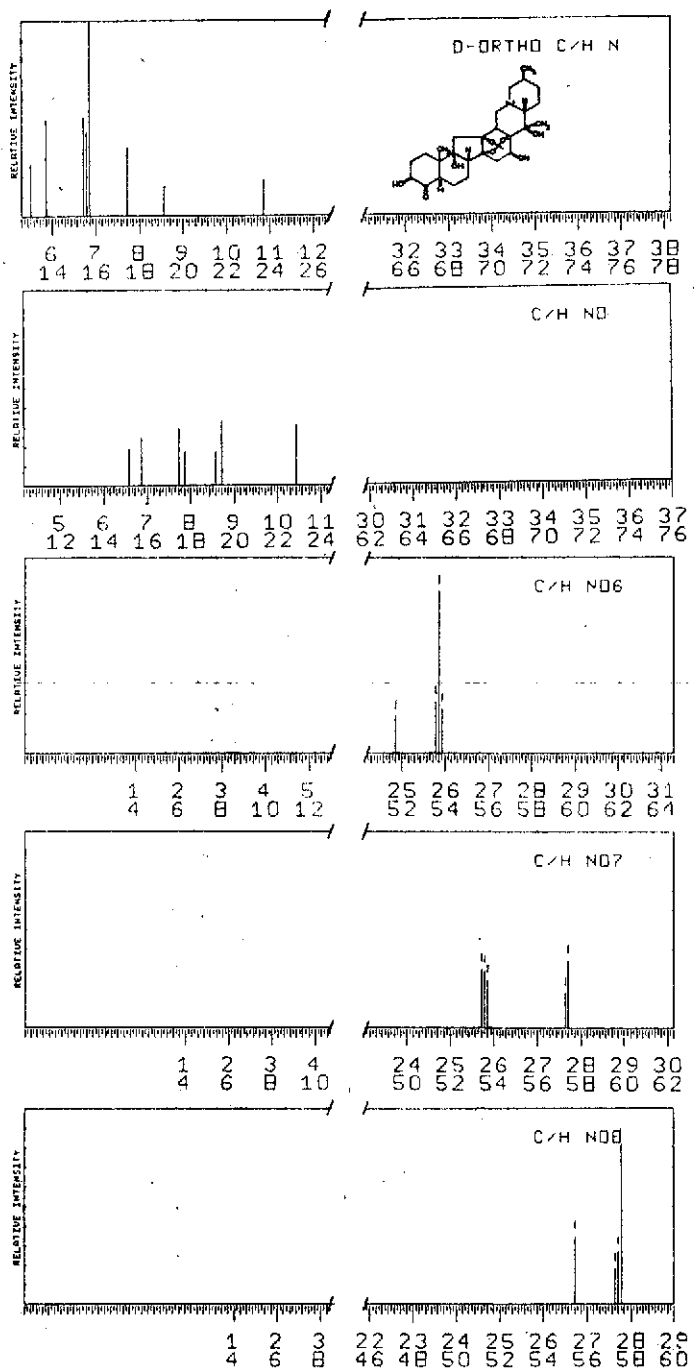

FIG 11. High resolution mass spectrum of cevagenine-D-ortho-acetate.

exhibit multiplets at all important peaks below m/e 80 (CH_2 *v.* N, CH_4 *v.* O, or NH_2 *v.* O), interpretation of peak shifts in the spectra of the deuterated compounds is an impossible task on the basis of the low resolution spectra only. Intensities (peak top) of the real-time data, where these multiplets are separated and deuterium content determined, are sufficiently quantitative to yield a clear formulation of the fragmentation processes occurring in such a molecule.

A final example is taken from studies of the fragmentation of Veratrum alkaloids,[21] which will serve to illustrate real-time data (CEC 21-110) on natural products of intermediate molecular weight. Cevine (Fig 10) and cevagenine-ring D ortho acetate (Fig 11) have relatively intense molecular ions at m/e 509 ($C_{27}H_{43}NO_8$) and 533 ($C_{29}H_{43}NO_8$) respectively. Their fragmentation patterns display a group of intense ions at high mass which are characteristic of the ring-ortho acetate derivatives possible and also a group of relatively low mass fragments containing the F-ring and the heterocyclic nitrogen.

CONCLUSIONS

A system for acquiring high resolution mass spectral data in real-time employing a Sigma 7 digital computer has been developed. At this stage of development, real-time data acquisition and display, followed by batch data reduction, provides extremely accurate mass measurements and reasonable intensity data. It is felt that this system offers several advantages over previous methods for determining high resolution data, including not only present capabilities, *e.g.* measurement of deuterium, carbon-13, some virtual doublets, *i.e.* C_3N *v.* H_2O_3, etc., but future potentialities for enhancement of accuracy in mass and intensity determinations. The high quality data presented, coupled with the flexibility, rapidity, and ease of such digital data acquisition, represents a significant state of the art advance in high resolution mass spectrometry.

The use of a digital computer for techniques of this nature offers additional advantages. In a real-time system the capability exists not only for data acquisition but also for a considerable amount of actual data reduction while the scan of the spectrum is taking place. An obvious goal is to provide the final output of masses, elemental composition, and intensities in suitable form for interpretation in a turn-round time of two or three minutes.

An additional advantage of such a computer is its capability for interaction both with the operator and with the mass spectrometer in terms of control of the various instrument and scanning parameters.

It may be of some interest to note that the data reduction procedure discussed above requires, from raw data to final plotted output, 10–12 sec of CDC 6600 central processor time for the average spectrum.

ACKNOWLEDGMENTS

Generous financial support was provided by the National Aeronautics and Space Administration, Grants NsG 243, Suppl. 5, and NGR 05-003-134.

I would also like to express appreciation to my colleagues, without whose ability and conscientiousness this research would not be possible: R. W. Olsen, Roderick Jones, R. E. Furey, Jan Hansir, John McConnell, Deborah Allen, Fred Walls, James Wilder, Dr Davies H. Smith, Dr Peter Schulze, and Dr Pierre Longevialle; and to the Lawrence Radiation Laboratory Computer Center for CDC 6600 time.

I also wish to thank M. Evans, of AEI, Manchester, for his help with the preliminary MS-9 (modified) data.

REFERENCES

1. For discussion of demanding problems accompanying the application of computers to scholarly disciplines, see "Digital Computer Needs in Universities and Colleges", National Academy of Sciences, National Research Council Publ. 1233.
2. Budzikiewicz, H., Djerassi, G., and Williams, D. H., *in* "Mass Spectrometry of Organic Compounds", San Francisco, Holden-Day, 1967.
3. Beynon, J. H., *in* "Advances in Mass Spectrometry", Vol. 1. J. D. Waldron, Ed. Pergamon, 1959, p. 328.
4. Nier, A. O., *in* "Nuclear Masses and their Determination", H. Hintenberger, Ed., London, Pergamon, 1957, p. 185.
5. (*a*) Bommer, P., McMurray, W., and Biemann, K. 12th Annual Conf. on Mass Spectrometry and Allied Topics, Montreal, 7–12 June 1964, p. 428.
   (*b*) Biemann, K., Bommer, P., Desiderio, D. M., and McMurray, W. J., *in* "Advances in Mass Spectrometry", Vol. 3, Elsevier, 1966, p. 639.
   (*c*) *Ibid.*, p. 701.
6. Olsen, R. W., 13th Annual Conf. on Mass Spectrometry and Allied Subjects, St. Louis, Mo., 16–21 May 1965.
7. Venkataraghavan, R., Board, R. D., Amy, J. W., and McLafferty, F. W. Paper this conference.
8. Venkataraghavan, R., McLafferty, F. W., and Amy, J. W. *Analyt. Chem.*, 1967, **39**, 178.
9. Biemann, K., Bommer, P., and Desiderio, D. M. *Tetrahedron Lett.*, 1964, (26), 1725.
10. Burlingame, A. L. EUCHEM Conf. on Mass Spectrometry, Sarlat, France, 7–12 September 1965; Burlingame, A. L., and Smith, D. H., *Tetrahedron*, in press.
11. Venkataraghavan, R., and McLafferty, F. W. *Analyt. Chem.*, 1967, **39**, 278.
12. Habfast, K. E., and Maurer, K. H. Abstr. 14th Annual Conf. on Mass Spectrometry and Allied Topics, 22–27 May 1966, Dallas, p. 271.
13. Banner, A. E. Abstr. 13th Annual Conf. on Mass Spectrometry and Allied Topics, 16–21 May 1965, St. Louis, Mo., p. 193; Green, B. N., Merren, T. O., and Murray, J. G. Abstr. 13th Annual Conf. on Mass Spectrometry and Allied Topics, 16–21 May 1965, St. Louis, Mo., p. 204.
14. Campbell, A. J., and Halliday, J. S. Abstr. 13th Annual Conf. on Mass Spectrometry and Allied Topics, 16–21 May 1965, St. Louis, Mo., p. 200.
15. Merritt, Jr, C., Issenberg, P., Bazinet, M. L., Green, B. N., and Murray, J. G. *Analyt. Chem.*, 1965, **37**, 1037; McMurray, W. J., Green, B. N., and Lipsky, S. *Analyt. Chem.*, 1966, **38**, 1194.
16. Boettiger, H. G. 15th Annual Conf. on Mass Spectrometry and Allied Topics, Denver, Colo., 14–19 May 1967.
17. Olsen, R. W., and Burlingame, A. L. 13th Annual Conf. on Mass Spectrometry and Allied Topics, 16–21 May 1965, St. Louis, Mo.
18. This technique has recently been shown to be applicable to the recording of conventional mass spectra; see Hites, R. A., and Biemann, K. *Analyt. Chem.*, 1967, **39**, 965; also this conference.
19. McMurray, W. J., Lipsky, S. R., and Green, B. N. this conference; Merritt, Jr, C., Issenberg, P., and Bazinet, M. L. this conference; Bowen, H. C., Chenevix-Trench, T., Drackley, S. D., Faust, R. C., and Saunders, R. H. *J. scient. Instrum.*, 1967, **44**, 343; Bowen, H. C., Shields, D. J., and Stainer, H. M. This conference.
20. Burlingame, A. L., Olsen, R. W., and Smith, D. H., 15th Annual Conf. on Mass Spectrometry and Allied Topics, Denver, Colo., 14–19 May 1967; Burlingame, A. L., Olsen, R. W., and Smith, D. H. ACS–APS Spec. Conf. on Computers in Chemistry, La Jolla, Calif., 26–30 June 1967; Burlingame, A. L., Smith, D. H., and Olsen, R. W. *Analyt. Chem.*, 1968, **40**, 13; Burlingame, A. L., Olsen, R. W., and Smith, D. H. *J. phys. Chem.*, submitted
21. Longevialle, P., and Burlingame, A. L. *Bull. Soc. chim. Fr.*, in preparation.

MS received 28 September 1967

Fatty Acids Derived from the Green River Formation Oil Shale by Extractions and Oxidations[1]) – A Review

A. L. Burlingame, Patricia A. Haug[2]), Heinrich K. Schnoes[3]) and Bernd R. Simoneit

Space Sciences Laboratory, University of California
Berkeley, California, USA

The Green River Formation oil shale (Eocene - - 52 x 10^6 years) is a carbon rich sedimentary rock thought to be the end result of sedimentation of algae and protozoa in a series of freshwater lakes. An extensive investigation of the carboxylic acids occurring in this shale has been undertaken to elucidate the nature and biopaleontological relationships of these components and to allow correlations with previous studies on the alkanes isolated from this formation.

The exhaustive benzene/methanol extract consisted of 2.2 percent (0.04 % of the shale) acids which, after successive GLC separations of the methyl esters, were identified individually by low resolution mass spectrometry. The major components found were C_7–C_{12} normal carboxylic acids; C_9–C_{10} isoprenoid acids; C_{12}–C_{18} normal α, ω-dicarboxylic acids; C_{16}, C_{18} and C_{19} β-methyl-n-α, ω-dicarboxylic acids; and C_{10} and C_{12} ketoacids. In minor amounts were found benzoic-, phenyl alkanoic-, naphthoic-, cyclic-, mono-unsaturated- and cycloaromatic acids.

The acids liberated from the mineral-kerogen matrix after HF/HCl treatment of exhaustively extracted shale amounted to 31.5 percent of the extract (0.06 percent of the shale). Again, separations were carried out by GLC techniques and structural identification of individual components, as well as homologous series by high and low resolution mass spectrometry. This fraction consisted mainly of C_5–C_{32} normal acids; C_8–C_{22} branched-chain acids; and C_3–C_{18} n-α, ω-dicarboxylic acids. In small amounts were found: C_4–C_{16} methylketoacids; C_5–C_{18} monounsaturated and/or cyclic acids; C_7–C_{15} benzoic acids; C_{11}–C_{14} naphthoic acids; and C_{10}–C_{15} cycloaromatic acids.

Subsequent oxidation of the kerogen concentrate with chromic acid successively for 3,6 15 and 24 hours yielded substantial quantities of fatty acids (0.60 percent of the shale), which were identified by the same techniques used for the previous fractions. The major homologous series found were: C_3–C_{35} normal acids; C_3–C_{27} branched-chain acids; and C_4–C_{22} α, ω-dicarboxylic acids. The minor constituents were: C_4–C_{20} methylketoacids; C_5–C_{26} monounsaturated and/or cyclic acids; C_7–C_{18} benzoic acids; C_{11}–C_{13} naphthoic acids; C_{10}–C_{18} cycloaromatic acids; di- and tricarboxylic aromatic acids; and tetracyclic- and pentacyclic monocarboxylic acids.

---

[1]) This review represents Part XXVII in the Series High Resolution Mass Spectrometry in Molecular Structure Studies. For Part XXVI, see A.L. Burlingame and B.R. Simoneit, Nature, in press.

[2]) Present address: Department of Chemistry, Rice University, Houston, Texas

[3]) Present address: Department of Biochemistry, University of Wisconsin, Madison, Wisconsin

Introduction

The Green River Formation Oil Shale, a sedimentary rock of Eocene age (ca. 52×10^6 years) was presumably formed by deposition of organic debris from a non-marine environment. The sediment is extremely rich in organic carbon (The carbon-hydrogen analysis of the oil shale used in these studies is 20.1 percent Carbon, 2.3 percent Hydrogen, 0.6 percent Nitrogen, 0.3 percent Sulphur and 67.0 percent residue) yielding an average of 40 gallons of crude oil per ton of shale. The organic matter, which is thought to derive mainly from algae (Bradley, 1966) and protozoan remains, is sedimented with silt consisting predominantly of carbonate minerals. Available geologic and geochemical evidence supports the view that the shale has not been subjected to either high temperatures or pressures, suggesting that the organic matter should be relatively well preserved.

Partly because of its potential economic value as a rich source of petroleum and partly because of its intrinsic scientific interest, the sediment has been quite actively investigated in recent years. Chemical studies have been concerned with both the shale oil resulting from retorting of bulk sediment, and the organics solvent extractable from the oil shale. Results based on the former method, which must involve considerable degradation of the organic material, are of lesser interest from the paleobiochemical viewpoint, and most of the detailed structural and stereochemical data are derived from extraction experiments.

Chemical analyses, although far from complete, are in agreement with the general assumption that biological precursors are a major source of the fossil organic matter. Thus, the presence of homologous series of normal and isoprenoidal hydrocarbons has been established. Normal alkanes ranging from C_{13} to C_{33} (lower homologues are probably lost in extraction procedures) exhibit an odd over even predominance not unlike the pattern observed for present-day biological alkane mixtures (Eglinton, Scott, Belsky, Burlingame, Richter and Calvin, 1966). Isoprenoidal alkanes (C_{15}, C_{16}, C_{18} to C_{20}) have been identified (Eglinton, Scott, Belsky, Burlingame, Richter and Calvin, 1966; Robinson, Cummins and Dinneen, 1965; Cummins and Robinson, 1964). Steranes, triterpanes and C_{40}-terpenoidal hydrocarbons, among which cholestane, ergostane, sitostane, lupane (Burlingame, Haug, Belsky and Calvin, 1965), gammacerane (Hills, Whitehead, Anders, Cummins and Robinson, 1966) and perhydro-β-carotene (Murphy, McCormick, Eglinton, 1967) are fairly convincingly characterized.

The fact that the aliphatic isoprenoidal, steroidal, triterpenoidal and tetraterpenoidal alkanes are prominent components of the saturated hydrocarbon fraction (Haug, 1967) represents excellent evidence for the biological origin of the organic matter extractable from this oil shale.

Next to the hydrocarbon fraction, the acidic constitutents of the extractables and those formed upon demineralization and matrix oxidation have received most experimental attention and comprise the subject of this review. A homologous series of straight-chain carboxylic acids from C_{10} to C_{34} was reported by Lawlor and Robinson (1965); normal acids of similar or more limited range have also been found by several other investigators (Haug, 1967; Abelson and Parker, 1962). Oxidation experiments of shale kerogen have yielded a series of normal acids up to C_{35} (Burlingame and Simoneit, 1968). The presence of *iso* and *anteiso* acids has been claimed on the basis of g.l.c. and infrared data in one study (Leo and Parker, 1966), but this finding has not yet been confirmed by other workers. The occurrence of isoprenoidal acids (C_8, C_9, C_{14} to C_{17}, C_{19} to C_{21}) is well established (Haug, 1967; Eglinton, Douglas, Maxwell, Ramsay and Ställberg-Stenhagen, 1966; Douglas, Douraghi-Zadeh, Eglinton, Maxwell and Ramsay, 1968); phytanic and norphytanic acids are major components of this fraction, paralleling to some extent the distribution of isoprenoidal alkanes. The isoprenoidal skeleton also occurs linked to the kerogen matrix – a finding of importance in correlation of the organic polymer structure to the extractables in this oil shale (Burlingame and Simoneit, 1968). A recent study of the isoprenoid acid methyl esters by gas chromatography has shown a diastereoisomeric composition which is compatible with a chlorophyll derivation for these acids (MacLean, Eglinton, Douraghi-Zadeh, Ackman and Hooper, 1968). In addition, the occurrence of oxo-acids (Haug, Schnoes and Burlingame, 1967) and several series of aromatic carboxylic acids (Haug, Schnoes and Burlingame, 1968) has been reported.

Porphyrin constituents of the shale and its shale oil have been investigated recently. Homologous series of alkylated etio-porphyrins, carboalkoxy porphyrins, cycloalkyl- and alkylbenzoporphyrins appear to be present (Morandi and Jensen, 1966; Baker, Yen, Dickie, Rhodes and Clark, 1967).

Much of the chemical work thus far has been directed toward the discovery and structural elucidation of compounds thought to be directly related to common biological precursor material. The emphasis on the search for isoprenoidal and triterpenoidal alkanes and isoprenoidal acids is a reflection of current interest in this field. For a deeper understanding of both the biological and diagenetic processes which contributed to the genesis of shale organics, a broadening of the research effort would appear desirable. Such should include the study of additional compound classes, the kerogen material, quantitative data on the occurrence and distribution of certain compounds as well as compound classes relative to others, and data detailing the nature of isolated organics in the rock matrix.

Some data bearing on the distribution of hydrocarbons as a function of depth of deposition are available from the work of Robinson, Cummins and Dinneen (1965) who found that the chain length of isoprenoidal alkanes tended to decrease with depth (while total content increases), and the interesting finding of Eglinton,

Douglas, Maxwell, Ramsay and Ställberg-Stenhagen (1966) of the predominance of the C_{12} acid at the 1200 ft. level of the shale. However, in most cases data presently available do not permit sound speculation as to specific sources of the compounds found, diagenetic transformation pathways, or the relationships between different compound classes.

Since previous investigations were aimed usually at the isolation of specific compounds or compound classes and are based on one method of extraction and isolation, giving thus perhaps a somewhat distorted picture of the amounts and range of certain compound types present, we thought it of some interest to obtain data on the total distribution of compounds resulting from different extraction methods.

Table 1. Organic acid fractions of the Green River Formation, per 100 g oil shale sample (~45 % kerogen concentrate).

1. **First Extract** (ϕ H – MeOH)
   totals: 1300 mg
   acids: 8 mg
2. **Exhaustive Extract** (ϕ H – MeOH)
   totals: 440 mg
   acids: (heptane) 30 mg
   (ether) 18 mg
3. **Matrix Entrapped Acids** (after demineralization HF/HCl)
   totals: 190 mg
   acids: (heptane) 60 mg
   (ether) 1.5 mg
4. **Oxidation** (3 hour, CrO_3-H_2SO_4)
   totals: 145 mg
   acids: (heptane) 60 mg
   (ether) 34 mg
5. **Oxidation** (9 hour, CrO_3-H_2SO_4)
   totals: 225 mg
   acids: (heptane) 35 mg
   (ether) 150 mg
6. **Oxidation** (24 hour, CrO_3-H_2SO_4)
   totals: 398 mg
   acids: (heptane) 48 mg
   (ether) 320 mg
7. **Oxidation** (48 hour, CrO_3-H_2SO_4)
   totals: 685 mg
   acids: (heptane) 274 mg
   (ether) 360 mg

We chose to investigate the carboxylic acids obtainable from the oil shale of the Green River Formation by three experimental procedures:

(a) direct extraction of the whole shale with organic solvents,
(b) demineralization of the exhaustively extracted shale followed by extraction, and
(c) successive oxidations of the residue remaining after demineralization ("kerogen").

Our data are as yet of a preliminary nature, requiring in many cases verification by identification of individual compounds only partly accomplished by this study, but they provide information on the total acid content, range and nature of acids contained in, and bound to, the polymer and mineral matrices (Table I).

The oxidation experiments were carried out in a stepwise fashion up to 48 hour total duration, at which time all organic matter was essentially degraded. These results do not bear on the acids occurring as such in the shale, but give some insight into the composition of the kerogen material.

Part I: Exhaustive Extraction of Shale

Experimental

In order to minimize contamination, several precautions were followed throughout these studies. All microlabware was treated with chromic acid, rinsed with distilled water and distilled organic solvents; this same procedure was applied to most of the glassware used in the large scale workup. All solvents used were A.C.S. reagent grade and redistilled in all glass stills. Other reagents used were checked for organic contaminants and treated to remove any that were present.

Shale samples from the Colorado Green River Formation were collected from a cliff-outcrop at Parachute Creek, 8 miles northwest of Grand Valley, Colorado, latitude N 39° 37′, longitude W 108° 7′, at an elevation of 7300 feet. After removal of the outer one-half inch of rock surface from several large pieces and rinsing with solvent, 5.3 kg of shale was broken into small fragments (3–20 mesh) and ultrasonically extracted in batches with benzene/methanol (4:1 v/v). These extracts were not further investigated. Further treatment of the shale is illustrated in an abbreviated form by the flowsheet of Figure 1. The shale was pulverized (about 200 mesh) and extracted twice (in batches of 500 g of shale to 2 l of 4:1 benzene/methanol) for twenty minutes with mechanical stirring and sonication. From this extract, 55 g of hexane soluble material was obtained. This material was divided into two portions of 26 and 29 g respectively, each dissolved in 500 ml of hexane and extracted three times with 100 ml portions of 1 *N* NaOH. The aqueous solutions were combined, extracted three times with 100 ml of hexane, filtered, acidified to pH 1 and

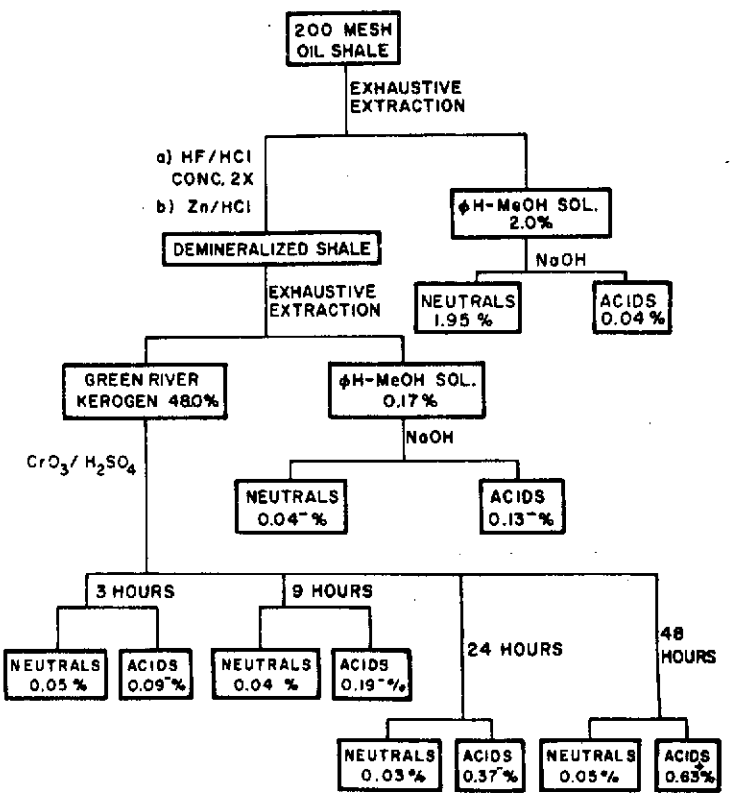

Fig. 1. Experimental flowsheet for the isolation of the various acid fractions from the Green River Formation oil shale

extracted with three 50 ml volumes of hexane. A total of 0.28 g of acidic material was obtained in this way. Acids were separated from phenols by extraction with a saturated solution of $NaHCO_3$ of half of this acidic material in 10 ml of hexane. The acids thus obtained were treated with BF_3/MeOH reagent and refluxed for one hour. Esters were analyzed by gas chromatography without further fractionation. Esters collected from one g.l.c. run (5 % SE-30, on 80–100 mesh Aeropak 30, 10′ x 1/4″ column, Helium carrier gas, flow rate of 50 ml/minute, programmed from 50° – 280° at 2°/minute) were analyzed by mass spectrometry without further purification. From a second separation on the same column (programmed at 4°/minute) collected fractions were rechromatographed [6′ x 1/4″ column, 3 % HIEPF 8 BP on 80/100 mesh Gaschrom Q (Applied Science), flow rate of 50 ml/minute, programmed at 6°/minute] and subsequently analyzed by mass spectrometry. Fractions from a third gas chromatogram (using the SE-30 column, conditions as for the

first case) were analyzed by high resolution mass spectrometry. Identifications are based on the data from these three analyses. A typical gas chromatogram of the total ester mixture is shown in Figure 2 (10′ x 1/16″ column, of 3 % SE-30 on 80/100 mesh Aeropak 30, flow rate 30 ml/minute, programmed from 50° to 280° at 2°/minute).

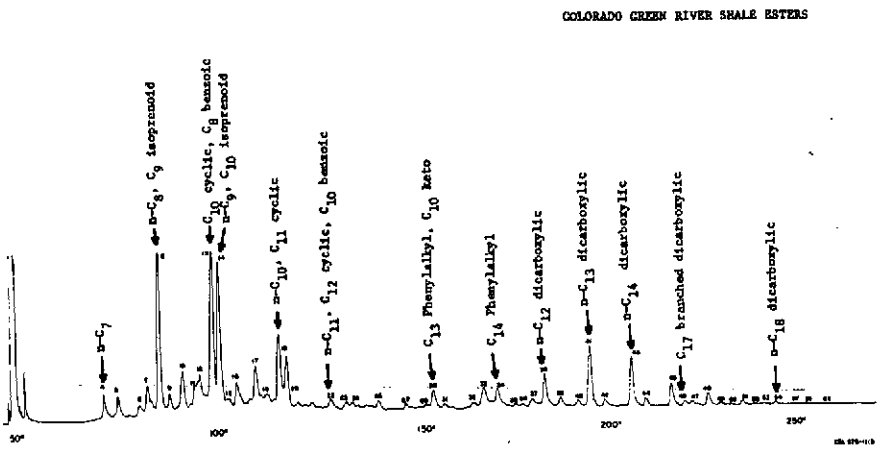

Fig. 2. Gas chromatogram of the total acid esters isolated from the first extract. Column conditions: 10 ft. x 1/16 in.; 3 percent SE-30 on 80/100 mesh Aeropak 30; 30 ml/minute helium; programmed from 50 °C to 280 °C at 2 °C/minute

A sample of the extracted oil shale described above was further extracted by the following procedure. After sieving the sample through 200 mesh it was Soxhlet extracted for one week with 3:1 benzene/methanol and then treated by ultrasonication with portions of the same solvent system until no more organics could be solubilized. All extracts were combined and the solvent evaporated under vacuum, yielding 440 mg organics per 100 g sample. The extract was dissolved in heptane and the acids were removed with 6 *N* NaOH. From the acidified aqueous solution 30 mg of acids were extracted with heptane and a subsequent diethyl ether extract yielded another 18 mg of more polar acids. Both fractions were esterified with BF_3/methanol and the heptane soluble acid ester fraction was clathrated with urea (Burlingame and Simoneit, 1968), yielding 1:1 normals/branched-cyclics. The total, normal and branched-cyclic fractions, were chromatographed on a 5 ft. x 1/8 in. column, packed with 3 % SE-30 on Chromosorb Q and programmed from 100° to 250° at 10°/minute with a flow rate of 40 ml/minute. The gas chromatograms of the heptane soluble acids are shown in Figure 3. The g.l.c. trace of the total ether soluble acids is shown in Figure 4. The labeled peaks were checked by coinjection of standards and identified from their retention times, low resolution mass spectra

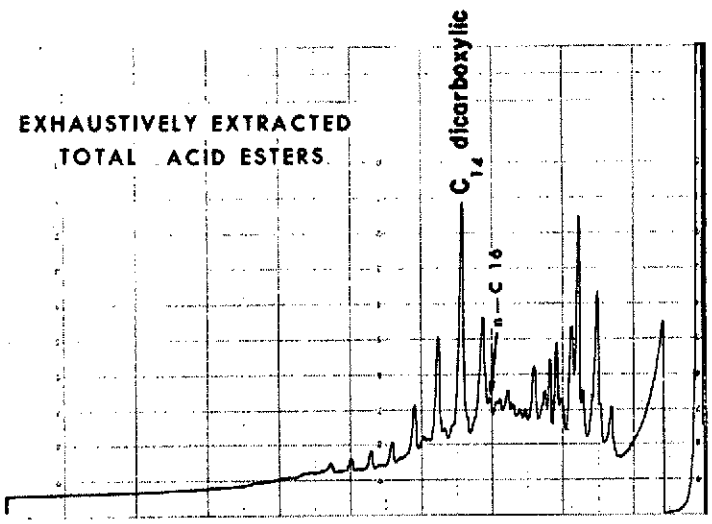

Fig. 3. Gas chromatogram of the total heptane soluble acid esters isolated from the second exhaustive extract. Column conditions: 5 ft. x 1/8 in.; 40 ml/minute helium; programmed 100 °C to 250 °C at 10 °C/minute

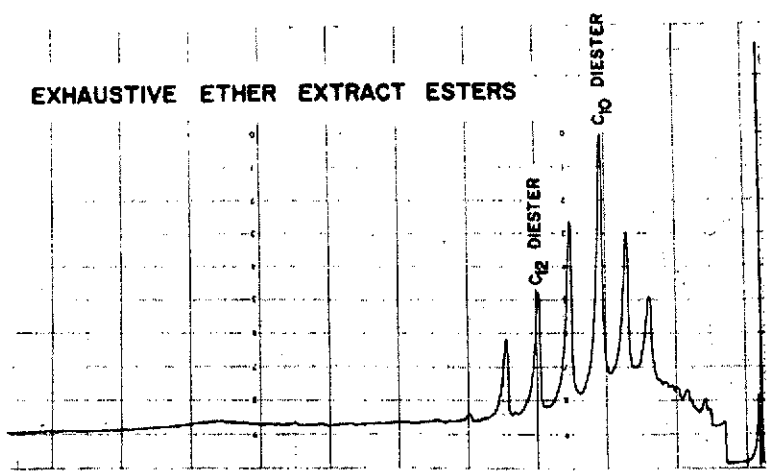

Fig. 4. Gas chromatogram of the total ether soluble acid esters isolated from the second, exhaustive extract. Column conditions as in Figure 3

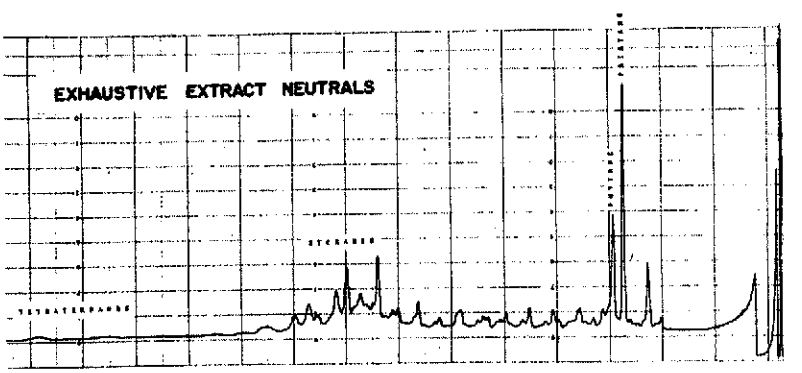

Fig. 5. Gas chromatogram of the neutral fraction isolated from the second, exhaustive extract. Column conditions as in Figure 3

and correlations with high resolution mass spectral data. For comparison the neutral and basic fraction from this extract was also analyzed by gas chromatography (Figure 5) and high resolution mass spectrometry (Figure 6).

All unit resolution mass spectra were obtained either on a modified G.E.C. – A.E.I. MS–902 or a C.E.C. 21–110B mass spectrometer using a direct insertion probe for sample introduction or an all glass introduction system for very volatile samples. The ion source temperature was kept as low as possible to achieve volatilization of samples, usually around 100°–150°. High resolution mass spectra were recorded *via* photoplate (C.E.C. 21–110B) (Burlingame, 1966) or *via* direct on-line computer data acquisition and processing (Burlingame, 1968; Burlingame, Smith, Merren and Olsen, 1968). High resolution mass spectral data are presented as heteroatomic plots (Burlingame and Smith, 1968).

Results

Data presented in this section are based on two sets of experiments. The first approach, as detailed in the experimental part, involved the extraction of relatively large quantities of rock and removal of acids from the total extract thus obtained. In order to insure more complete extraction of organic matter, the extracted rock powder from the large scale experiments was subjected to further exhaustive Soxhlet and ultrasonic extraction. In this section we combine the results from these two extractions, although methods of identification and experimental procedures differed somewhat.

The various homologous acid series found are listed in Table II and are discussed in the same order. The range of distribution and maxima indicated in this table are derived mainly from high resolution mass spectra of total mixtures. They are not *a priori* indicative of relative abundances of compounds and must be considered with

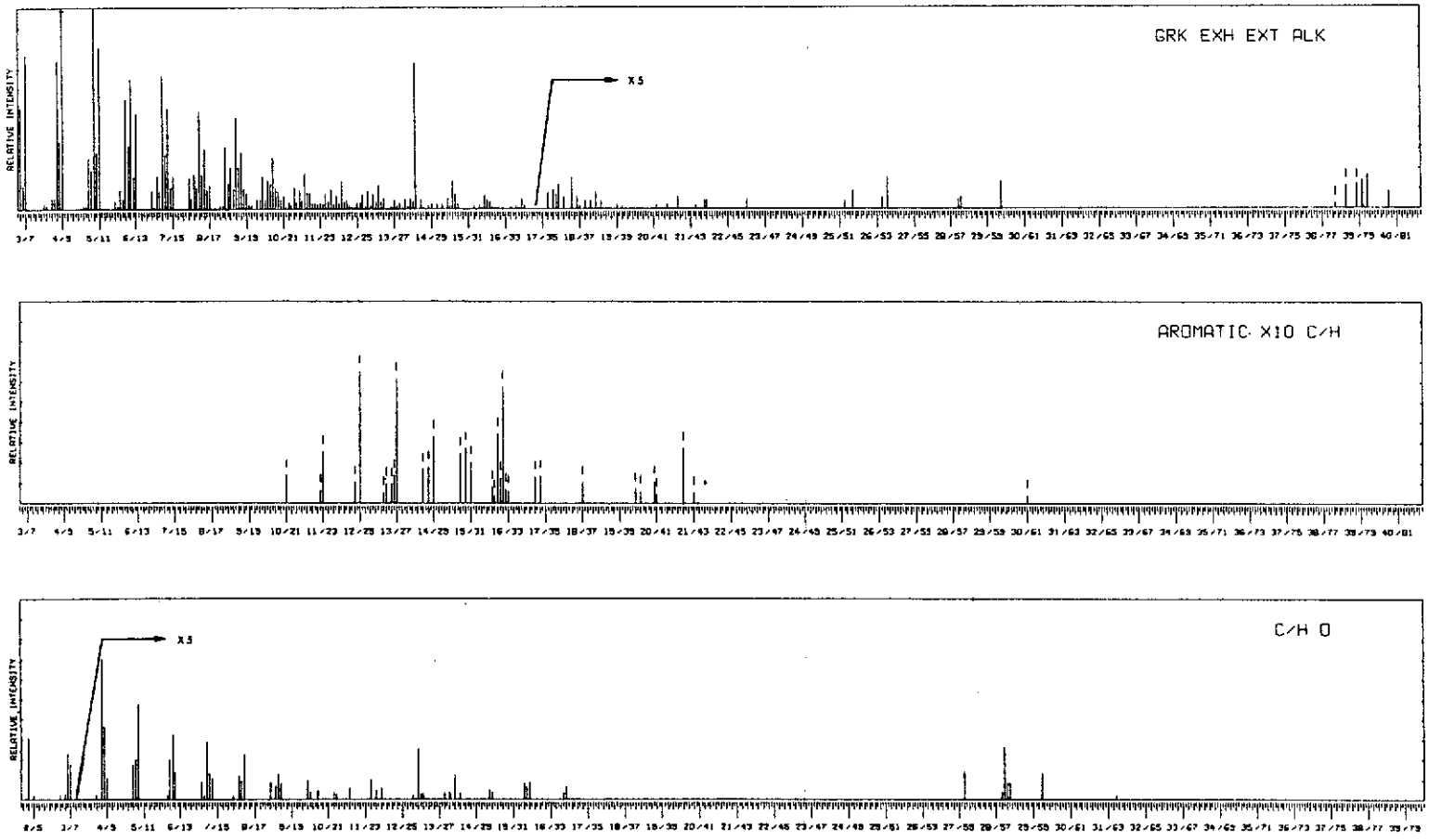

Fig. 6. High resolution mass spectral data for the neutral fraction isolated from the second, exhaustive extract

Table II. Organic acids from the exhaustive extracts of the Green River Formation oil shale (extracted with heptane and ether), listed as free acids.

	range	maximum concentration
1. **Normal Acids**		
first extract	C_7-C_{12}#+	C_8
exhaustive extract	C_5-C_{20}*	
2. **Branched Acids**		
first extract	C_9, C_{10}#+	C_9
exhaustive extract		
3. **Dicarboxylic Acids**		
first extract	$C_{12}-C_{18}$#+	C_{13}
exhaustive extract (heptane)	C_8-C_{15}*	
(ether)	C_8-C_{14}+	C_{10}
4. **Ketoacids**		
first extract	C_{11}, C_{14}#+	
exhaustive extract	C_5-C_{15}*	C_6
5. **Cyclic Acids** ($C_nH_{2n-2}O_2$)		
first extract	C_8-C_{12}#+	C_{10}
exhaustive extract	C_5-C_{16}*	
6. **Aromatic Acids** (phenyl $C_nH_{2n-8}O_2$)		
first extract	C_8-C_{14}#+	C_8
exhaustive extract	C_7-C_{17}*	C_8
7. **Aromatic Acids** (naphthyl $C_nH_{2n-14}O_2$)		
first extract	C_{12}, C_{13}#+	C_{12}
exhaustive extract	$C_{11}-C_{17}$*	C_{12}
8. **Aromatic Acids** ($C_nH_{2n-10}O_2$)		
first extract	$C_{13}-C_{15}$#+	C_{14}
exhaustive extract	$C_{10}-C_{17}$*	C_{10}

\# Determined by low resolution mass spectrometry of isolated samples
\+ Determined from gas chromatogram
* Determined by high resolution mass spectrometry

some caution, since the relative abundances of molecular ions vary with compound type in addition to the non-linearity in photoplate response characteristics with ion beam intensity for high resolution mass spectrograms (Venkataraghavan, McLafferty and Amy, 1967). Relative ion beam intensity measurements are accurate to the 1–2 % level for the real-time high resolution data (Burlingame, Smith, Merren and Olsen, 1968). Figure 7 represents the high resolution mass spectrum of this fraction -- sorted according to heteroatomic content (i.e., C/H, C/H O, C/H O_2, etc. ions).

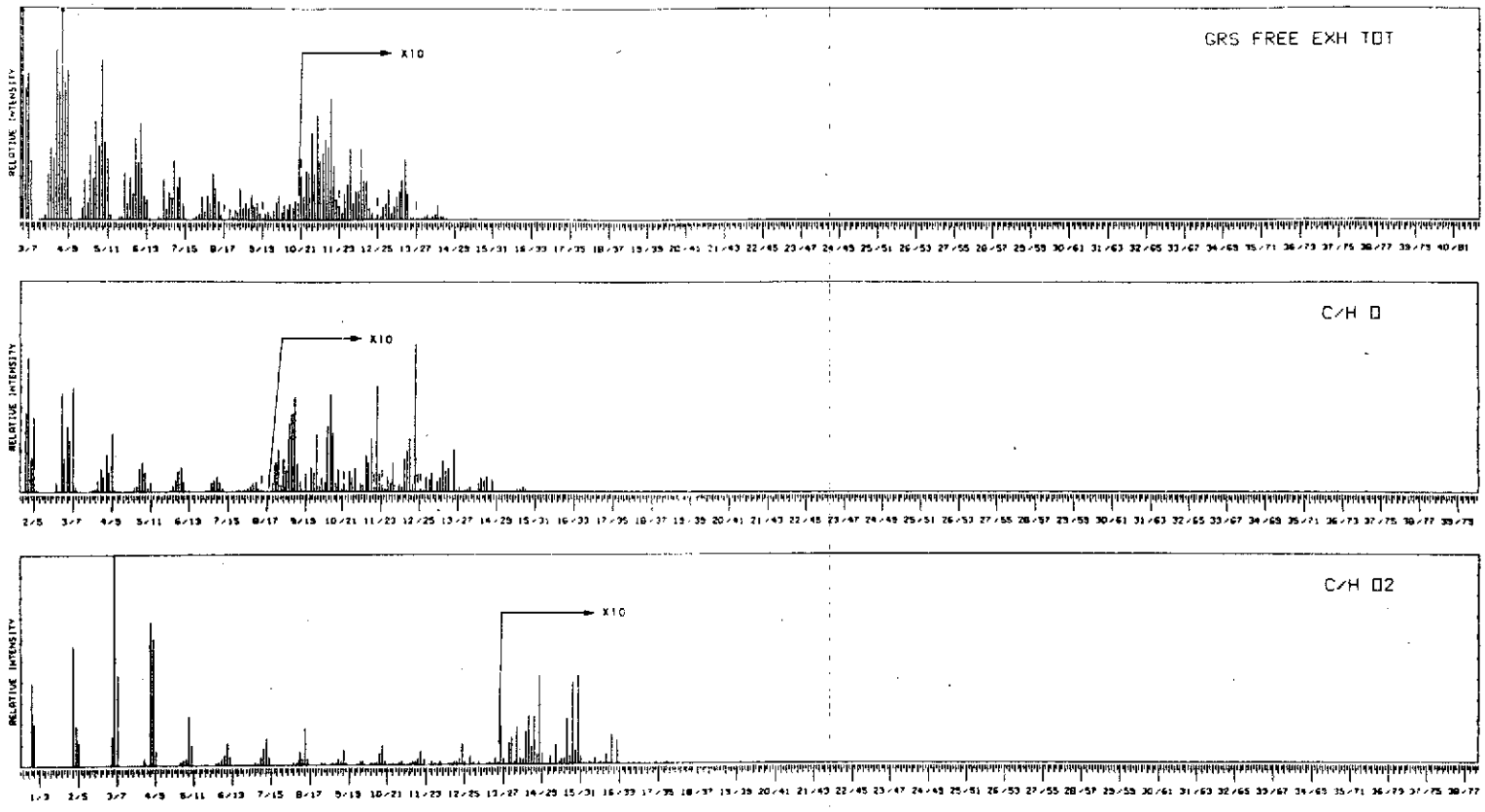
GRS FREE EXH TOT
X10
RELATIVE INTENSITY
C/H 0
X10
RELATIVE INTENSITY
C/H 02
X10
RELATIVE INTENSITY

Part of Fig. 7

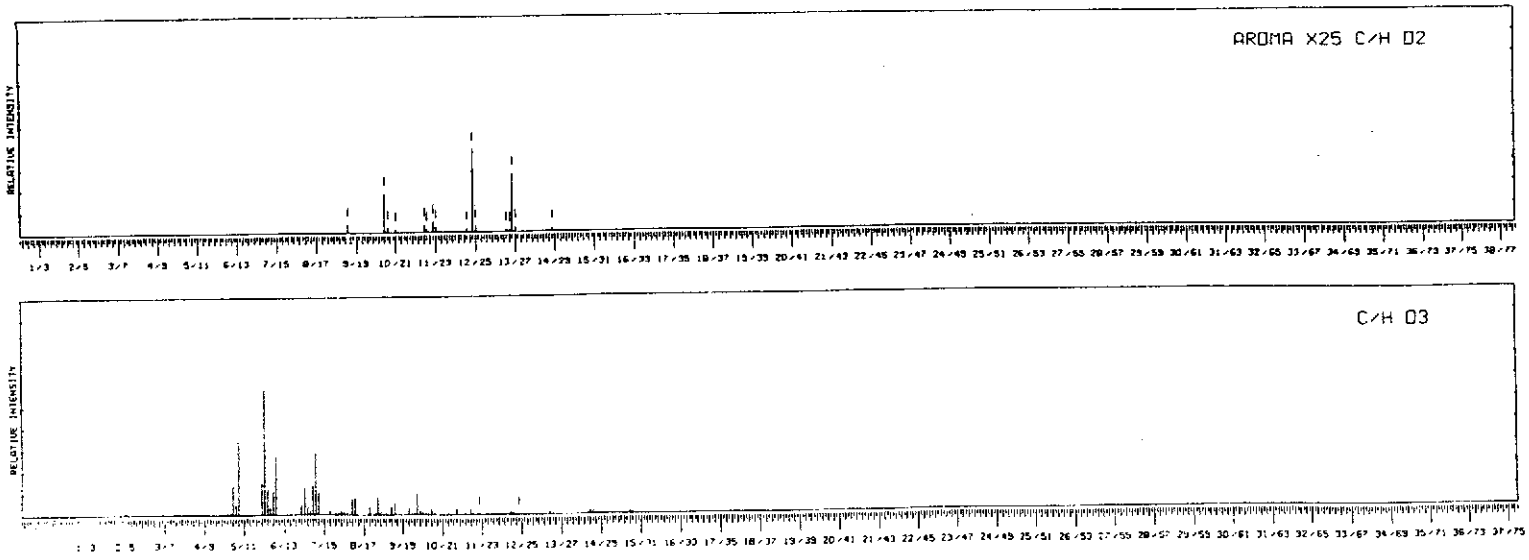

Fig. 7. High resolution mass spectral data for the total acid esters isolated from the second, exhaustive extract

The extraction experiments revealed a distribution of normal saturated acids ranging from C_5 up to C_{20}. From the first extraction five normal acids (C_7-C_{11}) were isolated and identified by mass spectrometry (present in peaks labelled 4, 8, 14, 19 and 22 in Figure 2). The high resolution mass spectrum of the total heptane soluble acid ester mixture (Figure 7) from the second exhaustive extraction exhibits molecular ions corresponding to saturated acids ranging from C_5 to C_{20}. For example, the molecular ion of the C_6 acid is found at $C_7H_{14}O_2$ (since the mass spectrum is that of the methyl ester mixture) in the C/H O_2 plot (Burlingame and Smith, 1968) of Figure 7. Higher homologues of this class are readily identifiable from this plot. The gas chromatogram of this ester mixture (Figure 3) shows some components above C_{10}, but our data indicate that the major acids obtained by direct extraction are relatively low molecular weight compounds. Only two branched acids, the C_9 and C_{10} isoprenoid acids, have been isolated from the extract. The g.l.c. pattern indicates that higher homologues are present, but no definite identifications were made. Results from the second extraction indicate that the branched acids represent only a very minor part of the total acid mixture. Pristanic and phytanic acids are certainly not major constituents of this mixture.

Seven saturated straight-chain α,ω-dicarboxylic acids (C_{12} to C_{18}, Haug, Schnoes and Burlingame, 1967) have been identified as constitutents of the first extract. In addition, the C_{13}, C_{15} and C_{16} dicarboxylic acids bearing one α-methyl substituent are present (Haug, Schnoes and Burlingame, 1967).

In the high resolution mass spectrum of the second exhaustive extract (Figure 7) a series of α,ω-dicarboxylic acids ranging from C_8 to C_{15} is apparent. The molecular ions are of very low abundance and are omitted from Figure 7 but the corresponding peaks resulting from losses of CH_3O and ketene (typical for this class of compounds) can be seen in the C/H O_3 and C/H O_2 plots respectively. The ether soluble acids from the second extraction (Figure 4) were shown to be a homologous series of saturated dicarboxylic acids (C_8 to C_{14}) by low resolution mass spectrometry. Thus a homologous series ranging from C_8 to C_{18} has been isolated from the shale by direct extraction. It is interesting to note that the ether-soluble acids exhibit a maximum at C_{10} (Figure 4) whereas the dicarboxylic acids obtained in the first extraction maximize at C_{13}, C_{14} (Figure 2, peaks 41, 43).

A series of ketoacids is indicated by the high resolution mass spectra of the total acid mixture. They appear to comprise all homologues from C_5 to C_{15}. As shown in Figure 7, the molecular ions of this series are found at positions $C_nH_{2n-2}O_3$ in the C/H O_3 plot and the peaks arising from elimination of CH_3O and C_3H_5O are prominently displayed in the C/H O_2 plot. Two of these were isolated from the acids

of the first extraction and identified as the C_{11} and C_{14} methylketo acids (methyl 10-oxoundecanoate and methyl 13-oxotetradecanoate) by low and high resolution mass spectrometry (Haug, Schnoes and Burlingame, 1967).

Cyclic acids ranging in molecular weight from 150 to 212 (C_8 to C_{12}) have been isolated from the first extraction but no definite compounds have yet been identified. A similar series of cyclic and/or unsaturated acids is indicated by the high resolution mass spectrum (Figure 7) which shows peaks although of very low intensity corresponding to molecular ions of cyclic acid esters from C_5 to C_{16}.

There appears to be a relatively abundant series of aromatic acids. The first extraction yielded a series ranging from C_8 to C_{14} among which methyl substituted benzoic acids (C_8 to C_{10}) are particularly prominent. Several (C_{11}, C_{12}, C_{13} and C_{14}) phenylalkanoic acids were also isolated. These acids could not be definitely identified, but the general structural type is readily recognized from the mass spectral fragmentation pattern. A similar distribution of aromatic acids in the heptane soluble mixture of the second extract is evident from the high resolution mass spectrum (Figure 7). Acids of composition $C_nH_{2n-8}O_2$ ranging from C_7 to C_{17} with an apparent maximum at C_8 were detected. Condensed aromatic systems are also present. From the high resolution mass spectrum a series of naphthyl carboxylic acids ranging from C_{11} (naphthoic acid) to C_{17} with a maximum at C_{12} are apparent.

Peaks corresponding to molecular ions of indane carboxylic acids (C_{10} to C_{17}) were observed. The C_{10} and C_{11} acids of this series appear to be major constituents. These data show that the bulk of these acid fractions obtained by direct extraction of whole shale material consists of low molecular weight normal and dicarboxylic acids. Cyclic acids appear to be important contributors to the acids below C_{12}, and keto and aromatic acids, while distributed over a wide mass range, are present in rather small amounts. The branched-chain acids represent a surprisingly small fraction of the total acids. In contrast to this the neutral and basic fraction of this extract included compounds up to C_{40} as evidenced by the high resolution mass spectrum (Figure 6). The presence of several C_{40} compounds, probably tetraterpenoidal hydrocarbons, is indicated by the peaks at $C_{40}H_{78}$ (corresponding to the molecular ion of perhydro-β-carotene, Murphy, McCormick and Eglinton, 1967), $C_{40}H_{70}$, $C_{40}H_{68}$, $C_{40}H_{66}$, $C_{40}H_{62}$, and $C_{40}H_{58}$ in the C/H plot. The peaks of composition $C_{30}H_{52}$ and $C_{29}H_{48}$ may be attributed to triterpanes. Particularly interesting are high mass ions in the C/H O plot, since their compositions, $C_{32}H_{52}O$, $C_{30}H_{48}O$ and $C_{29}H_{46}O$ and the corresponding $M-CH_3$ peaks suggest triterpenoidal ketones. This is a class of compounds not yet reported for this sediment, but now preliminary data suggest that a detailed search for them might be a promising undertaking.

Part II: Extract of Demineralized Shale

Experimental

The oil-shale exhaustively extracted as described in Part I was digested twice at room temperature for two days each with 1:1 concentrated hydrofluoric acid/hydrochloric acid. To remove sulfides and free sulfur, the residue was further treated with zinc dust in *6N* hydrochloric acid at room temperature (Forsman and Hunt, 1958). By repeated ultrasonic extractions with 4:1 benzene/methanol, an extract weighing 190 mg was isolated upon evaporation of solvent from a 100 g sample. The exhaustively extracted residue, i.e., the kerogen concentrate, had a carbon-hydrogen analysis of 65.9 %C, 8.2 %H, 0.66 %N and 0.9 %S based on a mineral-free sample. The extract was dissolved in heptane and treated with *6N* sodium hydroxide solution. The basic aqueous extract after back-extraction with heptane was acidified, and extracted first with heptane (3 x) and then diethyl ether (3 x). The heptane soluble acids amounted to 60 mg and the ether soluble acids to 1.5 mg. The acid fractions were esterified with BF_3/methanol and the heptane soluble acid esters were then clathrated with urea, yielding a normal and branched-cyclic fraction in the ratio of approximately 1:3. The three fractions were gas chromatographed under the same conditions as described above; the g.l.c. traces of the total normal and branched-cyclic fractions are illustrated in Figure 8. The ether soluble acid esters exhibit a g.l.c. pattern very similar to the gas chromatogram shown in Figure 3. Since the weight of this fraction was so low, it was not further studied. For correlation purposes the gas chromatogram of the neutral and basic fraction isolated from the demineralization is shown in Figure 9 (conditions as usual). An example of the high resolution mass spectral data for the total (heptane soluble) acid extract is shown in Figure 10 and for the neutral and basic fraction in Figure 11.

Results

Inspection of Table III shows that extraction of the demineralized shale yields essentially the same type of acids found in the exhaustive extraction of the shale described in Part I. However, significant differences in distribution and range of compounds are apparent. For example, the range of normal acids was found to extend up to C_{30} (by g.l.c. analysis, Figure 8) and C_{32} (by high resolution mass spectrometry, see Figure 10). The acids show maxima at C_{16} and C_{26}, whereby however, the high molecular weight acids clearly predominate (Figure 8). In the fraction containing branched acids, phytanic and norphytanic acid are major components. A homologous series of isoprenoidal acids from C_{15} to at least C_{21} is apparent from the gas chromatogram (Figure 8); a high resolution mass spectrum of this fraction shows peaks corresponding to molecular ions of saturated acids from C_8 to C_{22}, which, of course, may not necessarily all represent isoprenoidal acids.

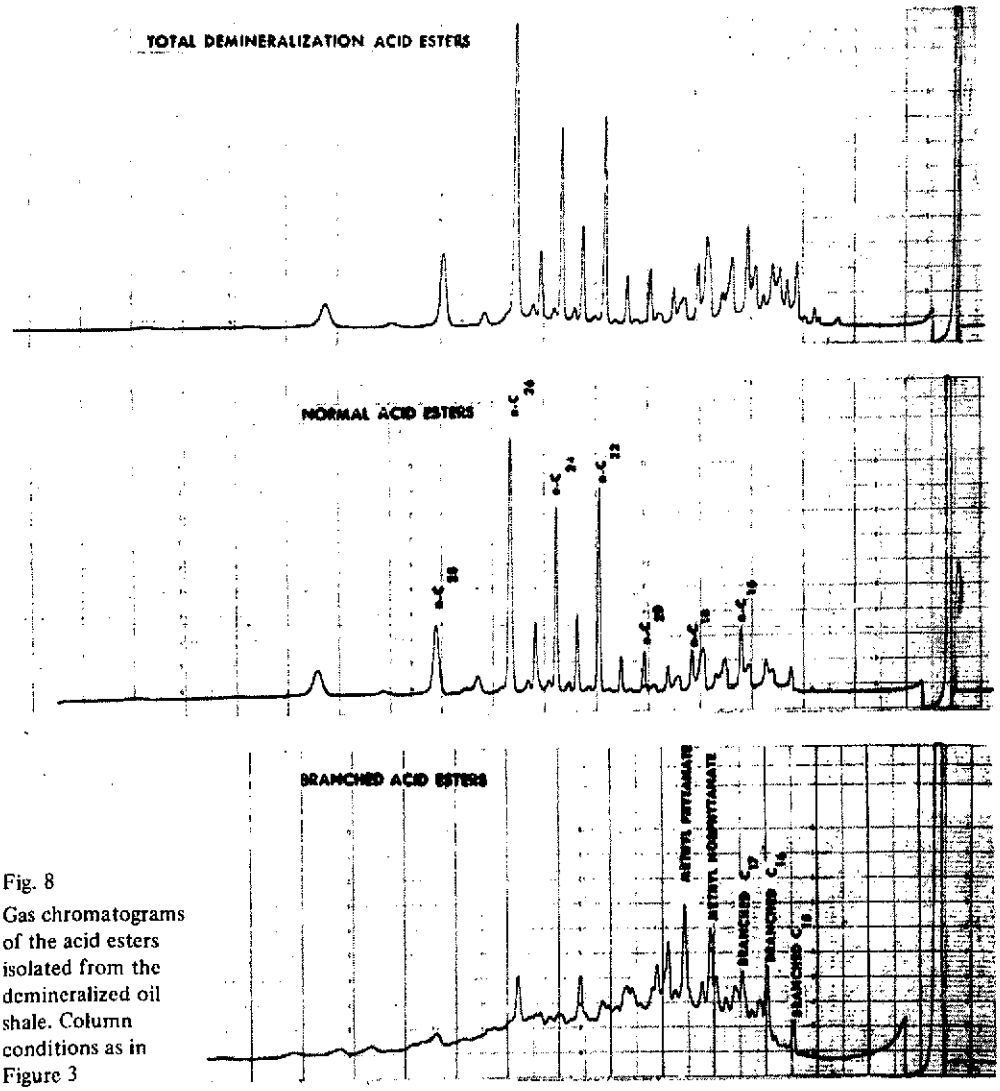

Fig. 8
Gas chromatograms of the acid esters isolated from the demineralized oil shale. Column conditions as in Figure 3

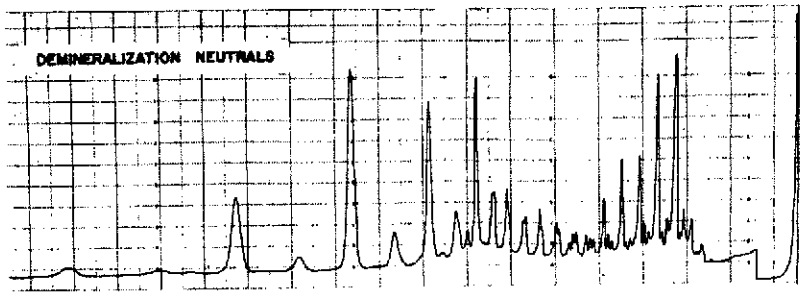

Fig. 9
Gas chromatogram of the neutral fraction isolated from the demineralized oil shale. Column conditions as in Figure 3

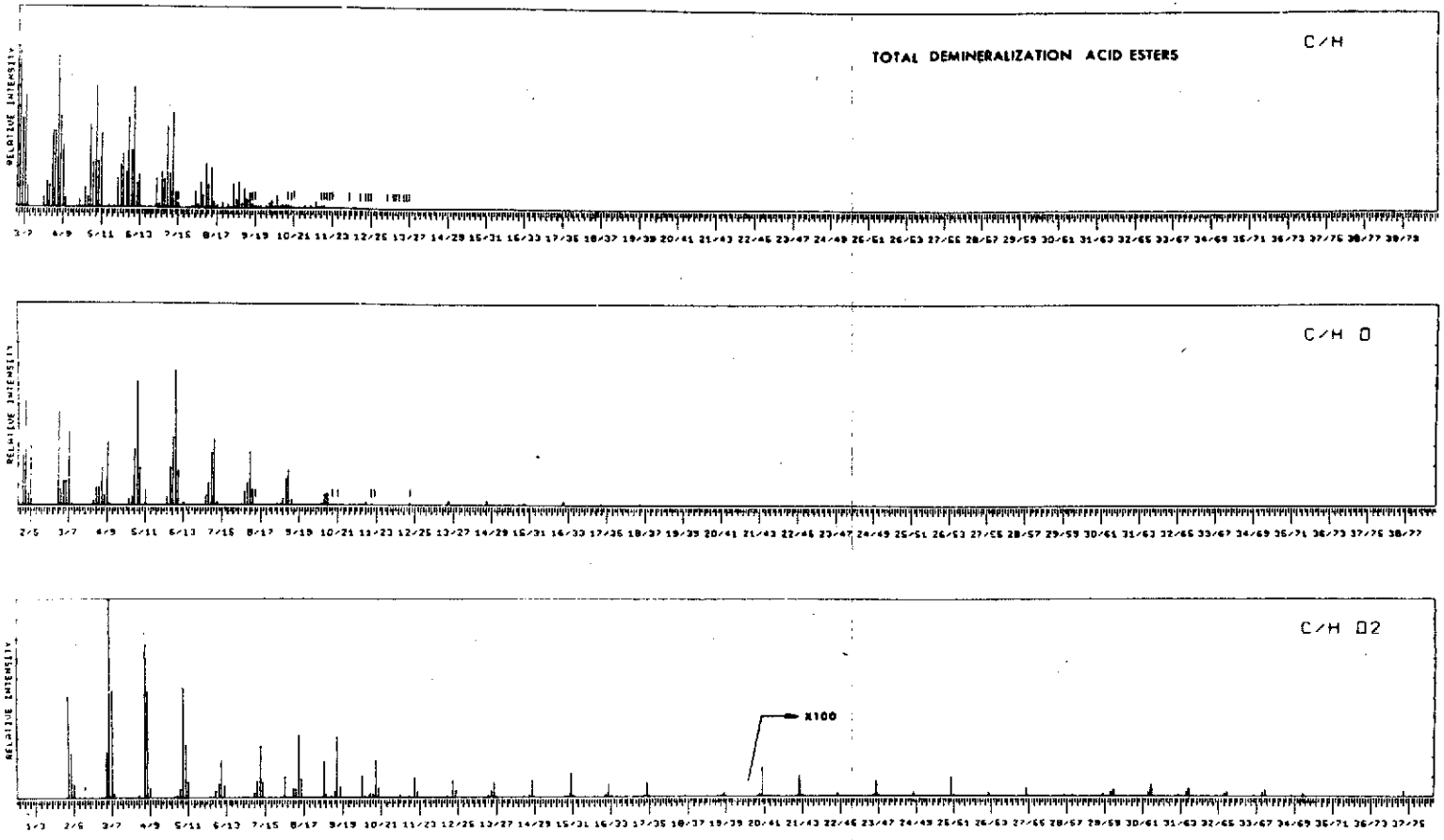

Part of Fig. 10

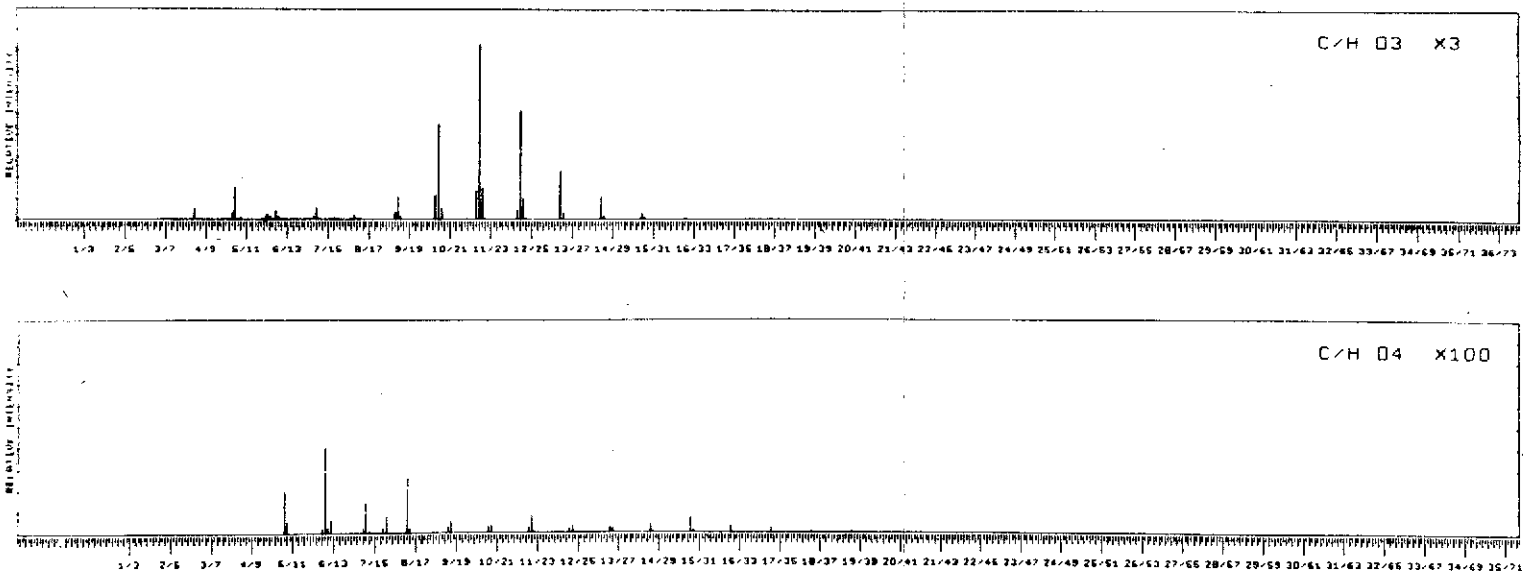

Fig. 10. High resolution mass spectral data for the total acid esters isolated from the demineralized oil shale

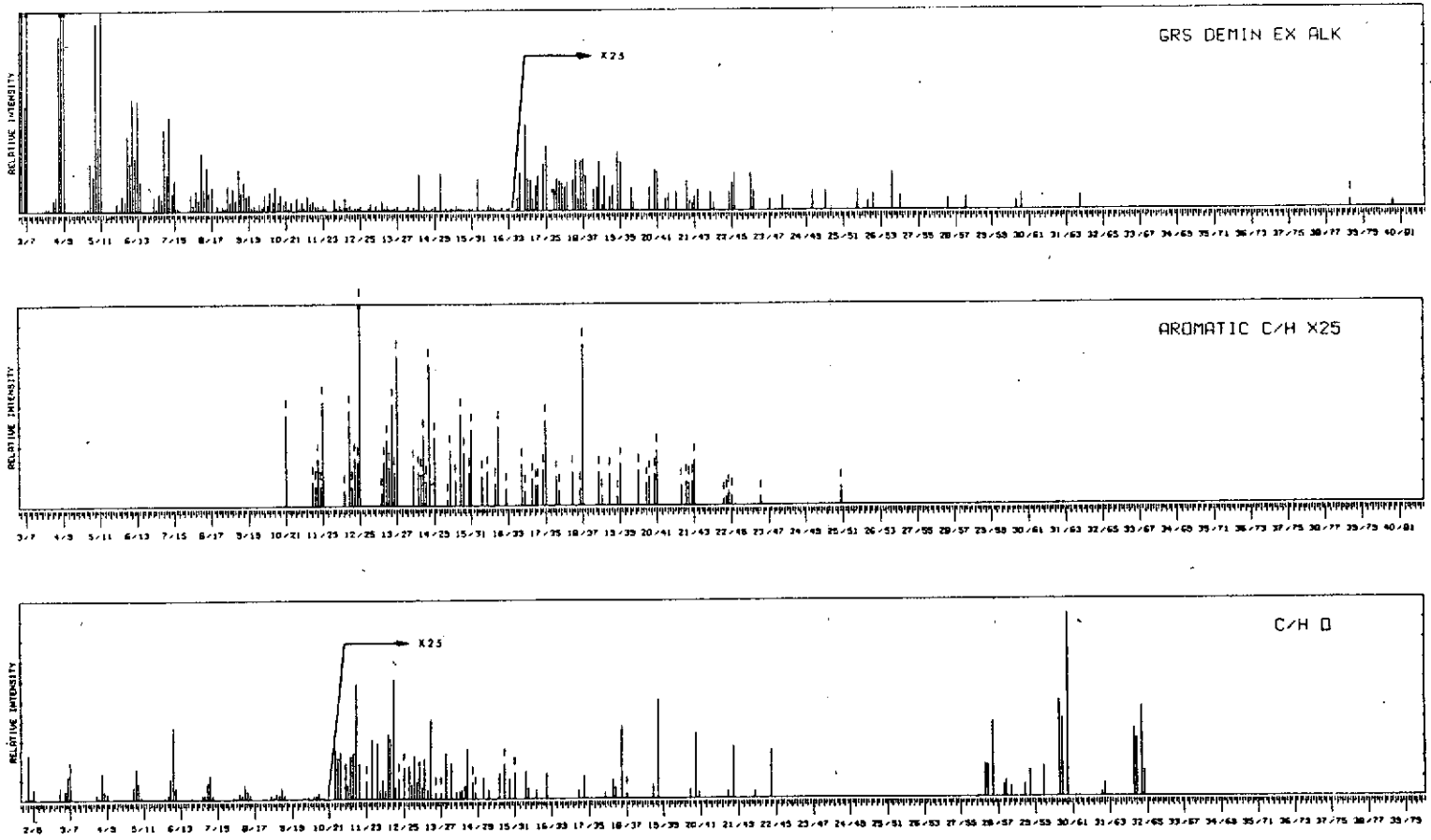

Part of Fig. 11

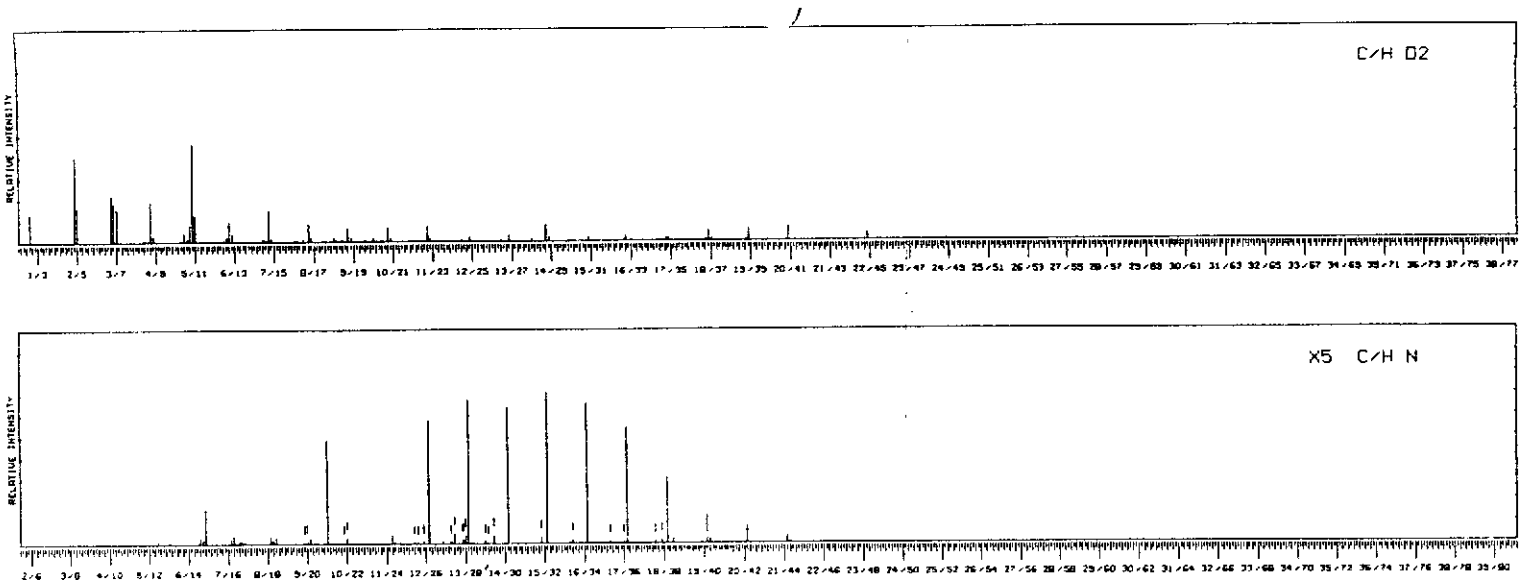

Fig. 11. High resolution mass spectral data for the neutral fraction isolated from the demineralized oil shale

Table III. Organic acids from the demineralized, exhaustively extracted oil shale of the Green River Formation, listed as free acids.

	range	maximum concentration
1. **Normal Acids**	C_5-C_{22}*	C_{16}, C_{24}
	C_8-C_{30}+	
2. **Branched Acids**	C_8-C_{22}*	C_{20}
	$C_{15}-C_{21}$+	
3. **Dicarboxylic Acids**	C_3-C_{18}*+	C_6
4. **Methylketoacids**	C_4-C_{16}*	C_{10}
5. **Mono-unsaturated and Cyclic Acids** ($C_nH_{2n-2}O_2$)	C_5-C_{18}*	C_6, C_{14}
6. **Aromatic Acids** (phenyl $C_nH_{2n-8}O_2$)	C_7-C_{15}*	C_9
7. **Aromatic Acids** (naphthyl $C_nH_{2n-14}O_2$)	$C_{11}-C_{14}$*	C_{11}
8. **Aromatic Acids** ($C_nH_{2n-10}O_2$)	$C_{10}-C_{15}$*	C_{11}
9. **Aromatic Acids** ($C_nH_{2n-12}O_2$)	$C_{10}-C_{13}$*	C_{10}
10. **Pentacyclic Acids**	$C_{28}-C_{34}$*	C_{30}

* Determined by high resolution mass spectrometry
\+ Determined from gas chromatograms

Dicarboxylic acids are represented by the series extending from about C_3 to C_{18}. The gas chromatogram shows a maximum at C_{14} for this series (the peak immediately preceding the C_{18} normal acid in the gas chromatogram of Figure 8 represents the C_{14} α,ω-dicarboxylic acid ester). Molecular ions of this series are apparent in the C/H O_4 plot of the high resolution mass spectrum (Figure 10). Peaks at $C_6H_{10}O_4$ and $C_8H_{14}O_4$ corresponding to C_4 and C_6 acids are particularly prominent, but these should not necessarily be taken as an accurate reflection of the relative abundance of these acids. Intense peaks in the C/H O_3 plot of Figure 10, provide further evidence for dicarboxylic acids. For example, the peaks at ($C_nH_{2n-3}O_3$) correspond to fragments resulting from loss of methoxyl radical from the molecular ion of dicarboxylic acids.

Indications of other classes of acids are based mainly on high resolution data. Thus, a series of ketoacids is apparent from the C/H O_3 plot of Figure 10, ranging apparently from C_4 to C_{16}. The peaks at $C_nH_{2n-2}O_3$ correspond to the molecular ions of these acids. Although at first sight these peaks must be regarded with some suspicion as definite indication of ketoacids since they might conceivably be explained as isotope and/or rearrangement ions, the results of the previous section and experiments to be mentioned later very clearly substantiate the occurrence of ketoacids in the sediment. A homologous series of apparently cyclic acids extends from about C_6 to C_{18}. Aromatic acids belonging to the phenyl ($C_nH_{2n-8}O_2$) series and naphthyl ($C_nH_{2n-14}O_2$) series are observed. The former appear to comprise the series from C_7 to C_{15}, the latter the group from C_{11} to C_{15}. Other groups, the homologues of the series $C_nH_{2n-10}O_2$ and $C_nH_{2n-12}O_2$, appear in various high resolution mass spectra. These occur, however, in fairly narrow distribution and low abundance, and might represent (at least partially) degradation products of other series. Special attention should be drawn however, to a series of apparently pentacyclic acids which are observed in the high resolution spectra of both the total and branched cyclic acids. Referring to the C/H O_2 plot of Figure 10, one notes, for example, the peaks of composition $C_{29}H_{48}O_2$ (m/e 428), $C_{30}H_{50}O_2$ (442), $C_{31}H_{52}O_2$ (456), $C_{32}H_{54}O_2$ (470), $C_{33}H_{56}O_2$ (484), $C_{34}H_{58}O_2$ (498) and $C_{35}H_{60}O_2$ (512). The series appears to maximize at C_{31} which would correspond to a C_{30} pentacyclic carboxylic acid. The suggestion of triterpenoidal acids appears obvious, but needs to be verified by more definitive experiments.

A comparison of the acids and the neutral and basic material from this extraction is provided by the gas chromatogram of Figure 9 and the high resolution mass spectrum of Figure 11. The C/H plot again shows some high mass ions such as $C_{40}H_{78}$ and $C_{40}H_{62}$ as well as polycyclic compounds in the region from C_{29} to C_{32}, some of which do not seem to represent triterpenoidal material, however. Prominent high mass C/H O peaks are observed which may represent ketonic material. The peaks $C_{30}H_{50}O$ and $C_{29}H_{48}O$ suggest the presence of triterpenoidal ketones. The corresponding peaks due to the loss of methyl radical from these molecular ions are also observed. The elemental compositions of most of the other ions, however, do not suggest triterpenoidal molecules. No more detailed interpretation can be advanced at this point.

Of interest also is the relative abundance of nitrogen compounds (C/H N plot of Figure 11), which was not observed in the neutral and basic fraction of the exhaustive extract. They appear to represent a homologous series of quinolines ranging in composition from $C_{13}H_{15}N$ to $C_{22}H_{33}N$.

Part III: Extraction of Oxidized Kerogen

Experimental

Twenty-five grams of kerogen concentrate from the demineralization was refluxed for 3 hours with 3 M chromic acid in sulfuric acid. The residue was filtered, washed with water and extracted three times, each first with heptane then diethyl ether, using ultrasonication to insure thorough extraction. The spent chromic acid solution was also extracted with heptane and then ether. The respective extracts were combined and the acids separated from the neutrals with 6 *N* sodium hydroxide solution. Esterification with BF_3/methanol yielded 0.034 g (0.13 percent of the kerogen concentrate) total esters from the heptane extract and 0.018 g (0.07 percent) total esters from the ether extract. In the case of the heptane soluble acid extract, the normal esters were separated from branched-chain esters by clathration with urea. Since it was found that the acids in the ether extract are of lower molecular weight and greater functionality than the acids of the heptane extracts, these ether extracts were not subjected to urea clathration, but were only esterified with BF_3/methanol. The yield of normal esters, which were again extracted with heptane, was 0.016 g (0.06 percent) and the branched-chain esters extracted from the adduct solution amounted to 0.010 g (0.04 percent). The residual kerogen was further oxidized for an additional 6 hours, the yield being 0.018 g (0.07 percent) acids extractable with heptane and 0.080 g (0.32 percent) acids extractable with ether. Esterification with BF_3/methanol and urea-clathration of the heptane extract gave 0.009 g (0.04 percent) of normal and 0.005 g (0.02 percent) of branched-chain ester fractions. The kerogen remaining from the 9 hour oxidation was oxidized for an additional 15 hours, resulting in 0.024 g (0.10 percent) acids extractable with heptane and 0.150 g (0.06 percent) acids extractable with ether. Esterification with BF_3/methanol and clathration of the heptane extract gave 0.021 g (0.05 percent) of normal and 0.008 g (0.03 percent) of branched-chain ester fractions. The residue from the previous oxidation, which still had a 14.7 percent carbon content, was subjected to 24 hours further oxidation. This resulted in 0.092 g (0.67 percent) acids extractable with heptane and 0.120 g (0.88 percent) acids extractable with ether. Esterification with BF_3/methanol and clathration of the heptane extract gave 0.021 g (0.05 percent) of normal and 0.008 g (0.03 percent) of branched-chain ester fractions. The residue from the previous oxidation, which still had a 14.7 percent carbon content, was subjected to 24 hours further oxidation. This resulted in 0.092 g (0.67 percent) acids extractable with heptane and 0.120 g (0.88 percent) acids extractable with ether. Esterification with BF_3/methanol and clathration of the heptane extract yielded 0.058 g (0.43 percent) of normal and 0.022 g (0.16 percent) of branched-chain ester fractions. It should be pointed out at this time that in working up reasonably concentrated fatty acid solutions in heptane (during washing of an extract before esterification, for example) the higher molecular

weight acids tend to crystallize out. The low resolution mass spectrum of such a precipitate filtered off from the 48 hour oxidation extract is shown in Figure 12 and consists of normal acids ranging from C_{18} to C_{35}. The four oxidations, totalling 48 hours, removed all the organic carbon from the kerogen concentrate (elemental analysis of the final residue: 0.21 percent C, 0.41 percent H, 0.0 percent N, 0.05 percent S, and 97.1 percent residue).

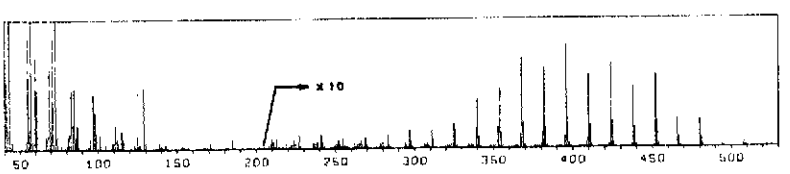

Fig. 12. Low resolution mass spectrum of the acid precipitate from the 48 hour oxidation

The total, normal and branched-chain ester fractions were chromatographed using the same conditions described earlier. The g.l.c. components were identified by their retention times, coinjection of standard compounds, low resolution mass spectra and then correlated to the high resolution mass spectra of the total mixtures. The g.l.c. patterns of the heptane soluble acid mixtures isolated from the 4 oxidations are virtually identical. There is an even/odd predominance in the normal acid fractions and the branched acids maximize at C_{16}. The 24 hour oxidation acid esters serve as illustration in Figure 13. The g.l.c. patterns of the ether soluble acid mixtures are also virtually identical and maximize at lower molecular weight acids. The ether extract acid esters from the 24 hour oxidation serve as illustration in Figure 14.

The high resolution mass spectral data of the total, branched and normal acid ester fractions and of the total ether extract ester fractions show that the various homologous acid series isolated from the 4 oxidations are the same and differ only in relative concentrations. Each fraction was subjected to increasing ion source temperatures (usually in the range 150°–270°) while several mass spectra were taken to insure complete volatilization. The high resolution mass spectral data of the normal esters from the 3 hour oxidation are shown in Figure 15 and similar data for the branched-cyclic esters from the 24 hour oxidation are shown in Figure 16. The high resolution mass spectral data for the total ether extract esters from the 9 hour oxidation are shown in Figure 17. This is a representative example for the four ether extract fractions isolated from the respective oxidations.

For correlation purposes, the gas chromatogram of the 9 hour oxidation neutral and basic fraction is shown in Figure 18 and the high resolution mass spectral data are shown in Figure 19.

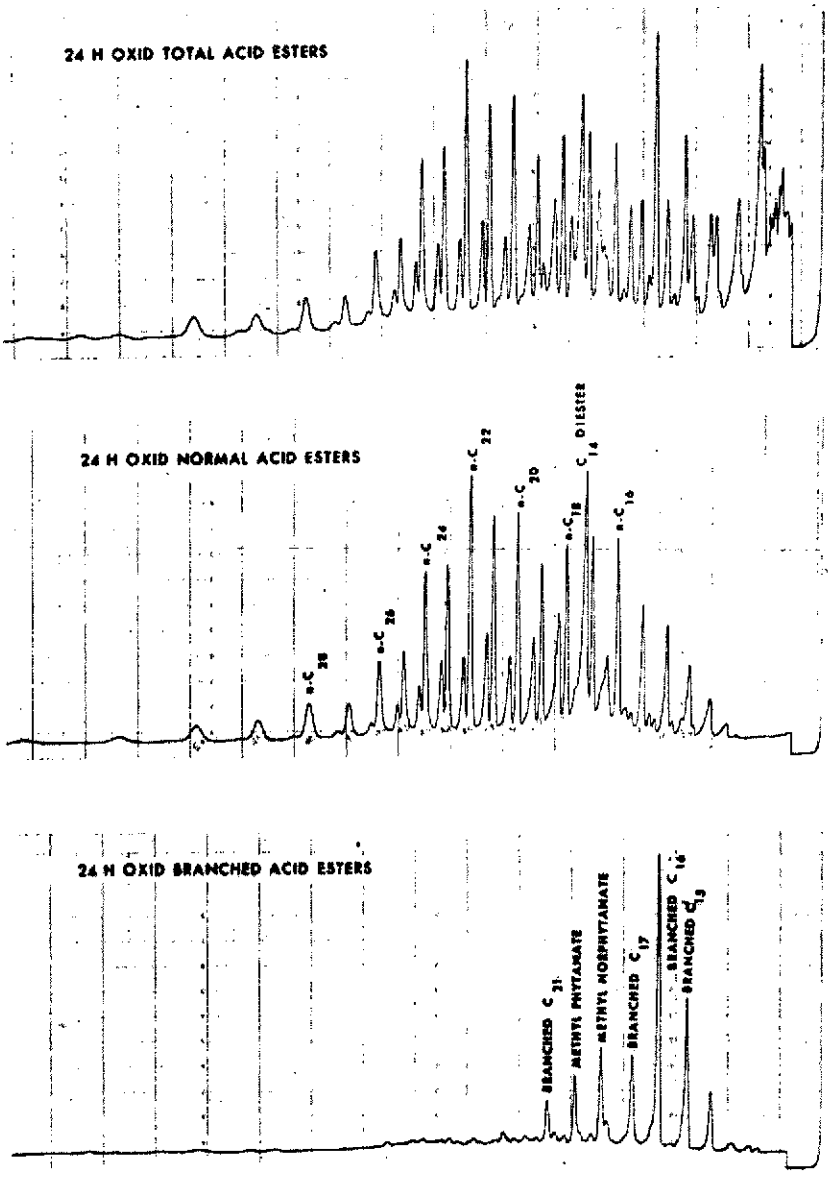

Fig. 13. Gas chromatogram of the heptane extract esters isolated from the 24 hour oxidation. Column conditions as in Figure 3

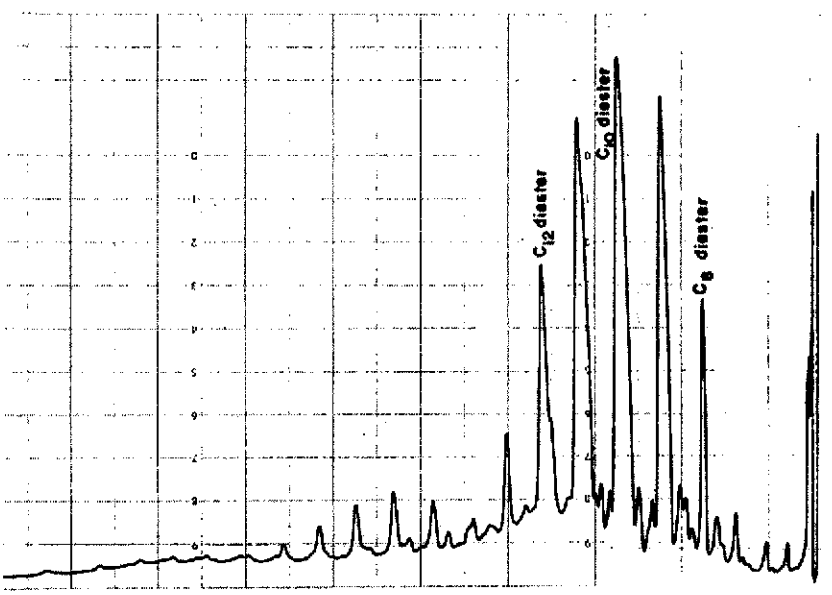

Fig. 14. Gas chromatogram of the ether extract esters isolated from the 24 hour oxidation. Column conditions as in Figure 3

Results

Each of the oxidation experiments yields the same type of acids, but differences are apparent in the relative abundance of the various classes of acids (Table IV). In Table I a summary of total amounts obtained in the 3, 9, 24 and 48 hour oxidations is presented. These data refer to successive oxidation steps on the same sample; after 48 hours of CrO_3/H_2SO_4 treatment all carbon is essentially removed from the "kerogen material". Both total organic matter and total heptane-extractable acids increase with successive oxidations; the tenfold increase in the amount of ether-extractable acids should be noted in particular, however. Another general trend evident from our data is the relative consistency of the range of acids within each series for the different oxidation experiments, and the decrease of branched acids relative to normal and dicarboxylic acids with extent of oxidation. Within each class of acids, the lower members of a homologous series tend to be concentrated in the ether extracts, the higher members are found in the heptane extracts.

Typical results for the 24 hour oxidation experiment are illustrated by the gas chromatograms of Figure 13. Normal, branched and dicarboxylic acids are major components in this mixture. The normals of the heptane extractable acids comprise

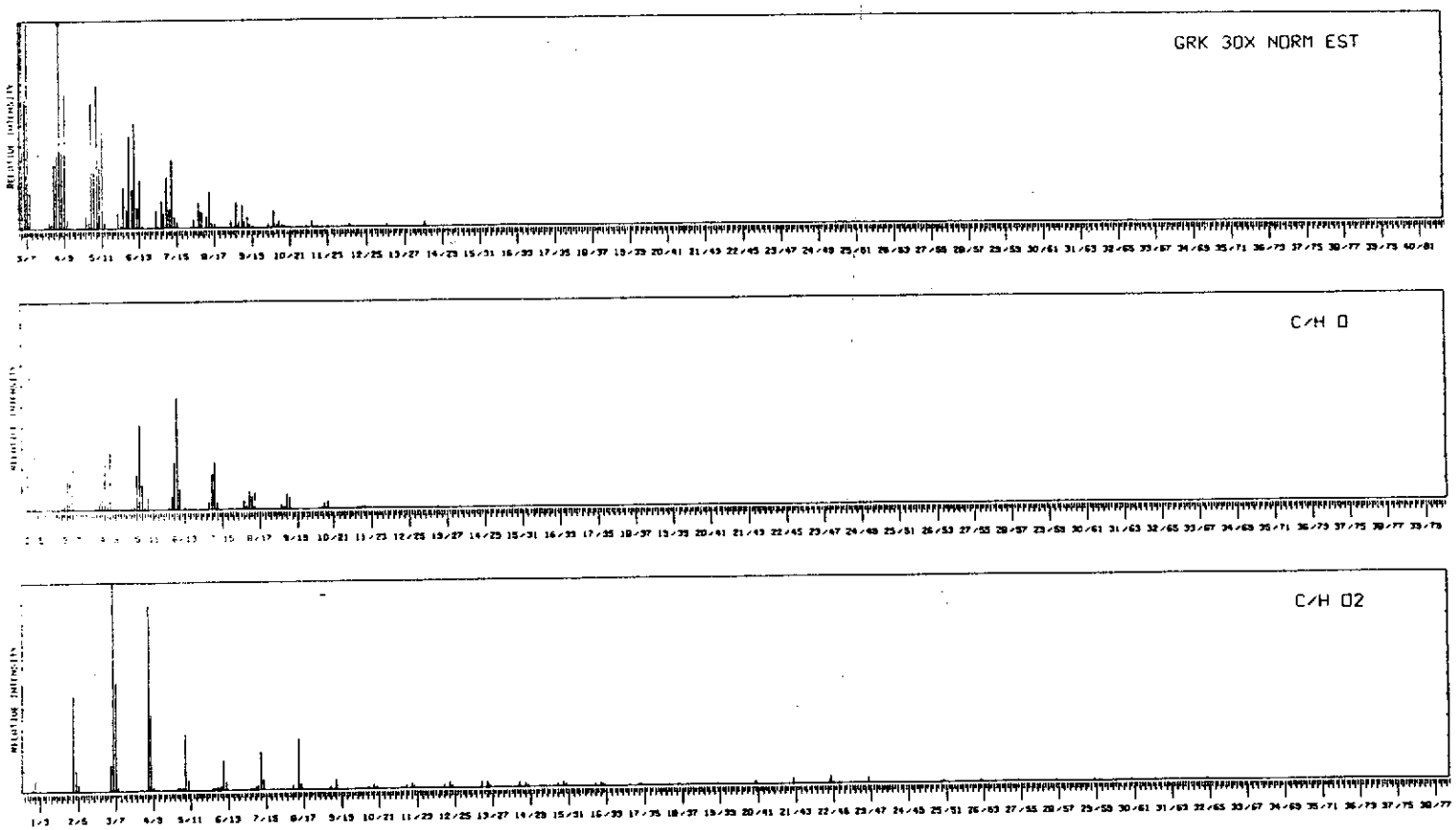

Part of Fig. 15

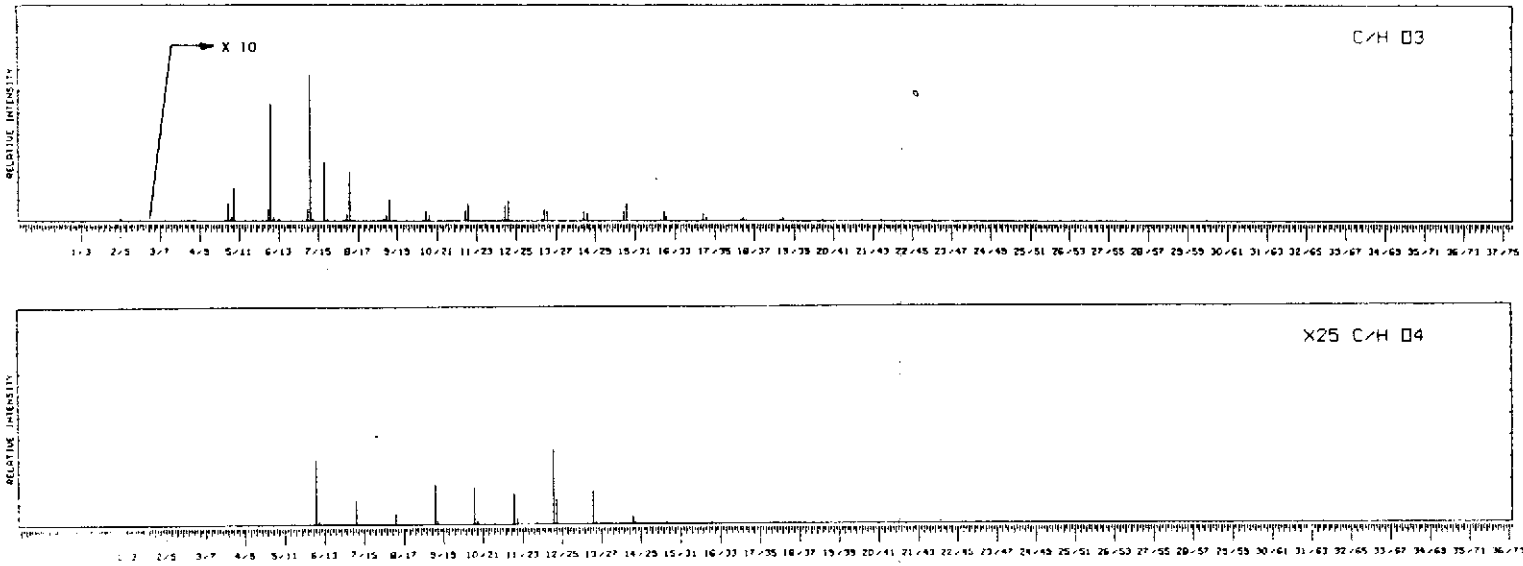

Fig. 15. High resolution mass spectral data for the normal acid esters from the 3 hour oxidation.

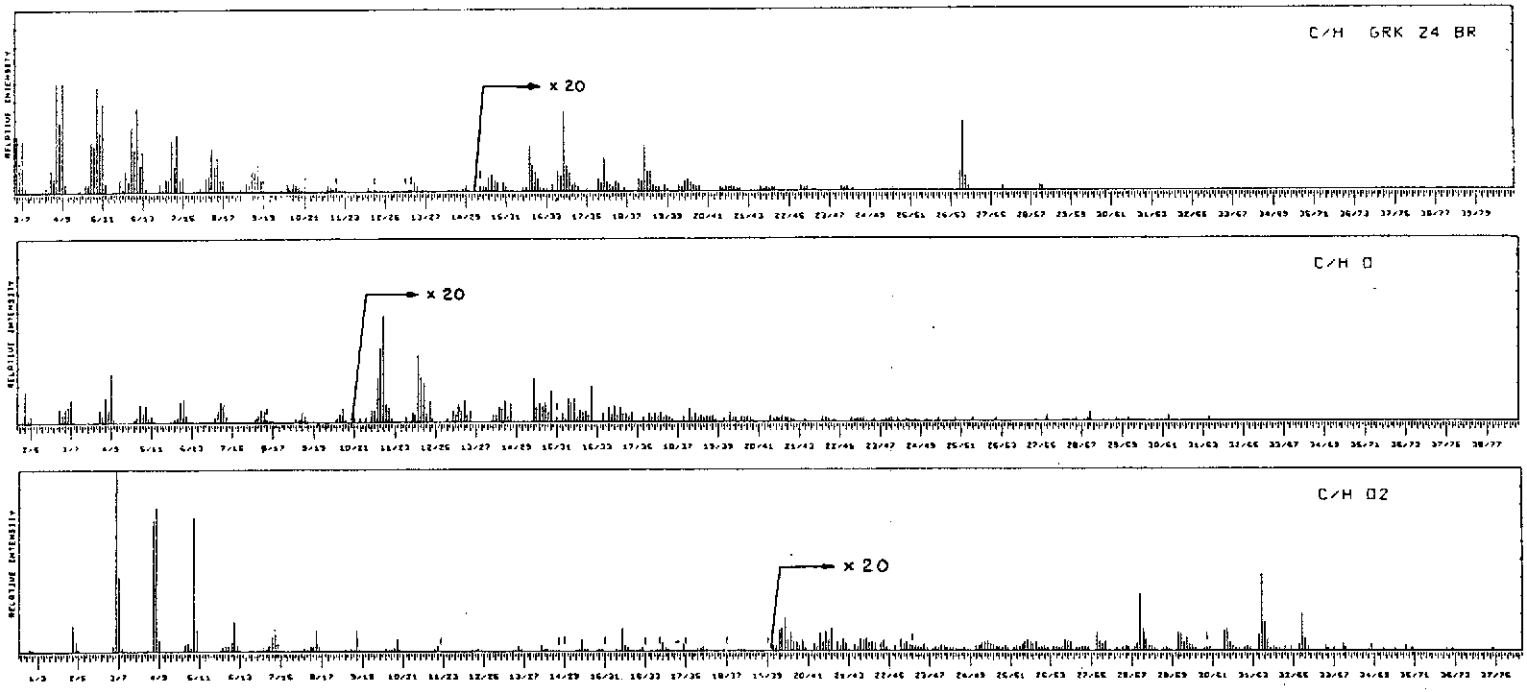

Part of Fig. 16

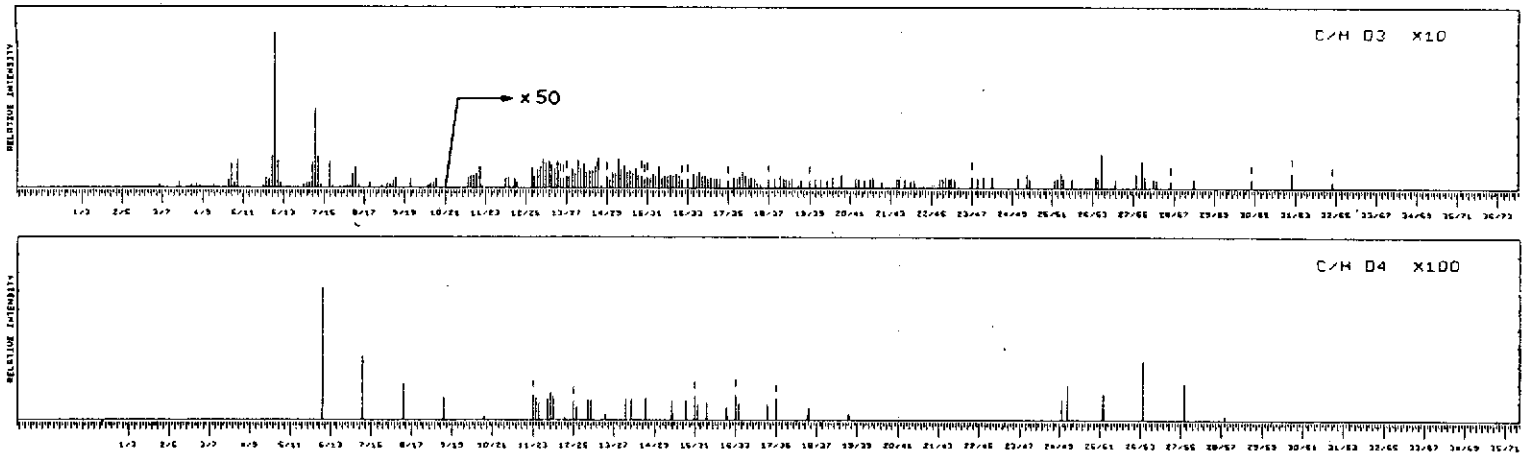

Fig. 16. High resolution mass spectral data for the branched acid esters from the 24 hour oxidation

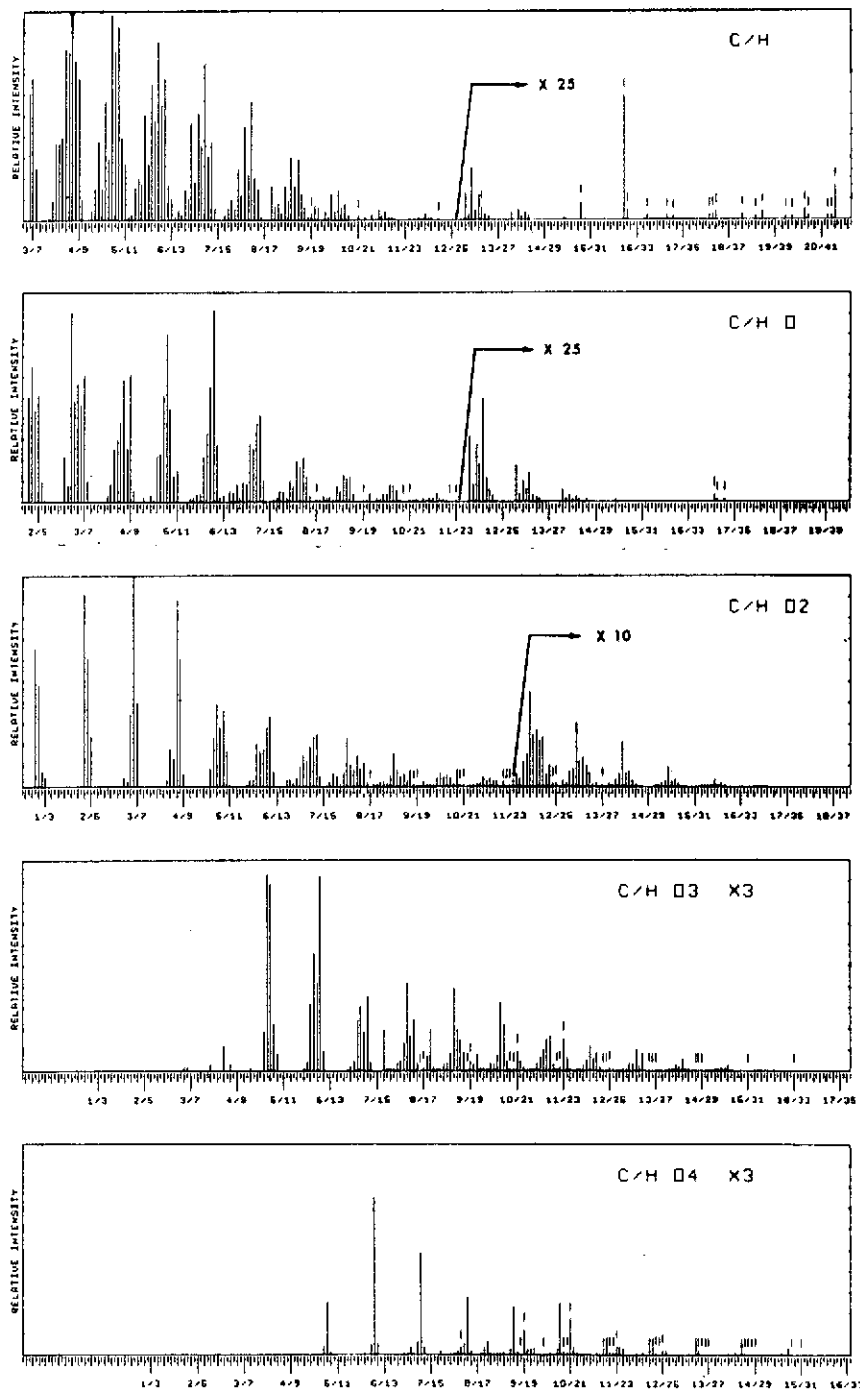

Part of Fig. 17

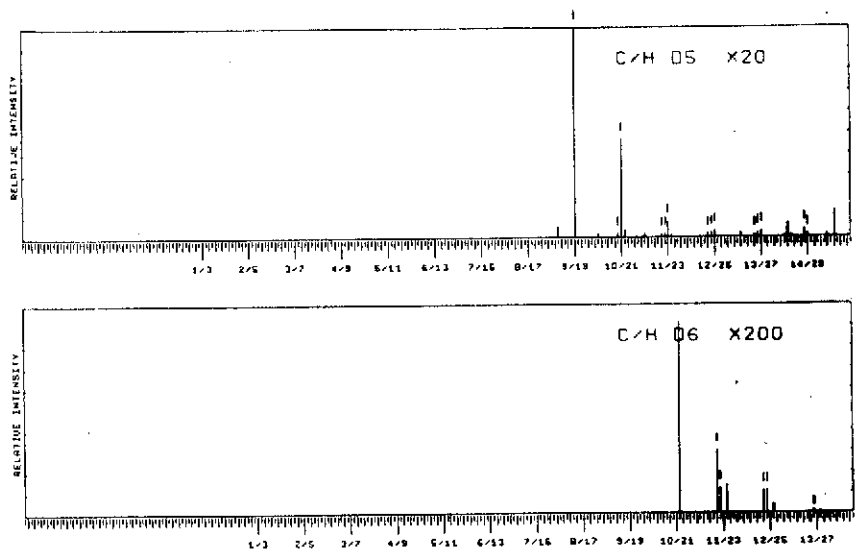

Fig. 17. High resolution mass spectral data for the total ether extract acid esters from the 9 hour oxidation

Fig. 18. Gas chromatogram of the neutral fraction isolated from the 9 hour oxidation. Column conditions as in Figure 3

the homologous series from C_8 to C_{30} with a maximum for the C_{22} acid. Phytanic and norphytanic acids were identified in the branched acid fraction but the range extends from C_{14} to C_{21}, maximizing at C_{16}. The remaining branched compounds are also isoprenoidal acids. Diacids are very prominent constituents; all normal dicarboxylic acids from C_{10} to C_{23} are present in the heptane-extractable mixture.

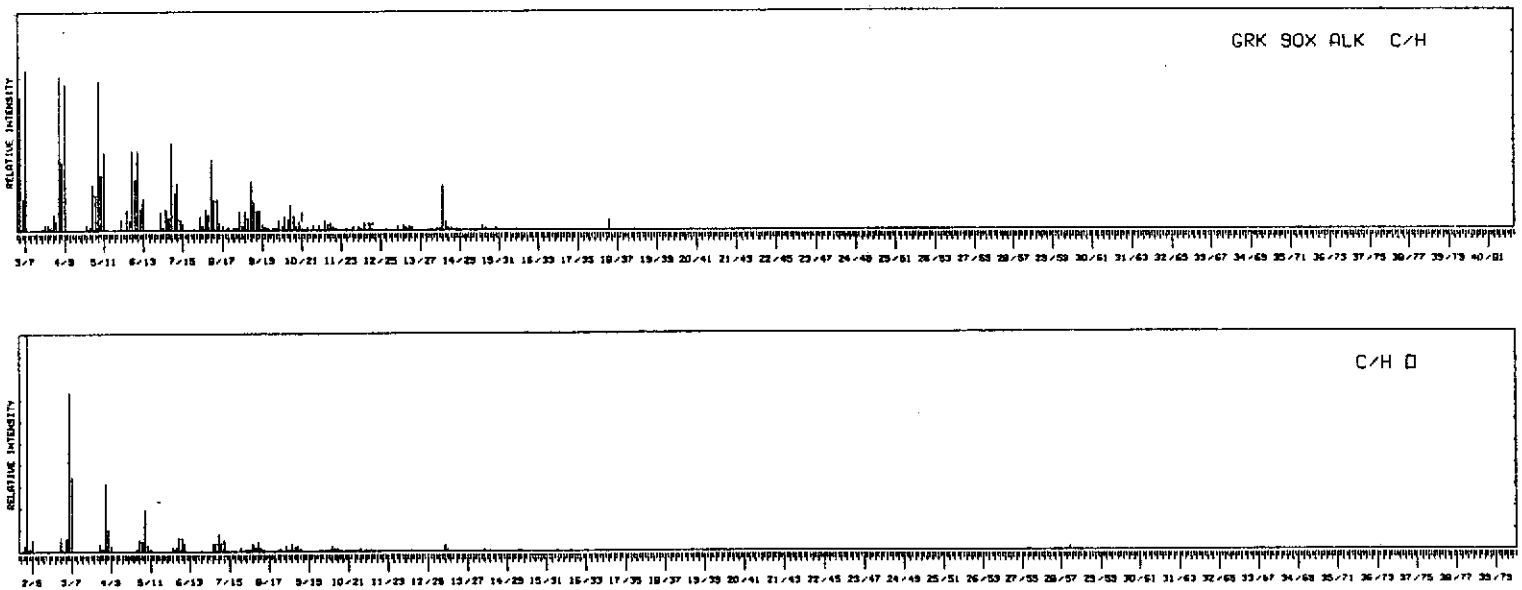

Fig. 19. High resolution mass spectral data for the neutrals from the 9 hour oxidation

Table IV. Organic acids from the stepwise oxidations of Green River Formation kerogen concentrate (listed as free acids), extracted with heptane and then ether.

	Range		Maximum Concentration	
	(Heptane)	(Ether)	(Heptane)	(Ether)
1. Normal Acids				
3 hour	$C_{10}-C_{30}$+ C_5-C_{33}*	C_5-C_8*	C_{22}	C_5
9 hour	C_9-C_{32}+ C_5-C_{34}*	C_5-C_9*	C_{22}	C_5
24 hour	C_9-C_{32}+ C_5-C_{34}*	C_5-C_8*	C_{22}	C_5
48 hour	$C_{10}-C_{33}$+ C_5-C_{36}*	C_5-C_{10}*	C_{22}	C_6
2. Branched-chain Acids				
3 hour	$C_{14}-C_{22}$+ C_5-C_{26}*	--	C_{16}	--
9 hour	$C_{14}-C_{22}$+ C_5-C_{26}*	--	C_{16}	--
24 hour	$C_{14}-C_{22}$+ C_5-C_{26}*	--	C_{16}	--
48 hour	$C_{14}-C_{22}$+ C_5-C_{26}*	--	C_{16}	--
3. Dicarboxylic Acids				
3 hour	C_9-C_{22}+ C_6-C_{14}*	C_8-C_{12}+ C_3-C_{13}*	C_{12}+*	C_4* C_{10}+
9 hour	C_4-C_6* $C_{14}-C_{17}$*	C_8-C_{12}+ C_3-C_{13}*	C_4 C_{15}	C_4* C_{10}+
24 hour	$C_{10}-C_{23}$+ C_4-C_{22}*	C_8-C_{12}+ C_3-C_{13}*	C_4* C_{14}+*	C_4* C_{10}+
48 hour	$C_{10}-C_{25}$+ C_5-C_{25}*	C_6-C_{10}+ C_3-C_{12}*	C_{17}+*	C_4* C_8+
4. Keto Acids				
3 hour	C_4-C_{12}+ C_4-C_{16}*	C_5-C_{10}*	C_6+* C_{14}*	C_6
9 hour	C_4-C_{16}*	C_5-C_{13}*	C_5 C_{14}	C_6
24 hour	C_4-C_{20}*	C_5-C_{13}*	C_6 C_{14}	C_6
48 hour	C_6-C_{17}*	C_5-C_{14}*	C_6 C_{14}	C_6

Table IV continued

		Range		Maximum Concentration	
		(Heptane)	(Ether)	(Heptane)	(Ether)
5.	**Cyclic Acids** (mono-unsaturated $C_nH_{2n-2}O_2$)				
	3 hour	C_5-C_{17}*	C_5-C_{12}*	C_{12}	C_6
	9 hour	C_5-C_{23}*	C_5-C_{14}*	C_{15}	C_6
	24 hour	C_5-C_{28}*	C_5-C_{14}*	C_{17}	C_6
	48 hour	C_5-C_{17}*	C_5-C_{14}*	C_{12}	C_6
6.	**Aromatic Acids** (phenyl $C_nH_{2n-8}O_2$) #				
	3 hour	C_7-C_{18}*	C_7-C_{13}*	C_7	C_7
	9 hour	C_7-C_{18}*	C_7-C_{15}*	C_9 C_{14}	C_7
	24 hour	C_7-C_{18}*	C_7-C_{14}*	C_9 C_{15}	C_7
	48 hour	C_7-C_{18}*	C_7-C_{12}*	C_{16}	C_7
7.	**Aromatic Acids** (naphthyl $C_nH_{2n-14}O_2$)				
	3 hour	C_{11}*	C_{11}*	C_{11}	C_{11}
	9 hour	C_{11}, C_{12}*	C_{11}, C_{12}*	C_{11}	C_{11}
	24 hour	C_{11}*	C_{11}, C_{12}*	C_{11}	C_{11}
	48 hour	none	C_{11}, C_{12}*	--	C_{11}
8.	**Aromatic Acids** ($C_nH_{2n-10}O_2$)				
	3 hour	C_{10}*	$C_{10}-C_{12}$*	C_{10}	C_{10}
	9 hour	$C_{10}-C_{18}$*	$C_{10}-C_{16}$*	C_{10}	C_{10}
	24 hour	$C_{10}-C_{19}$*	$C_{10}-C_{15}$*	C_{10}	C_{10}
	48 hour	$C_{10}-C_{19}$*	$C_{10}-C_{15}$*	C_{10}	C_{10}
9.	**Aromatic Acids** ($C_nH_{2n-12}O_2$)				
	3 hour	none	$C_{10}-C_{12}$*	--	C_{10}
	9 hour	C_{10}*	$C_{10}-C_{13}$*	C_{10}	C_{10}
	24 hour	C_{10}*	$C_{10}-C_{12}$*	C_{10}	C_{10}
	48 hour	C_{10}*	$C_{10}-C_{12}$*	C_{10}	C_{10}
10.	**Pentacyclic Acids**				
	3 hour	$C_{28}-C_{33}$*	none	C_{31}	--
	9 hour	$C_{28}-C_{33}$*	none	C_{30}	--
	24 hour	$C_{26}-C_{34}$*	none	C_{30}	--
	48 hour	$C_{29}-C_{32}$*	none	C_{30}	--

Table IV continued

		Range		Maximum Concentration	
		(Heptane)	(Ether)	(Heptane)	(Ether)
11.	**Tetracyclic Acids** ($C_nH_{2n-8}O_2$) #				
	3 hour	$C_{18}-C_{20}$*	none	C_{18}	--
	9 hour	$C_{18}-C_{26}$*	none	C_{20}	--
	24 hour	$C_{18}-C_{32}$*	none	C_{30}	--
	48 hour	$C_{18}-C_{32}$*	none	C_{30}	--
12.	**Dicarboxylic Aromatic Acids** ($C_nH_{2n-10}O_4$)				
	3 hour	none	C_8-C_{11}*	--	C_8
	9 hour	none	C_8-C_{13}*	--	C_8
	24 hour	none	C_8-C_{13}*	--	C_8
	48 hour	none	C_8-C_{12}*	--	C_8
13.	**Tricarboxylic Aromatic Acids** ($C_nH_{2n-12}O_6$)				
	3 hour	none	C_9-C_{12}*	--	C_9
	9 hour	none	C_9-C_{12}*	--	C_9
	24 hour	none	C_9-C_{13}*	--	C_9
	48 hour	none	C_9-C_{12}*	--	C_9

* Determined by high resolution mass spectrometry
\+ Determined from gas chromatogram
\# The aromatic acids are listed only to C_{18} since above C_{18} the data fit tetracyclic acids better.

The C_{14} component, dimethyl tetradecane-1,14-dioate is the major acid of this series (Figure 13). The lower dicarboxylic acids (C_8 to C_{12} in particular) are major constituents of the ether-extractable mixture (Figure 14). Small normal acids and/or branched-chain are present also (C_5 to C_8) but cannot be distinguished since the ether extract was not clathrated.

Essentially the same homologous series of these three acid types is present in all oxidation experiments (see Table IV for details). However, the amount of branched saturated acids markedly decreases relative to the normal and dicarboxylic acids with duration of oxidation (Table V). The presence of other classes of acids was

Table V. The relative percent abundance of isoprenoid acids *vs.* normal, dicarboxylic and ketoacids in the 4 oxidations.

Oxidation	Isoprenoids (percent of peak areas)	Others (percent of peak areas)
3 hour	60	40
9 hour	35	65
24 hour	16	84
48 hour	5	95

ascertained from the high resolution mass spectra. Referring back to the figures of the high resolution mass spectral data, a homologous series of normal acids up to $C_{32}H_{64}O_2$ is apparent from the C/H O_2 plot of Figure 15. Molecular ions of dicarboxylic acids can be seen in the C/H O_4 plot at $C_nH_{2n-2}O_4$. The M-CH_3O ions are found in the C/H O_3 plot; the last peak of the series $C_{21}H_{39}O_3$ would be derived from a C_{20} diacid ester. The isoprenoidal acids mentioned above appear in the C/H O_2 plot of Figure 16 at $C_nH_{2n}O_2$. Molecular ions for aliphatic oxoacids $C_nH_{2n-2}O_3$ are evident in the C/H O_3 plot of Figure 15. Peaks of composition $C_{11}H_{20}O_3$, $C_{12}H_{22}O_3$, $C_{13}H_{24}O_3$ etc., are major contributors, but the series appears to extend from about C_4 to C_{20}[1]). The ether extract of the 24 hour oxidation contains ketoacids comprising the lower homologous series from about C_5 to C_{13}.

Four series of aromatic acids are apparent from the high resolution mass spectra. In the heptane extract (Figure 16) the phenyl ($C_nH_{2n-8}O_2$) and naphthyl ($C_nH_{2n-14}O_2$) group appears to include homologues from n = 7 to 8 and n = 11, respectively. A distribution from n = 7 to 15 and n = 11 and 12 is found for the ether extractables. The other two aromatic series, $C_nH_{2n-10}O_2$ (indane carboxylic acids) and $C_nH_{2n-12}O_2$, occur in both the heptane and ether extracted mixtures. Table IV summarizes their distribution patterns, although these should be interpreted with some caution since the C/H O_2 plots of Figures 16 and 17 are quite complex.

The oxidation experiments yielded four new series of acids not obtained by extraction analyses; the high resolution spectrum of the branched fraction of the heptane soluble material gives definite indication of homologues of pentacyclic and tetracyclic acid constituents. For example, Figure 16 exhibits peaks of composition $C_{28}H_{46}O_2$, $C_{29}H_{48}O_2$, $C_{30}H_{50}O_2$, $C_{31}H_{52}O_2$, $C_{32}H_{54}O_2$, and $C_{33}H_{56}O_2$, which could be rationalized as molecular ions of perhaps triterpenoidal acids. Similarly, a series of compositions $C_nH_{2n-8}O_2$ (n = 18–20) can be noted. Both classes of compounds are absent in the ether-extractable acid mixture (see Figure 17). The ether extracts contain instead aromatic dicarboxylic and tricarboxylic acids. The ion of composition $C_{10}H_{10}O_4$ in Figure 17 corresponds to the molecular ion of a phthalic acid dimethyl ester. Higher homologues of this series are very minor constituents (Table IV). The most abundant compound of this class was identified

[1]) Confirmation that these compounds were indeed (ω - 1)-oxo-acids was provided by analysis of the real-time high resolution mass spectra on mixtures obtained in the following experiment: The normal acid ester fraction and the total ether fraction of the 24 hour oxidation acids were reduced with sodium borohydride and treated with silylating agent. Analysis of the real-time high resolution mass spectrum of these mixtures confirmed the presence of these ketoacids (W.J. Richter, B.R. Simoneit, D.H. Smith and A.L. Burlingame, unpublished results from this laboratory).

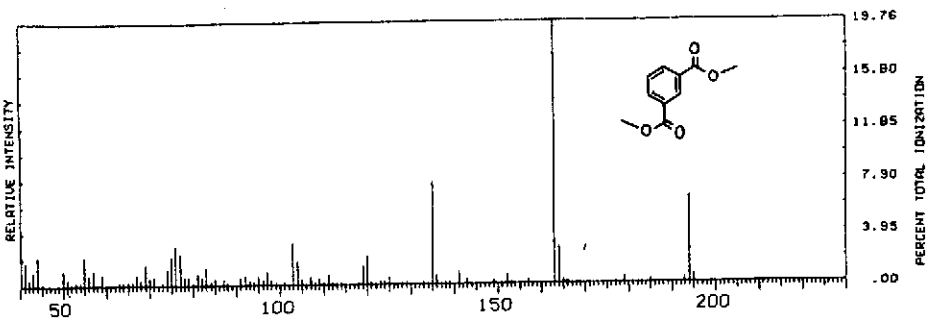

Fig. 20. Low resolution mass spectrum of dimethyl terephthalate isolated from the ether extract acids of the 24 hour oxidation

from its mass spectrum[1]) (Figure 20) as a phthalic acid ester, probably the *meta*-isomer. Tricarboxylic aromatic acids are indicated by the sequence $C_{12}H_{12}O_6$, $C_{13}H_{14}O_6$, $C_{14}H_{16}O_6$ in Figure 17. Again the lowest homologue is the most abundant species.

Monocyclic and/or mono-unsaturated acids of the general formula $C_nH_{2n-2}O_2$ were observed in all oxidation experiments. Table IV gives a summary of these results. For the 24 hour oxidation these acids appeared to comprise the series from C_5 to C_{28} in the heptane extract (Figure 16) and C_5 to C_{14} in the ether extract (Figure 17).

Part IV: Discussion of Results

Comparison of the data of Table I reveals the interesting fact that the amount of acids obtainable by various methods - - two extractions and demineralization followed by extraction - - increases. The first extraction yielded only 8 mg of acids out of a total of 1300 mg hexane soluble extract, the exhaustive extraction and demineralization gave 38 and 60 mg of acids for 440 and 190 mg of total extract, respectively. The low yield of acids from the first extract may well be due to incomplete removal of acidic material, since these experiments were conducted on a relatively large scale, making no attempt at quantitative removal of all acidic material from the total. However, the trend is too marked to be ignored. The differences between the first extract and the exhaustive extract can be ascribed to the more polar nature of the acidic materials, resulting in an artificial concentration of them in the exhaustive extract.

The high yield of acids relative to "neutral" organics from the demineralization experiment, however, suggests that the bulk of these acids are bound to the inorga-

[1]) Data was obtained *via* capillary g.l.c. – M.S. techniques using Apiezon L as liquid phase. Perkin Elmer, Model 900 gas chromatograph coupled to a G.E.C. – A.E.I. MS 902 mass spectrometer on-line to an S.D.S. Sigma 7 Computer.

nic matrix, perhaps as calcium salts. Part of them could also be derived by hydrolysis of the kerogen material. Not surprisingly, the yield of acids increases with length of oxidation; particularly marked is the increase of the more polar (and probably more functionalized) acids; i.e., the ether extractable material (see Table I). The branched-chain (isoprenoid) acids drastically decrease in concentration vs. the normal, dicarboxylic and oxo-acids as the oxidation time increases. These results are summarized in Table V and can also be discerned in Figure 21: The three-hour oxidation yields a mixture in which isoprenoidal acids predominate (note in particular the abundance of the C_{16} branched acid), whereas the 48 hour oxidation yields only minor amounts of branched acids (Figure 21).

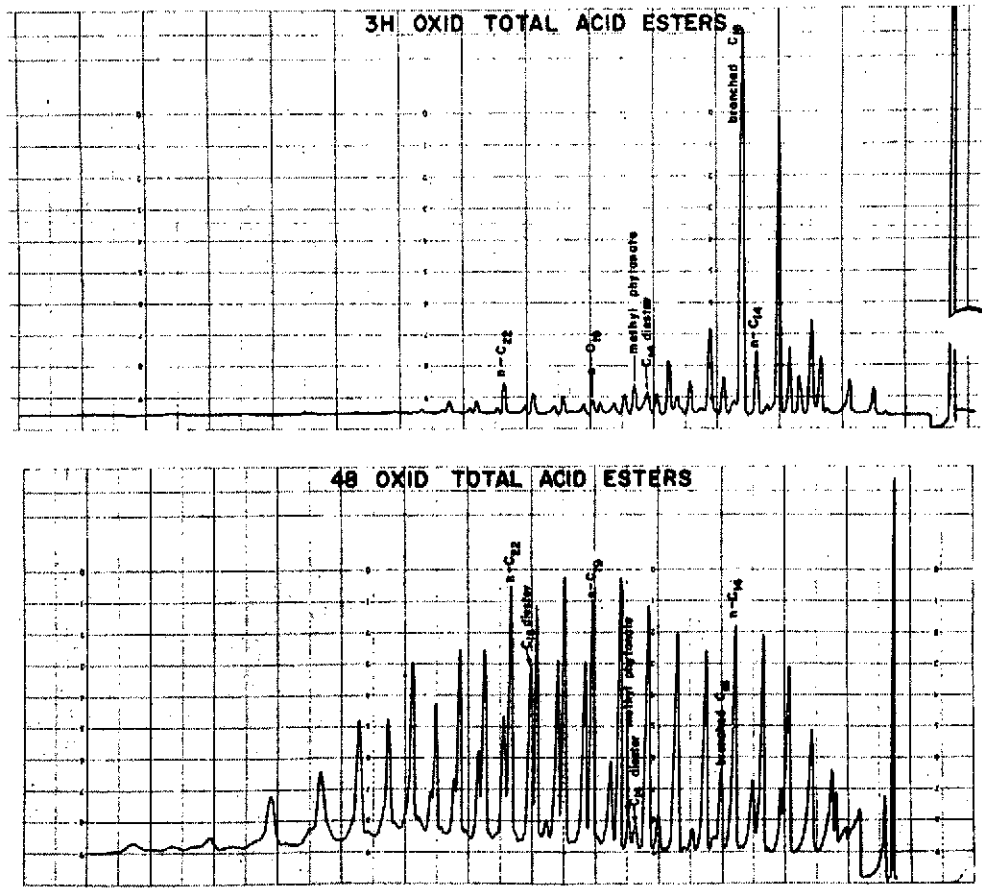

Fig. 21. Gas chromatograms of the total acid esters isolated from the 3 and 48 hour oxidations. Column conditions as in Figure 3

More important than these observations are the differences in distribution of acids due to different extraction-isolation methods. The first extraction and exhaustive extraction not unexpectedly yield essentially the same mixtures. A notable characteristic of these extracts is the absence of any appreciable quantity of both the higher normal and branched (isoprenoidal) acids. Instead, saturated dicarboxylic acids are the major acid constituents of the higher weight material. By contrast, demineralization yields an acid mixture in which higher normal acids are very prominent, maximum about C_{22}, and which contains a series of isoprenoidal acids in the branched-cyclic fraction, with phytanic acid as the most abundant. However, the isoprenoidal acids are far less prominent in our extracts than in those of Eglinton et al. (1966) from a core sample of shale from Sulfur Creek which contained phytanic acid as the major single component of the total acid fraction. If these differences reflect the different shale samples, conclusions as to ancient geologies extrapolated for the entire shale but based on analysis of a single sample may well have to be advanced with some caution. Furthermore, our data appear to show that relative abundances of certain compound types may be a function of methods of isolation and therefore not necessarily indicate a specific source material.

The acids obtained by oxidation could arise by several processes;

(a) "loosening" of the kerogen matrix and removal of entrapped compounds which might subsequently be partially oxidized,
(b) hydrolysis of ester linkages to give acids and alcohols, the latter being oxidized to carboxylic acids, and
(c) oxidative cleavage of carbon-carbon bonds.

All three processes probably contribute and their relative importance is difficult to assess. However, some arguments may be advanced to support the view that a major portion of the acids is derived from carbon-carbon bond cleavage of side chains attached to the kerogen. Hydrolysis of kerogen in aqueous boiling base yields relatively small amounts of acidic and neutral material suggesting that hydrolyzable linkages are not predominant structural features of the kerogen material. If this process were to be an important one for the generation of acids, the assumption that oxidation makes hydrolyzable sites more accessible to solvent by partially rupturing the kerogen matrix would have to be made. The fact that branched acids are major constituents (relative to normals) in the 3 hour oxidation experiments would also suggest that carbon-carbon bond cleavage is a major process rather than simple hydrolysis or oxidation of entrapped compounds. The latter processes would be expected to yield an acid mixture rather similar to that obtained by extraction methods; whereas, carbon-carbon bond cleavages might be expected to occur at a greater rate for branched structures. The predominance of the C_{16} branched acid in these mixtures is perhaps a further indication of this process, for this acid would result from cleavage of the C_{13}–C_{14} bond (next to tertary allylic carbon atom in

phytol) in an isoprenoidal carbon chain. This would indicate polymer cross-linking at the allylic centers during kerogen formation. A suggested substituent structure of kerogen is illustrated in Figure 22, showing the various hydrolyzable side-chains and oxidation sites. The carbon-carbon bonded substitutents should dominate over the carbon-oxygen substituents.

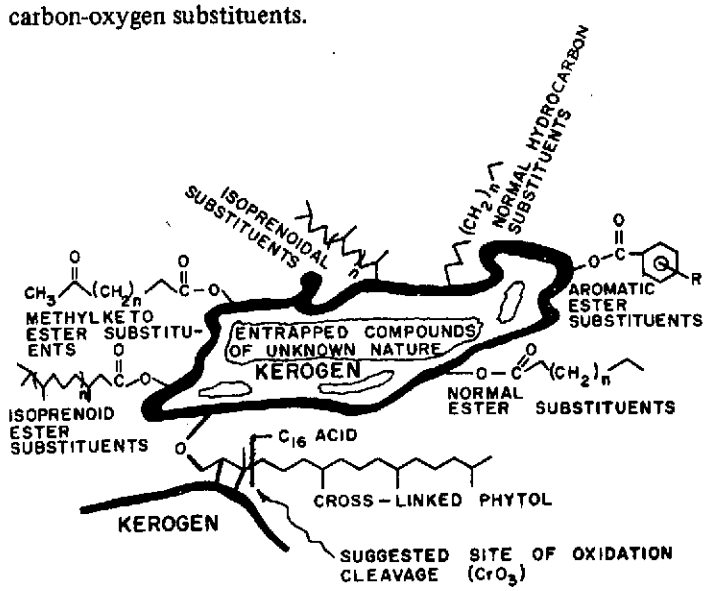

Fig. 22. The substituent structure suggested for kerogen

More extensive oxidation (9, 24 and 48 hours) leads not only to more acidic material in the total product mixture, but also to the predominant formation of normal acids and polyfunctional acids, in particular dicarboxylic acids. Our experiments do not yet point to any conclusion as to the structural attachments of the fragments obtained by oxidation. In particular, experiments with model compounds to determine the product distribution to be expected from these kinds of oxidation processes are needed. Data on the rate of oxidation of certain structural types also would be of interest.

Acknowledgements: We thank Mrs. Ellen Scott for technical assistance in Parts II and III, one of us (B.R.S.) for collection of the shale specimen, and Dr. D.H. Smith for assistance with the real-time high resolution data.

The work was supported by the U.S. National Aeronautics and Space Administration, Grants NGL 05-003-003, NGR 05-003-134 and NAS 9-7889.

References

Abelson, P.H. and Parker, P.L. (1961): Fatty Acids in Sedimentary Rocks, Carnegie Inst. Wash. Yearbook, 61, 181.

Baker, E.W., Yen, T.F., Dickie, J.P., Rhodes, R.E. and Clark, L.F. (1967): Mass Spectrometry of Porphyrins II. Characterization of Petro-Porphyrins, J.Am. Chem. Soc., 89, 3631.

Bendoraltis, J.G., Brown, B.L. and Hepner, L.S. (1962): Isoprenoid Hydrocarbons in Petroleum. Isolation of 2, 6, 10, 14-tetramethylpentadecane by High Temperature Gas Liquid Chromatography, Anal. Chem., 34, 49.

Bradley, W.H. (1966): Tropical Lakes, Copropel, and Oil Shale. Geol. Soc. Am. Bull., 77, 1333.

Burlingame, A.L. (1966): Application of High Resolution Mass Spectrometry in Molecular Structure Studies. In W.L. Mead, Ed., Advances in Mass Spectrometry, Vol. 3, Institute of Petroleum, London, p. 701.

Burlingame, A.L. (1968): Data Acquisition, Processing and Interpretation via Coupled High Speed Real-Time Digital Computer and High Resolution Mass Spectrometer Systems. International Mass Spectrometry Conference, Sept. 25–29, 1967, Berlin, in E. Kendrick, Ed., Advances in Mass Spectrometry, Vol. 4, The Institute of Petroleum, London, p. 15.

Burlingame, A.L., Haug, P., Belsky, T. and Calvin, M. (1965): Occurrence of Biogenic Steranes and Pentacyclic Triterpanes in an Eocene Shale (52 Million Years) and in an Early Precambrian Shale (2.7 Billion Years). A Preliminary Report. Proc. U. S. Nat. Acad. Sci., 54, 1406.

Burlingame, A.L. and Simoneit B.R. (1968): Isoprenoid Fatty Acids Isolated from the Kerogen Matrix of the Green River Formation (Eocene). Science, 160, 531.

Burlingame, A.L. and Simoneit, B.R. (1968): Analysis of the Mineral Entrapped Fatty Acids Isolated from the Green River Formation. Nature, 218, 252.

Burlingame, A.L. and Simoneit, B.R.: High Resolution Mass Spectrometry of Green River Formation Kerogen Oxidations, Nature, in press.

Burlingame, A.L. and Smith, D.H. (1968): Automated Heteroatomic Plotting as an Aid to the Presentation and Interpretation of High Resolution Mass Spectral Data, Tetrahedron, 24, 5749.

Burlingame, A.L., Smith, D.H., Merren, T.O. and Olsen, R.W.: Real-time High Resolution Mass Spectrometry, Proc. 16th Ann. Conf. on Mass Spectrometry and Allied Topics, May 12–17, 1968, Pittsburgh, Pa., p. 109.

Cummins, J.J. and Robinson, W.E. (1964): Normal and Isoprenoid Hydrocarbons Isolated from Oil Shale Bitumen, J. Chem. Eng. Data, 9, 304.

Douglas, A.G., Douraghi-Zadeh, K., Eglinton, G., Maxwell, J.R. and Ramsay, J.N.: Fatty Acids in Sediments including the Green River Shale (Eocene) and Scottish Torbanite (Carboniferous). In G.D. Hobson and G.C. Speers, Eds., Advances in Organic Geochemistry, Pergamon Press, London, in press.

Eglinton, G., Douglas, A.G., Maxwell, J.R., Ramsay, J.N. and Ställberg-Stenhagen, S. (1966): Occurrence of Isoprenoid Fatty Acids in the Green River Shale, Science, 153, 1133.

Eglinton, G., Scott, P.M., Belsky, T., Burlingame, A.L., Richter, W.J. and Calvin, M. (1964): Occurrence of Isoprenoid Alkanes in a Precambrian Sediment. In G.D. Hobson and M.C. Louis, Eds., Advances in Organic Geochemistry 1964, International Series of Monographs in Earth Sciences, Vol. 24, Pergamon Press, Oxford, 1966, pp. 41–74.

Forsman, J.P. and Hunt, J.M. (1958): In Habitat of Oil by L.G. Weeks, Ed., Am. Assoc. Petrol. Geol.

Haug, P.A. (1967): Applications of Mass Spectrometry to Organic Geochemistry. Ph.D. Thesis, University of California, Berkeley.

Haug, P., Schnoes, H.K. and Burlingame, A.L. (1967): Keto-Carboxylic Acids Isolated from the Colorado Green River Shale (Eocene). Chem. Comm. No. 21, 1130.

Haug, P., Schnoes, H.K. and Burlingame, A.L. (1967): Isoprenoid and Dicarboxylic Acids from the Colorado Green River Shale (Eocene). Science, 158, 772.

Haug, P., Schnoes, H.K. and Burlingame, A.L. (1968): Aromatic Carboxylic Acids Isolated from the Colorado Green River Formation (Eocene). Geochim. Cosmochim Acta., 32, 358–361.

Hills, J.R., Whitehead, E.V., Anders, D.E., Cummins, J.J. and Robinson, W.E. (1966): An Optically Active Triterpane, Gammacerane, in Green River, Colorado, Oil Shale Bitumen. Chem. Comm., 752.

Lawlor, D.L. and Robinson, W.E. (1965): Fatty Acids in Green River Formation Oil Shale. Paper presented at the Detroit Meeting, Amer. Chem. Soc., Div. Petrol. Chem., May 9, 1965.

Leo, R.F. and Parker, P.L. (1966): Branched Chain Fatty Acids in Sediments. Science, 152, 649.

Morandi, J.R. and Jensen, H.B. (1966): Comparison of Porphyrins from Shale Oil, Oil Shale, and Petroleum by Absorption and Mass Spectroscopy. J. Chem. Eng. Data, 11, 81.

Murphy, M.T.J., McCormick, A. and Eglinton, G. (1967): Perhydro-β-carotene in the Green River Shale, Science, 157, 1040.

Robinson, W.E., Cummins, J.J. and Dinneen, G.U. (1965): Changes in Green River Oil Shale Paraffins with Depth. Geochim. Cosmochim. Acta, 29, 249.

Venkataraghaven, R., McLafferty, F.W. and Amy, J.W. (1967): Automatic Reduction of High Resolution Mass Spectral Data. Anal. Chem., 39, 178.

Discussion

W.G. Meinschein: You suggest that in demineralizing your samples with mineral acids you are saponifying some esters. Do you believe the release of fatty acids from their salts may also be an important source of the acids obtained after your demineralization procedure with HCl and HF?

A.L. Burlingame: Yes. c.f. Burlingame, A.L. and Simoneit, B.R., Nature, 218, 252 (1968).

E.V. Whitehead: What do you regard as the effect of strong acids used in the separation or the possible polymerisation of naturally occurring unsaturated compounds liberated from the kerogen?

A.L. Burlingame: We do not have any evidence of olefinic substances liberated from this kerogen – with the possible exception of the C_{40} regions (c.f. perhydro-β-carotene and lower degrees of unsaturation (presumably rings – not double bonds of the olefinic variety).

Of course, we have evidence for the presence of tetra substituted double bonds in cyclic and polycyclic substances, e.g. Δ^8- in the lanosterol skeleton. We have developed an approach in determining the structures of enzymic steroid products by functionalisation of the hindered Δ^8-double bond with RuO_4 and subsequent high resolution mass spectral analysis, c.f. van Tamelen et al., J. Am. Chem. Soc. 89, 3284 (1968).

H. Kroepelin: Prof. Schmidt-Colerus, Denver[1]) has found in the methanol extract from Green River shale high molecular polymer acids (hydro-abietic and dehydro-abietic type). Have you observed these acids also?

A.L. Burlingame: We have not observed tricyclic aromatic acids of the resin variety occurring in nature (e.g. pine tree, etc.) in the Green River formation. We have evidence for their presence in the Tasmanites (see A.L. Burlingame, P.C. Wszolek and B.R. Simoneit; the fatty acid content of tasmanites, this conference).

On the other hand, we do have evidence for polycyclic acids in the C_{30} range, possibly the steroidal or triterpenoidal variety.

M. Louis: L'auteur a-t-il une idée de l'origine des acides benzene carboxyliques présents dans le schiste de Green River?

Est-ce que le milieu (lacustre) de dépot de la matière organique peut être responsable de la formation d'une partie des composés oxygénés (phénols, ac. benzène carboxyliques)?

A.L. Burlingame: A suggestion regarding the possible biological precursors I for the phenyl alkanoic acids has been presented by us previously (Haug, P., Schnoes, H.K and Burlingame, A.L. Geochim. Cosmochim. Acta, 32, 358–362 (1968)); whereas the lower homologs quite possibly are oxidation products of higher weight precursors.

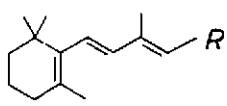

I

[1]) Paper presented at the UN-Symposium "Utilisation of oil shale", Tallinn, September 1968.

International Journal of Mass Spectrometry and Ion Physics
Elsevier Publishing Company, Amsterdam - Printed in the Netherlands

A COMBINED ELECTRON IMPACT–FIELD IONIZATION SOURCE AND ITS APPLICATION IN ORGANIC GEOCHEMISTRY*

P. SCHULZE, B. R. SIMONEIT AND A. L. BURLINGAME
Space Sciences Laboratory, University of California, Berkeley, Calif. 94720 (*U.S.A.*)

(Received July 12th. 1968; in revised form October 8th, 1968)

SUMMARY

A standard electron impact ion source for the C.E.C. 21-110B double-focusing mass spectrometer has been modified so that it can be used as a field ionization source. Switching from one mode of operation to the other is easy and can be done in a short time. The performance of the source is discussed with respect to sensitivity and high resolution. Photographic and on-line computer recording of field ionization mass spectra have been used. A procedure has been developed which permits mass measurement of the molecular ions despite the fact that there are no fragment ions and that perfluorokerosene which is normally used is not suitable as a mass marker.

The advantage of such a combination source coupled with a double-focusing mass spectrometer becomes evident in mixture identification. During studies on the composition of the total solvent extract, as well as the hydrocarbon and fatty acid fractions, from carbonaceous geological sediments, the spectra obtained in the field ionization mode have been compared to those generated upon electron impact.

INTRODUCTION

Since the first demonstration of the field ionization (FI) and dissociation phenomena in connection with mass separation by Inghram and Gomer[1], considerable effort has been expended, particularly by the pioneering studies of Beckey and co-workers[2,3], in the development of techniques which have permitted exploration of the scope of the phenomenon in conjunction with organic molecules.

* This represents Part XXIV in the series High Resolution Mass Spectrometry in Molecular Structure Studies. For Part XXIII, see A. L. BURLINGAME, *Proceedings Chromato-Mass Spectrometry Symposium, Moscow, May* 21–28, 1968, in press.

In addition to playing a significant role in the development of instrumental techniques, Beckey and co-workers have established a firm theoretical basis upon which the understanding of the ionization and dissociation processes may evolve[4]. The results of early studies by Beckey and Wagner[5] and Beckey and Schulze[6,7] on the behavior of homologous series of aliphatic compounds have demonstrated that a minimal amount of energy is transferred to the molecular ion during ionization, a fact manifested in the observed suppression of fragmentation in FI mass spectra compared with the case of electron impact (EI) spectra. Since molecular ions are comparatively abundant under FI conditions, the technique has obvious potential in determining the components of mixtures of hydrocarbons and petroleum[8,9]. Such studies have been carried out by Mead on paraffin waxes with molecular weights up to 700[10].

Various authors have pointed out the desirability of having the conventional EI ion source combined with an FI source in order to take advantage of what may be considered complementary modes of operation. In the FI mode usually very intense molecular ion peaks are obtained, from which empirical formulae can be determined. The EI mode, on the other hand, provides an extensive fragment ion spectrum from which structural information may be derived. FI data help to determine whether peaks at even mass numbers in the EI mass spectra are due to rearrangement processes or are molecular ions of minor components in a mixture. Recently, Beckey[11] has suggested that a comparison of FI and EI mass spectra may be helpful in determining whether fragment ions resulting from EI are due to single-bond ruptures or to multi-step fragmentation and/or rearrangement processes.

In this laboratory, the scope of FI studies in the analysis of complex mixtures of carboxylic acids derived from carbonaceous sediments is being explored as an adjunct to high-resolution mass analysis and on-line digital data acquisition both in the FI and EI[12] modes. In acid fractions obtained from carbonaceous sediments, several homologous series of compound types are generally present. For example, in the appropriate fraction from the Green River Formation, nominal mass 186 consists of a mixture of methyl naphthoate, methyl (ω-1)-oxononanoate and methyl decanoate. In order to distinguish among, and identify, these components, it is necessary to have the combined EI/FI source attached to a high-resolution mass spectrometer which permits accurate mass measurement to determine the elemental composition of the molecular ions in question. With a single-focusing mass spectrometer it was, until recently, impossible to get a resolution in excess of 300 (10 % valley definition) due to the energy spread exhibited by ions in FI. Brunnée et al. have shown[13] that a resolution of 800 can be achieved in a single-focusing instrument if the total voltage applied to a FI wire is increased to 17 kV. As such a high voltage may cause difficulties such as flashovers, gas discharges, etc., the application of FI mass spectrometry with single-focusing instruments to compounds of high molecular weight is limited.

In the following section the modifications necessary to convert a standard

ion source of a C.E.C. 21-110B double-focusing mass spectrometer into a combined EI/FI source are described and examples of its performance are given. A recent communication by Chait et al.[14] reports accurate mass measurements using a combined EI/FI source developed in their laboratory on a C.E.C. 21-110B mass spectrometer.

EXPERIMENTAL

The requirements which have to be met when constructing such a combination source are the following: (1) the combination should permit quick and easy interconversion of both modes of operation; (2) the sensitivity in the EI mode should not be decreased by the modification and should be as high as possible in the FI mode; (3) the resolution should be kept as high as possible in both modes; (4) it should be possible in both modes to run not only samples from the heated inlet system, but also solid samples which have to be introduced into the ion source via a direct introduction probe.

The emitter itself can be a wire, a blade or a tip. A tip was not used in this research, however, because the total ion current is too low, although it still may have some advantages if a higher degree of fragmentation than can be obtained with blades or wires is desired. In this laboratory Wollaston wires have not been used due to practical considerations. As Beckey and co-workers[15,16] have shown, wires yield much higher sensitivities than do razor blades, but the easier handling of a blade was considered to be more important than obtaining higher sensitivity. However, with the present system, Wollaston wires still can be used. Furthermore, a blade may be used without much preparation and conditioning. It should be mentioned, however, that when a new razor blade is first introduced, acetone is used for testing the performance of the blade. During this procedure the ion beam intensity increases slightly, which indicates a conditioning process.

Since an existing EI ion source was to be modified, it was desirable not to change the geometry of the ionization chamber to any degree and thereby to avoid possible influence on performance in the EI mode. Therefore, the FI emitter was placed behind the repeller plates while using these as the cathode (see Fig. 1). Since this might reduce the sensitivity for substances introduced through the direct introduction probe, which is in the plane of the electron beam, it is also possible to use the first slit of the ion-accelerating electrodes as the cathode. A vacuum lock was constructed and mounted in place of the window onto the cover flange of the 21-110B source housing. Thus, it is easy to change the emitter blade and to adjust it by means of a support rod to the desired position. The blade support rod is connected to a micrometer screw, which permits precise determination of the optimum distance from emitter to repeller or from emitter to first slit. It is also possible to rotate the emitter, thus allowing alignment of the FI emitter exactly

parallel with the slit of the repellers, which is necessary to give best results. Of course, the emitter may also be positioned perpendicular to the slit as recommended for wire emitters by Beckey *et al.* [15]

The blade is mounted in a small copper clamp which is surrounded by a quartz tube. This tube, when pushed into the back hole of the ion source chamber, insulates the blade from the source block. A copper coupling serves as electrical contact by means of a spring connection. Another insulator separates this copper piece from the blade support rod, which is maintained at ground potential.

Several experiments were carried out for the purpose of maximizing the total ion beam intensity, which was measured with the beam monitor between the electric and magnetic sectors. In placing the blade behind the repellers or behind the first slit, respectively, an increase in ion beam intensity was always observed when the blade position was behind the repellers, regardless of whether the sample was introduced via a heated glass inlet or a direct introduction probe. The reason for this is probably due to the electrostatic lens effect of the first slit, in combination with the source block. Placing the blade perpendicular to the slit of the repellers resulted in a decrease in transmitted ion beam intensity. The total ion currents obtained at this stage were still rather small (in the range of 10^{-13} amps or less for acetone). It was necessary, therefore, to make small modifications in the ion optics and also to change the type of emitter slightly.

While opening the first slit of the ion source from 0.7 mm to 1.0 mm and the slit between the focus plates from 1.0 mm to 1.5 mm did not increase appreciably the sensitivity in the FI mode, this change did increase considerably the resolution of the instrument obtainable in the EI mode. Prior to this modification the instrument was capable of a resolution not in excess of 20,000. Afterwards, it was not difficult to obtain a resolution of 32,000. The well-known doublet at *m/e* 142 in the mixture of methylnaphthalene and dimethylnaphthalene could be fully separated on the photographic plate as well as by using electron multiplier detection.

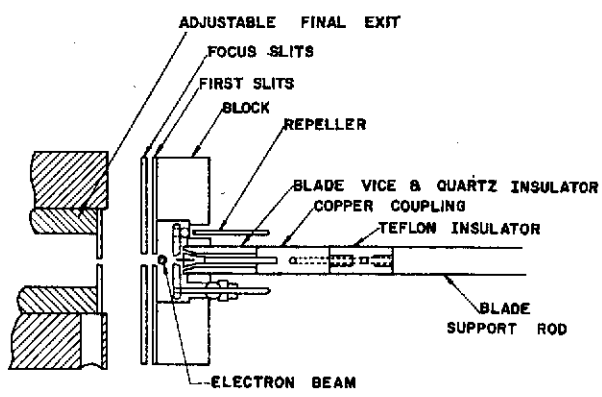

Fig. 1. The FI/EI combination source (schematic). For potentials in the FI mode, see text.

The modification of the emitter blade consisted of using not only single blades but also two or three blades, which were spotwelded together. The total ion current increased approximately proportional to the number of blades, although an exploratory experiment with an emitter of five blades did not verify this relation. In this case, only a slight increase was observed in comparison to a three-blade emitter. Therefore, in all experiments described hereafter a three-blade emitter was used.

By varying the potential at one of the focus plates a triple image was observed in the case of a three blade emitter. Fig. 2 shows this behavior for the molecular ion of acetone measured at the collector. The total ion beam observed on the beam

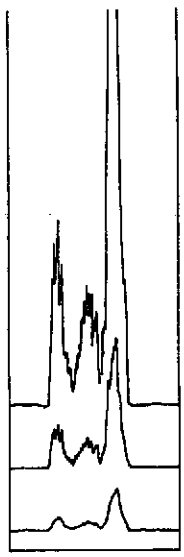

Fig. 2. Variation of the intensity of the molecular ion of acetone with changing focus potential using a threefold blade ($m/e = 58$).

monitor shows the same dependence on the focus potential. This means that the ions coming from each single blade are focussed separately onto the entrance slit of the mass spectrometer. As can be seen, the ion intensity coming from the outer blades is greater than from the center one. This is probably due to the fact that these blades are closer to the repeller electrodes and, therefore, the field strength at these blades is higher. In addition to the higher field strength at the outer blades, the direction of the field vectors in front of a multiple blade emitter is changed by the field of the adjacent blades to such an extent that more ions from each blade are emitted in a forward direction than from a single blade. This is assumed to be mostly responsible for the higher ion beam currents of multiple-blade emitters compared to a single blade.

Experiments were carried out to determine the dependence of the ion beam intensity on the distance from repeller to emitter. Three sets of modified repeller electrodes were used as indicated in Fig. 3. One set was cut down flat to a thickness

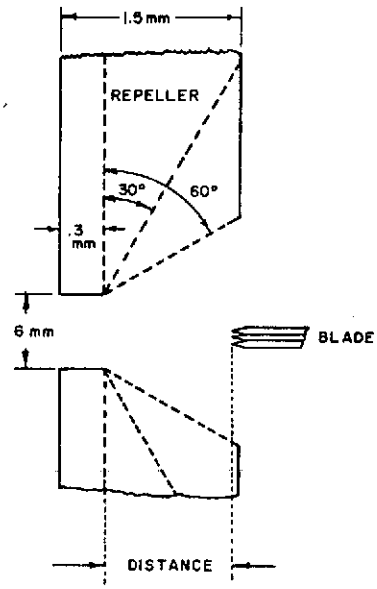

Fig. 3. Shape of the repellers.

of 0.3 mm. In the second case, the electrodes were bevelled to 30°, leaving a 0.3 mm slit depth, and in the third case a 60° bevel was used. The results are shown in Fig. 4. The intensity increases in all cases with decreasing distance. In the case of

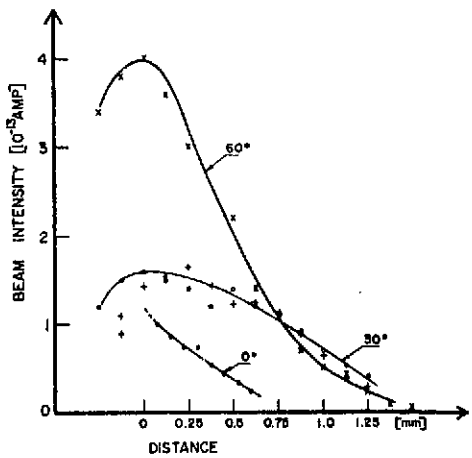

Fig. 4. Change of ion beam intensity (as measured with the beam monitor between electric and magnetic sectors) with distance from emitter to repeller. Pressure of acetone in the ionization chamber is estimated to be approximately 2×10^{-4} torr.

flat repeller electrodes (0°) the highest beam intensity is obtained when the blade is about to enter the space between the repellers and becomes very unstable as soon as the blade is just between the repeller electrodes. The beam intensity drops rapidly to zero as the blade moves further within the space between the repellers. In the case of a 30° and 60° bevel, the intensity is higher and does not drop abruptly to zero when the emitter enters the space. The increase in ion current with decreasing distance is very likely due to a higher ionizing field strength, rather than to more favorable ion optics. The stability of the ion beam is much better when the blade is close to the space between the 60° bevelled repeller electrodes than it is in the case of a flat repeller. The potentials normally used in the ion source were: emitter: +7450 V; repellers: −4000 to −5000 V; block: 0 V; and focus: +3200 V.

The resolution which could be obtained with this source was greater than 30,000 in the EI mode as already mentioned and greater than 20,000 in the FI mode. Fig. 5 shows the doublet at *m/e* 99 in cyclohexanone in the FI mass spectrum. The

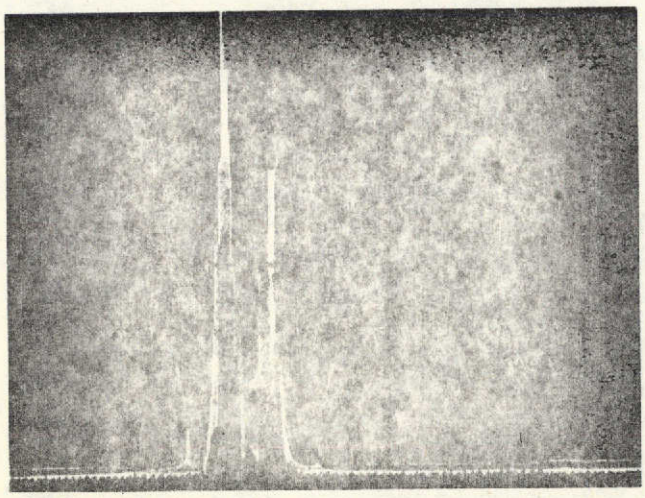

Fig. 5. Resolution obtained in the FI Mode with the electron multiplier detector ($C_5{}^{13}CH_{10}O^+$ and $C_6H_{11}O^+$). $m/e = 99$; $M/\Delta M = 22{,}000$.

larger peak represents the molecular ion containing ^{13}C while the other is the molecular ion with one hydrogen atom attached. The theoretical value for $M/\Delta M$ in this case is 22,000. Fig. 6 shows the trace from a recording microphotometer of the same doublet recorded on a photographic plate.

PROCEDURE

It is well-known that FI mass spectra do not exhibit many fragment ions. This, and the fact that perfluorokerosene cannot be used as an internal mass stand-

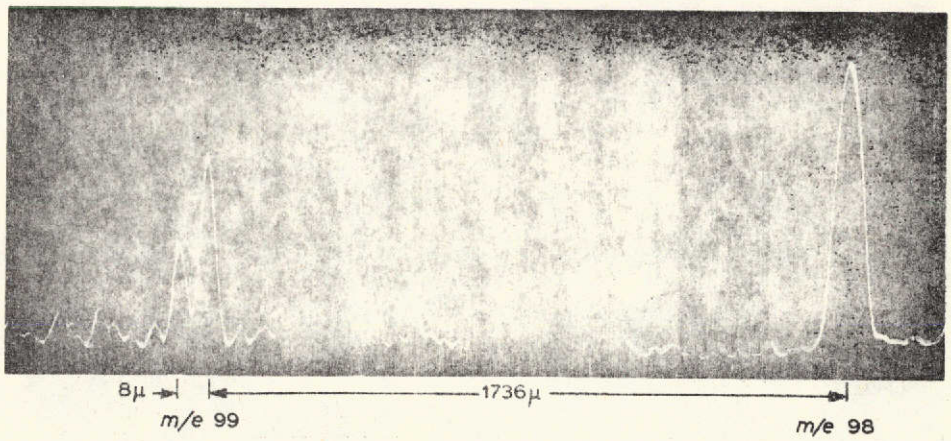

Fig. 6. Microphotodensitometer trace of the photographic record of the same doublet as in Fig. 5.

ard, makes it difficult even in low-resolution FI mass spectrometry to determine the masses of unknown compounds or mixtures of compounds. It is usually not too difficult to establish a mass scale if one is interested in the behavior of known compounds in an FI source. In investigating mixtures or homologues, it is sufficient to add just one known substance in order to define a mass scale although when dealing with unknown compounds or unknown mixtures, a proper choice may be difficult. For these reasons a more general way to determine the masses in an FI mass spectrum has developed. As was shown by Smith et al.[17] of this laboratory, the magnetic scan reproducibility of the C.E.C. 21-110B is very good, if the magnetic field is scanned linearly in time which establishes a quadratic relationship between mass and time. That is, the time elapsed between the recording of two different masses is always the same. The scan reproducibility was verified by several scans of perfluorokerosene in the EI mode which were done with on-line coupling of the output of the electron multiplier via an A/D converter to a computer (S.D.S. Sigma-7).[18]

Using this quadratic, mass vs. time relationship obtained with perfluorokerosene in the EI mode as a calibration, it is possible to superimpose the observed elapsed times of a FI mass spectrum. In order to do this, it is necessary to correct for possible differences in the high voltage and for differences in the time and mass used as starting points. This can be done by adding known compounds to the sample and comparing the times of the masses from the known compounds in the FI mass spectrum with the times of the same masses determined by interpolation from the perfluorokerosene calibration curve.

The resulting time differences were extrapolated to higher masses using the relationship

$$\Delta t = A + B\sqrt{m}$$

where $\Delta t = t_{PFK} - t_{FI}$ and the constants A and B are determined from the calibration masses. Using these Δt-values and the calibration data of the perfluorokerosene spectrum, this relationship gives satisfactory results over a very broad mass range. The determined masses are not highly accurate if the calibration data deviate extensively from the quadratic relationship which fits best in the vicinity of the FI calibration masses. It is still possible, nevertheless, to determine unambiguously the nominal mass of an unknown compound.

APPLICATIONS

Various standard and geochemical compound mixtures were analysed. A FI mass spectrum obtained from a mixture of free fatty acids isolated form the Green River Formation kerogen[19] is shown, with the corresponding low-resolution EI mass spectrum, in Fig. 7. Since the temperature of the ion source chamber for the FI spectrum is higher in this specific example, only the higher acids are detected. It may be noted that the acids show a dominant (M + 1) peak. The FI calibration compounds used were acetone, methylbutanone and cycloheptanone. Note that the calibration lines are very far apart (approximately 300 mass units) from the masses which have been calculated, as can be seen from Fig. 7.

Table 1 (upper part) lists the calculated and theoretical masses of a mixture

TABLE 1

THEORETICAL AND CALCULATED MASSES OF METHYL ALKANOATES AND FREE FATTY ACIDS

	Mass		
Formula	*Theoretical*	*Calc.*	*Error*
Methyl alkanoates			
$C_{15}H_{30}O_2$	242.22	242.17	−0.05
$C_{16}H_{32}O_2$	256.24	256.17	−0.07
$C_{17}H_{34}O_2$	270.26	270.18	−0.08
$C_{18}H_{36}O_2$	284.27	284.17	−0.10
$C_{19}H_{38}O_2$	298.29	298.19	−0.10
$C_{20}H_{40}O_2$	312.30	312.18	−0.12
Free fatty acids			
$C_{25}H_{50}O_2$	382.38	382.16	−0.22
$C_{26}H_{52}O_2$	396.40	396.15	−0.25
$C_{27}H_{54}O_2$	410.41	410.11	−0.30
$C_{28}H_{56}O_2$	424.43	424.13	−0.30
$C_{29}H_{58}O_2$	438.44	438.11	−0.33
$C_{30}H_{60}O_2$	452.46	452.08	−0.38
$C_{31}H_{62}O_2$	466.47	466.06	−0.41
$C_{32}H_{64}O_2$	480.49	480.05	−0.44

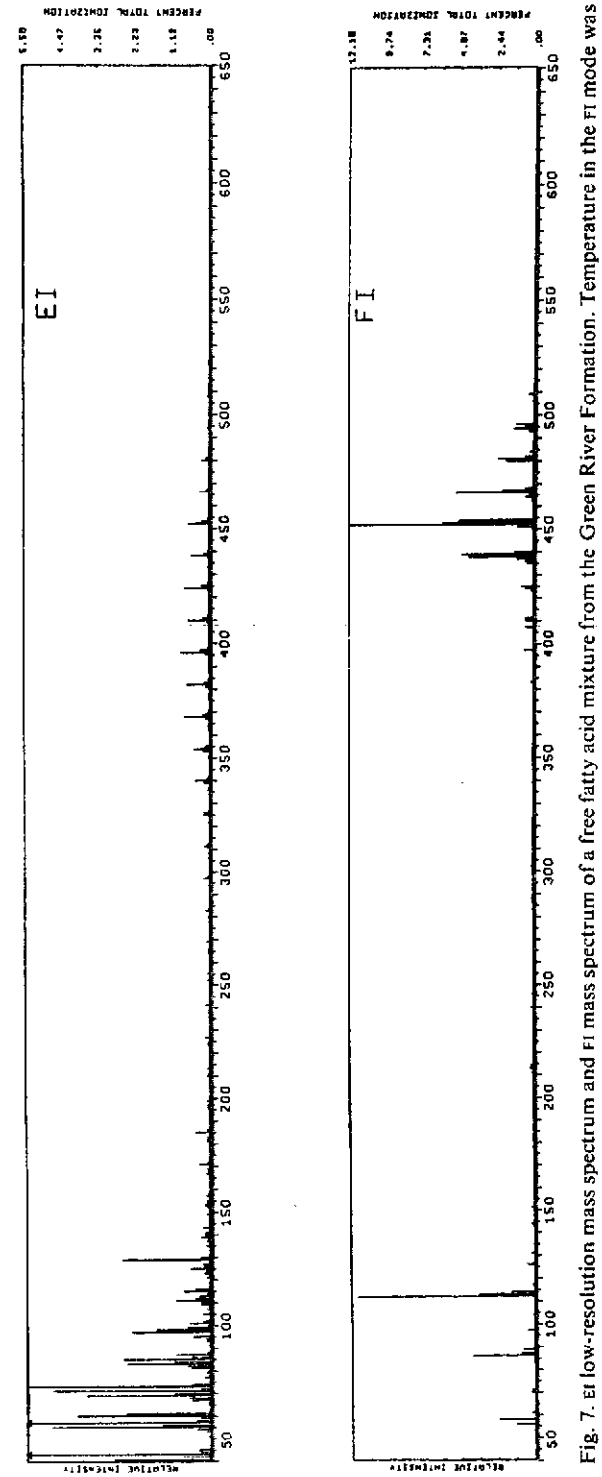

Fig. 7. EI low-resolution mass spectrum and FI mass spectrum of a free fatty acid mixture from the Green River Formation. Temperature in the FI mode was 25° higher than in the EI mode.

of known methyl alkanoates ranging from C_{15} to C_{20}, whose FI spectrum was determined as described above. In the lower part of Table 1, a second example of free fatty acids ranging from C_{25} to C_{32} obtained from Green River kerogen is presented. As can be seen, the error which is always negative increases with increasing mass. This was found for all spectra taken and calculated in this manner. Experiments in this laboratory are in progress using FI calibration standards closer in mass to the unknown compounds in order to reduce this error, and preliminary results are promising.

If accurate mass measurements are desired using either peak matching or the photoplate[14], the reference masses should be within a 14 mass unit region of the masses to be measured. On the other hand, with the present instrumentation it is more feasible to determine accurate masses using the EI mode provided the peaks of interest are present in the EI spectrum.

ACKNOWLEDGEMENTS

The authors wish to acknowledge the contribution of Mr. James Wilder, who carried out the ion source modifications, and that of Miss D. Allen for programming assistance. Financial support was provided by the National Aeronautics and Space Administration, Grants NsG 101 and NGR 05-003-134.

REFERENCES

1 M. G. INGHRAM AND R. GOMER, *Z. Naturforsch.*, 10a (1956) 863.
2 H. D. BECKEY, *Advan. Mass Spectry.*, 2 (1963) 1.
3 H. D. BECKEY, H. KNÖPPEL, H. G. METZINGER AND P. SCHULZE, *Advan. Mass Spectry.*, 3 (1966) 35.
4 H. D. BECKEY, *Z. Naturforsch.*, 19a (1964) 71.
5 H. D. BECKEY AND G. WAGNER, *Z. Naturforsch.*, 20a (1965) 169.
6 H. D. BECKEY AND P. SCHULZE, *Z. Naturforsch.*, 20a (1965) 1329, 1335.
7 H. D. BECKEY AND P. SCHULZE, *Ibid.*, 21a (1966) 214.
8 H. D. BECKEY AND G. WAGNER, *Z. Anal. Chem.*, 197 (1963) 58.
9 H. D. BECKEY, *Ibid.*, 197 (1963) 80.
10 W. L. MEAD, *Anal. Chem.*, 40 (1968) 743.
11 H. D. BECKEY, *J. Mass Spectry. Ion Phys.*, 1 (1968) 93.
12 A. L. BURLINGAME, D. H. SMITH, T. O. MERREN AND R. W. OLSEN, *Accounts Chem. Res.*, in press.
13 C. BRUNNÉE, G. KAPPUS AND K. H. MAURER, *Z. Anal. Chem.*, 232 (1967) 17.
14 E. M. CHAIT, T. W. SHANNON, J. W. AMY AND F. W. MCLAFFERTY, *Anal. Chem.*, 40 (1968) 835.
15 H. D. BECKEY, H. KRONE AND F. W. ROELLGEN, *J. Sci. Instr. Ser.* 2, 1 (1968) 118.
16 H. D. BECKEY, H. HEISING, H. HEY AND H. G. METZINGER, *Advan. Mass Spectry*, 4 (1968) 817.
17 D. H. SMITH, R. W. OLSEN AND A. L. BURLINGAME, 16th Ann. Conf. on Mass Spectrometry and Allied Topics, Pittsburgh, Pa., May 12–17, 1968.
18 A. L. BURLINGAME, *Advan. Mass Spectry.*, 4 (1968) 15.
19 For detailed discussion of these researches, see A. L. BURLINGAME AND B. R. SIMONEIT, *Science*, 160 (1968) 531; *Nature*, in preparation.

(Reprinted from Nature, Vol. 222, No. 56244, pp. 741-747, May 24th 1969)

High Resolution Mass Spectrometry of Green River Formation Kerogen Oxidations

by

A. L. BURLINGAME
B. R. SIMONEIT
Space Sciences Laboratory,
University of California,
Berkeley, California 94720

Extracts of a Green River Formation kerogen consisted chiefly of normal, isoprenoid, dicarboxylic, keto and various aromatic acid series. The kerogen seems to be polymer matrix, highly cross-linked by saturated hydrocarbons containing some aromatic nuclei, heteroatoms and many long isoprenoid and normal side chains.

Most previous investigations of oil shale from the Green River Formation of Eocene age have dealt with the solvent soluble matter. The presence of various homologous series in the hydrocarbon fraction has been established[1-4], while other studies have reported the presence of homologous series of normal fatty acids[5,6], isoprenoid acids[7-10], dicarboxylic acids[10], (ω-1) oxocarboxylic acids[11] and aromatic acids[12]. The same homologous series of acids have been found trapped in varying relative concentrations and distribution in the mineral–kerogen matrix[13]. The trapped acids probably occur chiefly as alkaline earth salts. Exhaustive solvent extraction accounts for approximately 2 per cent of the organic carbon; retorting yields about 13 per cent organics (35 gallons of naphtha are distilled from a ton of oil shale[14]). Such thermal distillation cracks roughly 10 per cent of the polymeric matter known collectively as kerogen. The sample used in these studies has an elemental analysis of 20·1 per cent C, 2·3 per cent H, 0·6 per cent N, 0·3 per cent S and 67·0 per cent residue. There have been few degradation studies to elucidate the molecular structures of the kerogen constituents. Exhaustive oxidation using alkaline permanganate yielded about 96 per cent of the organic carbon as water-soluble products[15] and oxidation under milder conditions has yielded dicarboxylic acids up to C_8 (ref. 16). Chromic acid oxidation under reflux for 6 h resulted in a complex mixture of acids[17], although only the normal acids C_{14}–C_{30} were identified. From these data and the retort pyrolysis studies, it has been concluded that the Green River Formation kerogen is non-benzenoid as well as non-coaly; in other words, it is essentially aliphatic in nature[18].

We report here the acids isolated from the controlled, stepwise degradation of kerogen by means of successive chromic acid oxidations lasting for 3, 6, 15 and 24 h. The isoprenoid fatty acids occur in all four fractions[19], decreasing in concentration as the oxidation time increases. Dicarboxylic acids, ketoacids, aromatic and cyclic acids, as well as polyfunctional acids, are present and increase in concentration, especially in the more polar extraction medium of diethyl ether (becoming smaller with regard to molecular weight), as the oxidation time increases. This means that in the early oxidation the long aliphatic side-chains of the kerogen matrix are removed and, as the oxidation proceeds, become depleted and then the breakdown of the cross links of the kerogen polymer matrix takes over. The "side chain-poor" kerogen, judging from the products isolated, is highly cross-linked and not very aromatized.

The oil shale sample was obtained from Parachute Creek, 8 miles north-west of Grand Valley, Colorado (108° 7′ W; 39° 37′ N; elevation 7,300 feet). The pulver-

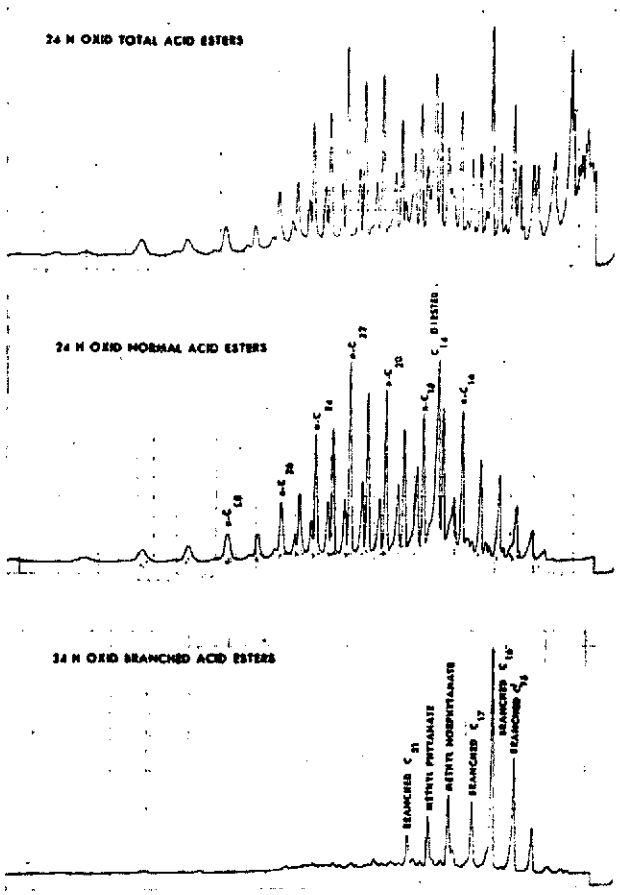

Fig. 1. Gas chromatogram of the heptane extract esters isolated from the 24 h oxidation. Column conditions: 5 feet × 1/8 inch; 40 ml./min helium; programmed from 100°–250° at 10°/min.

ized sample (to pass 200 mesh) was exhaustively extracted with a 4 : 1 mixture of benzene/methanol. This was followed by two digestions of 2 days each at room temperature using 1 : 1 concentrated hydrofluoric acid/hydrochloric acid. The residue, that is, the kerogen concentrate, was exhaustively extracted with 4 : 1 benzene/methanol using ultrasonication. The elemental analysis of the kerogen concentrate was 65·9 per cent C, 8·2 per cent H, 0·66 per cent N and 0·90 per cent S based on a mineral free sample. Twenty-five g of kerogen concentrate was refluxed for 3 h with 3 M chromic acid in sulphuric acid. The residue was filtered off, washed with water and extracted three times each, first with heptane and then with diethyl ether, using ultrasonication to ensure thorough extraction. The spent chromic acid solution was also extracted with heptane and then ether. The respective extracts were combined and the acids separated from the neutrals.

Esterification with BF_3 in methanol yielded 0·034 g (0·13 per cent of the kerogen concentrate) total esters from the heptane extract and 0·018 g (0·07 per cent) total esters from the ether extract. Normal esters were separated from branched-chain esters by clathration with urea[19]. Because it was found that the acids in the ether extract are of lower molecular weight and greater functionality than the acids of the heptane extracts, these ether extracts were not subjected to urea clathration, but were only esterified with BF_3 in methanol. The yield of normal esters, which were again extracted with heptane, was 0·016 g (0·06 per cent) and the branched-chain esters extracted from the adduct solution amounted to 0·010 g (0·04 per cent). The residual kerogen was further oxidized for an additional 6 h, the yield being 0·018 g (0·07 per cent) acids extractable with heptane and 0·080 g (0·32 per cent) acids extractable with ether. Esterification with BF_3 in methanol and clathration of the heptane extract gave 0·009 g (0·04 per cent) of normal and 0·005 g (0·02 per cent) of branched-chain ester fractions.

The kerogen remaining from the 6 h oxidation was oxidized 15 h more, resulting in 0·024 g (0·10 per cent) acids extractable with heptane and 0·150 g (0·60 per cent) acids extractable with ether. Esterification with BF_3 in methanol and clathration of the heptane extract gave 0·021 g (0·09 per cent) of normal and 0·008 g (0·04 per cent) of branched-chain ester fractions. The residue from the previous oxidation, which still had a 14·7 per cent carbon content, was subjected to further oxidation for 24 h. This resulted in 0·092 g (0·67 per cent) acids extractable with heptane and 0·120 g (0·88 per cent) acids extractable with ether. Esterification with BF_3 in methanol and clathration of the heptane extract yielded 0·058 g (0·43 per cent) of normal and 0·022 g (0·16 per cent) of branched-chain ester fractions. In working up reasonably concentrated fatty acid solutions in heptane, during washing of an extract before esterification, for example, the higher molecular weight acids crystallize out of solution. The low resolution mass spectrum[20] of such a precipitate filtered off from the 48 h oxidation extract consists of normal acids ranging from C_{18}–C_{35}. This molecular ion distribution was confirmed by obtaining a field ionization mass spectrum of the free acid mixture[21] using digital acquisition of the spectrum on a C.E.C. 21-110*B* mass spectrometer on-line to an SDS Sigma 7 computer[22]. The four oxidations, totalling 48 h, removed all the organic carbon from the kerogen concentrate (elemental analysis of the final residue gave 0·21 per cent C, 0·41 per cent H, 0·0 per cent N, 0·05 per cent S and 97·1 per cent residue). In summary, the respective oxidations, labelled 3, 9, 24 and 48 h, are listed in Table 1 with their yields of total and acid extracts.

Table 1. OXIDATION EXTRACTS OF GREEN RIVER FORMATION KEROGEN CONCENTRATE, EXPRESSED/100 G OF OIL SHALE SAMPLE

(Equivalent to approximately 45 g kerogen concentrate)

Oxidation	Total extract	Acids (heptane)	Acids (ether)
3 h	145 mg	60 mg	34 mg
9 h	225 mg	35 mg	150 mg
24 h	398 mg	48 mg	320 mg
48 h	685 mg	274 mg	360 mg

The total, normal and branched-chain ester fractions were chromatographed on a 5 foot × 1/8 inch column, packed with 3 per cent *SE*-30 on 'Chromosorb' and programmed from 100° to 250° C at 10°/min with a flow rate of 40 ml./min. The gas liquid chromatography (GLC) components were identified by their retention times, coinjection of standard compounds and low resolution mass spectra, and then correlated to the high resolution mass spectra of the respective fractions. The high resolution mass spectra were determined on both a C.E.C. 21-110*B* mass spectrometer and a modified GEC-AEI *MS* 902 mass spectrometer[22], each equipped with a direct inlet to the ion source.

The GLC patterns of the heptane soluble acid ester mixtures isolated from the four oxidations are virtually

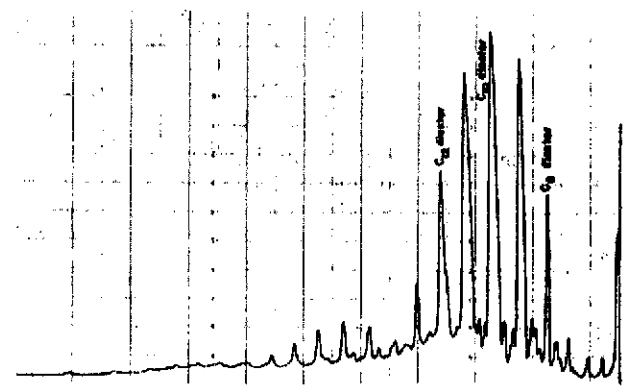

Fig. 2. Gas chromatogram of the ether extract esters isolated from the 24 h oxidation. Column conditions as in Fig. 1.

identical. There is an even/odd predominance in the normal acid fractions and the branched acids maximize at C_{16}. The 24 h oxidation esters serve as illustration in Fig. 1. The GLC patterns of the ether soluble acid mixtures are also virtually identical but maximize with lower carbon number acids. The ether extract acid esters from the 24 h oxidation serve as illustration in Fig. 2.

The high resolution mass spectral data of the total, branched and normal acid ester fractions[20] and of the total ether extract ester fractions[20] show that the various homologous acid series isolated from the four oxidations are the same and differ only in relative concentrations. Each fraction was subjected to increasing ion source temperatures, usually in the range 150°–270° C, to ensure complete volatilization while several mass spectra were taken. The partial high resolution mass spectral data[23] for the 3 h oxidation normal esters is shown in Fig. 3*a* and the C/H O_2 plot of the 24 h oxidation branched-cyclic esters appears in Fig. 3*b*. The even/odd predominance of the monocarboxylic acids is evident in the high resolution mass spectra of the total and normal fractions. The partial high resolution mass spectral data for the total ether extract esters from the 9 h oxidation are shown in Fig. 4. This is a representative example for the four ether extract fractions isolated from the respective oxidations.

Table 2. ORGANIC ACIDS FROM THE STEPWISE OXIDATIONS OF GREEN RIVER FORMATION KEROGEN CONCENTRATE (LISTED AS FREE ACIDS), EXTRACTED WITH HEPTANE AND THEN ETHER (THE MAXIMUM RANGE FOR THE FOUR OXIDATIONS ARE LISTED)

	Range (Heptane)	Range (Ether)	Maximum concentration (Heptane)	Maximum concentration (Ether)
Normal acids	C_{10}–C_{33}† C_5–C_{34}*	C_5–C_{19}*	C_{22}	C_5
Branched-chain acids	C_{14}–C_{22}† C_5–C_{26}*		C_{16}	
Dicarboxylic acids	C_8–C_{23}† C_5–C_{25}*	C_5–C_{13}† C_5–C_{12}*	C_{12}†*	C_4† C_{10}†
Ketoacids	C_4–C_{12}† C_6–C_{20}*	C_5–C_{14}*	C_6†* C_{14}*	C_6
Cyclic acids (mono-unsaturated $C_nH_{2n-2}O_2$)	C_5–C_{28}*	C_5–C_{14}*	C_{12}	C_6
Aromatic acids (phenyl $C_nH_{2n-6}O_2$) ‡	C_7–C_{28}*	C_7–C_{15}*	C_9	C_7
Aromatic acids (naphthyl $C_nH_{2n-14}O_2$)	C_{11}, C_{12}*	C_{11}, C_{12}*	C_{11}	C_{11}
Aromatic acids ($C_nH_{2n-10}O_2$)	C_{10}–C_{18}*	C_{10}–C_{18}*	C_{10}	C_{10}
Aromatic acids ($C_nH_{2n-12}O_2$)	C_{10}*	C_{10}–C_{13}*	C_{10}	C_{10}
Pentacyclic acids	C_{24}–C_{34}*	None	C_{30}	
Tetracyclic acids ($C_nH_{2n-8}O_2$)	C_{18}–C_{32}*	None	C_{24}, C_{30}	
Dicarboxylic aromatic acids ($C_nH_{2n-10}O_4$)	None	C_8–C_{13}*		C_8
Tricarboxylic aromatic acids	None	C_8–C_{12}*		C_9

* Determined by high resolution mass spectrometry.
† Determined from gas chromatogram.
‡ The aromatic acids are listed only to C_{19}, because above C_{19} the data fit tetracyclic acids better.

Results

Because the homologous series (Table 2) found in the heptane extracts of all four oxidations are essentially the same, the 3 h extracts will be discussed in detail and compared with those from the longer oxidations. The gas chromatogram of the normal acid esters exhibits peaks for three homologous series. Normal acids ranging from C_{10}–C_{30} with C_{22} as largest are the major constituent series, and dicarboxylic acids from C_6–C_{22} with C_{12} as largest, as well as ketoacids from C_4–C_{13} with C_6 as largest, are the minor constituent series. The gas chromatogram of the branched-chain esters exhibits peaks for the isoprenoid acid esters ranging from C_{14}–C_{22} with C_{16} as largest and

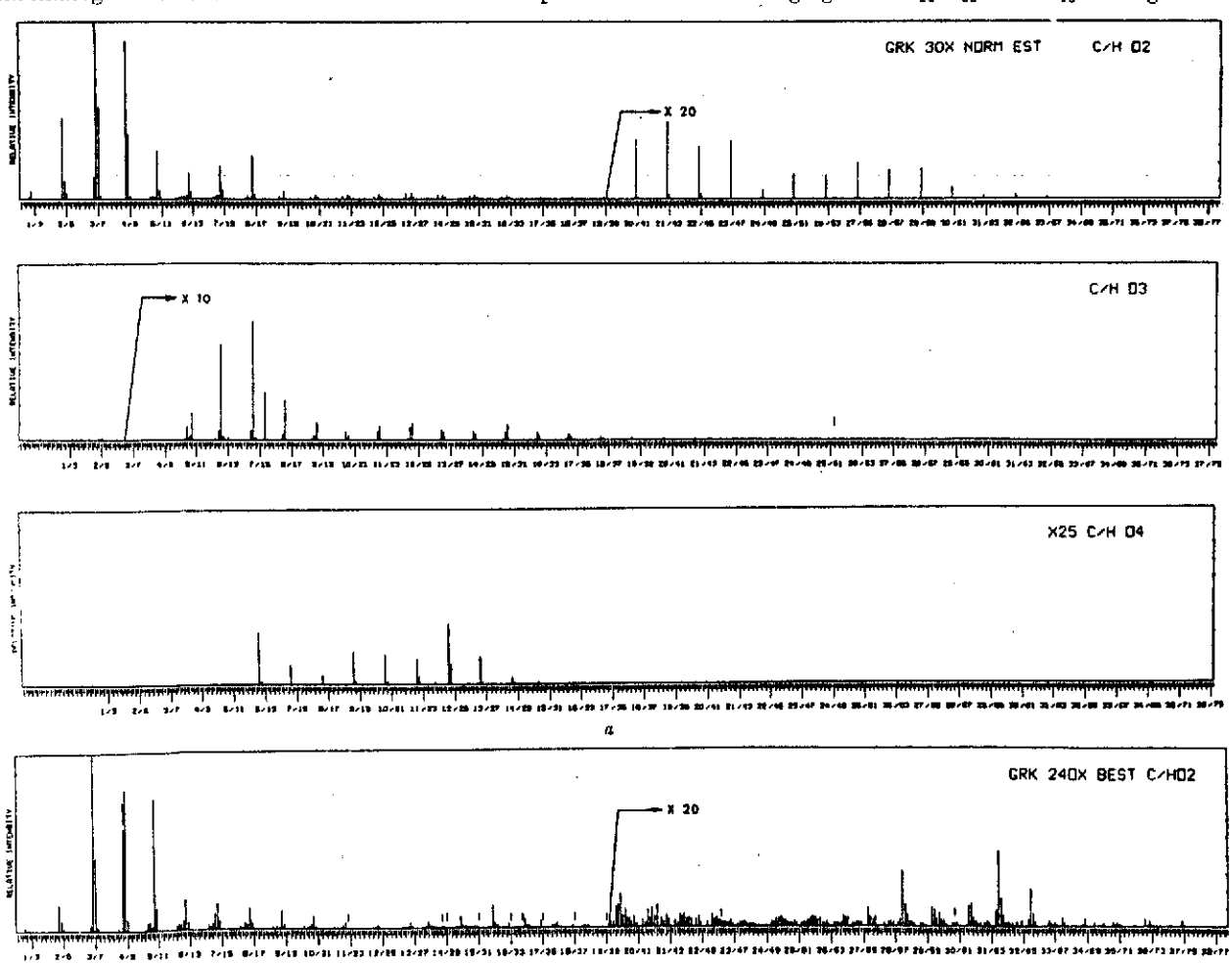

Fig. 3. *a*, Partial high resolution mass spectral data for the 3 h oxidation normal acid esters. *b*, Partial high resolution mass spectral data for the 24 h oxidation branched-cyclic acid esters.

C_{18} and C_{23} being absent. In the gas chromatogram of the total esters 40 per cent of the peak areas can be attributed to the normal, dicarboxylic and ketoacids and 60 per cent to the isoprenoid acids.

High resolution mass spectra of the total, normal and branched ester fractions showed molecular ion compositions corresponding to the same homologous series as indicated in the gas chromatograms together with several other trace acid series. The normal acids range from C_5–C_{33} with C_{22} most intense. The branched-chain acids range from C_6–C_{26} with C_{16} most intense and C_{18} and C_{23} entirely absent (the ester molecular ions of the C_8 and C_{13} acids are of low relative abundance). The presence of esters of $\leq C_4$ cannot be definitely determined from a high resolution mass spectrum alone because of the McLafferty rearrangement. Thus the lower limit of the normal and branched esters is at C_5 as a result of greater dyna c range. Dicarboxylic acids are indicated from C_6–C_{14} with C_{17} most intense. Although the molecular ions of this series are small, they were detectable and further substantiated by the presence of the strong peaks as a result of losses of 31 ($CH_3O\cdot$) and 73 ($C_3H_5O_2$) mass units (Fig. 5) (ref. 24). For example, in Fig. 3*a* the C_{18} diester has its molecular ion $C_{14}H_{26}O_4$ in the C/H O_4 plot; the loss of $CH_3O\cdot$ results in the peak at $C_{13}H_{23}O_3$ in the C/H O_3 plot and the following loss of ketene (unpublished results of W. J. Richter, D. H. Smith and A. L. B.) results in the peak at $C_{11}H_{21}O_2$ in the C/H O_2 plot. Ketoacids ranging

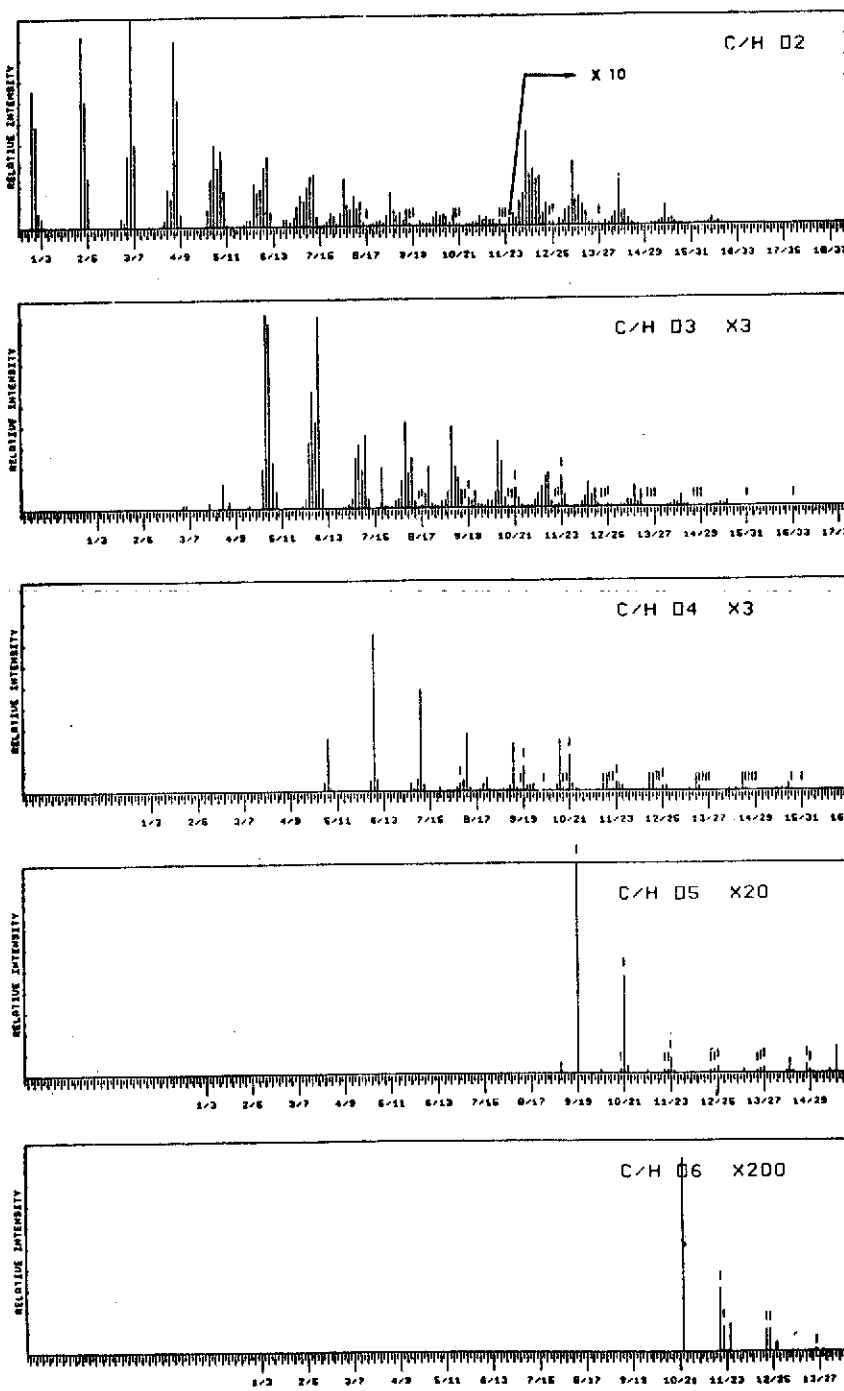

Fig. 4. Partial high resolution mass spectral data for the total ether extract acid esters from the 9 h oxidation.

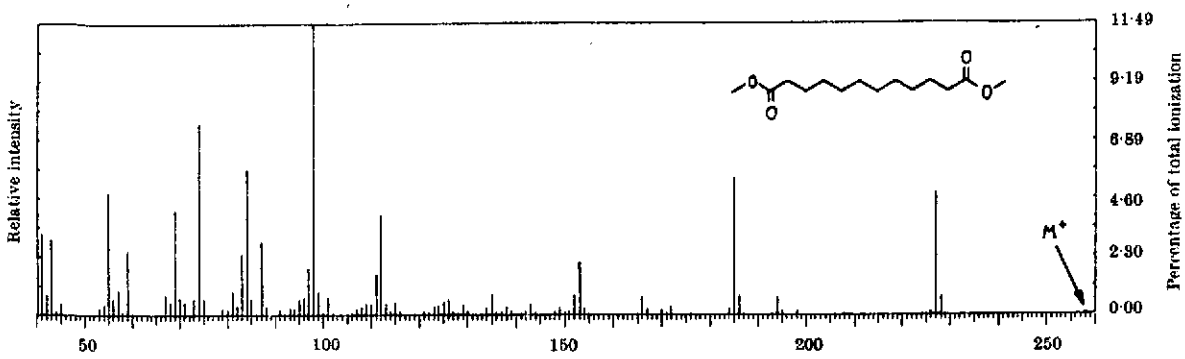

Fig. 5. Low resolution mass spectrum of dimethyl 1,12-dodecanedioate isolated from the ether extract esters of the 24 h oxidation by capillary GLC–MS techniques.

from C_4–C_{16} with a primary mode at C_6 and a secondary mode at C_{14} are present. The molecular ions are reasonably intense and this identification is further substantiated by the strong losses of $CH_3O\cdot$ and C_3H_5O (ref. 25 and unpublished results of W. J. Richter, D. H. Smith and A. L. B.). For example, in Fig. 3*a* the molecular ion of the C_{11} ketoacid is at $C_{12}H_{22}O_3$ in the C/H O_3 plot; loss of $CH_3O\cdot$ results in the peak at $C_{11}H_{19}O_2$ in the C/H O_2 plot and M–C_3H_5O in the peak $C_9H_{17}O_2$ also in the C/H O_2 plot. A confirmation of the oxoacids is discussed later.

The following acid series do not stand out in the gas chromatogram patterns and their presence is established by low and high resolution mass spectrometry. Cyclic and/or mono-unsaturated acids ranging from C_5–C_{17} with a maximum at C_{12} are found. Their molecular ions, strong loss of $CH_3O\cdot$ and cyclohexyl and alkylcyclohexyl ions are evident. A phenyl alkanoic acid series ranging from C_7 (benzoic acid, also the most abundant) to C_{16} is indicated by the elemental compositions of the molecular ions and the respective strong losses of $CH_3O\cdot$ in the high resolution mass spectra of the branched-cyclic fraction. Methyl naphthoate ($C_{12}H_{10}O_2$) and methyl indanoate ($C_{11}H_{12}O_2$) are the only members of the more aromatic series which are present. At higher ion source temperatures in the mass spectrometer, a series of polycyclic acid esters volatilizes from the branched-cyclic ester fraction. This series of pentacyclic acids has molecular ion compositions of $C_nH_{2n-10}O_2$, where $n = 29$–34 and $C_{32}H_{54}O_2$ is most intense. Referring to Fig. 3*b*, the molecular ion $C_{32}H_{54}O_2$ is found in the C/H O_2 plot and its corresponding M–$CH_3\cdot$ peak at $C_{31}H_{51}O_2$ in the same plot.

The 9 h oxidation acids, isolated by heptane extraction, consist of the same homologous series as listed in Table 2. The cycloaromatic series $C_nH_{2n-12}O_2$, however, ranges over $n = 11$–19 with $C_{11}H_{12}O_2$ as most abundant. Also another polycyclic acid series is evident. This series of tetracyclic acids has molecular ion compositions of $C_nH_{2n-8}O_2$, where $n = 19$–27, as well as the peak corresponding to M–$CH_3\cdot$; $C_{21}H_{34}O_2$ is the most intense of the group. From the gas chromatogram of the total esters 65 per cent of the peak areas can be attributed to the normal, dicarboxylic and ketoacids and 35 per cent to the isoprenoid acids. The even/odd predominance of the normal acids is very apparent, as is the case in the previous oxidation.

The 24 h oxidation acids conform excellently to the pattern of the previous oxidations. The same homologous series are present with only minor extensions. The isoprenoid acid content, however, is still less as deduced from the gas chromatogram of the total esters. Only 16 per cent of the peak areas can be attributed to the isoprenoid acids, whereas 84 per cent is due to normal, dicarboxylic and ketoacids. The concentration abundance of dicarboxylic compared with normal acids has also increased substantially for this oxidation. The even/odd predominance of the normal acids is still preserved.

The 48 h oxidation acids, by far the largest heptane fraction of the four oxidations, consist of the same homologous series as described. The isoprenoid acids are almost depleted; 5 per cent of the gas chromatogram peak areas can be assigned to them and 95 per cent to the normal, dicarboxylic and ketoacids. This relationship is summarized in Table 3, and in Fig. 6 the two extremes are illustrated by the original gas chromatograms. Furthermore, the dicarboxylic acids are of still higher molecular weight and greater abundance than in the previous oxidation. The even/odd predominance of the normal acids is also still evident.

Table 3. THE RELATIVE PERCENTAGE ABUNDANCE OF ISOPRENOID ACIDS COMPARED WITH NORMAL, DICARBOXYLIC AND KETOACIDS IN THE FOUR OXIDATIONS

Oxidation	Isoprenoids (percentage of peak areas)	Others (percentage of peak areas)
3 h	60	40
9 h	35	65
24 h	16	84
48 h	5	95

The subsequent ether extracts from the four oxidations consist of essentially the same homologous series of lower weight and more polar acids. The yields of ether soluble acids are listed in Table 1 and the distributions of the various series found are shown in Table 2. The gas chromatograms of the four fractions are the same, the dicarboxylic acid series, ranging from C_6–C_{12}, comprising the major peaks (Fig. 2).

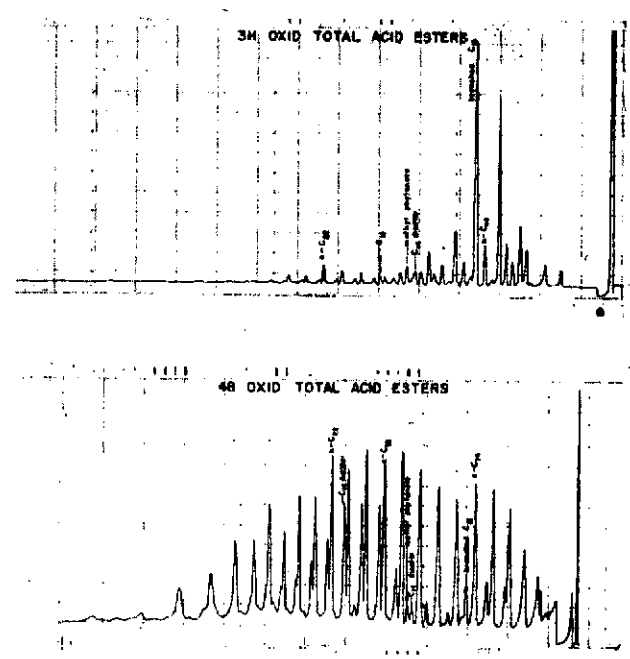

Fig. 6. Gas chromatograms of the total acid esters isolated from the 3 and 48 h oxidations. Column conditions as in Fig. 1.

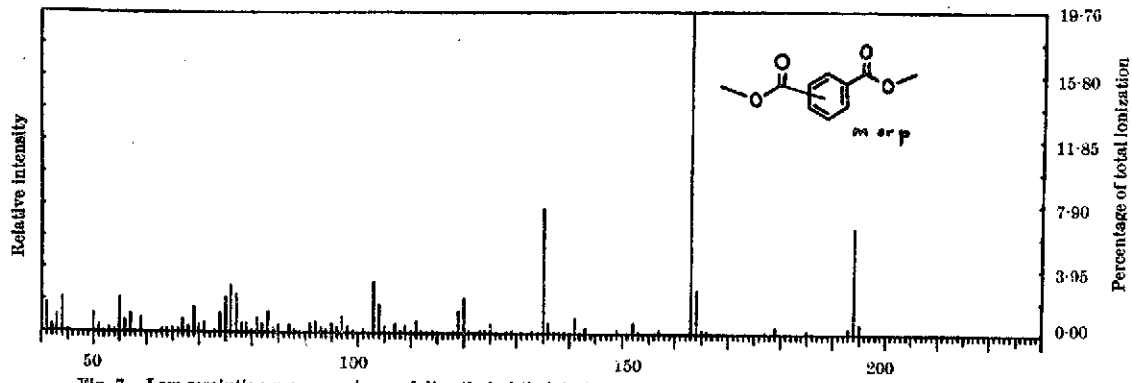

Fig. 7. Low resolution mass spectrum of dimethyl phthalate (m or p) isolated from the ether extract acids of the 24 h oxidation by capillary GLC–MS techniques.

High resolution mass spectrometry of the total fractions showed molecular ion compositions corresponding to the dicarboxylic acid series ranging from C_3–C_{12} with C_4 as the most intense. Referring to Fig. 4, the C_4 diacid has its molecular ion, $C_6H_{10}O_4$, in the C/H O_4 plot, the loss of $CH_3O\cdot$ results in the peak at $C_5H_7O_3$ in the C/H O_3 plot, and loss of ketene results in the peak at $C_3H_6O_2$ in the C/H O_2 plot. This series was also identified by capillary GLC–MS techniques, with 'Apiezon *L*' as liquid phase on a Perkin–Elmer model 900 gas chromatograph coupled to a GEC–AEI *MS*902 mass spectrometer on-line to an SDS Sigma 7 computer (for example, Fig. 5). There are also various other acid series present which are not resolved in the gas chromatogram because of their relatively low concentration. The fractions were not clathrated, so the normal and branched acids cannot be distinguished in the high resolution mass spectral data. Thus they are listed only as normals in Table 2 and range from C_5–C_{10} with C_5 most intense. Cyclic and/or mono-unsaturated acids, although of low intensity, are indicated from C_5–C_{14} with C_6 as maximum. Methylketo acids ranging from C_5–C_{14} with C_6 most intense are present. For example, in Fig. 4 the C_6 acid has its molecular ion, $C_7H_{12}O_3$, in the C/H O_3 plot and loss of $CH_3O\cdot$ to give $C_6H_{12}O_2$ and M–C_2H_3O to give $C_5H_{11}O_2$ can be found in the C/H O_2 plot. This series is further substantiated by borohydride reduction of the keto functionality, formation of the trimethylsilyl ether, and followed by high resolution mass spectrometry (unpublished results of W. J. Richter, B. R. S., D. H. Smith and A. L. B). The molecular ions of the ketoacids are absent in the mass spectral data of the reaction product and the series is indicated by the strong fragment ions containing SiO and SiO_2.

The various series of aromatic acids are well represented. The substituted phenyl acid series of $C_nH_{2n-8}O_2$ where $n=7$–13 is indicated by the molecular ions and strong loss of $CH_3O\cdot$ (benzoic acid is most abundant). The $C_nH_{2n-14}O_2$ series is only represented by naphthoic and methylnaphthoic acid. The bicycloaromatic acid series, $C_nH_{2n-10}O_2$, is present for $n=10$–15, indanoic acid being most concentrated. A second, more aromatized series is present as $C_nH_{2n-12}O_2$ for $n=10$–13, indenoic acid being most prevalent. Both these series can be seen in the C/H O_2 plot of Fig. 4. A dicarboxylic aromatic acid series is found as $C_nH_{2n-10}O_4$ for $n=8$–13, a phthalic acid (Fig. 7) being most abundant. Referring to Fig. 4, the molecular ion of the C_8 ester, $C_{10}H_{10}O_4$, can be seen in the C/H O_4 plot and the strong loss of $CH_3O\cdot$ is at $C_9H_7O_3$ in the C/H O_3 plot. A tricarboxylic aromatic acid series is also present with the compositions $C_nH_{2n-12}O_6$ for $n=9$–13, benzene tricarboxylic acid being the most intense. The molecular ion of the C_9 ester can be seen at $C_{12}H_{12}O_6$ in the C/H O_6 plot of Fig. 4; the diester of the same acid is at $C_{11}H_{10}O_6$ in the same plot; loss of $CH_3O\cdot$ from the triester results in the peak at $C_{11}H_9O_5$ in the C/H O_5 plot, and loss of $CH_3O\cdot$ from the diester in the peak at $C_{10}H_7O_5$ in the same plot.

The total yield of "generated" acids increases with the duration of oxidation. The increased yield of the more polar and more functionalized acids with the duration of oxidation—that is, the ether extractable acids (see Table 1)—is particularly marked. The isoprenoidal acids decrease drastically in concentration compared with the normal, dicarboxylic and ketoacids as the oxidation progresses. These results are summarized in Table 3, while the two extreme cases are illustrated in Fig. 6. The 3 h oxidation yields a mixture in which the isoprenoidal acids predominate; the abundance of the C_{16} branched acid should be noted particularly. The 48 h oxidation, however, yields only small amounts of branched acids (Fig. 6). The 9 h and 24 h oxidations are intermediate with respect to isoprenoid acid abundance. The branched acid fractions, isolated from urea adduction, show the same GLC distribution patterns (the 24 h oxidation, for example, in Fig. 1) with the C_{16} isoprenoid acids always as the chief constituent.

The acids obtained by oxidation could arise by several processes: (1) oxidative cleavage of carbon–carbon bonds; (2) hydrolysis of ester-linkages to give acids and alcohols, the latter being subsequently oxidized to acids; and (3) "loosening" of the kerogen matrix, thus liberating entrapped compounds. All three processes probably occur and it is difficult to determine their relative importance. The following arguments, however, strongly support the view that the major portion of the acids is derived from carbon–carbon bond cleavage of side chains and cross-links in the organic polymer matrix itself. The trend to decreasing relative abundance of isoprenoid acids (Table 3) with longer duration of oxidation indicates that preferential carbon–carbon bond cleavage occurs at branches in the side chains (compared with normal side chains); for example, oxidations of branched structures can be expected to occur at greater rates than straight chain oxidations. The predominance of 4,8,12-trimethyltridecanoic acid[19] in the branched fractions indicates cross-linking at the allyl rearrangement centre in phytol during polymer formation (structure I).

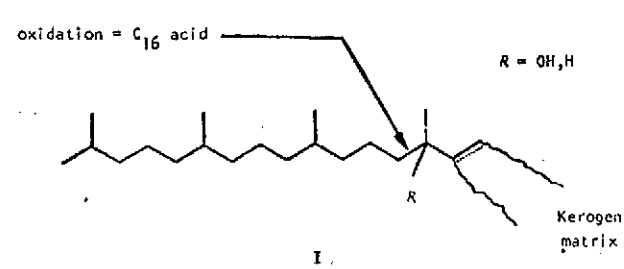

I

More extensive oxidation (9, 24 and 48 h) leads to the predominant formation of normal acids and polyfunctional acids—chiefly dicarboxylic acids. In the more polar extractions using diethyl ether are found smaller amounts of various aromatic acids with varying degrees of func-

tionality, as well as the aliphatic polyfunctional acids. The increase in concentration (with the period of oxidation) of the aromatic acids, especially the di and tricarboxylics, is further evidence for carbon–carbon bond cleavage and indicates the presence of some aromatic nuclei within the organic polymer (kerogen). The drastic increase of the dicarboxylic aliphatic acids with the duration of oxidation lends support to earlier conclusions regarding the aliphatic nature of the Green River Formation kerogen. The range (C_4–C_{25}) and smooth distribution of the dicarboxylic acids suggest a random aliphatic cross-linked polymer matrix. Further experiments to elucidate the structural attachments, rate of oxidation of certain structure types and reaction product and by-product distributions to be expected from this kind of treatment are in progress.

We thank Mrs Ellen Scott for technical assistance and the US National Aeronautics and Space Administration for support.

Received October 22, 1968; revised January 20, 1969.

[1] Eglinton, G., Scott, P. M., Belsky, T., Burlingame, A. L., Richter, W., and Calvin, M., in *Advances in Organic Geochemistry 1964* (edit. by Hobson, G. D., and Louis, M. C.), 41 (Pergamon, Oxford, 1966).

[2] Burlingame, A. L., Haug, P., Belsky, T., and Calvin, M., *Proc. US Nat. Acad. Sci.*, **54**, 1406 (1965).

[3] Hills, J., Whitehead, E., Anders, D., Cummins, J., and Robinson, W., *Chem. Commun.*, 752 (1966).

[4] Murphy, M. T. J., McCormick, A., and Eglinton, G., *Science*, **157**, 1040 (1967).

[5] Abelson, P. H., and Parker, P. L., *Carnegie Inst. Wash. Year Book*, **61**, 181 (1962).

[6] Lawlor, D. L., and Robinson, W. E., *Div. Pet. Chem. Amer. Chem. Soc.*, Detroit Meeting (May 9, 1965).

[7] Eglinton, G., Douglas, A. G., Maxwell, J. R., Ramsay, J. N., and Ståhlberg-Stenhagen, S., *Science*, **152**, 1133 (1966).

[8] Ramsay, J. N., thesis, Univ. Glasgow (1966).

[9] Douglas, A. G., Douraghi-Zadeh, D., Eglinton, G., Maxwell, J. R., and Ramsay, J. N., in *Advances in Organic Geochemistry 1966* (edit. by Hobson, G. D., and Spears, G. C.) (Pergamon, Oxford, in the press).

[10] Haug, P., Schnoes, H. K., and Burlingame, A. L., *Science*, **158**, 772 (1967).

[11] Haug, P., Schnoes, H. K., and Burlingame, A. L., *Chem. Commun.*, 1130 (1967).

[12] Haug, P., Schnoes, H. K., and Burlingame, A. L., *Geochim. Cosmochim. Acta*, **32**, 358 (1968).

[13] Burlingame, A. L., and Simoneit, B. R., *Nature*, **218**, 252 (1968).

[14] Dinneen, G. U., Van Meter, R. A., Smith, J. R., Bailey, C. W., Cook, G. L., Allbright, C. S., and Ball, J. S., *Bureau Mines Bull.*, 593 (US Govt. Printing Office, 1961).

[15] Robinson, W. E., Heady, H., and Hubbard, A., *Ind. Eng. Chem.*, **45**, 788 (1953).

[16] Robinson, W. E., Cummins, J. J., and Stanfield, K., *Ind. Eng. Chem.*, **48**, 1134 (1956).

[17] Hoering, T. C., and Abelson, P. H., *Carnegie Inst. Wash. Year Book*, **64**, 216 (1965).

[18] Forsman, J. P., in *Organic Geochemistry* (edit. by Breger, I. A.) (Pergamon, New York, 1963).

[19] Burlingame, A. L., and Simoneit, B. R., *Science*, **160**, 531 (1968).

[20] Burlingame, A. L., Haug, P. A., Schnoes, H. K., and Simoneit, B. R., in *Advances in Organic Geochemistry 1968* (edit. by Schenck, P. A., and Havenaar, I.) (Vieweg/Pergamon, Braunschweig, Germany, 1969).

[21] Schulze, P., Simoneit, B. R., and Burlingame, A. L., *J. Mass Spec. and Ion Phys.*, **2**, 181 (1969).

[22] Burlingame, A. L., in *Advances in Mass Spectrometry*, **4** (edit. by Kendrick, E.), 15 (The Institute of Petroleum, London, 1968).

[23] Burlingame, A. L., and Smith, D. H., *Tetrahedron*, **24**, 5759 (1968).

[24] Ryhage, R., and Stenhagen, E., *Arkiv Kemi*, **23**, 167 (1964).

[25] Ryhage, R., and Stenhagen, E., *Arkiv Kemi*, **15**, 545 (1960).

Reprinted from: COMPUTERS IN ANALYTICAL CHEMISTRY
(Plenum Press, 1969)

III. REAL-TIME HIGH-RESOLUTION MASS SPECTROMETRY

The Measurement of Accurate Molecular and Fragment Mass, and Relative Ionic Abundance: The Detection and Identification of Unresolved Isobaric Species.*

A. L. Burlingame, D. H. Smith, T. O. Merren,† and R. W. Olsen

Space Sciences Laboratory, University of California
Berkeley, California

A detailed description of the performance of a computer-coupled, high-resolution mass spectrometer system is presented. The results obtained from this system, which consist of accurate mass and intensity measurements for all ionic species present in a mass spectrum, are presented and discussed in the context of both system evaluation and application to organic analysis. The results indicate that mass measurement accuracies of 1 ppm or better are routinely obtainable through the use of the four-average technique, and that intensity measurement accuracy is limited only by ion statistics. Furthermore, system performance remains the same over a wide range of scan rates and mass spectrometer resolutions. Applications of such a system to organic analysis permits rapid acquisition and analysis of spectra and drastically reduces elemental composition ambiguities. A method for resolution of unresolved multiplets based on the mass measurement performance of the system is presented.

1. INTRODUCTION

The task of obtaining complete high-resolution mass spectra of complex organic molecules has involved use of computers for data processing for several years (1). The desirability of obtaining these spectra for structure elucidation or molecular fragmentation studies has been discussed (2). Our efforts have been directed toward developing more rapid and flexible

*Paper XXIII in the series High Resolution Mass Spectrometry in Molecular Structure Studies; for Part XXII, see A. L. Burlingame, D. H. Smith, and R. W. Olsen, *Anal. Chem.* (in preparation). Support of the National Aeronautics and Space Administration, Grants NGR 05-003-134, NsG 243, Suppl. 5, and NAS 9-7889, is gratefully acknowledged.

†Permanent address: G.E.C.–A.E.I., Ltd., Scientific Apparatus Division, Barton Dock Road, Urmston, Manchester, England.

means for acquiring such complete high-resolution mass spectra. This would be particularly suited for direct sample introduction employing capillary gas chromatographic techniques.

With the availability of improved performance, high-resolution mass spectrometers and high-speed digital computers, considerable interest has been expressed recently in linking these two devices in order to facilitate the task of data acquisition. These data are gathered while the experiment is in progress; thus the term "real-time." Several reports ([2]) have been presented on this subject, and a description of the performance of a prototype system for collecting complete high-resolution mass spectral data employing a digital computer in real-time has appeared from this laboratory ([3]). This system produced mass measurements accurate to about 5 ppm and adequate abundance measurements. Subsequent improvements in the system involving use of a different mass spectrometer-computer system and updating of interfacing have been discussed ([4]). These systems have proven to be quite flexible in terms of instrument operation, computer programing, and data display features, in addition to providing a rapid method for acquiring the vast amounts of data present in a high-resolution mass spectrum.

In this paper, we wish to discuss in some detail the quality of mass and intensity measurement data routinely obtainable from such a real time high resolution mass spectrometer. It was of considerable interest to perform a detailed evaluation of results obtained by this system. Such an evaluation provides a frame of reference in which system performance and limitations are well understood. Applications of such a computer-coupled high-resolution mass spectrometer system to routine problems in organic mass spectrometry can then proceed on a very firm footing.

These applications have led to development of a technique, based on mass measurement accuracy, for detection and identification of unresolved multiplets. Previous efforts directed toward the detection and identification of unresolved multiplets encountered in high-resolution mass spectra have concerned the mathematical deconvolution of the observed peak density profiles recorded on photographic plates ([5,6]). Difficulties have arisen in attempting such treatment from many factors associated with the reproducibility of line images on the photographic plate, e.g., nonlinearity of emulsion blackening characteristics over a wide dynamic range in intensity, "noisy" peaks, and so forth. The technique discussed in this paper is quite insensitive to instrument parameters such as resolution and peak shape.

2. EXPERIMENTAL

A detailed description of the mass spectrometer computer system will appear elsewhere ([7]). Briefly, the system includes an Associated Electrical

Industries, Ltd. modified MS-902 high-resolution mass spectrometer, capable of providing a resolution of 1 part in 50,000. Spectra are scanned by sweeping the magnetic field to cover a selected high-mass to low-mass range. The voltage output of an electron multiplier–amplifier system is digitized by an analog-to-digital (A/D) converter. The A/D output is linked to a Scientific Data Systems Sigma-7 computer. The output consists of peak voltage profiles recorded on magnetic tape and/or displayed on a cathode ray tube adjacent to a mass spectrometer. The tape is processed at a later time. Masses are calculated by relating the sample peak times to those of perfluorokerosene (PFK) through an exponential relationship of mass to time (Mass $\propto e^t$).

3. SYSTEM EVALUATION

The evaluation of data obtained by direct digitization on–line to the Sigma-7 will be concerned first with mass measurement accuracy and will delineate the performance which can be expected of the system described. Subsequently, relative abundance measurements will be evaluated and discussed. Before presenting the results, however, the method of calculation of the number of ions, N, in a peak will be discussed. The quantity N is used in evaluation of relative abundance measurements.

3.1. Calculation of *N*

The total number of ions may be estimated for each peak (singlet or multiplet) from the raw digital data. In practice, N is calculated and output during data reduction on the Sigma-7. N is calculated using the relationship derived below.

With reference to the peak depicted in Fig. 1, consider an element, of duration t seconds, of a peak, the element containing n ions.

The rate of arrival of n ions is therefore n/t per sec. If e is the charge of an electron, then the current i is given (in amperes) by

$$i = \frac{en}{t}$$

This ion current strikes the first dynode of an electron multiplier and is amplified by a factor G, the gain of the multiplier. On the last dynode, therefore, the current is

$$i = \frac{Gen}{t}$$

Attached to the last dynode is an amplifier, which has an input resistance R. The voltage E generated for this increment is then given by

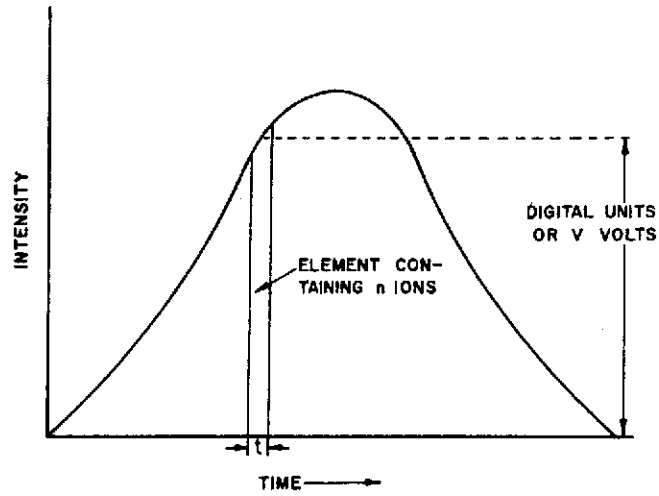

Figure 1. Illustration of parameters used in derivation of equation 1.

$$E = iR = \frac{RGen}{t}$$

The element of time considered t is the time between successive digitizations by the A/D, so that

$$t = \frac{1}{f}$$

where f is the digitization rate.

$$E = GRenf$$

Now, let the voltage level represented by one binary "bit" on the A/D converter be v volts.* If one observes c bits, then

$$E = cv$$
$$\therefore cv = GRenf$$

and

$$n = \frac{cv}{GRef}$$

The total number of ions is then given by a summation over all time elements per peak:

$$\Sigma n = N = \Sigma c \times \frac{v}{GRef} \qquad (1)$$

*The output of the A/D is a binary number, from 0 to $2^{14} - 1$ since there are 14 bits plus sign for this particular A/D. Therefore, 0–10 V represents 0 bits to 16,383 bits.

The summation over c is simply the peak area obtained by summation of the data points comprising a peak profile. The other parameters are noted before data are taken.

There is an additional consideration of importance, and that is the fact that the measured multiplier gain depends on the elemental composition of the particular ionic species impinging upon the electron multiplier ([8]). The gain is generally measured using a peak of PFK. It has been determined that the gain is 10–15% higher for the hydrocarbon or oxygen containing ions, depending on the particular elemental composition, than for the peaks of perfluorokerosene. It should be kept in mind, therefore, that the calculated number of ions represents an *upper* limit on N.

3.2. Mass Measurement Accuracy

In order to assess the accuracy of mass measurement attainable, nine successive scans were made at 25,000 resolution, with a scan rate of 35 sec/decade in mass. The data were digitized at 24 kHz. Perchlorobutadiene was chosen for the scans as a compound in which the masses of the fragment ions are known unambiguously. The sample flow rate into the ion source from a heated glass inlet system was less than 10 ng/sec.

For each of the runs, the differences between the observed and true masses were calculated for all peaks. Figure 2a shows the distribution of errors in the resulting 266 accurate mass values covering the mass range 100–266 with intensities greater than 2% of the base peak. Histogram A in Fig. 2a illustrates the percentage of errors (absolute values are plotted) falling within the ranges 0–2, 2–4 ppm and so forth. It can be seen that in 70% of the measurements, the observed mass differs from the true mass by less than 2 ppm.

An improvement in accuracy has been obtained by calculating the mean mass for several scans. If the errors in individual observed masses are random, then both precision and mass accuracy should be improved by a factor of two, taking the mean mass in four scans, and a factor of three taking the mean mass for nine scans. If, however, the observed deviations are due to systematic errors in the data acquisition and/or data reduction systems, mass measurement accuracy taking the mean of several scans should not be significantly better than for single scans.

To evaluate the data, mean masses were calculated for scans 1–4 and 5–8 of the nine scans. The 58 differences obtained are plotted in Fig. 2a as histogram B. In this case, the ranges are 0–1, 1–2 ppm and so forth. Comparison with histogram A shows that the errors are reduced by about a factor of two, with 77% of the errors now less than 1 ppm.

The mean differences for all nine scans are shown in Fig. 2a as histogram C, plotted over the ranges 0.0–0.5, 0.5–1.0 ppm, and so forth. Again the

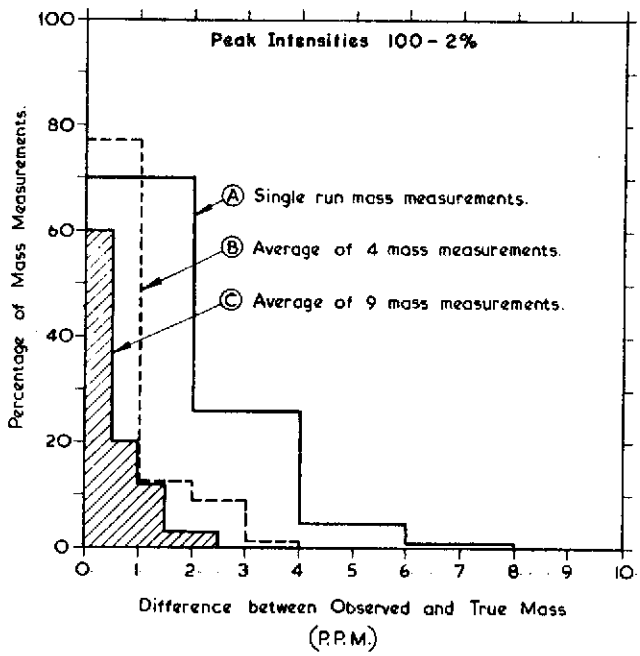

Figure 2a. Distribution of mass measurement errors at resolution of 25,000.

accuracy has been improved. In this case, 60% of the values are less than 0.5 ppm. These improvements are all consistent with observed mass measurement accuracy being a result of random rather than systematic errors.

Figure 2b shows that a further improvement in accuracy is obtained if only those peaks greater than 10% of the base peak are considered. The values plotted in the histograms were obtained exactly as for Fig. 2a. Seventy-eight percent of the differences are less than 2 ppm for single measurements, 88% are less than 1 ppm for the mean of four scans, and 71% are less than 0.5 ppm for the mean of nine scans. Furthermore, comparison of the histograms in Figs. 2ab shows that the larger errors are eliminated considering the smaller dynamic range.

The mass measurement accuracy described above is obtained for a total consumption of perchlorobutadiene of less than 0.5 μg in an individual scan and less than 2 μg for a group of four scans. Independent experiments on other organic compounds indicate that similar performance is obtained for similar sample quantities. The improved accuracy observed for peaks greater than 10% of the base peak in the above results would be expected to apply to all peaks down to 2% of the base peak if five times as much sample were used.

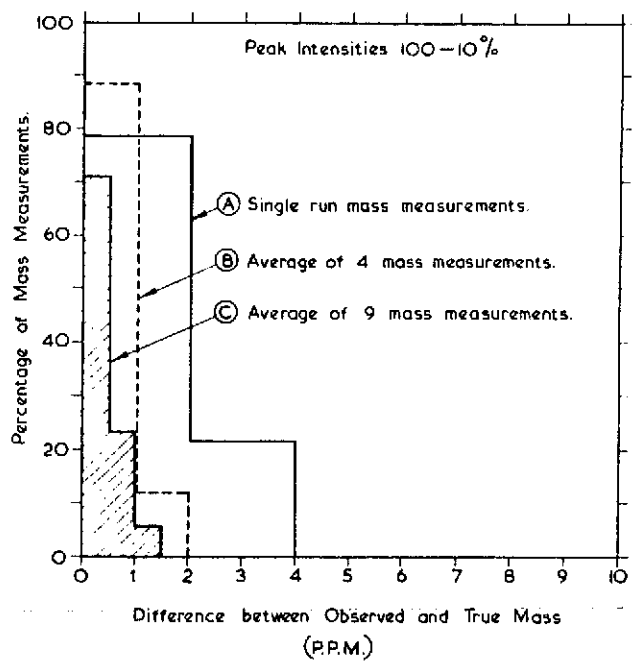

Figure 2b. Distribution of mass measurement errors at resolution of 25,000.

Some representative observed errors are tabulated in Table I. Errors for a representative single scan, averages for scans 1–4 and averages for scans 1–9 are expressed in ppm and in millimass units (mmu). The results of scans 1–9 are those used for histogram C in Fig. 2b. The only value larger than 1 ppm in the 9 average column is that at *m/e* 260, 1.15 ppm. The root-mean-square value is calculated for each column, since this value can be taken as a characteristic measure of performance for the particular number of scans considered.

The results indicate that a significant improvement in accuracy is achieved by taking four scans of a spectrum, and from both the sample and data handling points of view, the four-average method yields a practical improvement. Furthermore, the lack of systematic errors does enable mass measurement accuracy to be improved by multiple scans to about 0.5 ppm for peaks above 2% of the base peak.

The magnitudes of errors in millimass units for the above data provide an indication of the tolerances that must be considered for the acceptance or rejection of possible elemental compositions based on the observed mass. In Table I, for example, the R.M.S. value of 0.30 mmu with the largest observed error 0.91 mmu indicates the small tolerances that need be considered

TABLE I.

Species	Nominal mass	Error, ppm			Error, mmu			Relative intensity
		1	(1–4)	(1–9)	1	(1–4)	(1–9)	
C_4Cl_2	118	−0.83	−0.87	−0.29	−0.098	−0.103	−0.034	24.6
	120	−0.41	0.12	0.03	−0.049	0.014	0.004	16.8
C_3Cl_3	141	−0.64	−0.42	−0.31	−0.090	−0.059	−0.044	21.6
	143	−1.26	0.09	0.17	−0.180	0.013	0.024	21.6
C_4Cl_3	153	−0.83	0.46	0.12	−0.127	0.070	0.018	14.6
	155	0.83	0.71	0.63	0.129	0.110	0.098	14.5
C_4Cl_4	188	−0.82	−0.49	−0.41	−0.154	−0.092	−0.077	28.4
	190	−1.66	−0.36	−0.43	−0.315	−0.068	−0.082	36.6
	192	0.33	0.10	−0.44	0.063	0.019	−0.084	17.5
C_4Cl_5	223	−0.91	0.54	0.37	−0.203	0.121	0.083	62.0
	225	−0.61	−0.51	−0.26	−0.137	−0.115	−0.058	100.0
	227	0.91	−0.09	0.12	0.206	−0.020	0.027	62.1
	229	0.92	0.23	0.27	0.211	0.051	0.062	20.3
C_4Cl_6	258	2.34	1.77	0.96	0.605	0.457	0.248	21.3
	260	2.54	1.61	1.15	0.660	0.418	0.299	40.9
	262	2.88	1.70	0.91	0.705	0.445	0.238	31.2
	264	3.45	1.12	0.75	0.910	0.296	0.198	13.8
	RMS VALUE	1.59	0.859 ppm	0.547	0.382	0.209 mmu	0.132	

for only a single scan of a spectrum. Obtaining multiple scans yields the tabulated improvements in accuracy, and the resulting reduction of composition ambiguities possible. The R.M.S. value for nine scans is 0.13 mmu, with a largest error of 0.3 mmu.

Similar experiments were carried out at a resolution of 11,300 with a reduced sample flow rate (2.5 ng/sec). These results are presented as histograms in Figs. 3a and 3b as for the results at 25,000 resolution. The histograms show that the accuracy of mass measurement achieved at a resolution of 11,300 is very similar to that at a resolution of 25,000. For example, for the intensity range 100–2%, Fig. 31, 73% of the four-average mass measurements fall less than 1 ppm from the true value, and 63% of the ten average measurements fall less than 0.5 ppm. Consideration of the intensity range 100–10%, Fig. 3b, indicates results comparable to those shown in Fig. 2b.

At lower resolution, therefore, mass measurement accuracy is main-

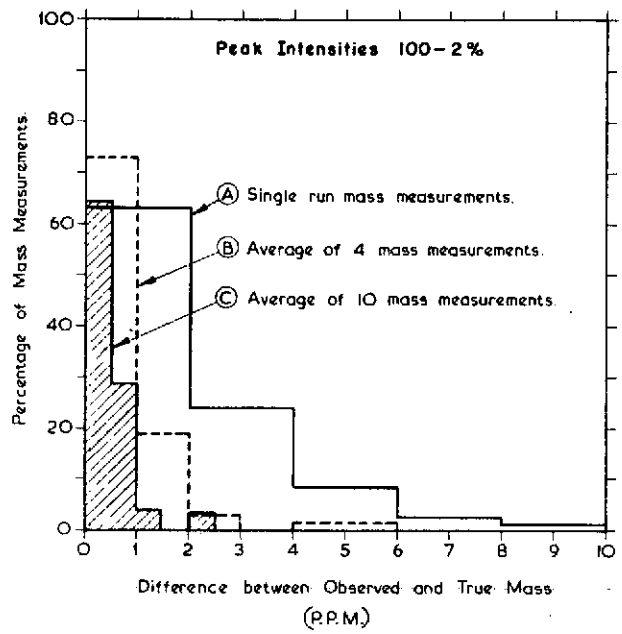

Figure 3a. Distribution of mass measurement errors at resolution of 11,000.

tained using smaller sample quantities. For this experiment, less than 0.5 μg flowed into the ion source for the period during which four scans were taken. Since Figs. 2a, 2b, 3a, and 3b demonstrate that improved accuracy is obtained on more intense peaks, a corresponding improvement would be obtained for peaks above 2% of the base peak at a higher sample flow rate.

Results of experiments on other organic samples indicate the results obtained over a dynamic range of 500–1. A representative example is a series of eight scans of the spectrum of methyl arachidate (discussed in a subsequent section), the methyl ester of n-C_{20} acid, at a resolution of 25,000. For these data, 65% of mass measurements (averaged over eight scans) fall within 1 ppm of the true mass, considering peaks above 0.2% of the base peak, and masses above m/e 100. Considering all masses above m/e 40 over this dynamic range, 61% of mass measurements are within 1 ppm of the true mass. The largest error noted is that of m/e 44 ($C_2\,{}^{13}C_1H_7$), 0.22 mmu, or 5.0 ppm. The slight decrease in mass accuracy below m/e 100 is relatively unimportant, because there are many fewer possible ambiguities in elemental composition.

3.3. Intensity Measurement Precision and Accuracy

Use of a chlorinated compound permits a detailed study of intensity measurement accuracy. The intensity ratios of peaks containing the same

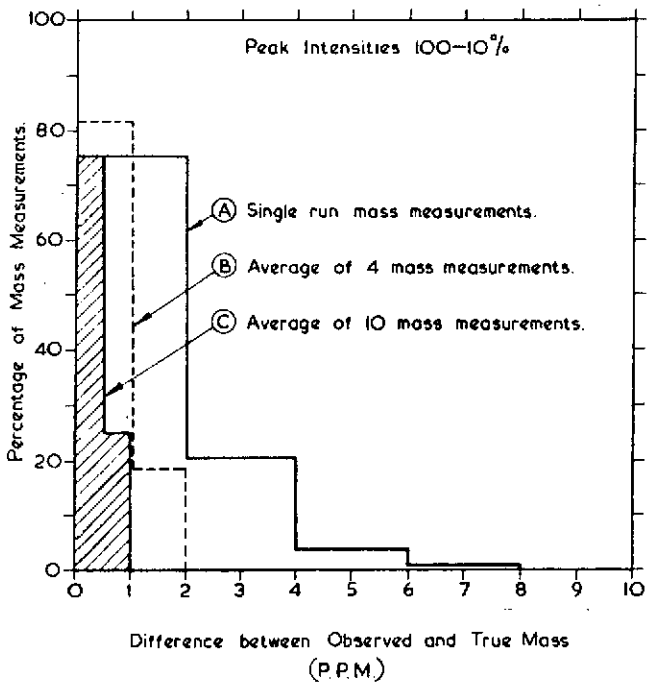

Figure 3b. Distribution of mass measurement errors at resolution of 11,000.

number of carbon and chlorine atoms can be calculated from the formula $(a+b)^m$ where m is the number of chlorine atoms, and $a=0.758$ and $b=0.242$ are the natural abundances of ^{35}Cl and ^{37}Cl. Intensity measurement precision may be evaluated by comparing the observed deviations in intensity with theoretical deviations based on ion statistics.

The evaluation of precision and accuracy can be accomplished as follows. Peak intensity measurements may be conveniently expressed as percentages of the total of isotopic peaks in a group, that is,

$$\frac{N_i}{\sum_i N_i} \times 100$$

where N_i is the number of ions in peak i (obtained as discussed in Section 1 above) and $\Sigma_i N_i$ is the total number of ions in the group.

The percentage abundances can be assigned theoretical standard deviations according to the equation

$$\sigma_{\text{theor}} = \frac{\sqrt{N_i}}{\sum_i N_i} \times 100$$

This form of the equation for σ_{theor} results in the standard deviation expressed in the same units (percentage of total ions in the group) as the abundance value itself.

Nine successive scans of the spectrum of perchlorobutadiene at each of two resolutions, 11,300 and 30,000, were obtained, and these data used to evaluate intensity measurement. Representative data in Table II compare the mean observed abundances with the true abundances, and the observed standard deviations with the theoretical value.

Precision may be evaluated by comparing the observed and theoretical standard deviations. It can be seen that they agree very closely, indicating that variations in intensity measurements are fully accounted for by ion statistical considerations. This confirms the conclusions reached by McMurray *et al.* ([2]) on a limited number of peaks at 10,000 resolution, and extends them to a larger number of peaks, a wider intensity range and resolutions as high as 30,000.

Intensity measurement accuracy may be evaluated by comparing the observed and true abundances. A qualitative comparison indicates excellent agreement, judged in terms of the accuracy of intensity measurement desired in organic mass spectrometry. A quantitative assessment involves comparison with the expected standard deviation of the mean, that is, the theoretical standard deviation divided by $\sqrt{n}$ where n is the number of scans from which the mean is calculated. Since n is 9 for both sets of scans, the errors in the mean abundances should be compared with the theoretical standard deviations divided by 3 ($\sigma_{theor}/\sqrt{9}$).

It may be seen from the table that 76% of the errors are less than one-third of a theoretical standard deviation. One hundred percent of the errors are less than 2 $\sigma_{theor}/\sqrt{9}$. The expected percentages of the errors, due entirely to statistical factors, are 68% and 96%, respectively. This close agreement indicates that no significant systematic errors are present in the mass spectrometer or data acquisition and processing systems. As with the precision, therefore, accuracy of intensity measurement is shown to be limited by ion statistical considerations.

4. APPLICATIONS TO ORGANIC ANALYSIS

The results presented above were intended to provide a detailed evaluation of the mass spectrometer–computer system. With this evaluation in hand, it is now possible to examine results obtained on organic samples of interest for a mass spectroscopist. Specifically, it is of interest to examine how the conclusions arrived at in the preceding sections can be used for analysis of typical, everyday spectra.

One of the more important results observed above is that four repeated

TABLE II.

Species	*m/e*	True abundance	Resolution 11,300				Resolution 30,000			
			Mean observed abundance	Standard deviation	Theoretical standard deviation	Error in mean abundance	Mean observed abundance	Standard deviation	Theoretical standard deviation	Error in mean abundance
C_4Cl_6	258	19.0	18.8	±0.5	0.5	−0.2	18.8	±1.3	1.5	−0.2
	260	36.3	36.5	±0.4	0.7	+0.2	36.6	±2.2	2.1	+0.3
	262	29.0	28.9	±0.8	0.7	−0.1	28.7	±1.6	1.9	−0.3
	264	12.4	12.4	±0.3	0.4	0.0	12.6	±0.9	1.2	+0.2
	266	2.96	3.00	±0.17	0.22	+0.04	3.12	±0.41	0.61	+0.16
	268	0.38	.35	±0.12	0.07	−0.03	0.38	±0.20	0.22	0.00
	270	.02	—	—	—	—	—	—	—	—
C_4Cl_5	223	25.0	25.0	±0.5	0.4	0.0	24.5	±1.5	1.2	−0.5
	225	39.9	39.6	±0.5	0.5	−0.3	40.2	±1.6	1.5	+0.3
	227	25.6.	25.7	±0.4	0.4	+0.1	25.8	±0.9	1.2	+0.2
	229	8.16	8.31	±0.20	0.24	+0.15	8.24	±0.54	0.68	+0.08
	231	1.32	1.34	±0.14	0.09	+0.02	1.25	±0.15	0.26	−0.07
	233	.08	—	—	—	—	—	—	—	—
C_4Cl_4	188	33.0	33.1	±0.7	0.8	+0.1	32.7	±1.6	2.3	−0.3
	190	42.2	42.3	±0.5	0.8	+0.1	42.2	±2.5	2.6	0.0
	192	20.2	20.3	±0.8	0.6	+0.1	20.5	±2.3	1.8	+0.3
	194	4.31	4.35	±0.27	0.28	+0.04	4.56	±0.72	0.85	+0.25
	196	0.30	—	—	—	—	—	—	—	—
C_4Cl_3	141	43.6	43.7	±1.1	1.1	+0.1	43.8	±5.1	3.3	+0.2
	143	41.7	41.6	±1.1	1.1	−0.1	42.3	±2.3	3.3	+0.6
	145	13.3	13.3	±0.5	0.6	0.0	12.8	±1.9	1.8	−0.5
	147	1.42	1.38	±0.28	0.20	−0.04	1.10	±0.53	0.57	−0.32
C_4Cl_2	118	57.5	56.8	±1.3	1.3	−0.7	57.7	±3.6	4.3	+0.2
	120	36.7	37.4	±1.1	1.1	+0.7	36.0	±3.9	3.4	−0.7
	122	5.80	5.81	±0.48	0.42	+0.01	6.30	±1.37	1.41	+0.50

scans of a spectrum will yield mass measurement accuracies of between one and two ppm. It may be expected that in most situations it is possible to obtain four spectra of a compound. To illustrate the information that may be obtained by knowing the mass measurement errors expected from the system, eight successive scans of the spectrum of methyl arachidate (n-$C_{19}H_{39}COOCH_3$) were recorded at 10,000 resolving power.* Mass measurement accuracy was evaluated by calculating average mass differences (in ppm), between assigned and observed mass, for spectra 1–4, 5–8, and 1–8. Some data representative of those observed for the complete spectrum are presented in Table III.

An examination of Table III reveals two sets of measurement accuracy data. One set, the majority of the table, includes those data that compare favorably with what is expected from the previous sections. The other set, comprising nominal masses 70, 88, 130, 186, and 214, include those data

TABLE III. Mass Measurement Accuracy. Methyl Arachidate

Assigned composition	Assigned mass	Average difference, ppm.			Average intensity
		1–4	5–8	1–8	
C_3H_5	41.03912	−0.51	−1.62	−1.06	7.81
$C_2{}^{13}CH_4$	42.04247	−0.48	−1.97	−1.32	0.26
C_3H_6	42.04694	−1.03	0.26	−0.39	2.49
$C_2H_3O_2$	59.01330	1.32	0.85	1.08	1.43
C_5H_9	69.07042	−0.53	−0.37	−0.45	12.45
C_5H_{10}	70.07824	−11.86	−12.53	−12.20	3.50
$C_3H_6O_2$	74.03677	0.27	−0.95	−0.34	100.00
$C_4H_7O_2$	87.04459	0.43	0.68	0.50	65.14
$C_4H_8O_2$	88.05242	−27.48	−25.30	−26.39	5.51
$C_5H_9O_2$	101.06024	−0.35	0.67	0.16	6.81
C_6H_{13}	121.10172	−0.76	−1.55	−1.15	0.98
$C_7H_{13}O_2$	129.09155	−1.52	−0.38	−0.95	7.19
$C_7H_{14}O_2$	130.09936	−9.03	−7.87	−8.45	2.30
$C_8H_{15}O_2$	143.10719	0.25	−0.37	−0.06	19.84
$C_{12}H_{19}$	163.14866	−0.18	0.82	0.32	0.39
$C_{11}H_{22}O_2$	185.15414	0.28	−0.09	0.10	4.93
$C_{11}H_{23}O_2$	186.16196	−12.79	−12.21	−12.45	1.13
$C_{13}H_{25}O_2$	213.18544	0.62	−0.13	0.25	2.05
$C_{13}H_{26}O_2$	214.19326	−10.05	−8.68	−9.38	0.70
$C_{18}H_{34}$	250.26603	−0.48	1.17	0.25	0.18
$C_{18}H_{35}O_2$	283.26368	0.25	−0.46	−0.10	8.82
$C_{19}H_{37}O_2$	297.27933	−0.51	0.47	−0.02	1.82
$C_{21}H_{42}O_2$	326.31846	−0.28	−0.63	−0.45	15.34

*Spectra scanned at 35 sec/decade with a digitization rate of 24 kHz.

that exhibit very high differences. These entries may then represent unresolved doublets, with the contribution from the second peak shifting the peak position sufficiently to yield errors higher than expected.

To illustrate this situation in more detail, peak profiles from one scan of the resolved ^{13}C *vs.* CH doublet at *m/e* 42 ($\Delta M = 0.00446$ amu) and the suspected unresolved doublets at *m/e* 70, 88, and 130 are presented in Figs. 4 and 5. Peak widths at 10,000 resolution, 35 sec/decade, should be $\sim 1500\,\mu$sec. At a digitization rate of 24 kHz, the peaks should be ~ 36 clock pulses wide at the 5% level. Calculated positions of the center of gravity (labeled C.G. in the figures) are indicated. It is observed that the profiles of *m/e* 70 and 88 do indeed indicate unresolved doublets. These doublets, as will be described below, are due to ^{13}C *vs.* CH. The presence of an unresolved ^{13}C isotope peak under the peak profile should result in a shift of the center of gravity to lower mass, resulting in a negative difference when compared to the mass of an assigned composition including CH, rather than ^{13}C. This is exactly what is observed in Table III (note the large negative differences of *m/e* 70, 88, 120, 186, and 214). The profile of *m/e* 130 (Fig. 5) which is only slightly suggestive of an unresolved doublet, is a particularly striking example of how little the center of gravity need be shifted to yield a large mass measurement error.

Further investigations were carried out by recording repetitive scans

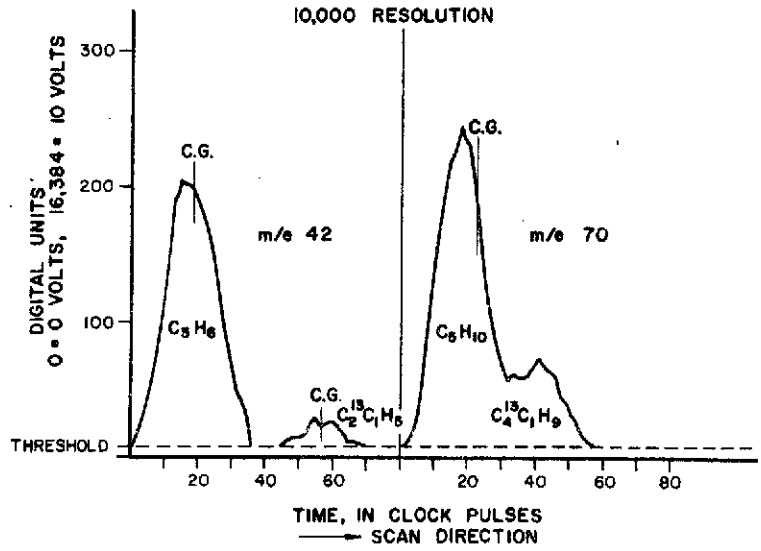

Figure 4. Peak profiles of *m/e* 42 and *m/e* 70 at a resolution of 10,000. Scan rate 35 sec/decade in mass. Clock rate 24 kHz. Mass spectrum of methyl arachidate.

TABLE IV. Doublet Recognition

Nominal mass	Assigned composition	Resolution					
		10,000 (8 scans)		25,000 (9 scans)		30,000 (6 scans)	
		Difference*	Rel. int., %	Difference	Rel. int., %	Difference	Rel. int., %
70	C_5H_{10}	−12.20 (U)†	3.50	0.67	4.10	0.43	4.32
	$C_4{}^{13}C_1H_9$			1.03	0.85	−1.06	0.67
88	$C_4H_8O_2$	−26.39 (U)	5.51	−0.63	2.58	1.57	2.52
	$C_3{}^{13}CH_7O_2$			−0.25	3.17	0.69	2.61
130	$C_7H_{14}O_2$	−8.45 (U)	2.30	−0.67	2.12	0.63	2.10
	$C_6{}^{13}C_1H_{13}O_2$			0.52	0.55	0.21	0.45
186	$C_{11}H_{22}O_2$	−12.45 (U)	1.13	−13.90 (U)	1.08	0.09	0.60
	$C_{10}{}^{13}C_1H_{21}O_2$					−1.12	0.38
214	$C_{13}H_{26}O_2$	−9.38 (U)	0.70	−10.39 (U)	0.47	−0.47	0.20
	$C_{12}{}^{13}C_1H_{25}O_2$					0.97	0.24

*Difference, in ppm, of average and assigned mass.
†'U' indicates unresolved doublet.

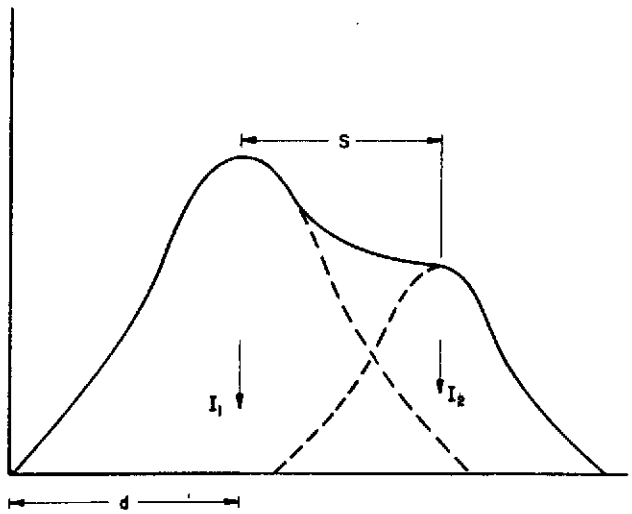

Figure 6. Illustration of parameters used in derivation of equation 2.

peak I_1 be d from the origin. The calculated position of the doublet is given by:

$$\frac{I_1 + (d+S)I_2}{I_1 + I_2}$$

The shift E of the larger peak is given by:

$$E = \frac{I_1 d + (d+S)I_2}{I_1 + I_2} - d$$

$$= \frac{I_2 S}{I_1 + I_2} \qquad (2)$$

E, which may be regarded as the error, may be expressed in ppm by expressing the mass separation S as $\Delta M/M$, the difference in mass divided by the mass, time 10^6. The value S does *not* depend on the actual physical separation of the peaks. It is merely the separation of the centers of gravity of the two peaks comprising the doublet. Thus equation (2) is *independent* of mass spectrometer resolution.

The equation is plotted in Fig. 7 for the two error confidence limits of 1 and 2 ppm. Doublets, with appropriate separation S and intensity ratios, falling in the hatched region should be detectable on the basis of mass measurement error at the indicated confidence level. For example, if one is confident that a series of mass measurements should yield an accuracy of better than 1 ppm for single, resolved peaks, then doublets with a separation $\Delta M/M = 4$ ppm are detectable if $I_2/I_1 \geq 35\%$, and doublets with $\Delta M/M =$ 20 ppm are detectable if $I_2/I_1 \geq 5\%$.

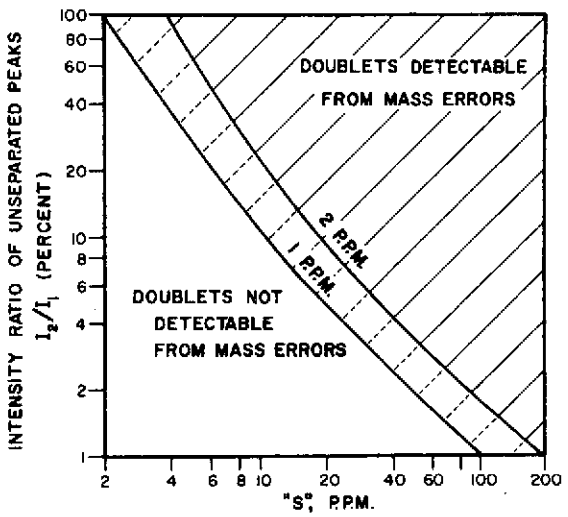

Figure 7. Intensity ratio of unseparated peaks *vs.* the separation $S = \Delta M/M$ for the error confidence limits of 1 and 2 ppm.

Equation (2) may be applied and tested for the CH *vs.* ^{13}C doublets noted above. Intensity I_2, the ^{13}C contribution, may be calculated on the basis of the corresponding peak one mass unit lower. S and $(I_1 + I_2)$ are known quantities. Subtraction of the calculated error from the observed error yields a mass measurement error for the CH species. As may be seen from the results tabulated in Table V, this procedure works quite well.

TABLE V.

Nominal mass	Observed error, ppm	Mass measurement error, CH species, ppm
70	−12.20	0.2
88	−26.39	−0.1
130	−8.45	−0.3
186	−12.45	−0.3
214	−9.38	−0.8

Thus, one obvious use of equation (2) is immediately suggested. This equation could readily be incorporated into a data reduction scheme to eliminate ^{13}C isotopic contributions to unresolved doublets, be they ^{13}C *vs.* CH or ^{13}C *vs.* another species, resulting in a new measured mass to match with a composition.

The above discussion indicates that a detailed knowledge of the mass measurement capabilities of the system provides one criterion, but not necessarily the only one, to screen the real time data for suspected unresolved

multiplets. Judicious use of equation (2), based on knowledge of the elemental composition of the intact molecule and the calculated mass of the multiplet from the center of gravity, then allows calculation of the accurate mass and intensity of the peaks comprising the multiplet. Equation (2) may be applied in an iterative fashion for multiplets of higher order than doublets. Indeed, this method has been applied successfully to several triplets of the type ^{13}CH *vs.* CH_2 *vs.* CD ([9]). This simple mathematical procedure lends itself readily to automatic calculation by appropriate computer programing, and this method is currently being pursued in more detail in this laboratory.

This technique of multiplet resolution appears to offer distinct advantages over the technique of deconvolution in applications to electrically detected mass spectra. In addition to being mathematically much simpler to apply, a distinct advantage to those not having access to a large computer, multiplet resolution based on only two pieces of data, the accurate mass and intensity, eliminates many of the problems, such as peak profile smoothing and introduction of several empirical parameters, associated with application of deconvolution techniques ([5,6]).

For further applications to organic analysis, it is perhaps desirable to examine some of the results obtained on spectra of compounds with molecular weights considerably higher than those of perchlorobutadine and methyl arachidate, discussed previously. These spectra indicate that mass measurement accuracy is maintained at the higher masses. Two examples will be discussed briefly.

The first example is concerned with spectra obtained on several steroid derivatives related to lanosterol. Mass measurements on one member of the series serve as an illustration. Four successive spectra were obtained on a sample of dihydrolanosterolenedione acetate (I) on the direct introduction probe.* Table VI presents some of the more prominent peaks in the spectrum above mass 350, with assigned mass and composition and average difference in ppm indicated.

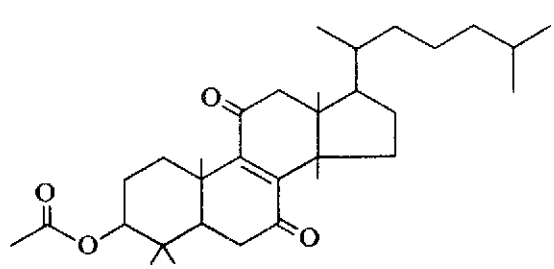

(I)

*Spectra taken at 10,000 resolution, 24 kHz digitization rate.

TABLE VI. Dihydrolanosterolenedione Acetate—High Mass

Assigned mass	Assigned composition	Average diff., ppm
356.27151	$C_{24}H_{36}O_2$	−0.39
372.23004	$C_{23}H_{32}O_4$	1.10
385.23787	$C_{24}H_{33}O_4$	−0.16
410.35485	$C_{29}H_{46}O_1$	1.36
420.33920	$C_{30}H_{44}O_1$	1.76
423.32629	$C_{29}H_{43}O_2$	1.20
438.34976	$C_{30}H_{46}O_2$	0.50
456.36032	$C_{30}H_{48}O_3$	0.75
470.37597	$C_{31}H_{50}O_3$	1.04
483.34741	$C_{31}H_{47}O_4$	1.16
498.37089	$C_{32}H_{50}O_4$ (M^+)	2.18

The second example involves the spectrum of Rifamycin S (II), a member of a new series of antibiotics.*

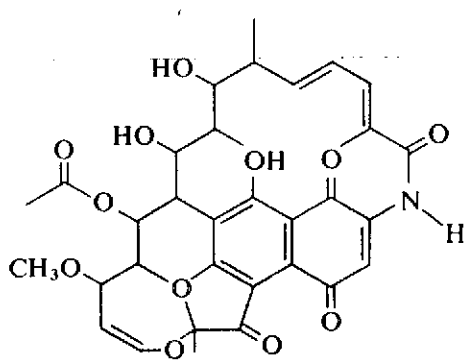

(II)

Some representative data (single-spectrum mass measurements) for Rifamycin S are tabulated in Table VII.

TABLE VII.

Species	Observed mass	Assigned mass	Composition	Difference, mmu	Relative intensity, %
M^+	695.29448	695.29415	$C_{37}H_{45}NO_{12}$	0.33	1.53
$M-CH_2O$	665.28346	665.28359	$C_{36}H_{43}NO_{11}$	−0.13	1.46
$M-CH_3OH$	663.27001	663.26794	$C_{36}H_{41}NO_{11}$	2.07	0.99

*We wish to thank Professor Sensi and Dr. Lancini for providing us with this sample.

The data in Tables VI and VII indicate that generalizations based on system evaluation at lower masses are extendable to higher masses. Mass measurement accuracy is maintained at these higher masses.

CONCLUSIONS

A detailed examination of the technique of real-time high resolution mass spectrometry has been carried out. Evaluation of the system shows root mean square mass measurement accuracies of 0.5–3.0 ppm depending on the number of scans taken and the dynamic range covered by the data. The utility of the "four average" technique to provide accuracies sufficient to drastically limit elemental composition ambiguities has been described. Intensity measurement precision and accuracy has been shown to be limited only by ion statistical considerations.

This examination permits one to analyze data from organic samples of interest on the basis of known mass and intensity measurement performance of the system. Development of an equation to predict or analyze mass measurement errors greater than known limitations of the system has been described, and its application to doublets involving ^{13}C isotopic contributions has been illustrated. Data presented indicate retention of mass measurement accuracy to much higher masses than studied in the section on system evaluation.

It is felt that the data presented above provide an indication of the future potential of utilization of real-time computers in the field of high-resolution mass spectrometry.

REFERENCES

1. P. Bommer, W. J. McMurray, and K. Biemann, 12th Annual Conference on Mass Spectrometry and Allied Topics, Montreal (June 7–12, 1964), p. 428.
   A. L. Burlingame, EUCHEM Conference on Mass Spectrometry, Sarlât, France, September 7–12, 1965.
2. A. L. Burlingame, *Advances in Mass Spectrometry, Vol. 4* (E. Kendrick, ed.), The Institute of Petroleum, London (1968), p. 15.
   W. J. McMurray, S. R. Lipsky, and B. N. Green, *ibid.*, p. 77.
   C. Merritt, Jr., P. Issenberg, and M. L. Bazinet, *ibid.*, p. 55.
   H. C. Bowen, E. Clayton, D. J. Shields, and H. M. Stanier, *ibid.*, p. 257.
   H. C. Bowen, T. Chenerix-Trench, S. D. Drackley, R. C. Faust, and R. H. Saunders, *J. Sci. Instrum.* **44**, 343(1967).
   W. J. McMurray, B. N. Green, and S. R. Lipsky, *Anal. Chem.* **38**, 1194(1966).
3. A. L. Burlingame, D. H. Smith, and R. W. Olsen, *Anal. Chem.* **40**, 13(1968).
4. A. L. Burlingame, D. H. Smith, R. W. Olsen, and T. O. Merren, 16th Annual Conference on Mass Spectrometry and Allied Topics, Pittsburgh (May 12–17, 1968).
   D. H. Smith, R. W. Olsen, and A. L. Burlingame, *ibid.*
5. D. D. Tunnicliff and P. A. Wadsworth, *private communication*.

6. R. Venkataraghavan, F. W. McLafferty, and J. W. Amy, *Anal. Chem.* **39**, 178(1967).
7. A. L. Burlingame, D. H. Smith, and R. W. Olsen, *Anal. Chem.* (*in preparation*).
8. C. La Lau, Mass discrimination caused by electron-multiplier detectors, *in: Topics in Organic Mass Spectrometry* (A. L. Burlingame, ed.). Wiley–Interscience, New York (in press).
9. A. L. Burlingame and D. H. Smith, unpublished results.